



Universidad del País Vasco Euskal Herriko Unibertsitatea



Cyclic carbonates from CO<sub>2</sub> and vegetable oils as bio-precursors for non-isocyanate polyurethanes development:  
**A journey from monomer synthesis to industrial application**

2022, Donostia-San Sebastián.

**Ander Centeno Pedraza.**



Cyclic carbonates from  
CO<sub>2</sub> and vegetable oils as bio-precursors  
for non-isocyanate polyurethanes  
development:  
A journey from monomer synthesis to  
industrial application

A dissertation presented by:

**Ander Centeno Pedraza**

In fulfilment of the Requirements for the degree of:

**Doctor in Applied Chemistry and Polymeric Materials**

Advisors: **Dr. Zoraida Freixa** and **Dr. Pablo Ortiz**

**University of the Basque Country UPV/EHU**

**Donostia-San Sebastián 2022**



*"It's the questions we can't answer that teach us the most. They teach us how to think. If you give a man an answer, all he gains is a little fact. But give him a question and he'll look for his own answers."*

Patrick Rothfuss



# ACKNOWLEDGEMENTS

Escribir estas palabras significa que el final de una de las aventuras más increíbles llega a su fin. Esto no hubiera sido posible sin el apoyo de toda la gente maravillosa con la que he tenido la suerte de coincidir. Por ello, en estas páginas me gustaría agradecer de corazón a todas las personas que considero parte de esta tesis y que me han hecho ser mejor investigador y persona.

Creo que no hay mejor forma de empezar que agradeciendo a mis directores de tesis. A Pablo Ortiz, por la confianza depositada en mí y darme total libertad para aplicar mis ideas. Valoro enormemente que me hayas ayudado a ser una persona-investigador autosuficiente. A Zoraida Freixa por estar siempre que lo he necesitado y tu inagotable dedicación. Aprecio muchísimo toda tu ayuda y empeño en enseñarme y ayudarme a sacar este proyecto adelante. Gracias a los dos por haberme hecho no solo mejor investigador, sino también mejor persona.

Gracias Eduardo, creo que todo agradecimiento que te escriba no será ni una mínima parte de todo lo que has hecho por mí durante estos 4 años. Fuiste una de las razones para que me embarcara en este viaje, y no me equivocaba. Gracias por poner las bases de la tesis, pero especialmente por transmitir la pasión e inagotable motivación que sientes por la investigación. Tus consejos, conocimiento y valores han sido la clave para poder crecer y tener las ideas más claras. Estaré eternamente agradecido por todo lo que has creído en mí y valorarme.

También me gustaría hacer una mención especial a José Ramon Ochoa. Gracias por seguirme de cerca, tus infinitos consejos y enseñarme que la pasión es la pieza fundamental de la investigación. Ha sido un placer poder coincidir contigo y poder aprender en cada una de las conversaciones.

Gracias también a Ali, Olga y Soraya, por tener siempre la “puerta” abierta para mí, por ayudarme, animarme y escucharme siempre que lo he necesitado. También

quiero dar las gracias a otras personas que de un modo u otro me han ayudado: Bea, Iker, Paqui, Susana y Tomás.

A mis compañeras de laboratorio que me abrieron las puertas un 26 de octubre de 2018, y me han hecho ser parte desde el primer día. A Jonatan por enseñarme todo lo que sabes y que pese a que te habré hecho más de 1.000.000 de preguntas todavía sigues contestándome con una sonrisa. A Leire por estar siempre dispuesta ayudarme, hacérmelo todo tan fácil y por las “discusiones” en el labo, creo que sin tu inagotable apoyo esta tesis no hubiera salido adelante. A Beñat por estar siempre interesado en los avances de mi tesis, tu entusiasmo por que un químico entienda a un ingeniero químico (y viceversa), y por los miles de cafés hablando de la Real. A Belen, por escucharme, entenderme y aconsejarme. A Cristina, Marta, Noelia y Silvia por enseñarme, invertir vuestro tiempo en mí y las risas en el laboratorio. Por último, no quiero olvidarme de todos los estudiantes que han pasado durante estos años por el laboratorio: Gorka, Igor, Mehwish, Melani, María, Ruben... Todxs los que sois o habéis sido parte de Química Sostenible habéis conseguido sacarme una sonrisa en los momentos más duros de estos 4 años.

I gratefully acknowledge Dr. Florian Lunzer for giving me the opportunity of going to Allnex -The coating Resin Company- for an internship. Especial Thanks to Dr Roland Feola, for being my mentor there, the scientific discussion and all the thing you tough me. To Sabine and Heike for making me part of the group and helping me to understand a new field. Thank you all three for helping me to make my stay as easy as possible. You are part of one of the most special times of my life. I would also like to thank the many other people who are part of Allnex-Graz. There are too many names to list here, but without a doubt, I am deeply grateful for all the help I received during the three and a half months of my stay.

También me gustaría dar las gracias al grupo de organometálicos, especialmente a Ane, Ariadna y Borja. A pesar de haber trabajado en sitios distintos, siempre que he necesitado me habéis hecho un hueco en el laboratorio y sentirme uno más del grupo.



A Amets, David y Jorge por el tiempo y la ayuda para que pudiese caracterizar los materiales.

A mis amigos, por preocuparse, aguantarme y entenderme. Gracias por las cenas interminables, los pogos en los conciertos y los buenos momentos.

Nere uniko lagunei, bereziki Axi, Elena, Jabino, Olaia eta Unaitori. Bidaia hau aspaldi hasi baitzen, eta zuen laguntza, ulermen, goxotasun eta animorik gabe, bidea oso bestelakoa izango zen. Eskerrik asko bihotzez.

A mi familia, por estar siempre conmigo. A la allalla, por educarme, enseñarme a no rendirme e inculcarme los reños que tienes. Eres y serás mi persona favorita. A la apapa, por hacerme reír y sacarme de quicio a la vez. Gracias por el interés que muestras en todo lo que hago y las innumerables preguntas sobre mis viajes y la química. A Borja por protegerme y tirarme de las orejas siempre que ha hecho falta. Gracias por preocuparte por mí y estar siempre que lo he necesitado. Aitziberri, zure pazientzia, ulertzeko gaitasuna eta goxotasunagatik. Zure milaka aholkuek, entzuteko gaitasuna, estresaren aurkako besarkadek... bidai honen zati oinarrizkoa egin zaituzte. Askotan ere, nire zamaren pisu asko zeureganatu duzu. Txantxetan esaten dizudan moduan abentura honetan ni Frodo eta zu Sam izan zara. Baina bereziki eskerrak eman nahi dizkizut nire egun txarrak, onak bihurtzeagatik, maite zaitut potola. Y, por último, a la ama, por escucharme, comprenderme y guiarme. Gracias por enseñarme que con trabajo y dedicación puedo conseguir todo lo que me proponga. Pero sobre todo porque con tu amor, cariño, dulzura y esfuerzo me lo has hecho todo más fácil. Siempre seremos un equipo, te quiero mucho ama.



## SUMMARY

Since the development of the reaction between alcohols and isocyanates in 1930s by Otto Bayer and co-workers, the expansion of polyurethanes (PUs) has reached such a point that modern life cannot be understood without them. In fact, the versatility of this polymer family has allowed the use of PU in numerous fields and applications, such as rigid and flexible foams for insulation or automotive industry, adhesives and sealants, coatings, biomedical materials, etc. However, the use of finite and non-renewable fossil-based feedstocks, and the increasing environmental and security concerns has spurred the research in new synthetic alternatives to traditional PUs. Consequently, alternative polyurethanes processes should take into consideration factors such as circular economy, renewability, reliability, low emissions and industrial feasibility. The design of a new class of polymers to substitute the current PUs is one of the greatest challenges in polymer chemistry.

The growing interest in process development in line with Green Chemistry principles has resulted in the research to use biomass as feedstock for PU synthesis. In this context, vegetable oils have attracted the greatest interest due to their widespread availability, non-toxicity, sustainability, inherent biodegradability, easy handling, low cost and the well-defined chemical structure. The fact that vegetable oils are triesters of glycerol with long-chain fatty acids, provides different active sites, which can be modified for the obtention of both polyols and isocyanates as intermediates of PUs. Nevertheless, the synthesis of a completely biomass-based PUs does not address the major drawback of PUs: The toxicity of isocyanates and their precursors.

To tackle this problem, the scientific community has focused its efforts on the replacement of isocyanates as chemical reagents, developing new chemical pathways for polyurethane synthesis by non-isocyanate routes. Up to now, the best way for the development of PUs aligned with non-isocyanate and Green Chemistry philosophy is the polyaddition reaction between cyclic carbonates and amines. Indeed, this route has allowed the synthesis of non-isocyanate polyurethanes (NIPUs) from carbonated vegetable oils.

In spite of the step forward in terms of sustainability, the synthesis of NIPUs from vegetable oils through polyaddition reaction has several drawbacks. In relation to carbonated precursor synthesis, the low CO<sub>2</sub> activity and the high steric hindrance of the oil structure prevent a high yield of the desired bio-based carbonate product. This leads to the need for high temperatures and pressures with long reaction times, together with the use of efficient catalytic systems. Therefore, the synthesis of carbonated vegetable oils requires reaction conditions that considerably increase the cost of the products and make more difficult the industrial implementation of the carbonated oils. To circumvent these drawbacks, in this thesis a series of economic and easy to prepare and to isolate catalysts have been tested in the cycloaddition reaction of CO<sub>2</sub>. On the other hand, most of the research on the synthesis of NIPUs has been focused on factors to improve the reactivity between the cyclic carbonates and the amines. However, few works have gone a step further and have tried to apply these products in the industry or at least characterize the product according to industrial standards. Therefore, in this thesis we have tried to make progress in this area, with the implementation of soybean oil-based NIPUs in the coatings industry, in addition to a comparison of the properties between NIPUs and PUs from vegetable oils.

In order to bring CSBO-based NIPUs closer to an industrial application, the thesis is structured in five chapters. **Chapter 1** discusses the current status of petrochemical-based polyurethanes and the possible solutions developed to obtain more sustainable polyurethanes in accordance with the principles of Green Chemistry, with special emphasis on the new generation of biomass based non-isocyanate polyurethanes. Additionally, the challenges that need to be addressed for sustainability and to make the process industrially viable are highlighted. Besides, the current situation of CO<sub>2</sub> cycloaddition to epoxides from vegetable oil or derivatives is described, as well as the properties and applicability of NIPUs from carbonated oils.

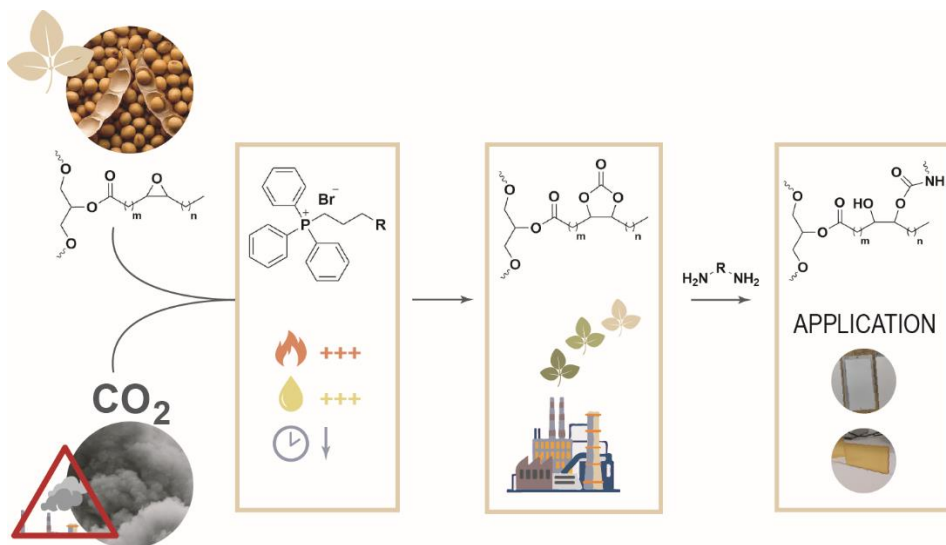
In **Chapter 2**, the optimization of the carbonation of soybean oil through the development of new catalysts is presented. Specifically, a series of economic and easy to prepare and to isolate ionic liquids based in phosphonium cation and a halogen anion have been designed, prepared, fully characterized and tested in the

cycloaddition reaction of CO<sub>2</sub> to epoxidized soybean oil (ESBO). In order to find the optimal reaction conditions, the influence of the cation and the anion on the performance of the ionic liquid and several reaction parameters such as reaction temperature, catalyst concentration, total pressure and reaction time have been studied and are deeply discussed.

**Chapter 3** deals with the synthesis and characterization of non-isocyanate polyurethanes through the polyaddition reaction between carbonated soybean oil and different amines and molar ratios. NIPUs synthesis was accompanied by a detailed study of the properties of soybean oil-based NIPUs through a series of characterization techniques to analyse the influence of these parameters in the final properties and determine their versatility. Additionally, a comparison of the properties obtained with those of traditional vegetable oil-based PUs has also been carried out.

**Chapter 4** focuses on the applicability of NIPUs from CSBO in the coatings industry under industry-required conditions. For that goal, two different strategies have been pursued. The first focuses on the development of NIPU coatings by combining carbonated soybean oil and industrial amines directly in the formulation. The second approach is based on the development of 2K hybrid NIPU-epoxy coatings via the synthesis of CSBO-based amino hardeners. The obtained NIPU coatings were characterized by means of complementary techniques used in the coating industry and compared to commercial epoxy coating benchmarks.

**Chapter 5** brings together the main conclusions obtained throughout this research, in addition to possible future work to create more sustainable polyurethanes with greater potential.



Graphical abstract 1. Thesis graphical abstract.

# RESUMEN

Desde que en la década de 1930 Otto Bayer y sus colaboradores desarrollaron la reacción entre alcoholes e isocianatos, la expansión de los poliuretanos (PUs) ha llegado a tal punto que es incomprendible entender la vida moderna sin estos materiales. De hecho, la versatilidad de esta familia de polímeros ha permitido el uso de los PUs en numerosos campos y aplicaciones, como espumas rígidas y flexibles para el aislamiento o la industria del automóvil; adhesivos y selladores; revestimientos; materiales biomédicos; etc. Sin embargo, el uso de materias primas finitas y no renovables de origen fósil, junto con la creciente preocupación por el medio ambiente y la seguridad han impulsado la investigación de nuevas alternativas sintéticas a los PUs tradicionales. Por este motivo, el proceso para desarrollar PUs alternativos debe tener en cuenta estos factores: economía circular, reciclabilidad, seguridad, bajas emisiones y viabilidad industrial. El diseño de una nueva clase de polímeros para sustituir a los actuales PUs es uno de los mayores retos en la química de polímeros.

El creciente interés por el desarrollo de procesos afines a los principios de la Química Verde ha impulsado a el uso de la biomasa como materia prima para la síntesis de PUs. En este contexto, la disponibilidad, no toxicidad, sostenibilidad, inherente biodegradabilidad, fácil manejo, bajo coste y estructura química bien definida, convierte a los aceites vegetales en una de las materias primas con mayor potencial para el desarrollo de distintos productos. El hecho de que los aceites vegetales sean triésteres de glicerol con ácidos grasos de cadena larga, proporciona diferentes sitios activos, que pueden ser modificados para la obtención de polioles e isocianatos, como intermedios de PUs. No obstante, la síntesis de un PUs completamente basado en la biomasa no aborda el principal inconveniente de los PUs: La toxicidad de los isocianatos y sus precursores.

Para afrontar este problema, la comunidad científica ha focalizado sus esfuerzos en la sustitución de los isocianatos como reactivos químicos, desarrollando nuevas vías químicas para la síntesis de poliuretanos por rutas sin isocianatos. En la actualidad,

la reacción de poliadición entre carbonatos cíclicos y aminas es considerada la vía de mayor potencial para el desarrollo de PUs por estar acorde a la filosofía de evitar el uso de los isocianatos y la Química Verde. De hecho, esta ruta ha permitido la síntesis de poliuretanos sin isocianato (NIPUs) a partir de aceites vegetales carbonatados.

A pesar del paso adelante en términos de sostenibilidad, la síntesis de NIPUs a partir de aceites vegetales por medio de la poliadición presenta varios inconvenientes. En primer lugar, la baja actividad del CO<sub>2</sub> y el alto impedimento estérico de la estructura del aceite limita la reactividad y alto rendimiento del precursor carbonatado. Esto implica el uso de altas temperaturas y presiones con largos tiempos de reacción. Por esta razón, la síntesis de aceites vegetales carbonatados requiere unas condiciones de reacción que aumentan considerablemente el coste de los productos y dificultan su implantación industrial. Para sortear estos inconvenientes, en esta tesis se han ensayado una serie de catalizadores económicos, fáciles de preparar y aislar en la reacción de cicloadición entre el CO<sub>2</sub> y aceite de soja epoxidado (ESBO). En segundo lugar, la mayor parte de la investigación sobre la síntesis de NIPUs a partir de aceites vegetales se ha centrado en factores para mejorar la reactividad entre los carbonatos cíclicos y las aminas. Sin embargo, son pocos los trabajos que han ido un paso más allá y han tratado de aplicar estos productos en la industria o, al menos, caracterizar el producto de acuerdo con los estándares industriales. Por ese motivo, uno de los objetivos de esta tesis ha sido avanzar en la aplicabilidad de los NIPUs a base de aceite de soja, empleando estos materiales en la industria de los recubrimientos. Asimismo, se ha realizado una comparación de las propiedades entre NIPUs y PUs de aceites vegetales con la intención de conocer la eficiencia de los NIPUs respecto a sus análogos con isocianatos.

Con el fin de acercar los NIPU basados en aceite de soja carbonatado (CSBO) a una aplicación industrial, la tesis se estructura en cinco capítulos. En el **Capítulo 1** se discute el estado actual de los poliuretanos de base materias primas de origen petroquímico y las posibles soluciones desarrolladas para obtener poliuretanos más sostenibles de acuerdo con los principios de la Química Verde, con especial énfasis en la nueva generación de poliuretanos sin isocianato basados en biomasa. Además, se destacan los retos que hay que abordar para la sostenibilidad y para que el proceso



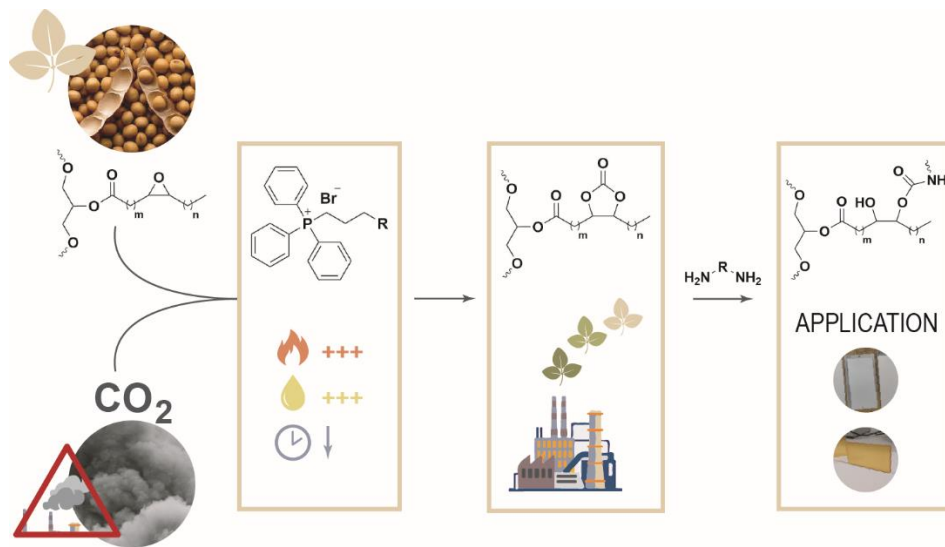
sea viable industrialmente. Asimismo, se describe la situación actual de la cicloadición de CO<sub>2</sub> a epóxidos procedentes de aceites vegetales o derivados, así como las propiedades y aplicabilidad de los NIPUs procedentes de aceites carbonatados.

En el **Capítulo 2** se realiza la optimización de síntesis del aceite de soja carbonatado mediante el desarrollo de nuevos catalizadores. En concreto, se han diseñado, preparado, caracterizado y ensayado una serie de líquidos iónicos económicos basados en un catión fosfonio y un anión halógeno en la reacción de cicloadición de CO<sub>2</sub> a ESBO. Con el fin de conocer las condiciones óptimas de reacción, se ha estudiado la influencia del catión y del anión en el rendimiento del líquido iónico, además de varios parámetros de reacción como la temperatura de reacción, la concentración del catalizador, la presión total y el tiempo de reacción.

El **Capítulo 3** se presenta la síntesis y caracterización de poliuretanos sin isocianatos mediante la reacción de poliadición entre CSBO y diferentes aminas y proporciones molares. Además de, la síntesis de NIPUs, se ha realizado un estudio detallado de las propiedades de los NIPUs basados en aceite de soja mediante una serie de técnicas de caracterización para analizar la influencia de estos parámetros en las propiedades finales y determinar su versatilidad. También, se ha realizado una comparación de las propiedades obtenidas con las de los PUs tradicionales basados en aceites vegetales.

El **Capítulo 4** se centra en la aplicabilidad de NIPUs de CSBO en la industria de los recubrimientos. Para ello, se han seguido dos estrategias diferentes. La primera se centra en el desarrollo de recubrimientos de NIPU mediante el uso directo de aceite de soja en una formulación compuesta por aminas de uso industrial y el aceite. La segunda estrategia se enfoca en el desarrollo de recubrimientos híbridos NIPU-epoxi mediante la síntesis de amino endurecedores a base de CSBO. Los recubrimientos de NIPU obtenidos se caracterizaron mediante técnicas complementarias utilizadas en la industria de los recubrimientos y se compararon con las referencias de los recubrimientos epoxi comerciales.

El **Capítulo 5** agrupa las principales conclusiones obtenidas a lo largo de esta investigación, además de posibles trabajos futuros para crear poliuretanos más sostenibles y con mayor potencial.



**Graphical abstract 2.** Thesis graphical abstract

# LIST OF ABBREVIATIONS

[BDBU][Br]	1-butyl-2,3,4,5,7,8,9,10-octahydropyrido[1,2-a][1,3]diazepin-1-ium bromide
[BMeIm][Cl]	1- <i>n</i> -butyl-3-methylimidazolium chloride
[BMePh][I]	1-butyl-4-methylpyridinium iodide
[BMPyr][I]	1-butyl-1-methylpyrrolidinium iodide
[BPy][I]	1-butylpyridinium
[BTBD][Br]	1-butyl-3,4,6,7,8,9-hexahydro-2H-pyrimido [1,2-a]pyrimidin-1-ium bromide
[BTCP][Br]	Butyltricyclohexylphosphonium bromide
[BTPP][Br]	Butyltriphenylphosphonium bromide
[CBTPP][Br]	(3-carboxypropyl)triphenylphosphonium bromide
[COTPP][Br]	(7-carboxyheptyl)triphenylphosphonium bromide
[CTMA][Br]	Cetyltrimethylammonium bromide
[DTCP][Br]	Dodecyltricyclohexylphosphonium bromide
[DTPP][Br]	Dodecyltriphenylphosphonium bromide
[ETPP][Br]	Eicosiltriphenylphosphonium bromide
[H <sup>+</sup> ]	Hydrogen ion-Acid compound
[HBIIm][Cl]	1-hydroxypropyl-3- <i>n</i> -butylimidazolium chloride

<b>[HPhBPhIm][Br]</b>	1-butyl-4-(2-hydroxyphenyl)-3-phenyl-1 <i>H</i> -imidazolium bromide
<b>[HPhBPhIm][I]</b>	1-butyl-4-(2-hydroxyphenyl)-3-phenyl-1 <i>H</i> -imidazolium iodide
<b>[HPhDPhIm][Br]</b>	1-butyl-4-(2-hydroxyphenyl)-3-butyl-1 <i>H</i> -imidazolium bromide
<b>[HPhDPhIm][I]</b>	1-butyl-4-(2-hydroxyphenyl)-3-butyl-1 <i>H</i> -imidazolium iodide
<b>[HPhDPhP][Br]</b>	(2-hydroxyphenyl)diphenylpropyl phosphonium bromide
<b>[HPTPP][Br]</b>	(3-hydroxypropyl)triphenylphosphonium bromide
<b>[HTPP][Br]</b>	Hexadecyltriphenylphosphonium bromide
<b>[O]</b>	Oxidant
<b>[OMeIm][Br]</b>	1- <i>n</i> -octyl-3-methylimidazolium bromide
<b>[OMeIm][Cl]</b>	1- <i>n</i> -octyl-3-methylimidazolium chloride
<b>[OMeIm][I]</b>	1- <i>n</i> -octyl-3-methylimidazolium iodine
<b>[OTPP][Br]</b>	Octyltriphenylphosphonium bromide
<b>[OTPP][I]</b>	Octyltriphenylphosphonium iodine
<b>[PPN][Cl]</b>	Bis(triphenylphosphine)iminium chloride
<b>[TBA][Br]</b>	Tetra- <i>n</i> -butylammonium bromide
<b>[TBA][Cl]</b>	Tetra- <i>n</i> -butylammonium chloride
<b>[TBA][F]</b>	Tetra- <i>n</i> -butylammonium fluoride

<b>[TBA][I]</b>	Tetra- <i>n</i> -butylammonium iodine
<b>[TBA][OH]</b>	Tetrabutylammonium hydroxide
<b>[TBHEP][Br]</b>	Tri- <i>n</i> -butyl-(2-hydroxyethyl)phosphonium bromide
<b>[TBHEP][Cl]</b>	Tri- <i>n</i> -butyl-(2-hydroxyethyl)phosphonium chloride
<b>[TBHEP][I]</b>	Tri- <i>n</i> -butyl-(2-hydroxyethyl)phosphonium iodine
<b>[TBP][Br]</b>	Tetra- <i>n</i> -butylphosphonium bromide
<b>[TBP][Cl]</b>	Tetra- <i>n</i> -butylphosphonium chloride
<b>[TBP][I]</b>	Tetra- <i>n</i> -butylphosphonium iodine
<b>[TDMeIm][Br]</b>	1- <i>n</i> -tetradecyl-3-methylimidazolium bromide
<b>[TES][I]</b>	Triethylsulfonium iodide
<b>[THA][Br]</b>	Tetra- <i>n</i> -heptylammonium bromide
<b>[TOP][Br]</b>	Tetra- <i>n</i> -octylphosphonium bromide
<b>[TPhHEP][Br]</b>	(2-hydroxyethyl)triphenylphosphonium bromide
<b>[TPhHEP][Cl]</b>	(2-hydroxyethyl)triphenylphosphonium chloride
<b>[TPhHEP][I]</b>	(2-hydroxyethyl)triphenylphosphonium iodine
<b>°C</b>	degree centigrade
<b>μm</b>	micrometre
<b>1K</b>	One-component coatings
<b>2K</b>	Two-component coatings

<b>AH</b>	Amino hardener
<b>AsA</b>	Ascorbic acid
<b>ATR</b>	Attenuated Total Reflection
<b>ATR-FTIR</b>	Attenuated Total Reflection Fourier Transform Infrared Spectroscopy
<b>ca.</b>	Circa (about)
<b>CAGR</b>	Compound annual growth rate
<b>Cat.</b>	Catalyst
<b>CDCl<sub>3</sub></b>	Deuterated chloroform
<b>CHA</b>	Cyclohexylamine
<b>CLSO</b>	Carbonated linseed oil
<b>cm</b>	centimetre
<b>CMR</b>	Carcinogenic, mutagenic, and toxic to reproduction
<b>Conv.</b>	Conversion
<b>CRM</b>	Critical Raw Material
<b>CSBO</b>	Carbonated soybean oil
<b>CSBO-AHs</b>	CSBO-based NIPU amino hardeners
<b>CSFO</b>	Carbonated sunflower oil
<b>DABCO</b>	1,4-Diazabicyclo[2.2.2]octane

<b>DAO</b>	1,8-diaminooctane
<b>DBU</b>	1,8-Diazabicyclo[5.4.0]undec-7-ene
<b>DETA</b>	2,2'-Diaminodiethylamine
<b>DFT</b>	Dry film thickness
<b>DMAP</b>	4-(Dimethylamino)pyridine
<b>DMSO-<i>d</i><sub>6</sub></b>	Deuterated dimethyl sulfoxide
<b>DSC</b>	Differential Scanning Calorimetry
<b>dTG</b>	Derivative Thermo-Gravimetric Analysis
<b>EDA</b>	1,2-diaminoethane
<b>ELSO</b>	Epoxidized linseed oil
<b>Equiv.</b>	Equivalent
<b>ESBO</b>	Epoxidized soybean oil
<b>ESFO</b>	Epoxidized sunflower oil
<b>FA</b>	Fatty acid
<b>FTIR</b>	Fourier Transform Infrared Spectroscopy
<b>g</b>	gram
<b>GC</b>	Gel-content
<b>GC-MS</b>	Gas Chromatography Mass Spectrometry
<b>h</b>	hour

<b>HBD</b>	Hydrogen Bond Donor
<b>HCMC</b>	Protonated carboxymethyl cellulose
<b>IL</b>	Ionic liquid
<b>Impact d</b>	Direct impact
<b>Impact id</b>	Indirect impact
<b>IPDA</b>	Isophoronediamine
<b>Jeff D400</b>	JEFFAMINE D-400 Polyetheramine
<b>MBCHA</b>	Methylenebis(cyclohexylamine)
<b>MDI</b>	Methylene diphenyl diisocyanate
<b>MEK</b>	Methyl ethyl ketone
<b>mL</b>	millilitre
<b>MOF</b>	Metal-Organic-Framework
<b>MPa</b>	megapascal
<b>MR</b>	Molar ratio
<b>MW</b>	Microwave
<b>Mw</b>	Weight average molecular weight
<b>mW</b>	miliwatt
<b>m-XDA</b>	m-xylenediamine
<b>NIPU</b>	Non-isocyanate polyurethane



<b>NMR</b>	Nuclear Magnetic Resonance
<b>P</b>	Pressure
<b>PDI</b>	Pentamethylene diisocyanate
<b>PEG</b>	Polyethyleneglycol
<b>PHU</b>	Polyhydroxyurethane
<b>PPC</b>	Propylene carbonate
<b>ppm</b>	Parts per million
<b>PU</b>	Polyurethane
<b>PUD</b>	Waterborne polyurethane dispersion
<b>PVC</b>	Polyvinyl chloride
<b>QSPR</b>	Quantitative structure-property relationship
<b>r.p.m</b>	Revolutions per minute
<b>Ref.</b>	Reference
<b>RIM</b>	Reaction injection moulding
<b>s</b>	second
<b>SBU</b>	Solvent-borne urethane solution
<b>Select.</b>	Selectivity
<b>SI</b>	Swelling index
<b>SiO<sub>2</sub>-I</b>	Silica-supported 4-pyrrolidinopyridinium iodide

<b>T</b>	Temperature
$T_5$	Temperature in which the sample loss 5 wt% of its initial mass
$T_{50}$	Temperature in which the sample loss 50 wt% of its initial mass
<b>TAEA</b>	Tris(2-aminoethyl)amine)
<b>TBD</b>	1,5,7-Triazabicyclo[4.4.0]dec-5-ene
<b>TCP</b>	Tricyclohexylphosphine
<b>TDI</b>	Toluene diisocyanate
<b>TETA</b>	Triethylenetetramine
<b>TFtert-BOH</b>	2,2,2-trifluoro-tert-butanol
$T_g$	Glass transition temperature
<b>TGA</b>	Thermo-Gravimetric Analysis
$T_m$	Melting temperature
<b>TMPE</b>	Thermomorphing polyethylene
$T_{onset}$	Decomposition temperature
<b>TPP</b>	Triphenylphosphine
<b>TPU</b>	Thermoplastic polyurethane resin
<b>USD</b>	United States Dollar

<b>VO</b>	Vegetable oil
<b>vs.</b>	Versus
<b>wt. %</b>	Weight given as a percentage



# TABLE OF CONTENTS

<b>ACKNOWLEDGEMENTS.....</b>	<b>I</b>
<b>SUMMARY .....</b>	<b>V</b>
<b>RESUMEN .....</b>	<b>IX</b>
<b>LIST OF ABBREVIATIONS.....</b>	<b>XIII</b>
<b>CHAPTER 01.....</b>	<b>1</b>
<b>1.1 POLYURETHANES: PAST, PRESENT, AND FUTURE.....</b>	<b>3</b>
1.1.1 Traditional polyurethanes.....	3
1.1.2 Biomass-based polyurethanes .....	6
1.1.3 Non-isocyanate polyurethanes .....	12
<b>1.2 CARBONATED VEGETABLE OIL SYNTHESIS: CATALYTIC SYSTEMS FOR THE EFFECTIVE FIXATION OF CO<sub>2</sub> INTO EPOXIDIZED VEGETABLE OILS AND DERIVATES. ....</b>	<b>16</b>
1.2.1 Homogeneous catalytic systems.....	17
1.2.2 Heterogeneous catalytic systems .....	40
<b>1.3 CARBONATED SOYBEAN OIL AS PRECURSOR FOR NON-ISOCYANATE POLYURETHANES .....</b>	<b>43</b>
<b>1.4 AIM AND OUTLINE OF THE THESIS .....</b>	<b>44</b>
<b>1.5 REFERENCES.....</b>	<b>45</b>

<b>CHAPTER 02 .....</b>	<b>55</b>
<b>2.1 BACKGROUND.....</b>	<b>57</b>
<b>2.2 OBJECTIVES .....</b>	<b>60</b>
<b>2.3 EXPERIMENTAL.....</b>	<b>60</b>
2.3.1 Materials.....	60
2.3.2 Synthesis and characterization of the prepared ionic liquids .....	61
2.3.3 Catalytic study .....	62
2.3.4 Solubility test of the employed catalysts .....	62
<b>2.4 RESULTS AND DISCUSSION .....</b>	<b>63</b>
2.4.1 Synthesis and characterization of ionic liquids .....	63
2.4.2 Catalytic study .....	65
<b>2.5 CONCLUSIONS .....</b>	<b>73</b>
<b>2.6 REFERENCES .....</b>	<b>74</b>
<b>CHAPTER 03 .....</b>	<b>79</b>
<b>3.1 BACKGROUND.....</b>	<b>81</b>
<b>3.2 OBJECTIVES .....</b>	<b>83</b>
<b>3.3 EXPERIMENTAL.....</b>	<b>84</b>
3.3.1 Materials.....	84
3.3.2 Synthesis and characterization of CSBO.....	85
3.3.3 Influence of [DTPP][Br] in the reaction between cyclic carbonate and amine .....	85
3.3.4 Synthesis and characterization of CSBO-based NIPUs .....	86
<b>3.4 RESULTS AND DISCUSSION .....</b>	<b>87</b>

---

3.4.1	Synthesis and characterization of CSBO .....	87
3.4.2	Influence of [DTPP][Br] in the reaction between cyclic carbonate and amine. .....	88
3.4.3	Synthesis and characterization of CSBO-based NIPUs .....	90
<b>3.5</b>	<b>CONCLUSIONS .....</b>	<b>104</b>
<b>3.6</b>	<b>REFERENCES.....</b>	<b>105</b>
 <b>CHAPTER 04.....</b>		 <b>109</b>
<b>4.1</b>	<b>BACKGROUND .....</b>	<b>111</b>
<b>4.2</b>	<b>OBJECTIVES.....</b>	<b>114</b>
<b>4.3</b>	<b>EXPERIMENTAL .....</b>	<b>115</b>
4.3.1	Materials .....	115
4.3.2	Synthesis and characterization of CSBO .....	115
4.3.3	Synthesis and characterization of NIPU coatings by direct use of CSBO ....	115
4.3.4	Synthesis and characterization of NIPU-epoxy hybrid coatings by modified CSBO .....	116
<b>4.4</b>	<b>RESULTS AND DISCUSSION .....</b>	<b>118</b>
4.4.1	Synthesis and characterization of NIPU coatings by direct use of CSBO ....	119
4.4.2	Synthesis and characterization of NIPU-epoxy hybrid coatings by modified CSBO .....	122
<b>4.5</b>	<b>CONCLUSIONS .....</b>	<b>141</b>
<b>4.6</b>	<b>REFERENCES.....</b>	<b>143</b>
 <b>CHAPTER 05.....</b>		 <b>149</b>

<b>5.1 CONCLUSIONS</b> .....	<b>151</b>
<b>5.2 FUTURE WORK</b> .....	<b>153</b>
<b>5.3 PUBLISHED RESEARCH</b> .....	<b>155</b>
<b>LIST OF FIGURES</b> .....	<b>157</b>
<b>LIST OF TABLES</b> .....	<b>162</b>
<b>LIST OF SCHEMES</b> .....	<b>164</b>
<b>METHODS</b> .....	<b>167</b>
<b>EPOXIDE CONTENT DETERMINATION</b> .....	<b>169</b>
<b>GAS CHROMATOGRAPHY MASS SPECTROMETRY (GC-MS)</b> .....	<b>169</b>
<b>NUCLEAR MAGNETIC RESONANCE SPECTROSCOPY (NMR)</b> .....	<b>170</b>
<b>THERMOGRAVIMETRIC ANALYSIS (TGA)</b> .....	<b>170</b>
<b>DIFFERENTIAL SCANNING CALORIMETRY ANALYSIS (DSC)</b> .....	<b>171</b>
<b>MELTING POINT DETERMINATION</b> .....	<b>171</b>
<b>FOURIER TRANSFORM INFRARED SPECTROSCOPY (FTIR)</b> .....	<b>172</b>
<b>DETERMINATION OF THE DEGREE OF CROSS-LINKING OF THE POLYMERIC NETWORK</b> .....	<b>172</b>
<b>AMINE NUMBER DETERMINATION</b> .....	<b>173</b>
<b>VISCOSITY AND FORMULATIONS POT-LIFE DETERMINATION</b> .....	<b>173</b>
<b>COATING DRYING DETERMINATION</b> .....	<b>174</b>
<b>COATING HARDNESS DETERMINATION</b> .....	<b>175</b>
<b>DETERMINATION OF THE RESISTANCE OF COATINGS TO SEPARATION FROM SUBSTRATE</b> .....	<b>176</b>



---

<b>COATING SOLVENT RESISTANCE DETERMINATION .....</b>	<b>178</b>
<b>COATING GRADUAL DEFORMATION RESISTANCE DETERMINATION .....</b>	<b>178</b>
<b>COATING RAPIDLY DEFORMATION RESISTANCE DETERMINATION .....</b>	<b>179</b>
<b>COATING CORROSION RESISTANCE DETERMINATION .....</b>	<b>179</b>
<b>REFERENCES .....</b>	<b>180</b>
<b>APPENDIX.....</b>	<b>181</b>
<b>CHAPTER 2.....</b>	<b>183</b>
A1. Synthesis of ionic liquids .....	183
A2. $^1\text{H}$ and $^{31}\text{P}\{^1\text{H}\}$ NMR spectra of the prepared ionic liquids .....	187
A3. TG profiles of the prepared and benchmark ionic liquids .....	198
A4. TG isothermal profiles of the [TBA][Br] (12) and the prepared [DTPP][Br] (5) ionic liquids: 180 °C (left) and 200 °C (right). .....	199
A5. Products isolated by flash chromatography column purification.....	199



# CHAPTER 01

---

## INTRODUCTION

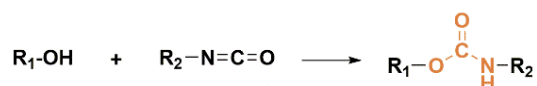
The *section 1.2* of this chapter has been submitted as publication.



## 1.1 Polyurethanes: Past, present, and future

### 1.1.1 Traditional polyurethanes

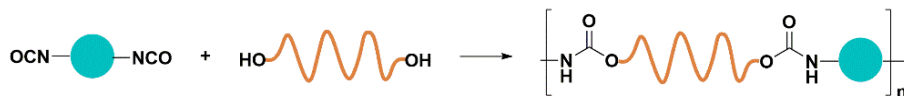
In the first decades of 20<sup>th</sup> century, the development of synthetic polymers prompted the explosive growth of the polymer industry with the creation of polyvinyl chloride (PVC), polyethylene, polyamides (nylon) or polyurethanes (PUs). The expansion has reached such a point that many of these polymer families are currently an inseparable part of modern life. PUs chemistry has not stopped growing since in the 1930s Otto Bayer and co-workers developed the reaction between alcohols and isocyanates (**Scheme 1.1**)<sup>1</sup> The growth of PUs technology in the next decades was attributed to their potential use as substitutes of other materials and the development of a great variety of polyols, which allowed the use of PU in numerous fields and applications: Shoe soles, clothing fibbers, seat cushions, wall and ceiling insulation, paints and coatings, bed mattresses, adhesives, etc (**Figure 1.1**).<sup>2</sup> Furthermore, the continuous expansion of the polyurethane industry in recent years has turned PUs into the fifth most utilized type of polymer, with a market value of over \$50 billion in 2021. This market is forecast to register a compound annual growth rate (CAGR) of 5% during the period 2022-2027.<sup>3,4</sup>



**Scheme 1.1.** Synthesis of an urethane compound.

Traditionally, PUs are formed by a polyaddition reaction between a diol (or polyol), and a diisocyanate (or polyisocyanate) (**Scheme 1.2**). It is important to emphasize that, depending on the final application, the manufacturing process may undergo some modifications.<sup>5</sup> Variations on the type and proportion of diisocyanate, polyol, and chain extender (if needed) offer a wide range of macromolecular structures, which translates into diverse properties. These, in turn, make them suitable for any different applications: rigid and flexible foams for insulation or automotive industry, adhesives and sealants, coatings, biomedical materials, etc<sup>6,7</sup>. Indeed, the diversity of

isocyanates and polyols has made PUs one of the most versatile materials in modern life.



**Scheme 1.2.** PU from diisocyanate and diol.

PUs are usually classified as thermosets and thermoplastics. The functionality and composition of the precursors determine whether a PU is a thermoset or a thermoplastic, and hence their final application. Highly functionalized reagents ( $\geq 3$ ) result in a PU with large degree of chemical cross-linking producing thermoset materials, which are present in numerous applications within the foams field, as flexible or rigid, and parts made by reaction injection moulding (RIM). These materials are largely employed as insulators in the construction industry, or in furniture and automotive businesses for seat cushioning. Additionally, thermoset urethane polymers are also applied in numerous industrial and household articles, such as shoes, helmets, sports equipment, floor mats, etc. PUs made from purely difunctional components are thermoplastics. Unlike thermoset products, these are not chemically cross-linked, and the behaviour is closely related to the physical cross-link generated via phase separation and hard segment crystallization. Thermoplastic PU resin (TPU), solvent-borne urethane solution (SBU) and waterborne PU dispersions (PUD) are the categories possible in thermoplastic polyurethanes. As previously mentioned, the diversity of chemistry and availability of many building blocks has allowed the use of PUs in numerous fields. For instance, TPU are present in shoe-soles, wire and cable jackets, skiing-shoes and rollers, protective films, catheters, implants, automotive parts, etc. SBU and PUD are applied as coatings, adhesives, or binders in many industries, such as automotive, aerospace, textile or furniture. However, although the two categories are very well differentiated, it should be noted that in some of the applications, such as coatings or adhesives, they may be used as a combination of thermoplastic and thermoset.<sup>8,9</sup>

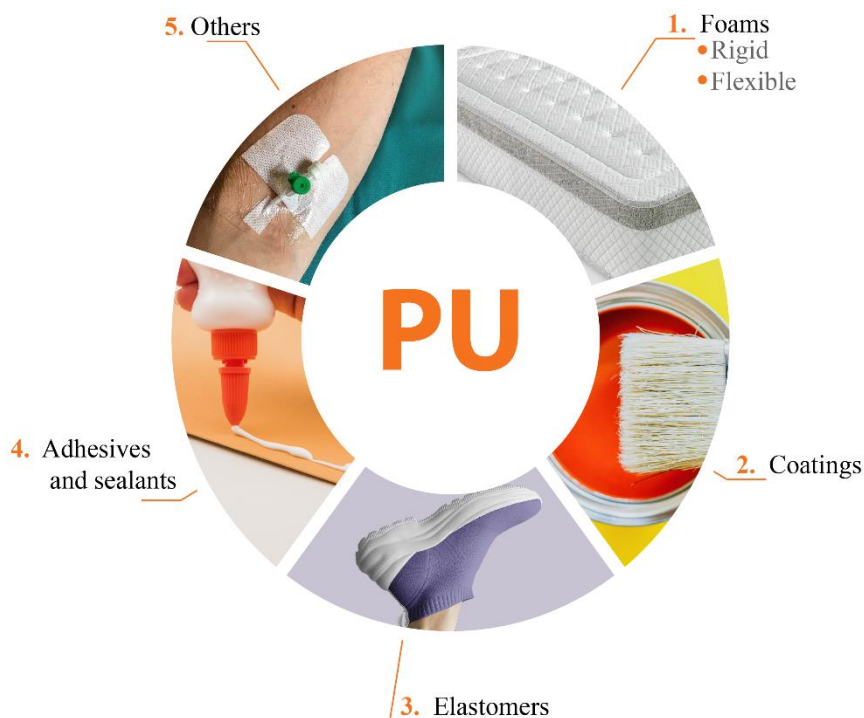


**Figure 1.1.** Main applications of traditional polyurethanes.

Despite the usefulness of PUs in numerous industries, the course towards Green Chemistry revealed two main drawbacks in PUs traditional synthesis. On the one hand, the use of petroleum-based resources. Most of the polyols and polyisocyanates are derived from petrochemicals<sup>10,11</sup>. Therefore, the high environmental impact of the consumption of non-renewable resources is pushing for more suitable polymers derived from biomass-based monomers, also known as bio-based monomers.<sup>8,12–14</sup> It is important to highlight that, this last appellation is the one used during this work for products developed from biomass. On the other hand, the evidenced toxicity of isocyanates. Although polyurethanes are not toxic compounds, considering the life cycle of isocyanate-based PUs there are several negative aspects. First, the industrial synthesis of isocyanates is based on a phosphogenation process, using a lethal and highly reactive gas, phosgene.<sup>15</sup> Secondly, the use of isocyanates raises severe health issues. Even some of the most commonly used isocyanates (methylene diphenyl diisocyanate (MDI) and toluene diisocyanate (TDI)) are classified as CMR

(carcinogenic, mutagenic, and toxic to reproduction).<sup>16-18</sup> Moreover, at the end of PUs life cycle, toxic substances are formed as a consequence of thermal degradation and also by hydrolysis of PUs wastes.<sup>19</sup> To be aware of the danger of the use of isocyanates it is worth reminding the disaster that occurred in Bophal (India) at the end of 1984. A methyl isocyanate leakage caused one of the deadliest industrial events, in which at least 2000 thousand people died, and 200.000 resulted injured.<sup>20</sup> Thereby, in the last decades, the use of highly toxic isocyanates is coming more restrictive through European regulation.<sup>21</sup>

Hence, the increasing environmental and security concerns have triggered both academia and industrial research putting significant efforts into finding synthetic alternatives to traditional PUs. The alternative process should consider factors such as circular economy, renewability, reliability, and low emissions.

### **1.1.2 Biomass-based polyurethanes**

As mentioned previously, most of the polyols and polyisocyanates used in the synthesis of polyurethanes nowadays are manufactured from fossil-based feedstocks. In fact, in order to avoid the use of petrochemical sources, the scientific community has focused on bio-based alternatives from biomass for the development of more suitable materials. Biomass is destined to be one of the sources of chemicals and materials in the near future, since our planet has enormous amount of available biomass, making it an almost unlimited source. This organic material comes from vegetable oils and animals, including crops, forest residues, animal wastes, municipal and industrial wastes, among others.<sup>22</sup> The development of renewable bio-based materials allows the manufacturing of products with a generally better environmental footprint coming from the reduction of greenhouse gas emissions.

So far, obtaining a 100% bio-based formulation has been hampered by the fact that most of the precursors are of petrochemical origin. However, in the last decades, there has been a considerable progress in developing bio-based polyols and polyisocyanates from diverse biomass sources. Indeed, both academic and industrial



research has employed a variety of biomass raw materials, such as amino acids<sup>23</sup>, sugars<sup>24</sup>, furans<sup>25</sup>, lignin<sup>26</sup>, cashew nut shell liquid<sup>27</sup> or algae<sup>28</sup> in order to increase the biobased content in PUs formulations. Even some of these bio-based monomers are commercially available. For example, Covestro sells Desmodour eco N7300<sup>8,29</sup> (a bio-based aliphatic polyisocyanate, pentamethylene diisocyanate (PDI)-trimer), derived from sugars. Other examples of bio-based compounds that have been used directly as a part of a formulation are mannitol,<sup>30</sup> a polyol derived from glucose, or lignin, which was used in PUs formulations to increase rigidity of automotive parts.<sup>31</sup>

Nevertheless, among the many renewable sources, vegetable oils have attracted the most interest due to their widespread availability, non-toxicity, sustainability, inherent biodegradability, easy handling, and low cost.<sup>32-36</sup> In addition, the well-defined chemical structure of vegetable oils is a distinctive feature compared to other biomass sources, allowing the different active points to be modified into products of high chemical, ecological and economic value.<sup>37</sup> The main components of vegetable oils are triglycerides, which are defined as esters of glycerol with three fatty acid (FA) chains. The chain length of fatty acids can vary between C12 and C24 and the number of unsaturations can vary between 0 and 3 per chain, providing different chemical and physical properties depending on the composition. **Figure 1.2** illustrates the composition of soybean oil, which is one of the most widely available vegetable oils in the world. Despite the fact that each type of vegetable oil has a certain percentage of fatty acids, it differs slightly depending on the variety, geographical area, and climatic conditions.<sup>38,39</sup>

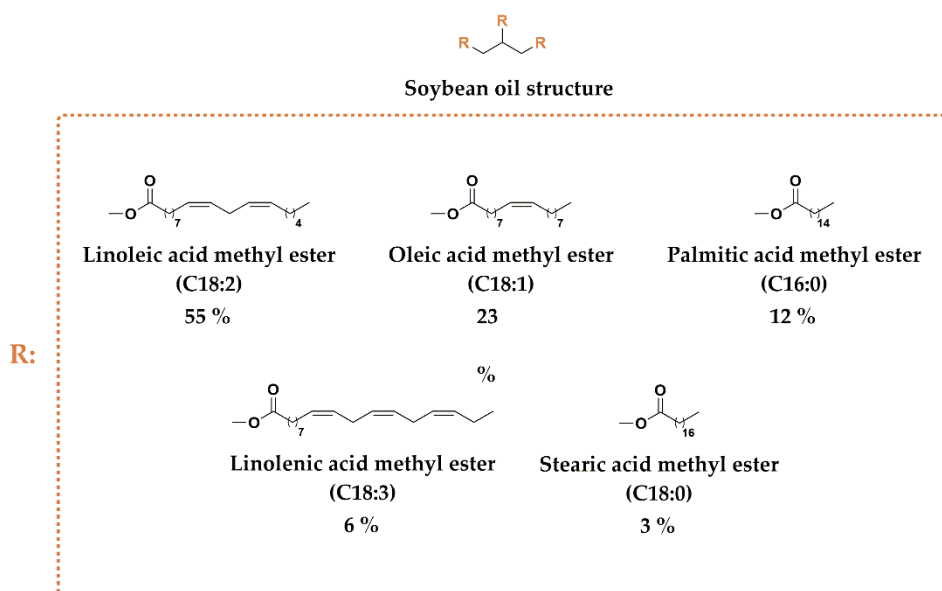


**Figure 1.2.** Soybean oil chemical composition.

Through the chemical modification of double bonds, ester groups and allylic positions presented in vegetable oils structure several bio-based monomers and polymers, such as polyesters, polyethers, polyurethanes, etc. can be synthesized.<sup>32,36</sup> The reactive sites present in the triglyceride structure are depicted in **Figure 1.3**.

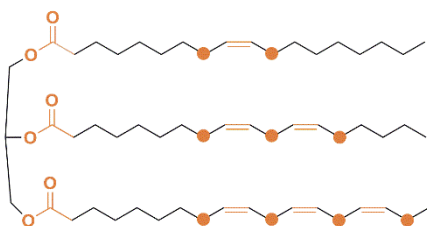


**Figure 1.3.** Triglyceride structure composed by oleic (top), linoleic (middle) and linolenic (bottom) acid methyl esters and reactive sites highlighted in orange.

The use of vegetable oil-based polyols is the most employed strategy to increase renewable content in PUs.<sup>14,40–42</sup> In fact, oleochemical-based polyols are employed in the production of rigid and flexible foams for the automotive industry or in applications, such as adhesives and glues.<sup>43–47</sup> Depending on the vegetable oil type,

two main alternatives are possible. On the one hand, PU formation reacting isocyanates and vegetable oils without chemical modifications, enabled by the presence of hydroxyl groups in fatty acid chains. This can only be brought employing castor and lesquerella oils (**Figure 1.4**), which are mainly composed by ricinoleic and lesquerolic hydroxylated fatty acids, respectively.<sup>48-50</sup>

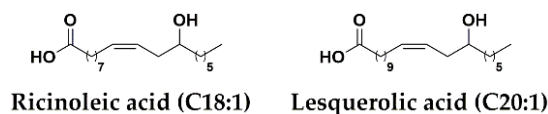


**Figure 1.4.** Ricinoleic and lesquerolic acid chemical structure.

On the other hand, most of the oils do not have hydroxyl groups in its natural form and need chemical transformations to create hydroxyl groups in the of fatty acid chains backbone. Epoxidation and subsequent epoxide ring-opening, ozonolysis, hydroformylation, thiol-ene coupling, transesterification and transamidation are the most studied chemical synthetic pathways for the obtention of vegetable oil-based polyols. **Figure 1.5** illustrates the possible routes for the synthesis of polyols based on vegetable oils.

Among the potential synthetic routes for the development of oleochemical polyols, the epoxidation/ring-opening is the most studied one.<sup>51</sup> This process consists of two main steps. First, the transformation of the unsaturations present in fatty acid chains into oxirane rings, and subsequently the formation of polyols through the epoxide ring-opening (**Figure 1.5-a**). The last step is a key factor in the polyol production since the type of ring-opening agent allows the optimization of polyol parameters, such as amount of O–H functionalities, availability of functional group, structure, etc.<sup>38,52,53</sup> Despite these parameters can be controlled, the polyols obtained through epoxidation have lower reactivity with isocyanates due to the formation of secondary O–H groups. This limiting factor has boosted the development of new processes to produce vegetable oil-based polyols.

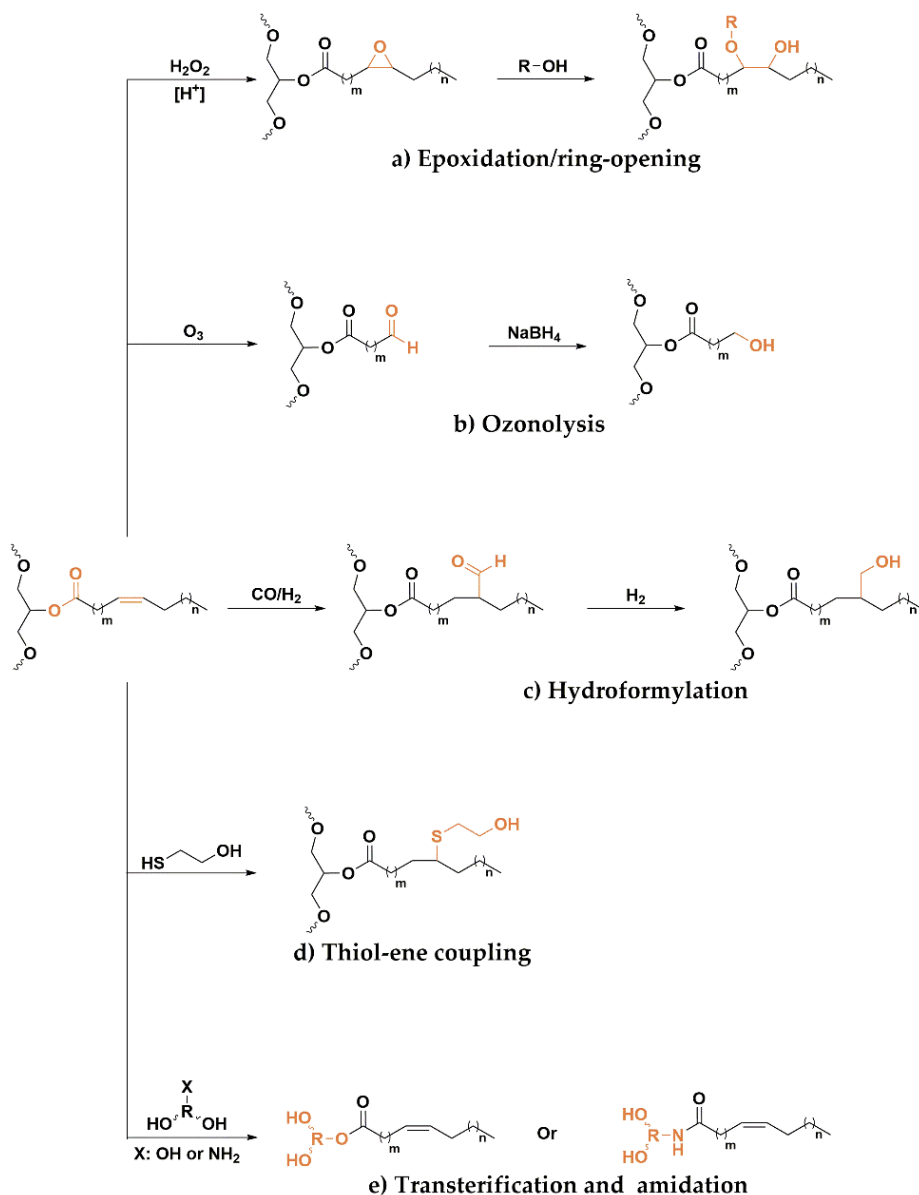


**Figure 1.5.** Main synthetic routes to form polyols from vegetable-oils.

Among the potential synthetic routes for the development of oleochemical polyols, the epoxidation/ring-opening is the most studied one.<sup>51</sup> This process consists of two main steps. First, the transformation of the unsaturations present in fatty acid chains into oxirane rings, and subsequently the formation of polyols through the epoxide

ring-opening (**Figure 1.5-a**). The last step is a key factor in the polyol production since the type of ring-opening agent allows the optimization of polyol parameters, such as amount of O–H functionalities, availability of functional group, structure, etc.<sup>38,52,53</sup> Despite these parameters can be controlled, the polyols obtained through epoxidation have lower reactivity with isocyanates due to the formation of secondary O–H groups. This limiting factor has boosted the development of new processes to produce vegetable oil-based polyols.

Ozonolysis is an alternative to the route that renders polyols with terminal primary hydroxyl groups after reduction of the formed aldehyde.<sup>54,55</sup> This synthetic route allows the introduction of primary hydroxyl groups in fatty acid chains through the cleavage of the carbon-carbon double bond. As in the case of the epoxidation process, the development of polyols is composed by two steps. First, the double bond oxidation in the presence of ozone leads the formation of unstable ozonide ring, which subsequently decomposes into an aldehyde. Afterward, the latter is reduced by hydrogenation, achieving polyols with hydroxyl primary groups (**Figure 1.5-b**). Despite reaching higher reactivity, this synthetic route has several drawbacks, such as limited O–H groups, the extreme temperature and pressure required for the process, and the use of toxic solvents.<sup>56</sup> Hence, the application of the ozonolysis mechanism is limited by process conditions.

Hydroformylation is another alternative that permits the synthesis of primary hydroxyl polyols with primary hydroxyl functionalities distributed along the fatty acid chain. In this approach, initially the reduction of the carbon-carbon double bond using syngas (CO/H<sub>2</sub>) forms an aldehyde group, which is immediately reduced to the corresponding alcohol (**Figure 1.5-c**).<sup>57</sup> Notwithstanding achieving primary functional groups, but the toxicity and flammability of the reactive gas mixture, as well as the cost of the catalyst limit the use and commercialization of polyols produced through hydroformylation process.

The last chemical process for the modification of the unsaturations present in fatty acid chains is the thiol-ene coupling.<sup>58</sup> This synthetic pathway produces polyols with primary hydroxyl groups in only one step, via the addition of the thiol (S–H) group

of a thioalcohol to the carbon-carbon double bond (**Figure 1.5-d**). It should also be emphasised the high activity of the reaction at mild reaction conditions and the versatility of the thiol-ene click reaction, since many multifunctional polyols have been recently reported.<sup>59-61</sup>

Although the modification of fatty acid chains has been focused on the carbon-carbon double bond, hydroxyl groups could also be introduced through the ester group. There are two main reaction pathways: (1) transesterification and (2) amidation process (**Figure 1.5-e**). The main difference between these two synthetic routes is in the nucleophilic reagent employed. In the transesterification, the nucleophile is a multifunctional alcohol, while in the amidation amines are used for the development of polyol-amides.<sup>62,63</sup> The unreacted fatty acid chains attached to the polyol are considered the major limiting factor of these processes, resulting in poor thermal and mechanical properties compared with petrochemical PUs.<sup>42</sup>

Although most efforts to increase the diversity of bio-based PUs, the main focus has been on the synthesis of vegetable oil-based polyols. Few research groups have explored the synthesis of isocyanates from triglycerides or derivatives. Multiisocyanates have been developed via the chemical modification of double bonds, allylic positions, acid groups presented in fatty acids, etc.<sup>8,29</sup> Even, Henkel Corporation and General Mills achieved the commercialization of a fatty acid-based diisocyanate.<sup>8</sup>

### 1.1.3 Non-isocyanate polyurethanes

The use of vegetable oil-based polyols and polyisocyanates leads to the obtention of PUs with at least a bio-based content of 60-70% in weight, and it even allows the direct use of existing industrial technologies and installations. Nevertheless, a completely bio-based polymer does not mean that it is safe, either because the precursors used are highly toxic, the synthesis route is hazardous, etc.<sup>64</sup> In particular, this is the major drawback of PU chemistry. Even if they are of biomass-origin, isocyanates are still as toxic as their fossil counterparts and, are also produced using the lethal phosgene.

Hence, the next generation of environmentally friendly PUs must address also these aspects. Among the arising strategies, several synthetic routes have been developed to avoid the application of extremely toxic gaseous phosgene.<sup>65</sup> Even if some of these alternatives achieve the synthesis of isocyanates in a safer manner, the toxicity related to this functional group is still present. For this reason, the scientific community has focused its efforts on the replacement of isocyanates as chemical reagents developing new chemical pathways for polyurethanes synthesis by non-isocyanate routes. The PUs obtained via these processes are named non-isocyanate polyurethanes (NIPUs), and the interest in them has only grown in the last few decades.<sup>66-69</sup>

Four main routes are known for the synthesis of non-isocyanate polyurethanes (NIPUs): (1) polycondensation, (2) rearrangements, (3) ring-opening and (4) polyaddition (**Figure 1.6**).<sup>70-75</sup> Although in the three first synthetic pathways the synthesis of NIPUs is obtained without using isocyanates directly, the employment of toxic substances is necessary for the obtention of the monomers, which goes against the Green Chemistry principles. The polycondensation mechanism allows NIPUs production through different reactions. However, the use of phosgene or derivatives is necessary for the synthesis of precursors. Although, some of the precursors, such as carbamates, can be synthesized avoiding the use of phosgene via the reaction between a carbonate and an amine, the need to remove the side products formed during the reaction (low molecular alcohols and/or acids) to shift the equilibrium, together with the high temperatures and long reaction time have restricted the extension of polycondensation for industrialization.<sup>19,76,77</sup> In the synthesis of NIPUs by rearrangement the employment of harmful reagents, such as acyl azides, carboxamides and hydroxyformic acids becomes this route less preferable.<sup>19,76,77</sup> Furthermore, the viability of a more secure route in the ring opening of cyclic carbamates and aziridines is affected by the use of phosgene in cyclic carbamates synthesis and the toxicity of aziridines.<sup>19,76,77</sup>

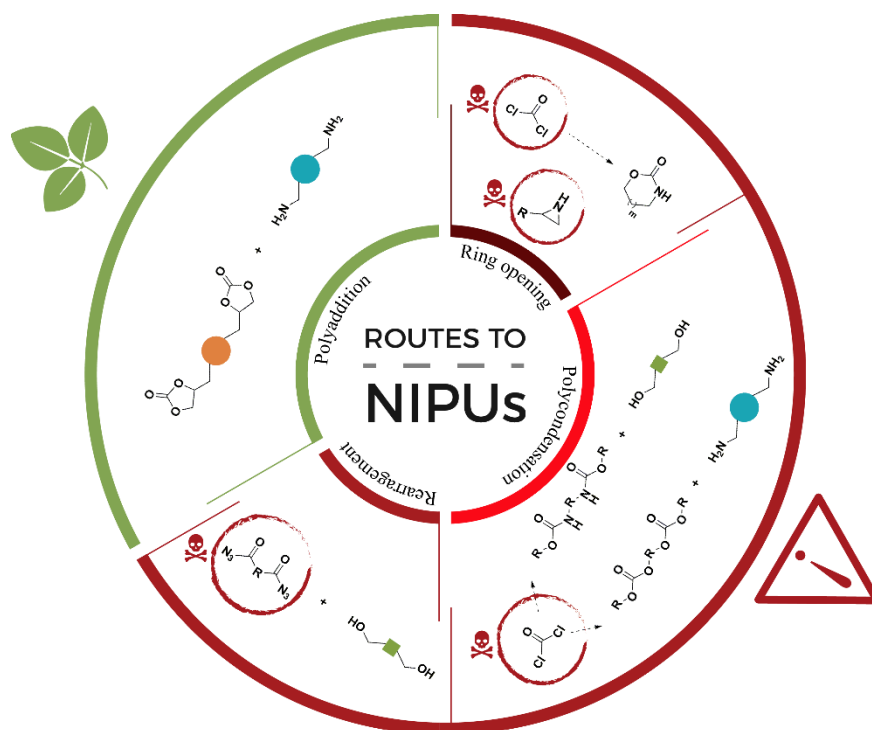
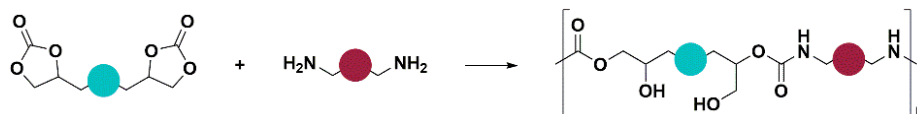


**Figure 1.6.** Main routes known for the synthesis of non-isocyanate polyurethanes.

In this way, the polyaddition reaction between cyclic carbonates and amines has gained much attention from both academic and industrial research.<sup>78,79</sup> The growing interest is not only related to the ability to avoid toxic precursors, but to the various functional benefits compared with the previously mentioned non-isocyanate routes and even traditional PUs.<sup>19,64,65,80,81</sup> Unlike polycondensation or ring-opening, the reactivity between cyclic carbonates and amines allows the polymerization at moderate temperatures and without a catalyst. Furthermore, the polyaddition involves the ring-opening of a cyclic carbonate with an amine, which leads to polymers named polyhydroxyurethanes (PHU) due to the presence of primary or secondary hydroxyl groups located at the  $\beta$ -carbon adjacent to the urethane group (**Scheme 1.3**). The formation of this functional group results in a new range of polyurethanes with different properties. In fact, the dangling hydroxyl groups contribute to intra- and intermolecular hydrogen bonding with the urethane carbonyl group, enhancing the chemical resistance to organic solvents compared to traditional



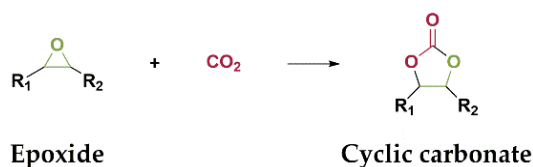
PUs. In addition, it brings the possibility of further functionalization of the obtained polymers.<sup>82</sup>



**Scheme 1.3.** Synthesis of non-isocyanate polyurethanes via polyaddition of bis(cyclic carbonate) to diamine.

Nevertheless, the great advantage is not only in the limited or null toxicity of cyclic carbonates and the novel properties related to the formed polyhydroxyurethane structure. Sustainability is the major potential of the polyaddition reaction. In fact, this reaction process enables the use of biomass sources and a greenhouse gas, namely carbon dioxide (CO<sub>2</sub>), as feedstocks to produce cyclic carbonates. Although several routes are used to produce cyclic carbonates, their industrial production is based on the cycloaddition reaction between CO<sub>2</sub> and oxirane rings (**Scheme 1.4**).<sup>83</sup> As is well known, climate change is related to the increase in CO<sub>2</sub> levels in the atmosphere, which have been rising since the industrial revolution due to the combustion of carbon sources. Therefore, the utilization of this greenhouse gas as chemical feedstock helps reducing its environmental impact.<sup>84</sup> As previously mentioned, one of the possibilities is to use it for the cycloaddition reaction between CO<sub>2</sub> and epoxides, becoming this route one of the most attractive alternatives for the reduction of CO<sub>2</sub> emissions and the achievement of a circular carbon economy.<sup>85,86</sup> Additionally, a wide range of biodegradable, renewable and sustainable resources can be converted into the carbonated bio-based precursors necessary for this route from the corresponding epoxide.<sup>19,77,87,88</sup> As described before for bio-based polyols, the numerous advantages related to vegetable oils structure have made triglycerides a reliable platform for the development of non-isocyanate polyurethanes. However, when manufacturing chemicals, along with the feasibility of the chemical process, the cost of the raw material must be taken into account. In the case of rapeseed, linsed and soybean oil, considered as the major oleo-based feedstocks the price did not exceed United States Dollar (USD) 1000/ton, with a price of USD 900/ton, USD 880/ton and USD 750/ton,

respectively. Moreover, the simple production of epoxidized oils through the oxidation of double bonds, together with the usability of this bio-based product, have resulted in the industrialization of the process.<sup>89</sup> In fact, the global epoxidized soybean oil market is expected to reach USD 691.7 million in 2026 at a compound annual growth rate of 10.7% during 2016-2026.<sup>90</sup> Therefore, soybean oil (and epoxidized analogue) has economic advantages over other vegetable oils. This opens the door for the production of vegetable oil-based NIPUs via two main step process. First, the CO<sub>2</sub> cycloaddition to oxirane ring to produce five-membered cyclic carbonates, and subsequently, the formation of NIPU networks reacting this carbonated oil with different amines.<sup>91</sup>



**Scheme 1.4.** General cycloaddition reaction of CO<sub>2</sub> to an epoxide.

## 1.2 Carbonated vegetable oil synthesis: Catalytic systems for the effective fixation of CO<sub>2</sub> into epoxidized vegetable oils and derivatives.

The cycloaddition of CO<sub>2</sub> to epoxidized vegetable oils was reported first by Tamami et al. two decades ago.<sup>91</sup> Due to the significant potential of carbonated oils in different fields, this bio-based material has gained much attention. In fact, the possibility of producing it from a greenhouse gas further increased the interest in this product. However, owing to the low activity of CO<sub>2</sub> and the high steric hindrance of oils structure, effective catalytic systems are necessary in order to obtain the carbonated oil.<sup>92,93</sup> Thereby, to solve these issues, much effort and intensive research have been devoted to the development of homogeneous and heterogeneous catalytic systems to circumvent both the low reactivity of the CO<sub>2</sub> molecule and the steric hindrance of the epoxidized vegetable oil and its derivatives.

This section is intended as a journey through the employed catalytic systems up to today aimed to improve the conversion and selectivity to the desired bio-based carbonated products of CO<sub>2</sub> chemical fixation by its cycloaddition to epoxidized vegetable oils or derivatives.

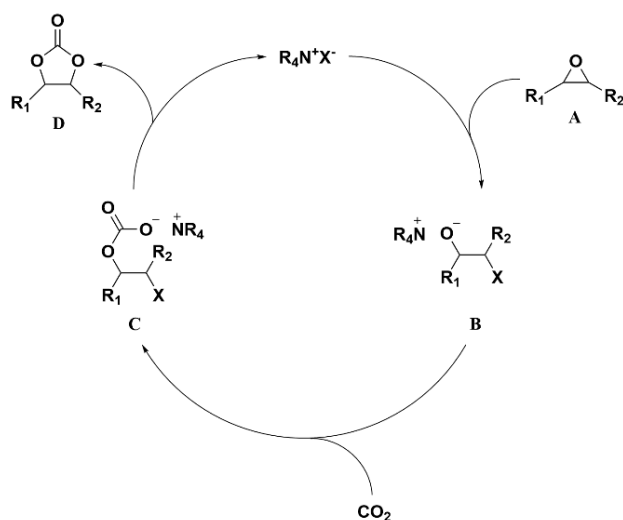
### 1.2.1 Homogeneous catalytic systems

In a homogeneous catalytic system, the catalyst and the reactant are presented in the same phase. These systems are usually more efficient than heterogenous catalysts, achieving larger conversion and better selectivities at milder reaction conditions (lower temperature, lower catalyst loading and reduced reaction time).<sup>94</sup> Indeed, a wide variety of homogeneous catalytic systems with different compositions has been developed for the reaction of CO<sub>2</sub> with epoxidized vegetable oils or derivatives.

Ionic liquids as catalysts in CO<sub>2</sub> cycloaddition reaction

#### *a) Non-functionalized ionic liquids catalysts*

Organic salts and ionic liquids have gained much attention in catalysis (both as catalysts and as reaction solvents) due to their low toxicity, availability, and affordability. The ones used as homogeneous catalysts in the CO<sub>2</sub> cycloaddition reaction are typically organic halides acting as Lewis bases, e.g., ammonium or phosphonium salts. In **Scheme 1.5** is depicted the commonly accepted reaction mechanism for the CO<sub>2</sub> cycloaddition to an epoxide. First, an alkoxide intermediate (**B**) is formed by the oxirane (**A**) opening with a nucleophile species (e.g., halide). Then the alkoxide attacks the CO<sub>2</sub> molecule forming the corresponding alkyl carbonate compound (**C**). Finally, the alkyl carbonate undergoes an intramolecular ring-closure forming the cyclic carbonate (**D**). When these Lewis bases are employed as the only catalyst, the nucleophilic attack of the halide anion to epoxide becomes the rate-determining step.<sup>95-97</sup>



**Scheme 1.5.** General three-step mechanism for the cycloaddition to an epoxide catalyzed by a tetraalkylammonium ionic liquid.

In **Figure 1.7**, Non-functionalized ionic liquid catalyst used in CO<sub>2</sub> cycloaddition to epoxidized oleochemicals. are summarized selected non-functionalized ionic liquid-based catalysts employed in the cycloaddition of CO<sub>2</sub> to epoxidized oleochemicals collected from the scientific literature.

Among the different ionic liquids employed as catalysts for the cycloaddition of CO<sub>2</sub> to oleochemicals to yield the corresponding cyclic carbonates, tetra-n-butylammonium bromide ([TBA][Br], **1**) stands out as the most commonly used one. Tamami et al. reported the first catalytic synthesis of carbonated soybean oil employing the [TBA][Br] as a catalyst. Fully carbonated soybean oil was achieved after 70h reaction at atmospheric pressure at 110 °C.<sup>91</sup> In the last two decades, many studies followed pioneer Tamami's work using [TBA][Br] as the catalyst for the CO<sub>2</sub> cycloaddition to epoxides but modifying some reaction parameters e.g., temperature, reaction time, pressure, etc. For instance, Doll et al. performed the synthesis of carbonated soybean oil and carbonated methyl oleate under scCO<sub>2</sub> conditions.<sup>98</sup> The substantially increased CO<sub>2</sub> amount due to the employment of scCO<sub>2</sub>, reduced to one-third the reaction time compared with Tamami's work. Several works studied the influence of the nature of the halide anion of the tetrabutylammonium ionic liquid (**1**-

4) or even the employment of a hydroxyl group (5) as a nucleophile.<sup>96,99–102</sup> Despite the differences in reaction conditions and vegetable oil derivatives used, it was found that the optimum balance between highest activity and highest selectivity was achieved when bromide was used as the anion. The highest reactivity was due to a good balance of the bromide anion between nucleophilicity ( $F^- > Cl^- > Br^- > I^-$ ) and leaving group character ( $I^- > Br^- > Cl^- > F^-$ ). In this regard, Alves et al. attributed the highest catalytic activity showed by ionic liquids bearing a bromide anion compared to those bearing an iodine anion to the smaller bromide size favouring its diffusion towards internal epoxides in the linseed oil triglycerides.<sup>100</sup> Doll et al. also performed the reaction between  $CO_2$  and epoxidized soybean oil or epoxidized methyl oleate with a non-halide catalyst, such as tetrabutylammonium hydroxide ([TBA][OH], 5). While [TBA][Br] showed the total conversion of the epoxide substrate, the catalyst bearing the hydroxide anion (5) exhibited null activity. This fact reveals the key role of halide anion in the synthesis of carbonated oleochemicals.<sup>98</sup> Moreover, Zheng et al. tested [TBA][Br] catalytic system in the cycloaddition of  $CO_2$  to epoxidized cottonseed oil methyl esters to the corresponding cyclic carbonated compounds using a microwave irradiated continuous-flow recycle batch reactor. The effect of microwave irradiation compared with conventional heating on the reaction kinetics was studied by the authors in the temperature range of 100–120 °C and the pressure range of 2.5 bar to 6 bar. As could be expected, the authors found that the activation energy of the carbonation reaction was slightly lower when MW irradiation was used as a heating source, achieving slightly higher conversion at 120 °C, 6 bar, [TBA][Br] 4 wt.% and 950 rpm after 7h.<sup>103</sup> Apart from tetrabutylammonium-based ionic liquids, other ammonium-based ionic liquids were successfully tested as catalysts. dos Santos et al. carried out a selection of the most suitable ionic liquids to be employed as catalysts in the synthesis of oleochemical carbonates by quantitative structure-property relationship (QSPR) modelling and exploratory analysis.<sup>104</sup> This theoretical approach allowed the authors the selection of 122 potential available catalysts for the target reaction. The molecular targets via a virtual screening and the structure-property relationship analysis, led to the selection of cetyltrimethylammonium bromide ([CTMA][Br], 6) as the most promising one based on its well-balanced properties such as bulkiness, lipophilicity, and nucleophilic character. In addition, experimental

results confirmed QSPR analysis, achieving with 5 wt.% [CTMA][Br] high conversions ( $\geq 98\%$ ) using several epoxidized vegetable oils (rice, soybean and canola oil) as starting materials at 120 °C and 50 bar after 48h reaction. Langanke et al., tested tetraheptylammonium bromide ([THA][Br], **7**) as catalyst (5 mol%) in the synthesis of a series of carbonated methyl esters showing slightly higher yield than the benchmark catalyst [TBA][Br] (**1**) 99% *vs.* 96% after 24h reaction at 100 °C and 117 bar.<sup>96</sup>

Imidazolium-based ionic liquids have also been extensively explored as catalysts in the cycloaddition reaction of CO<sub>2</sub> to epoxidized vegetable oils and derivatives. This work was pioneered by Langanke et al. employing 1-*n*-tetradecyl-3-methylimidazolium bromide ([TDMeIm][Br], **8**) as catalyst in the cycloaddition of CO<sub>2</sub> to several oleo derivatives achieving a yield comparable to the one obtained with [TBA][Br] (**1**) 94% *vs.* 96% after 24h reaction at 100 °C and 117 bar.<sup>96</sup> Afterwards, Alves et al. tested 1-*n*-octyl-3-methylimidazolium halides (**9-11**) as catalysts in the cycloaddition reaction of CO<sub>2</sub> to epoxidized linseed oil (ELSO). Not surprisingly, also in this case, bromine stood out as the best-suited anion. Indeed, [OMeIm][Br] (**10**) reached the same conversion (30%) than benchmark catalyst [TBA][Br] (**1**) after 5h at 100 °C and 100 bar.<sup>100</sup> B. Schäffer and co-workers used 1-*n*-butyl-3-methylimidazolium chloride ([BMeIm][Cl], **12**) as a catalyst in the synthesis of carbonated fatty acid esters from epoxidized methyl linoleate.<sup>99</sup> However, in contrast to the work of J. Langanke and M. Alves, the catalytic activity of [BMeIm][Cl] (**12**) was found to be much lower than the benchmark catalysts [TBA][Br] (**1**) (25% *vs.* 68% yield). Phosphonium-based ionic liquids have also been tested as catalysts in the cycloaddition of CO<sub>2</sub> to epoxidized vegetable oils and their derivatives. Tenhumberg et al., studied the influence of the anion in the selected tetrabutylphosphonium-based ionic liquids ([TBP][X], where X is an halide = [Cl] (**13**), [Br] (**14**) or [I] (**15**)), as catalysts instead of the traditional [TBA][Br] (**1**) ionic liquid, in the cycloaddition reaction CO<sub>2</sub> to an epoxidized methyl oleate.<sup>105</sup> Concerning the halide anion influence, the authors found the same trend as previously observed for [TBA][X] (**1-4**), confirming that the ionic liquid formed with bromide as anion shows the best catalytic performance. Indeed, in the presence of the bromide anion, 49% of epoxide was converted with 94% of selectivity towards the desired product. On the other hand, the employment of

chloride and iodine anions returned lower conversions 39% and 35%, with a selectivity towards the target products of 99% and 71%, respectively. Moreover, [TBP][Br] (**14**) showed superior activity than the benchmark [TBA][Br] (**1**) ionic liquid in terms of conversion 49% *vs.* 39% and selectivity 94% *vs.* 82% towards the desired carbonated methyl ester. On the other hand, [TBP][Br] (**14**) and [TBA][Br] (**1**) were also tested as catalyst by Alves et al. for the synthesis of carbonated linseed oil (CLSO). In contrast to N. Tenhumberg work, phosphonium-based catalyst (**14**) exhibited similar epoxide conversion to those achieved by using [TBA][Br] (**1**) as catalyst 28% *vs.* 30%, but selectivity was not reported in this work.<sup>100</sup> Very few articles report the use of triphenylphosphonium-based ionic liquids as catalysts for the synthesis of carbonated oleochemicals by cycloaddition of CO<sub>2</sub> to the corresponding epoxidized compound. Peña Carrodeaguas et al. achieved the synthesis of carbonated methyl ester at relatively mild reaction conditions (70 °C, 10 bar, 24h, 5 mol%) using bis(triphenylphosphine)iminium chloride ([PPN][Cl] (**17**)) as catalyst.<sup>101</sup> In this work, both [TBA][Br] (**1**) and [PPN][Cl] (**17**) reached quantitative conversion in the synthesis of carbonated methyl oleate. However, while the use of [PPN][Cl] (**17**) provided high chemo-selectivity and stereocontrol towards *cis*-isomer (96:4), [TBA][Br] (**1**) significantly reduced this stereoselectivity (51:49). Therefore, the authors proved that the use of [PPN][Cl] (**17**) was beneficial to produce almost exclusively the *cis*-configured carbonated methyl oleate. Other ionic liquids composed by different cations (**18-23**) were scarcely investigated. Alves et al. tested triethylsulfonium iodide ([TES][I] (**18**)), 1-butyl-1-methylpyrrolidinium iodide ([BMPyr][I] (**19**)), 1-butylpyridinium ([BPy][I] (**20**)), 1-butyl-2,3,4,5,7,8,9,10-octahydropyrido[1,2-a][1,3]diazepin-1-ium bromide ([BDBU][Br] (**21**)) and 1-butyl-3,4,6,7,8,9-hexahydro-2H-pyrimido [1,2-a]pyrimidin-1-ium bromide ([BTBD][Br] (**22**)) as catalysts (1 mol%) in the cycloaddition reaction of CO<sub>2</sub> to ELSO oil at 100 °C and 100 bar for 5h.<sup>100</sup> [TES][I] (**18**), [BMPyr][I] (**19**) and [BPy][I] (**20**) ionic liquids were less efficient evidenced by the poor performance in terms on conversion to the CLSO, 0%, 19% and 12%, respectively. The authors attributed their poor performance to the poor solubility of these ionic liquids in the reaction media. However, [BDBU][Br] (**21**) and [BTBD][Br] (**22**) exhibited much higher activity achieving conversions of 28% and 36%, respectively, to the CLSO, improving the results achieved by the benchmark catalyst

[TBA][Br] (**1**) that was found to be 30% to the CLSO. Schäffner et al. employed 1-butyl-4-methyl pyridinium iodide ([BMePh][I], (**23**)) in the cycloaddition of CO<sub>2</sub> to epoxidized methyl linoleate at 100 °C, 100 bar for 17h. The catalytic activity resulted similar as the one of [TBA][Br] (**1**) in terms of conversion (65% *vs.* 69%, respectively) and selectivity towards target product >99% with both ionic liquids.<sup>99</sup>

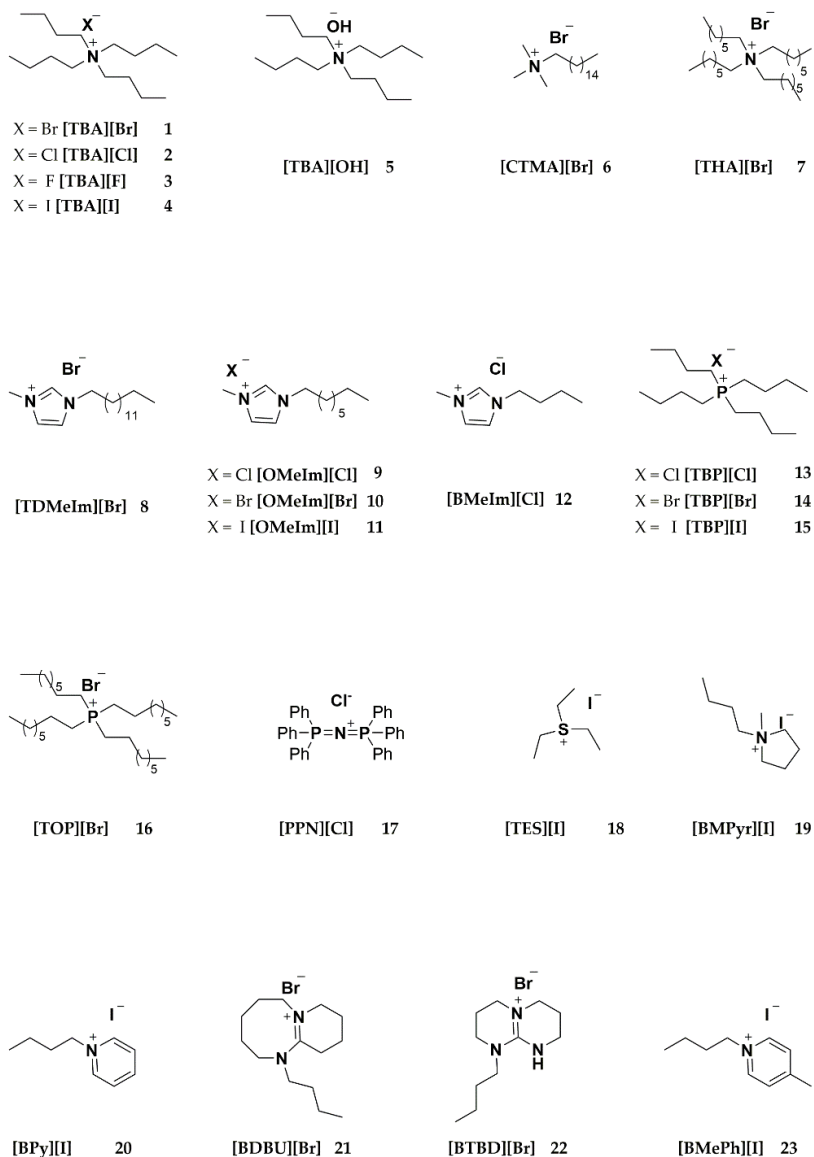


**Figure 1.7.** Non-functionalized ionic liquid catalyst used in CO<sub>2</sub> cycloaddition to epoxidized oleochemicals.



In **Table 1.1** are summarized the selected non-functionalized ionic liquids employed as catalysts, the reaction conditions, the conversion, and the selectivity to target products (when given) in the CO<sub>2</sub> cycloaddition to different vegetable oils or analogue molecules.

**Table 1.1.** Non-functionalized ionic liquid catalysts used in carbonated oleochemicals synthesis.

Catalyst	Epoxidized oleochemical	Reaction conditions				Conv. (%)	Select. (%) <sup>b</sup>	Ref.
		<i>T</i> (°C)	<i>P</i> (bar)	<i>Time</i> (h)	<i>Cat</i> (mol%)			
1	Soybean oil	110	1	70	5	100	-	91
	Methyl oleate	100	>103	20	5	100	-	98
	Soybean oil	100	>103	40	5	100	-	98
	Methyl linoleate	100	100	17	5 <sup>a</sup>	69	99	99
	Methyl oleate	100	117	24	5	97	>99	96
	Linseed oil	100	100	5	1	30	-	100
	Methyl oleate	100	50	16	2	39	82	105
	Methyl oleate	70	10	24	5	>99	>99	101
	Methyl oleate	100	5	24	5	83	87	102
	Cottonseed oil methyl ester	120	6	7	4 <sup>a</sup>	52	-	103
2	Methyl oleate	100	117	24	5	21	95	96
	Linseed oil	100	100	5	1	17	-	100
	Methyl oleate	70	10	24	5	6	99	101
	Methyl oleate	100	5	24	5	44	99	102
3	Methyl oleate	100	117	24	5	62	0	96
4	Methyl oleate	100	117	24	5	80	92	96
	Methyl linoleate	100	100	17	5 <sup>a</sup>	75	98	99
	Methyl oleate	100	5	24	5	70	59	102
	Linseed oil	100	100	5	1	26	-	100
5	Methyl oleate	100	>103	20	5	6	-	98
6	Rice bran oil					98	-	
	Canola oil	120	50	48	5 <sup>a</sup>	>99	-	104
	Soybean oil					>99	-	

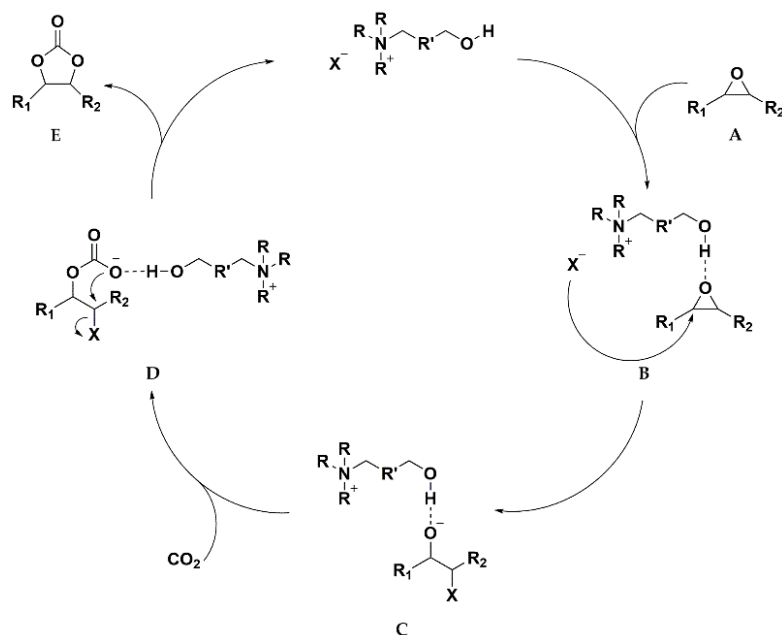
7	Methyl oleate	100	117	24	5	99	99	96
8	Methyl oleate	100	117	24	5	97	97	96
9	Linseed oil	100	100	5	1	20	-	100
10	Linseed oil	100	100	5	1	30	-	100
11	Linseed oil	100	100	5	1	25	-	100
12	Methyl linoleate	100	100	17	5 <sup>a</sup>	26	99	99
	Linseed oil	100	100	5	1	19	-	100
13	Methyl oleate	100	50	16	2	38	99	106
	Methyl oleate	100	50	16	2	39	99	105
	Linseed oil	100	100	5	1	28	-	100
14	Methyl oleate	100	50	16	2	38	99	106
	Methyl oleate	100	50	16	2	49	94	105
	Linseed oil	100	100	5	1	21	-	100
15	Methyl oleate	100	50	16	2	35	72	106
	Methyl oleate	100	50	16	2	35	71	105
17	Methyl oleate	70	10	24	5	53	99	101
18	Linseed oil	100	100	5	1	-	-	100
19	Linseed oil	100	100	5	1	19	-	100
20	Linseed oil	100	100	5	1	12	-	100
21	Linseed oil	100	100	5	1	28	-	100
22	Linseed oil	100	100	5	1	36	-	100
23	Methyl linoleate	100	100	17	5 <sup>a</sup>	65	>99	99

<sup>a</sup>catalyst in wt.%; <sup>b</sup>selectivity to the cyclic carbonate product.

### b) Functionalized (task-specific) ionic liquids

Functionalized ionic liquid refers to an ionic liquid that possesses a functional group or extra functionality, generally on the cation. These ionic liquids are known as task-specific ionic liquids, and their functionalization helps to enhance the performance of the ionic liquid in a specific application e.g., as catalyst.<sup>107,108</sup> In the cycloaddition reaction of CO<sub>2</sub> to low molecular weight epoxides, such as propylene oxide, butylene oxide, etc., it is found that the use of task-specific ionic liquids bearing an -OH, -COOH or -NH<sub>2</sub> functionalities (hydrogen donors) able to form hydrogen bonds enhance the catalytic performance of the ionic liquid.<sup>109-112</sup> Indeed, reported works

suggest that these functionalities able to donate hydrogen increased the rate of the epoxide ring opening (rate-determining step on the catalytic cycle) due to a synergetic effect between anion and hydrogen bond donor. As depicted in **Scheme 1.6**, the hydrogen donor moiety is able to polarize the C–O bond in the epoxide ring (**A**), making the carbon atom more electrophilic, thus facilitating the attack of the anion. It results in an easier epoxide ring-opening (**B**), yielding the corresponding alkoxide (**C**). Then the alkoxide attacks the CO<sub>2</sub> molecule forming the corresponding alkyl carbonate compound (**D**). Finally, the alkyl carbonate undergoes an intramolecular ring-closure forming the cyclic carbonate (**E**). In view of the promising results obtained by using task-specific ionic liquids in the CO<sub>2</sub> cycloaddition to low molecular weight epoxides, they were tested in the more challenging internal epoxides present in epoxidized vegetable oils and derivatives.



**Scheme 1.6.** General mechanism of CO<sub>2</sub> cycloaddition to an epoxide catalyzed by a tetraalkylammonium halide salt with hydroxyl terminal group.

In **Figure 1.8** and **Table 1.2** are summarized selected task-specific ionic liquid-based catalysts ionic liquids employed as catalysts, the reaction conditions, the conversion,

and the selectivity to target products (when given) in the CO<sub>2</sub> cycloaddition to different vegetable oils or analogue molecules.

**Table 1.2.** Task-specific (functionalized) ionic liquid catalysts used in carbonated oleochemicals synthesis.

Catalyst	Epoxidized oleochemical	Reaction conditions				Conv. (%)	Select. (%) <sup>a</sup>	Ref.
		<i>T</i> (°C)	<i>P</i> (bar)	<i>t</i> (h)	<i>Cat</i> (mol%)			
<b>24</b>	Methyl oleate	100	50	16	2	5	0	113
<b>25</b>	Methyl oleate	100	50	16	2	9	99	113
<b>26</b>	Methyl oleate	100	50	16	2	14	80	113
<b>27</b>	Methyl oleate	100	50	16	2	10	>99	113
<b>28</b>	Methyl oleate	100	50	16	2	22	97	113
<b>29</b>	Methyl oleate	100	50	16	2	24	98	113
<b>30</b>	Methyl oleate	100	25	16	5	99	98	113
	Sunflower oil					99	80	
	Soybean oil	80	25	24	5	97	77	
	Linseed oil					99	88	
<b>34</b>	Sunflower oil					97	98	114
	Halzenut oil					98	93	
	Olive oil					98	98	
	Pistachio oil	100	20	16	1	99	94	
	Almond oil					98	97	
	Rapeseed oil					99	95	
	Pumpkin oil					97	95	

<sup>a</sup>Selectivity to the cyclic carbonate product.

Büttner et al. tested several functionalized phosphonium-based ionic liquids (**24-30**) in the cycloaddition of CO<sub>2</sub> to epoxidized oleochemicals.<sup>113</sup> In this work, triphenylphosphonium- (**24-26**) and tributylphosphonium-based (**27-29**) ionic liquids lead to low conversion (5-24%) of methyl oleate epoxide in its cycloaddition with CO<sub>2</sub> to form in the corresponding carbonated methyl oleate at 100 °C, 50 bar for 16h.

Despite the low activity observed, the same authors prepared a series of phosphonium ionic liquids derived from phenol. Among them, 2-hydroxyphenyldiphenylpropyl phosphonium bromide ([HPhDPhP][Br] (**30**)) exhibited high potential in the synthesis of carbonated methyl oleate from the corresponding epoxide yielding good results in terms of conversion (99%) and selectivity (98%) at 100 °C and 25 bar after 16h. The authors attributed the catalytic activity enhancement to different factors, the bromide anion, the presence of an -OH group and its position (*ortho*) in the aromatic ring. In addition, due to its potential, the same ionic liquid (**30**) was tested as well in the synthesis of other three carbonated oils (high oleic sunflower oil, soybean oil, and linseed oil) with excellent reaction yields (isolated) up to 88% after 24h reaction at 80 °C and 25 bar. Martinez et al. synthesized waste oil-derived cyclic carbonates using as catalyst imidazolium-based task-specific ionic liquid bearing a phenolic ring in position 5 and [Br] and [I] as anions (**31-34**), achieving excellent conversion ( $\geq 97\%$ ) and selectivity ( $\geq 93\%$ ) to the target products after 16h at 100 °C and 20 bar with catalyst **34**.<sup>114</sup> The excellent catalytic performance of catalysts **34** was attributed to the high solubility of the catalyst boosted with the presence of butyl chains on nitrogen 1 instead of a phenyl ring compared to catalyst **33**. Furthermore, unlike previous works, the catalyst containing the iodine anion (**34**) showed higher activity than the analogue one containing the bromide anion (**32**), achieving at 100 °C and 20 bar 97% and 75% conversion, respectively, after 16h of reaction with 1 mol% of catalyst. These authors performed a recyclability test with task-specific ionic liquids, being one of the scarce examples of recyclability of the catalysts in the cycloaddition of CO<sub>2</sub> to vegetable oils epoxides. The ionic liquid **34** was reused for at least 5 cycles at different reaction times (2h, 5h and 16h) at 100 °C and 20 bar with 1 mol% of catalyst without significant loss of its activity. In addition, the catalyst can be recovered (up to 100%) from the reaction media by simple precipitation with diethyl ether.

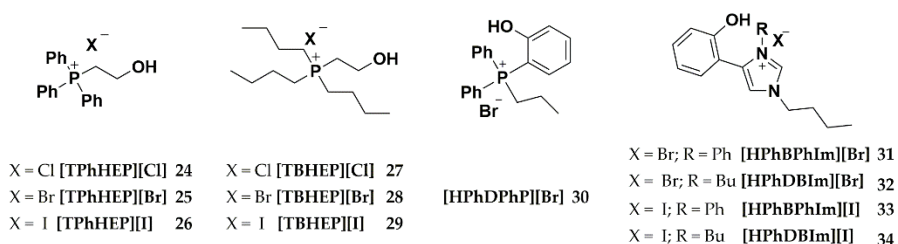


**Figure 1.8.** Task-specific ionic liquid catalyst used in CO<sub>2</sub> cycloaddition to epoxidized oleochemicals.

*c) Ionic liquid/Lewis acidic co-catalyst binary catalytic systems*

As previously mentioned, nucleophilic ionic liquids such as [TBA][Br] (**1**) are often used as catalysts in the synthesis of cyclic carbonated oils and derivatives from the cycloaddition of CO<sub>2</sub> to the corresponding epoxidized compounds. However, the steric hindrance of the internal epoxide rings in the vegetable oil structure makes difficult the epoxide ring-opening (generally the rate-determining step), hampering the overall reaction rate as well as the selectivity to the target products. Therefore, high temperatures (70-120 °C) and pressures (5-117 bar), as well as long reaction times (>20h) are generally required to achieve reasonable conversions. These harsh conditions can affect both the selectivity to the desired products and their industrial implementation. In this regard, several research groups tried to improve the catalytic performance in terms of conversion and selectivity towards desired products by adding a Lewis acid metal complex as co-catalysts. The CO<sub>2</sub> cycloaddition reaction mechanism of the catalytic systems formed by these catalytic systems is similar to that proposed for the task-specific ionic liquids (**Scheme 1.6**). In this case, the role of the functional group (epoxide ring-opening facilitation) is played by the metal complex that, due to its Lewis acid character, interacts with the oxygen atom making the adjacent carbon more electron deficient, and prompt for a nucleophilic attack by the anion of the employed ionic liquid.<sup>115</sup> These catalytic systems formed by an ionic liquid, mainly [TBA][Br] (**1**), and a Lewis acidic metal complex have been employed by several authors. Li et al. used a catalytic system formed by 1 equivalent (3 mol%) of [TBA][Br] (**1**) and 0.3 equivalents (1 mol%) of a Lewis acid co-catalysts to improve the catalytic performance in the synthesis of carbonated soybean oil by cycloaddition

of CO<sub>2</sub> to the corresponding epoxidized soybean oil at 120 °C and 10 bar in 20h.<sup>116</sup> The addition of SnCl<sub>4</sub>·5H<sub>2</sub>O (0.3 equiv.) as co-catalysts improved the catalytic performance of the employed ionic liquid (1) (1 equiv.) by around 25%, increasing the conversion from 71% to 89%. Under the optimized reaction conditions (140 °C and 15 bar), the catalytic system afforded the full conversion of epoxidized soybean oil after 30h. The same catalytic system but in different proportion, [TBA][Br] (1) 7.8 mol% (3.5 wt.%) and SnCl<sub>4</sub>·5H<sub>2</sub>O 9 mol% (5 wt.%), was tested by Schäffner et al. in the obtention of carbonated methyl linoleate via the CO<sub>2</sub> cycloaddition to the corresponding epoxide at 100 °C and 100 bar, achieving a conversion and selectivity of 64 % and 82 %, respectively after 17h.<sup>99</sup> Nevertheless, in this case, the [TBA][Br] (1) ionic liquid without the presence of the co-catalyst exhibited higher conversion (69% *vs.* 64%) and better selectivity (>99% *vs.* 82%) towards the desired carbonated product than the binary catalytic system. The authors justified the lower selectivity found to the strong Lewis acid character of SnCl<sub>4</sub>·5H<sub>2</sub>O co-catalyst, which could promote the hydrolysis of the epoxide methyl ester to the corresponding diol, thus decreasing the selectivity. Langanke et al. promoted the reaction between CO<sub>2</sub> and epoxidized methyl oleate using a catalytic system formed by 1 equivalent of [TBA][Br] (1) ionic liquid (2 mol%) and 1 equivalent of THA-Cr-Si-POM (tetraheptylammonium silicotungstates containing Cr (III), ((*n*-C<sub>7</sub>H<sub>15</sub>)<sub>4</sub>-N)<sub>5</sub>[CrSiW<sub>11</sub>O<sub>39</sub>]) (2 mol%).<sup>96</sup> After 6h at 100 °C and 125 bar the desired carbonate product was formed with high epoxide conversion (95%) and selectivity (98%). This binary catalytic system substantially improved the performance of [TBA][Br] (1) alone 11% *vs.* 95% and 81% *vs.* 98% in terms of conversion and selectivity, respectively. However, using epoxidized soybean oil as starting material, the catalytic activity was reduced in terms of conversion (41 % *vs.* 47%) and selectivity (60% *vs.* 73%) with respect to [TBA][Br] (1) alone, even when increasing the reaction time to 24h. The inferior catalytic performance achieved by the binary system compared to the [TBA][Br] (1) when using an epoxidized soybean oil as starting material, was attributed to the higher viscosity of the obtained carbonated products compared to the carbonated methyl oleate and the strong Lewis acidity character of the co-catalyst, thus hampering the reaction rate and favouring the hydrolysis of the epoxide rings, decreasing both the conversion and the selectivity of the studied reaction. Schäffner et al. tested a binary catalytic system formed by

[TBA][Br] (**1**) ionic liquid (3.5 wt.%) and Al-Salen complex (5 wt.%) in the synthesis of carbonated methyl linoleate from CO<sub>2</sub> and the corresponding epoxide at 100 °C and 100 bar.<sup>99</sup> The catalytic performance of the binary catalytic system was found to be superior to the [TBA][Br] (**1**) ionic liquid as the sole catalyst in terms of yield (75% *vs.* 65%) after 17h reaction. Farhadian et al. employed a catalytic system formed by 1 equivalent [TBA][Br] (**1**) ionic liquid (4 mol%) and 1 equivalent of Mn-based porphyrins as Lewis acid co-catalyst (4 mol%) to achieve the synthesis of fully carbonated sunflower oil (CSFO) (yield >99 %) from the cycloaddition of CO<sub>2</sub> to epoxidized sunflower oil (ESFO) after 30h at mild reaction conditions, 100 °C and atmospheric pressure.<sup>117</sup> A binary system formed with [TBA][Br] (**1**) ionic liquid (17 wt. %) and several Metal-Organic-Frameworks (MOFs) (10 wt.%) was tested by Cai et al. in the preparation of carbonated *o*-acetyl methyl ricinoleate from the cycloaddition of CO<sub>2</sub> to the corresponding epoxidized precursor.<sup>118</sup> Among the different binary catalytic systems tested by the authors, the one formed by [TBA][Br] (**1**) ionic liquid and UiO-66-NH<sub>2</sub> MOF showed the best catalytic performance achieving 94% conversion of the epoxidized precursor after 12h at 120 °C and 30 bar. Tenhumberg et al., tested several binary catalytic systems formed by a combination of 1 equivalent of [TBP][Br] (**14**) ionic liquid (2 mol%) with 1 equivalent of different metals as Al, Ca, Mo and W (2 mol%) in the synthesis of carbonated methyl oleate from CO<sub>2</sub> and the corresponding epoxide at 100 °C and 50 bar for 16h.<sup>105</sup> In all cases, the yield to the desired cyclic carbonates was considerably increased with conversions up to 99% by adding 2 mol% of a metal transition complex as co-catalyst compared to the conversion (49%) obtained using [TBP][Br] (**14**) ionic liquid as the sole catalyst, while the selectivity towards the desired carbonated product was comparable (93 % *vs.* 94 %). The best catalytic performance was achieved with the binary system containing MoO<sub>3</sub> as Lewis acidic co-catalyst, doubling the yield of the carbonated product compared to the use of the [TBP][Br] (**14**) ionic liquid as the only catalyst (84% *vs.* 46%). Under the optimized reaction conditions (100 °C and 50 bar), the catalytic system composed of 1 equivalent of [TBP][Br] (**14**) ionic liquid and 0.125 equivalents of MoO<sub>3</sub> afforded the conversion of four epoxidized vegetable oils into the corresponding carbonates with both conversions and selectivity towards the carbonated compounds higher than 99% after 20h reaction. The same authors tested



binary catalytic systems formed by [TBP][Br] (**14**) or [TOP][Br] (**16**) as the ionic liquids and different iron salts  $\text{FeF}_3$ ,  $\text{FeCl}_3$ ,  $\text{FeCl}_3 \cdot 6\text{H}_2\text{O}$ ,  $\text{FeBr}_3$ ,  $\text{FeBr}_2$ ,  $\text{Fe}(\text{acac})_3$ ,  $\text{Fe}(\text{OTf})_3$ ,  $\text{Fe}(\text{OAc})_2$ ,  $\text{Fe}(\text{stearate})_3$ ,  $\text{FeSO}_4 \cdot 7\text{H}_2\text{O}$  and  $\text{Fe}(\text{citrate})_3 \cdot (\text{aq})$  as the Lewis acidic co-catalyst in the synthesis of carbonated methyl oleate from cycloaddition of  $\text{CO}_2$  to epoxidized methyl oleate at  $100\text{ }^\circ\text{C}$  and 50 bar lasting for 16h.<sup>106</sup> Among the studied binary catalytic systems, the most efficient at the studied conditions was found to be the one formed by 1 equivalent of [TOP][Br] ionic liquid (2 mol%) and 0.125 equivalents of  $\text{FeCl}_3$  (0.25 mol%) as Lewis acid achieving yields of the target product as high as 95%. The presence of an iron-based Lewis acid as co-catalysts enhanced 100 % the conversion compared to the employment of [TOP][Br] (**16**) (>99% *vs.* 49%). The same catalytic system was tested in the optimized reaction conditions ( $100\text{ }^\circ\text{C}$  and 50 bar), in the synthesis of four carbonated oil by  $\text{CO}_2$  cycloaddition to the corresponding epoxidized oils exhibiting excellent yields ranging from 88% to 94% after 24h reaction. Peña Carrodeaguas et al. developed a catalytic system formed by 1 equivalent [PPN][Cl] (**25**) ionic liquid (5 mol%) and 0.1 equivalents of Aluminium(III)aminotriphenolate complex (0.5 mol%) as Lewis acidic co-catalyst in the synthesis of carbonated fatty acids methyl esters from  $\text{CO}_2$  cycloaddition to their corresponding epoxidized compounds.<sup>101</sup> The binary system, [PPN][Cl] (**17**) and Al-complex, afforded the production of carbonated methyl esters with excellent yields (up to >99%) at relatively mild reaction conditions,  $70\text{ }^\circ\text{C}$  and 10 bar, after 24h. The presence of Lewis acid as co-catalyst enhanced the conversion in a range of ca. 18–150% compared to the catalytic system without metal complex, depending on the epoxidized fatty acid employed as starting material.

In **Table 1.3** are summarized selected ionic liquid/Lewis acidic co-catalysts binary catalytic systems employed in the literature, the reaction conditions, the conversion, and the selectivity to target products (when given) in the  $\text{CO}_2$  cycloaddition to different vegetable oils or analogue molecules.

**Table 1.3.** Ionic liquid/Lewis acidic co-catalyst binary catalytic systems used in carbonated oleochemicals synthesis.

Catalyst (equiv.)	Co-catalyst (equiv.)	Epoxidized oleochemical	Reaction conditions				Conv. (%)	Select. (%) <sup>b</sup>	Ref.
			<i>T</i> (°C)	<i>P</i> (bar)	<i>t</i> (h)	<i>Cat</i> mol%			
1 (1)	SnCl <sub>4</sub> ·5H <sub>2</sub> O (0.3)	Soybean oil	140	15	30	3	98.6	-	116
1 (1)	SnCl <sub>4</sub> ·5H <sub>2</sub> O (1.4)	Methyl linoleate	100	100	17	3.5 <sup>a</sup>	64	82	99
1 (1)	<i>(n</i> -C <sub>7</sub> H <sub>15</sub> ) <sub>4</sub> -N) <sub>5</sub> [CrSiW <sub>11</sub> O <sub>39</sub> ] (1)	Methyl oleate	100	125	6	2	95	98	96
		Soybean oil	100	130	24	2	41	60	96
1 (1)	Al-salen (1.4)	Methyl linoleate	100	100	17	3.5 <sup>a</sup>	80	94	99
1 (1)	Mn-Porphyrin (1)	Sunflower oil	100	1	30	4	100	99	117
1 (1)	UiO-66-NH <sub>2</sub> (0.6)	Methyl ricinoleate	120	30	12	17 <sup>a</sup>	94	-	118
		Methyl oleate	100	50	16	2	95	91	
		High oleic sunflower oil					>99	95	
		Sunflower oil	100	50	20	2	99	98	105
14 (1)	MoO <sub>3</sub> (0.125)	Soybean oil					99	90	
		Linseed oil					97	79	
		Methyl oleate	100	50	16	2	≥99	96	
		Linseed oil					99	90	
16 (1)	FeCl <sub>3</sub> (0.125 eq)	High oleic sunflower oil	100	50	24	2	99	88	106
		Soybean oil					99	94	
17 (1)	Al-complex (0.1)	Fatty acid methyl ester	70	10	24	5	99	99	101

<sup>a</sup>catalyst in wt.%; <sup>b</sup>selectivity to the cyclic carbonate product

*d) Ionic liquid/hydrogen bond donor co-catalyst binary catalytic systems*

These binary catalytic systems are similar to previous ones formed by an ionic liquid and Lewis acidic co-catalysts, with a Hydrogen Bond Donor (HBD) compound playing the role of the Lewis acidic co-catalysts, increasing the rate of epoxide ring-opening, that is the rate-determining step in the catalytic cycle. In fact, the HBDs co-catalyst has two roles in the catalytic cycle (similar to the one depicted in **Scheme 1.6**): 1) interaction with the oxygen atom of the epoxide ring, making more electrophilic the adjacent carbon facilitating the ring-opening by the nucleophilic attack of the ionic liquid anion; and 2) stabilization of the alkoxide formed after the ring-opening through hydrogen bonds formation.<sup>113</sup> The HBD co-catalysts are a more sustainable and cheaper alternative to Lewis acidic co-catalyst, because most of the Lewis acidic ones contain a transition metal complex that could be considered as Critical Raw Material (CRM) due the current global situation and geopolitical issues, and because their extraction processes are far from being environmentally friendly.<sup>119</sup> Despite that, still very few research groups work in the design of binary catalytic systems formed by an ionic liquid as the main catalyst and a HBD compound as co-catalyst in the cycloaddition of CO<sub>2</sub> to epoxidized vegetable oils or derivatives to obtain carbonated analogue compounds. In this context, Mazo et al. evaluated the performance of a binary catalytic system formed by 1 equivalent of [TBA][Br] (**1**) ionic liquid and 3 equivalents of water as HBD co-catalyst in the synthesis of carbonated soybean oil (CSBO) from CO<sub>2</sub> and epoxidized soybean oil (ESBO) at 120 °C and atmospheric pressure.<sup>120</sup> They achieved good conversion of the ESBO (87%) but moderate selectivity (89%) towards the CSBO after 70h. The designed binary catalytic system improved the catalytic performance of [TBA][Br] (**1**) as the sole catalyst in terms of reaction time that was reduced ca. 30% to achieve similar conversion of the epoxide group, proving the promoting effect of H<sub>2</sub>O as co-catalyst. Alves et al. tested several binary catalytic systems formed by 1 equivalent of [TBA][Br] (**1**) ionic liquid (1 mol%) and 1 equivalent of a HBD co-catalysts (1 mol%). In total they tested 17 different HBDs compounds (multiphenolic or fluorolcohols), in the production of carbonated linseed oil from CO<sub>2</sub> and corresponding epoxidized linseed oil at 100 °C, 100 bar and 5h reaction time.<sup>100</sup> 14 out of the 17 HBDs co-catalysts tested improved

the conversion by at least ca. 33 % compared to the use of [TBA][Br] (**1**) ionic liquid as the sole catalyst ( $\geq 42\%$  vs. 32%). Quantitative conversion of ELSO into CLSO was achieved after 10h by employing a binary catalytic system formed by 1 equivalent of [TBA][Br] (**1**) ionic liquid (2.2 mol%) and 1 equivalent of 2,2,2-trifluoro-tert-butanol (TFtert-BOH) (2.2 mol%) as HBD co-catalyst at the optimized reaction conditions (120 °C and 50 bar). A binary catalytic system formed by [TBA][Cl] (**2**) ionic liquid and ascorbic acid (AsA) as HBD co-catalyst was designed and its catalytic performance was evaluated by Natongchai et al. in the synthesis of carbonated vegetable oils and fatty acids esters from CO<sub>2</sub> and the corresponding epoxidized compounds.<sup>102</sup> This binary catalytic system produced excellent results in the synthesis of targeted oleochemicals reaching conversions and selectivities up to 99% after 48h at mild reaction conditions, 80-100 °C and 5-10 bar.

In **Table 1.4** are summarized selected ionic liquid/HBDs co-catalysts binary employed as catalytic systems, the reaction conditions, the conversion and the selectivity to target products (when given) in the CO<sub>2</sub> cycloaddition to different vegetable oils or analogue substrates.

**Table 1.4.** Ionic liquid/HBD co-catalyst binary catalytic systems used in carbonated oleochemicals synthesis.

Catalyst (equiv.)	Co-catalyst (equiv.)	Epoxidized oleochemical	Reaction conditions				Conv. (%)	Select. (%) <sup>a</sup>	Ref.
			<i>T</i> (°C)	<i>P</i> (bar)	<i>t</i> (h)	<i>Cat</i> (mol%)			
<b>1</b> (1)	H <sub>2</sub> O (3)	Soybean oil	120	1	70	5	87	88	120
<b>1</b> (1)	TFtert-BOH (1)	Soybean oil	120	50	10	2.2	99	-	100
		Methyl oleate					99	99	
<b>2</b> (1)	AsA (1)	Olive oil	100	5	48	5	99	99	102
		Soybean oil					99	89	
		Canola oil					99	94	

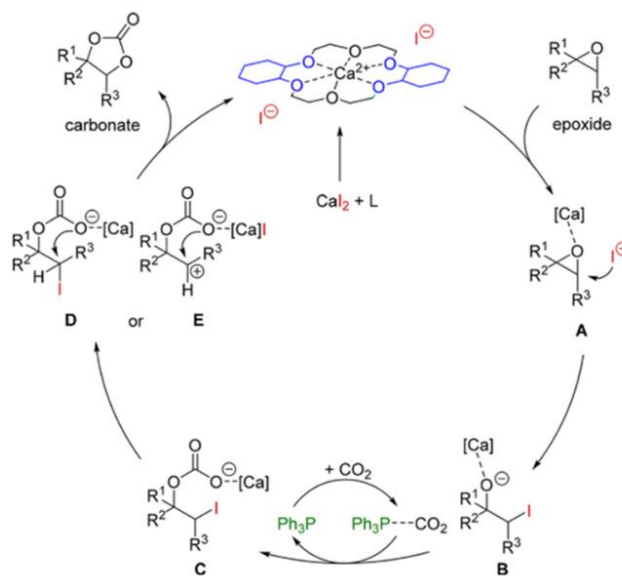
<sup>a</sup>selectivity to the cyclic carbonate product.

Other catalytic systems based on ionic compounds

Abundant, inexpensive, and nontoxic catalysts based on Na, Li or K metal salts are found as well to catalyze the cycloaddition reaction of CO<sub>2</sub> to low molecular weight epoxides with excellent results. Indeed, the synthesis of ethylene carbonate at an industrial scale is patented using alkali metal salts as a catalyst.<sup>83</sup> Nevertheless, the catalytic performance of this kind of metal salts in the preparation of carbonated oleochemicals and derivatives is generally negligible or poor. Doll et al. tested KBr and LiBr (3 mol%) metal salts as catalysts under supercritical conditions in the cycloaddition of CO<sub>2</sub> to epoxidized soybean oil achieving low conversion ( $\leq 6\%$ ) after 40h of reaction.<sup>98</sup> Schöffner et al., also observed poor conversions (2%) employing KI (5 wt.%) as a catalyst in the synthesis of carbonate fatty acids methyl esters from CO<sub>2</sub> and epoxidized fatty acid methyl esters at 100 °C and 100 bar for 17h.<sup>99</sup> As mentioned in previous catalytic systems, the addition of a co-catalyst (Lewis acid or HBD) often promotes the overall catalytic performance in terms of conversion and selectivity in the cycloaddition of CO<sub>2</sub> to epoxidized oleochemical reaction. Consequently, some authors designed catalytic systems containing a metal salt and an additive (co-catalysts) such as crown ethers or glycols (**Figure 1.9**) to try to improve the catalytic performance of the alkali metal salts in the synthesis of carbonated oleochemicals. The role of the crown ether is to enable the *in-situ* formation of a complex containing the metal (cation) and the halide (anion) of the alkali salt as depicted in **Scheme 1.7**. The “in situ” formed complex allows the epoxide activation due to the Lewis acidic character of the metal facilitating the nucleophilic ring opening by the halide anion in the cycloaddition of CO<sub>2</sub> to epoxides.<sup>121,122</sup> For the first time, Parzuchowski et al. tested a catalytic system composed by an alkali metal salt and crown ether in the cycloaddition of CO<sub>2</sub> to epoxidized oleochemicals.<sup>123</sup> This catalytic system was formed by KI (0.3 wt.%) and 18-crown-6 ether (0.2 wt.%) and tested in the synthesis of carbonated soybean oil from CO<sub>2</sub> and epoxidized soybean oil, achieving a conversion of 98.3% at 130 °C and 60 bar after 120h reaction. Schöffner et al. tested several catalytic systems formed by 5 wt.% of an alkali metal salt (KBr, KI, NaI, LiI and CsI) and 3.5 wt.% of a crown ether (18-crown-6, 15-crown-5 and 12-crown-4) in the reaction of CO<sub>2</sub> with epoxidized methyl linoleate at 100 °C, 100 bar and 17h reaction time.<sup>99</sup> The best results in terms of conversion (94%) were achieved with the

catalytic system formed by NaI and 15-crown-5 while in terms of selectivity (89% *vs.* 97%) were obtained with the catalytic system formed by KI and 18-crown-6. In general, the second catalytic system produced slightly better results in terms of yield of the targeted carbonated product (84% *vs.* 87%). All the other catalytic systems formed by other alkali metal salts tested by the authors exhibited insufficient conversions from 10% to 55%. The same authors, tested as well catalytic systems formed by alkali metal salts (5 wt.%) and glycols (HBDs) (3.5 wt.%) as co-catalysts at 100 °C, 100 bar and 17h reaction time in the reaction of CO<sub>2</sub> with epoxidized methyl linoleate. The authors justified the used of glycols as co-catalyst based on both their tuneable properties and low cost. Among the catalytic systems employed containing a glycol, the one formed by KI and polyethyleneglycol 400 (PEG400) showed the best catalytic performance in terms of conversion (84%) and selectivity (99%) although the catalytic system formed by KI and polyethyleneglycol 600 (PEG600) showed similar conversion (83%) and selectivity (99%). In this work, the authors observed that the epoxidized oleochemical conversion was reduced considerably when high molecular weight glycols ( $\geq 1000$  Mw) were employed in the catalytic systems due to the limited solubility of the heavy glycols. Longwitz et al. developed catalytic systems formed by 1 equivalent of CaI<sub>2</sub> (5 mol%) 1 equivalent of a crown ether (5 mol%) to be tested in the synthesis of carbonated methyl oleate from the epoxidized methyl oleate and CO<sub>2</sub> at relatively mild reaction conditions, 60 °C and 20 bar.<sup>124</sup> Among the designed catalytic systems, the one containing 18-crown-6-ether showed the highest activity in terms of conversion (>99%) and selectivity (>99%) to the targeted carbonated compound after 24h. The authors attributed the excellent catalytic performance of the catalytic system containing the 18-crown-6-ether to its higher solubility in the reaction media. The authors tested the same catalytic system at milder reaction conditions, 45 °C and 10 bar achieving a yield to the carbonated product of 24% after 24h of reaction time. To keep the milder reaction conditions (45 °C and 10 bar) and increase the overall reaction yield, the authors added 5 mol% of other additives (co-catalysts) to the catalytic system such as DABCO, TBD, DBU, DMAP or triphenylphosphine (TPP). Indeed, the presence of these co-catalysts improved the overall yield at least in ca. 330% from 24% to 81%. Even in the case of TPP, the yield increased by more than 400%, from 24% to 98%. The authors claimed the

improvement was due to the additives (co-catalysts) acting as activators of the CO<sub>2</sub> molecule. Taking into account these results, the authors proposed a mechanism in four steps for a catalytic system formed by CaI<sub>2</sub>, 18-crown-6-ether and TPP as shown in **Scheme 1.7**. Before the catalytic cycle starts must take place the “*in situ*” formation of a calcium complex with the crown ether. After, upon addition of the epoxide the Lewis acid character of the calcium makes easier the activation of the epoxide ring by interacting with the oxygen atom (**A**). Then the epoxide undergoes nucleophilic attack by the iodine anion yielding the corresponding alkoxide (**B**). After, the alkoxide attacks the CO<sub>2</sub> molecule previously activated by the TPP yielding the carbonate compound (**C**). Finally, the intramolecular ring closing takes place (**D** or **E**) liberating the catalyst and yielding the desired cyclic carbonate.



**Scheme 1.7.** Mechanism proposed by Longwitz et al. for the CO<sub>2</sub> cycloaddition to an epoxide catalyzed by CaI<sub>2</sub>, 18-crown-6-ether and TPP catalytic system (Credit: Longwitz et al.).<sup>124</sup>

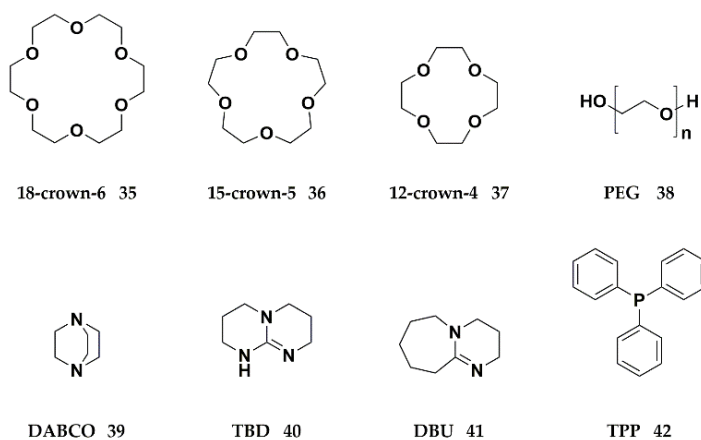


**Figure 1.9.** Additives employed as co-catalyst to improve the catalytic performance of alkali metal salts.

In **Table 1.5** are summarized the selected alkali metal salts/co-catalyst binary employed as catalytic systems, the reaction conditions, the conversion, and the selectivity to target products (when given) in the CO<sub>2</sub> cycloaddition to different vegetable oils or analogue substrates.



**Table 1.5.** Alkali metal salts/co-catalyst binary catalytic systems used in carbonated oleochemicals synthesis.

Catalyst (equiv.)	co-catalyst (equiv.)	Epoxidized oleochemical	Reaction conditions				Conv. (%)	Select. (%) <sup>b</sup>	Ref.
			<i>T</i> (°C)	<i>P</i> (bar)	<i>t</i> (h)	<i>Cat</i> mol%			
KBr	-	Soybean oil	100	>103	40	3	6	-	98
LiBr	-	Soybean oil	100	>103	40	3	0	-	98
KI	-	Fatty acid methyl ester	100	100	17	5 <sup>a</sup>	2	99	99
KI (1)	35 (0.7)	Soybean oil	130	60	120	0.3 <sup>a</sup>	98	-	123
KBr (1)	35 (0.7)	Methyl linoleate	100	100	17	5 <sup>a</sup>	55	97	99
KI (1)	35 (0.7)	Methyl linoleate	100	100	17	5 <sup>a</sup>	90	97	99
NaI (1)	36 (0.7)	Methyl linoleate	100	100	17	5 <sup>a</sup>	94	89	99
LiI (1)	37 (0.7)	Methyl linoleate	100	100	17	5 <sup>a</sup>	18	98	99
CsI (1)	35 (0.7)	Methyl linoleate	100	100	17	5 <sup>a</sup>	10	99	99
KI (1)	38 PEG400 (0.7)	Methyl linoleate	100	100	17	5 <sup>a</sup>	84	99	99
		Fatty acid methyl ester					>99	>99	
CaI <sub>2</sub> (1)	35 (1)/42 (1)	Sunflower oil	45	5	24	5	99	99	124
		Soybean oil					99	82	
		Linseed oil					80	65	

<sup>a</sup>catalyst in wt.%; <sup>b</sup>selectivity to the cyclic carbonate product.

### 1.2.2 Heterogeneous catalytic systems

Homogenous catalytic systems are the most extensively studied in the cycloaddition of CO<sub>2</sub> to epoxidized oils and/or derivatives to yield the corresponding cyclic carbonates. However, the relevance of an efficient and easy separation and reutilisation of the catalyst, as well as the development of more sustainable processes strongly push researchers to design easily recoverable and reusable heterogeneous catalytic systems.<sup>125</sup> Despite this strong interest in the use of heterogeneous catalytic systems due to their remarkable advantages, very few works (only 5 to the best of our knowledge) reported their use in the synthesis of carbonated oleochemicals from CO<sub>2</sub>. In this regard, Bähr et al. compared the catalytic performance of the benchmark [TBA][Br] (**1**) ionic liquid catalyst with a heterogeneous catalysts in the CO<sub>2</sub> cycloaddition to epoxidized linseed oil to yield the corresponding carbonated compound to be employed in the non-isocyanate polyurethanes synthesis.<sup>126</sup> The catalyst was a silica-supported 4-pyrrolidinopyridinium iodide (SiO<sub>2</sub>-I). At 140 °C and 30 bar, full conversion of the epoxidized linseed oil was achieved with [TBA][Br] (**1**) ionic liquid as catalyst after 20h reaction time, while 45h were needed to reach the same conversion with the heterogeneous catalysts (SiO<sub>2</sub>-I). The authors attributed the longer reaction time needed with the heterogeneous catalyst to the size of the silica pores, which limited the approach of the bulky epoxidized linseed oil. In fact, the authors suggest that as solution to improve the catalytic performance of SiO<sub>2</sub>-I catalysts would be to increase the silica pore size, tailoring the pore compartments as well as to increase the spacer length (linker) between the silica support and the alkyl ammonium groups. Schäffner et al. tested a heterogenized catalytic system prepared by impregnation of the benchmark [TBA][Br] (**1**) ionic liquid homogeneous catalyst on silica as support in the synthesis of carbonated methyl linoleate from CO<sub>2</sub> and epoxidized methyl linoleate at 100 °C and 100 bar.<sup>99</sup> After 17h of reaction, the conversion of the homogeneous system was found to be 4.6 times higher compared to the heterogenized system (15% *vs.* 69%) but the selectivity with both systems was similar >99% towards the carbonated product. The authors attributed the drop in conversion of the heterogenized systems to well-known mass transfer limitations in this kind of catalysts. With the objective of developing a kinetic model for the

synthesis of carbonated oleo compounds at industrial scale, Cai et al. tested a heterogeneous catalyst by supporting via a noncovalent linkage a task-specific ionic liquid [HBIIm][Cl] (1-hydroxypropyl-3-*n*-butylimidazolium chloride) and NbCl<sub>5</sub> on protonated carboxymethyl cellulose (HCMC) as support. The heterogeneous catalytic system ([HBIIm][Cl]-NbCl<sub>5</sub>/HCMC) was tested in the synthesis of carbonated fatty acid methyl esters obtained from cottonseed oil, and parameters such as temperature, pressure, stirring rate, particle size, and catalyst loading were investigated.<sup>127</sup> The optimal parameters to afford highly carbonation of the epoxidized compounds were found to be 170 °C, 30 bar, 500 r.p.m., 652 μm particle size and 0.71 mol/L catalyst amount. Akhdar et al. prepared several heterogeneous catalytic systems by covalent support of imidazolium-based ionic liquids with thermomorphic polyethylene (TMPE).<sup>128</sup> The catalytic performance of these prepared catalytic systems was evaluated for the ring opening of epoxidized methyl oleate with CO<sub>2</sub>. Among the heterogeneous catalytic systems tested, the one composed by bromide anion and N-methylimidazole cation ([MeIm][Br]-TMPE) produced the highest epoxide conversion (>99%) with a selectivity of 93% towards carbonated methyl oleate after 20h at 100 °C, 20 bar and using 4 mol% catalyst. Comparable catalytic activity to homogeneous [TBA][Br] (1) ionic liquid catalyst was achieved with this catalyst in terms of conversion (>99% *vs.* 96%) and selectivity (93% *vs.* 97%) at the same reaction conditions. However, while [TBA][Br] could not be recovered and reused, the prepared heterogenous catalyst could be easily recovered and reused up to 10 times without any significant loss of catalytic activity. Perez-Sena et al. evaluated the performance of various organic salts supported on silica gel and SBA-15 in the synthesis carbonated methyl oleate.<sup>129</sup> Among the tested catalytic systems, the 4-pyrrolidino pyridine supported on SBA-15 and doped with a molar ratio of 0.12 Zn/Si (Zn-SBA-15(0.12)-4PPI) (7.4 wt.%) was found to be the most active, reaching a suitable epoxide conversion (75%) and carbonate selectivity (91%) at 140 °C and 30 bar after 32h of reaction. The same catalytic system was used for the synthesis of carbonated methyl esters from cottonseed oil and tall oil under similar reaction conditions (140 °C, 30 bar, 7.4 wt.% and 23h). Nevertheless, the catalytic activity was considerably lower in terms of conversion (47% and 57%) and selectivity (85% and 60%) comparing with using methyl oleate as precursor.

In **Table 1.6** are summarized the selected employed heterogeneous catalytic systems, the reaction conditions, the conversion, and the selectivity to target products (when given) in the CO<sub>2</sub> cycloaddition to different vegetable oils or analogue substrates.

**Table 1.6.** Heterogeneous catalytic systems used in carbonated oleochemicals synthesis.

Catalyst	Epoxidized oleochemical	Reaction conditions				Conv (%)	Select (%) <sup>c</sup>	Ref.
		<i>T</i> (°C)	<i>P</i> (bar)	<i>t</i> (h)	<i>Cat</i> (mol%)			
SiO <sub>2</sub> -I	Linseed oil	140	30	45	3	100	-	126
<b>1</b> on SiO <sub>2</sub>	Methyl linoleate	100	100	17	2	15	99	99
HBimCl-NbCl <sub>5</sub> /HCMC	Cottonseed oil methyl ester	170	30	8	0.71 <sup>a</sup>	> 90	-	127
[MeIm][Br]-TMPE	Methyl oleate	100	20	20	4	> 99	93	128
Zn-SBA-15(0.12)-4PPI	Methyl oleate	140	30	32	7.4 <sup>b</sup>	75	91	
	Cottonseed oil methyl ester	140	30	23	7.4 <sup>b</sup>	47	85	129
	Tall oil methyl ester	140	30	23	7.4 <sup>b</sup>	57	60	

<sup>a</sup>catalyst in mol/L; <sup>b</sup>catalyst in wt.%; <sup>c</sup>selectivity to the cyclic carbonate product.

Nevertheless, among the employed catalytic system in the CO<sub>2</sub> cycloaddition to epoxidized oleochemical, it is difficult to extract conclusions about what is the best catalytic system, if any, reported so far due to the vast and diverse conditions (catalyst amount, temperature, pressure, reaction time, employed substrate etc.) employed in the different scientific literature dealing with this topic. It seems clear that the selection of the catalytic systems strongly depends on the nature of the selected bio-based substrate. Even if some advances have been made in this topic (mainly in last 5–6 years) deep and extensive studies are still required to make CO<sub>2</sub> chemical fixation into epoxidized bio-based compounds attractive for the synthesis of more sustainable polymers industry. In particular, it is necessary to develop cost-effective catalysts to

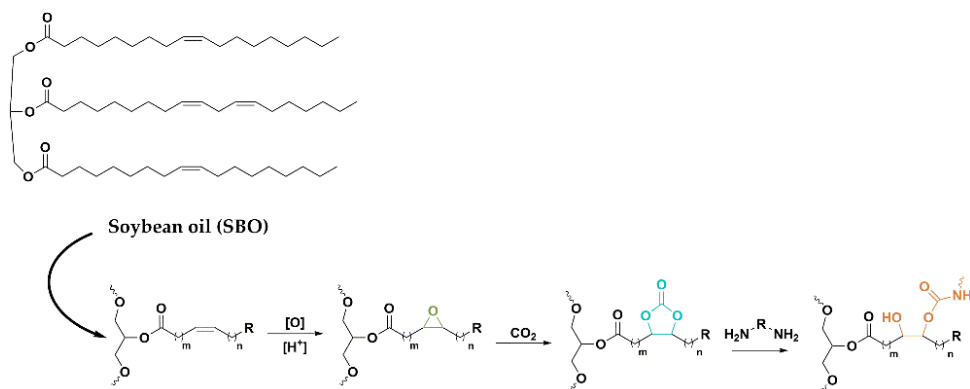
obtain carbonated oils with high yields under conditions that are attractive to the industry: low P and T and short reaction time.

### 1.3 Carbonated soybean oil as precursor for non-isocyanate polyurethanes

As previously mentioned, at the beginning of the 21<sup>st</sup> century, B. Tamami and co-workers developed for the first-time non-isocyanate polyurethanes (NIPUs) using carbonated soybean oil as a precursor.<sup>91</sup> As illustrates **Scheme 1.8** the synthesis of NIPUs from CO<sub>2</sub> and vegetable oils consists of three stages. First, the unsaturations present in the fatty acid chains are oxidized to epoxy groups. Then CO<sub>2</sub> is inserted into the oxirane ring to produce five-membered cyclic carbonates. Finally, the carbonated (soybean) oil reacts with amines to give the desired NIPU. The potential of this route for the valorisation of CO<sub>2</sub> and vegetable oil has prompted the publication of numerous papers in this field.<sup>19,64</sup> In many of these works, the influence of several factors, such as the cyclic carbonate amine ratio, amine structure, carbonate amount and oil type on the final polymer properties was studied. The resultant NIPUs exhibit a wide range of properties, with a tensile strength ranging from 0.1-20 MPa, elongation at break in the range of 3-477%, glass transition temperatures between -15 and 60 °C or decomposition temperatures (5 wt% weight loss) up to 386 °C. In view of the potential of vegetable oil-based NIPUs, there have been efforts to apply these materials in several fields, such as foams<sup>130,131</sup>, adhesives<sup>132</sup>, coatings<sup>133-135</sup> or tissue engineering.<sup>136</sup> The background related to the synthesis of NIPUs from vegetable oils, as well as the numerous factors that affect their performance and enable a wide range of properties are further detailed in the introduction of **Chapter 3**.

However, the reaction between amines and oleo-based cyclic carbonates presents significant disadvantages for the industrial application of the resulting NIPUs. The low reactivity of cyclic carbonates and amines aggravates the reaction conditions compared to isocyanates and alcohols, which react at room temperature. Even when using more severe reaction conditions (high temperature and long reaction times), vegetable oil-based NIPUs do not reach the features of their isocyanate analogues.

These less optimal operating conditions, along with the suboptimal properties of the final product, are a barrier for the industrial implementation vegetable oil-based NIPUs. It is important to note that in the **Chapter 4** introduction, the current status of carbonated vegetable oil-based NIPUs in the coatings industry has been detailed in depth.



**Scheme 1.8.** CSBO-based non-isocyanate polyurethanes synthesis process.

## 1.4 Aim and outline of the thesis

Epoxidized soybean oil is one of the few bio-based feedstock that contains epoxy groups in its structure and is produced in tons. This makes ESBO oil a widely available and low-cost precursor, making it an excellent candidate to be employed in the development of the new alternative to polyurethanes: Non-isocyanate polyurethanes. Although the polyaddition reaction is the most attractive route due to the inherent toxicity, the harsh reaction conditions, (high pressure, high temperature and long time) together with curing conditions far from what is required by the industry, hampers the process industrialization and the possible commercialization of both carbonated oils and vegetable oil-based NIPUs.

Hence the aim of the thesis has been to advance the introduction of carbonated soybean oil as a monomer for the synthesis of (partially) biobased NIPU, a more sustainable and safer alternative to PU. First, a new family of catalysts was designed and synthesized to improve the reaction conditions of  $\text{CO}_2$  cycloaddition to

epoxidized soybean oil. (**Chapter 2**) The goal was to find catalysts that could improve the reaction conditions in the synthesis of carbonated monomer in terms of temperature, pressure, time and yield. The carbonated soybean oil was reacted with diamines to synthesize vegetable oil-based NIPUs, which were characterized and compared with traditional PUs (**Chapter 3**). Finally, with the aim of bringing this chemistry closer to industrial level, an investigation of the use of these products in the field of coatings has been carried out, according to the specific synthesis and characterization requirements of this industry (**Chapter 4**).

## 1.5 References

- 1 O. Bayer, *Angew. Chem.*, 1947, **59**, 257–288.
- 2 M. F. Sonnenschein, *Polyurethanes. Science, Technology, Markets, and Trends*, Wiley, 2014.
- 3 B. Bizet, É. Grau, H. Cramail and J. M. Asua, *Polym. Chem.*, 2020, **11**, 3786–3799.
- 4 Polyurethane (PU) Coatings Market–Growth, Trends, COVID-19 Impact, and Forecast (2021-2026), <https://www.mordorintelligence.com/industry-reports/polyurethane-market>. (accessed February 5, 2022).
- 5 G. Boiteux, L. Cuvé and J.-P. Pascault, *Polymer*, 1994, **35**, 173–178.
- 6 E. Delebecq, J. Pascault and B. Boutevin, *Chem. Rev.*, 2013, **113**, 80–118.
- 7 H. W. Engels, H. G. Pirkl, R. Albers, R. W. Albach, J. Krause, A. Hoffmann, H. Casselmann and J. Dormish, *Angew. Chem. Int. Ed.*, 2013, **52**, 9422–9441.
- 8 T. An Phung Hai, M. Tessman, N. Neelakantan, A. A. Samoylov, Y. Ito, B. S. Rajput, N. Pourahmady and M. D. Burkart, *Biomacromolecules*, 2021, **22**, 1770–1794.
- 9 M. Szycher, *Handbook of Polyurethanes*, Taylor & Francis Group, London, 2<sup>nd</sup> edn., 2013.
- 10 C. G. Mothé and C. R. De Araújo, *Thermochim. Acta*, 2000, **357–358**, 321–325.

- 11 J. O. Akindoyo, M. D. H. Beg, S. Ghazali, M. R. Islam, N. Jeyaratnam and A. R. Yuvaraj, *RSC Adv.*, 2016, 6, 114453–114482.
- 12 Z. S. Petrović, *Contemp. Mater.*, 2010, I-1, 39–50.
- 13 A. Noreen, K. M. Zia, M. Zuber and S. Tabasum, *Prog. Org. Coatings*, 2016, **91**, 25–32.
- 14 A. Tenorio-Alfonso, M. C. Sánchez and J. M. Franco, *J. Polym. Environ.*, 2020, **28**, 749–774.
- 15 Y. Suryawanshi, P. Sanap and V. Wani, *Polym. Bull.*, 2019, **76**, 3233–3246.
- 16 M. H. Karol and J. A. Kramarik, *Toxicol. Lett.*, 1996, **89**, 139–146.
- 17 C. Bolognesi, X. Baur, B. Marczyński, H. Norppa, O. Sepai and G. Sabbioni, *Crit. Rev. Toxicol.*, 2001, **31**, 737–772.
- 18 L. Pollaris, F. Devos, V. De Vooght, S. Seys, B. Nemery, P. H. M. Hoet and J. A. J. Vanoirbeek, *Arch. Toxicol.*, 2016, **90**, 1709–1717.
- 19 M. Ghasemlou, F. Daver, E. P. Ivanova and B. Adhikari, *Eur. Polym. J.*, 2019, **118**, 668–684.
- 20 S. Diamond, The Bhopal disaster: How it happened. *The New York Times*, **28**, 1985.
- 21 *Of. J. Eur. Union*, 2009, **552**, 7–31.
- 22 S. V. Vassilev, D. Baxter, L. K. Andersen, C. G. Vassileva and T. J. Morgan, *Fuel*, 2012, **94**, 1–33.
- 23 M. Fabbri, M. Soccio, M. Costa, N. Lotti, M. Gazzano, V. Siracusa, R. Gamberini, B. Rimini, A. Munari, L. García-Fernández, B. Vázquez-Lasa and J. San Román, *Polym. Degrad. Stab.*, 2016, **132**, 169–180.
- 24 M. Y. Lu, A. Surányi, B. Viskolcz and B. Fiser, *Croat. Chem. Acta*, 2018, **91**, 299–307.
- 25 A. Basterretxea, X. Lopez De Pariza, E. Gabirondo, S. Marina, J. Martin, A. Etxeberria, D. Mecerreyes and H. Sardon, *Ind. Eng. Chem. Res.*, 2020, **59**, 10746–



- 10753.
- 26 D. J. Dos Santos, L. B. Tavares, J. R. Gouveia and G. F. Batalha, *Arch. Mater. Sci. Eng.*, 2021, **107**, 56–63.
- 27 M. Zhang, J. Zhang, S. Chen and Y. Zhou, *Polym. Degrad. Stab.*, 2014, **110**, 27–34.
- 28 Z. S. Petrović, X. Wan, O. Bilić, A. Zlatanić, J. Hong, I. Javni, M. Ionescu, J. Milić and D. Degruson, *J. Am. Oil Chem. Soc.*, 2013, **90**, 1073–1078.
- 29 B. V Tawade, R. D. Shingte, S. S. Kuhire, N. V Sadavarte, K. Garg, D. M. Maher, A. B. Ichake, A. S. More and P. P. Wadgaonkar, *Polyurethane Today*, 2017, **11**, 41–46.
- 30 P. Furtwengler and L. Avérous, *Polym. Chem.*, 2018, **9**, 4258–4287.
- 31 O. Faruk, M. Sain, R. Farnood, Y. Pan and H. Xiao, *J. Polym. Environ.*, 2014, **22**, 279–288.
- 32 K. K. Tremblay-Parrado, C. García-Astrain and L. Avérous, *Green Chem.*, 2021, **23**, 4296–4327.
- 33 U. Biermann, U. Bornscheuer, M. A. R. Meier, J. O. Metzger and H. J. Schäfer, *Angew. Chem. Int. Ed.*, 2011, **50**, 3854–3871.
- 34 Y. Y. Li, X. Luo and S. Hu, Polyols and polyurethanes from vegetable oils and their derivatives. *Bio-based Polyols and Polyurethanes*, 2015, 15-43.
- 35 L. Montero De Espinosa and M. A. R. Meier, *Eur. Polym. J.*, 2011, **47**, 837–852.
- 36 J. C. Ronda, G. Lligadas, M. Galià and V. Cádiz, *Eur. J. Lipid Sci. Technol.*, 2011, **113**, 46–58.
- 37 S. Miao, P. Wang, Z. Su and S. Zhang, *Acta Biomater.*, 2014, **10**, 1692–1704.
- 38 A. Zlatanić, C. Lava, W. Zhang and Z. S. Petrović, *J. Polym. Sci. Part B Polym. Phys.*, 2004, **42**, 809–819.
- 39 M. A. R. Meier, J. O. Metzger and U. S. Schubert, *Chem. Soc. Rev.*, 2007, **36**, 1788–1802.

- 40 Z. S. Petrović, *Polym. Rev.*, 2008, **48**, 109–155.
- 41 M. Alam, D. Akram, E. Sharmin, F. Zafar and S. Ahmad, *Arab. J. Chem.*, 2014, **7**, 469–479.
- 42 R. S. Malani, V. C. Malshe and B. N. Thorat, *J. Coatings Technol. Res.*, 2022, **19**, 201–222.
- 43 S. Das, M. Dave and G. L. Wilkes, *J. Appl. Polym. Sci.*, 2009, **112**, 299–308.
- 44 Z. Fang, Z. Yang, D. Ji, N. Zhu, X. Li, L. Wan, K. Zhang and K. Guo, *RSC Adv.*, 2016, **6**, 90771–90776.
- 45 C. S. Carriço, T. Fraga and V. M. D. Pasa, *Eur. Polym. J.*, 2016, **85**, 53–61.
- 46 A. Tenorio-Alfonso, M. C. Sánchez and J. M. Franco, *Polymers*, 2017, **9**, 132–146.
- 47 N. Gama, A. Ferreira and A. Barros-Timmons, *Int. J. Adhes. Adhes.*, 2019, **95**, 102413.
- 48 P. Ferreira, R. Pereira, J. F. J. Coelho, A. F. M. Silva and M. H. Gil, *Int. J. Biol. Macromol.*, 2007, **40**, 144–152.
- 49 E. Hablot, D. Zheng, M. Bouquey and L. Avérous, *Macromol. Mater. Eng.*, 2008, **293**, 922–929.
- 50 C. Sharma, S. Kumar, A. R. Unni, V. K. Aswal, S. K. Rath and G. Harikrishnan, *J. Appl. Polym. Sci.*, 2014, **131**, 40668–40676.
- 51 C. Zhang, R. Ding and M. R. Kessler, *Macromol. Rapid Commun.*, 2014, **35**, 1068–1074.
- 52 S. Miao, S. Zhang, Z. Su and P. Wang, *J. Polym. Sci. Part A Polym. Chem.*, 2010, **48**, 243–250.
- 53 P. Rojek and A. Prociak, *J. Appl. Polym. Sci.*, 2012, **125**, 2936–2945.
- 54 P. Tran, D. Graiver and R. Narayan, *J. Am. Oil Chem. Soc.*, 2005, **82**, 653–659.
- 55 M. Desroches, M. Escouvois, R. Auvergne, S. Caillol and B. Boutevin, *Polym. Rev.*, 2012, **52**, 38–79.

- 56 J. M. Raquez, M. Deléglise, M. F. Lacrampe and P. Krawczak, *Prog. Polym. Sci.*, 2010, **35**, 487–509.
- 57 T. Vanbésien, E. Monflier and F. Hapiot, *Eur. J. Lipid Sci. Technol.*, 2016, **118**, 26–35.
- 58 C. Resetco, B. Hendriks, N. Badi and F. Du Prez, *Mater. Horizons*, 2017, **4**, 1041–1053.
- 59 C. K. Park, J. H. Lee, I. S. Kim and S. H. Kim, *J. Appl. Polym. Sci.*, 2020, **137**, 48304–48315.
- 60 P. Alagi, Y. J. Choi, J. Seog and S. C. Hong, *Ind. Crops Prod.*, 2016, **87**, 78–88.
- 61 M. Desroches, S. Caillol, V. Lapinte, R. Auvergne and B. Boutevin, *Macromolecules*, 2011, **44**, 2489–2500.
- 62 U. Stirna, A. Fridrihsone, B. Lazdiņa, M. Misāne and D. Vilsone, *J. Polym. Environ.*, 2013, **21**, 952–962.
- 63 S. Jayavani, S. Sunanda, T. O. Varghese and S. K. Nayak, *J. Clean. Prod.*, 2017, **162**, 795–805.
- 64 B. Nohra, L. Candy, J. F. Blanco, C. Guerin, Y. Raoul and Z. Mouloungui, *Macromolecules*, 2013, **46**, 3771–3792.
- 65 O. Kreye, H. Mutlu and M. A. R. Meier, *Green Chem.*, 2013, **15**, 1431–1455.
- 66 J. Guan, Y. Song, Y. Lin, X. Yin, M. Zuo, Y. Zhao, X. Tao and Q. Zheng, *Ind. Eng. Chem. Res.*, 2011, **50**, 6517–6527.
- 67 M. S. Kathalewar, P. B. Joshi, A. S. Sabnis and V. C. Malshe, *RSC Adv.*, 2013, **3**, 4110–4129.
- 68 G. Rokicki, P. G. Parzuchowski and M. Mazurek, *Polym. Adv. Technol.*, 2015, **26**, 707–761.
- 69 L. Maisonneuve, O. Lamarzelle, E. Rix, E. Grau and H. Cramail, *Chem. Rev.*, 2015, **115**, 12407–12439.
- 70 L. Ubaghs, N. Fricke, H. Keul and H. Höcker, *Macromol. Rapid Commun.*, 2004,

- 25, 517–521.
- 71 P. Deepa and M. Jayakannan, *J. Polym. Sci. Part A Polym. Chem.*, 2008, **46**, 2445–2458.
- 72 D. V. Palaskar, A. Boyer, E. Cloutet, C. Alfos and H. Cramail, *Biomacromolecules*, 2010, **11**, 1202–1211.
- 73 S. Neffgen, H. Keul and H. Höcker, *Macromolecules*, 1997, **30**, 1289–1297.
- 74 O. Ihata, Y. Kayaki and T. Ikariya, *Angew. Chem.*, 2004, **116**, 735–737.
- 75 D. C. Webster and A. L. Crain, *Prog. Org. Coatings*, 2000, **40**, 275–282.
- 76 A. Cornille, R. Auvergne, O. Figovsky, B. Boutevin and S. Caillol, *Eur. Polym. J.*, 2017, **87**, 535–552.
- 77 C. Carré, Y. Ecochard, S. Caillol and L. Avérous, *ChemSusChem*, 2019, **12**, 3410–3430.
- 78 H. Blattmann, M. Fleischer, M. Bähr and R. Mülhaupt, *Macromol. Rapid Commun.*, 2014, **35**, 1238–1254.
- 79 F. D. Bobbink, A. P. Van Muyden and P. J. Dyson, *Chem. Commun.*, 2019, **55**, 1360–1373.
- 80 O. Figovsky, L. Shapovalov, A. Leykin, O. Birukova and R. Potashnikova, *Chem. Chem. Technol.*, 2013, **7**, 79–87.
- 81 J. Datta and M. Włoch, *Polym. Bull.*, 2016, **73**, 1459–1496.
- 82 C. Hahn, H. Keul and M. Möller, *Polym. Int.*, 2012, **61**, 1048–1060.
- 83 M. North, R. Pasquale and C. Young, *Green Chem.*, 2010, **12**, 1514–1539.
- 84 L. M. Alsarhan, A. S. Alayyar, N. B. Alqahtani and N. H. Khadary, *Sustainability*, 2021, **13**, 11625.
- 85 T. Sakakura, J. C. Choi and H. Yasuda, *Chem. Rev.*, 2007, **107**, 2365–2387.
- 86 Q.-W. Song, Z.-H. Zhou and L.-N. He, *Green Chem.*, 2017, **19**, 3707–3728.
- 87 D. Miloslavskiy, E. Gotlib, O. Figovsky and D. Pashin, *Int. Lett. Chem. Phys.*

- Astron.*, 2014, **81**, 20–29.
- 88 M. A. C. Mhd. Haniffa, K. Munawar, Y. C. Ching, H. A. Illias and C. H. Chuah, *Chem. An Asian J.*, 2021, **16**, 1281–1297.
- 89 S. M. Danov, O. A. Kazantsev, A. L. Esipovich, A. S. Belousov, A. E. Rogozhin and E. A. Kanakov, *Catal. Sci. Technol.*, 2017, **7**, 3659–3675.
- 90 Epoxidized Soybean Oil Market by Raw Material. Application, End-use Application-Global Forecast to 2026 [https://www.marketsandmarkets.com/Market-Reports/epoxidized-soybean-oil-market-27777113.html?gclid=EAIaIQobChMIgOHKjp399gIVHY1oCR1LfQufEAAYA SAAEgLKc\\_D\\_BwE](https://www.marketsandmarkets.com/Market-Reports/epoxidized-soybean-oil-market-27777113.html?gclid=EAIaIQobChMIgOHKjp399gIVHY1oCR1LfQufEAAYA SAAEgLKc_D_BwE). (accessed August 15, 2022).
- 91 B. Tamami, S. Sohn and G. L. Wilkes, *J. Appl. Polym. Sci.*, 2004, **92**, 883–891.
- 92 F. Castro-Gómez, G. Salassa, A. W. Kleij and C. Bo, *Chem. A Eur. J.*, 2013, **19**, 6289–6298.
- 93 M. Alves, B. Grignard, R. Mereau, C. Jerome, T. Tassaing and C. Detrembleur, *Catal. Sci. Technol.*, 2017, **7**, 2651–2684.
- 94 K. Kiatkittipong, M. A. A. M. Shukri, W. Kiatkittipong, J. W. Lim, P. L. Show, M. K. Lam and S. Assabumrungrat, *Processes*, 2020, **8**, 548-570.
- 95 H. Y. Ju, M. D. Manju, K. H. Kim, S. W. Park and D. W. Park, *J. Ind. Eng. Chem.*, 2008, **14**, 157–160.
- 96 J. Langanke, L. Greiner and W. Leitner, *Green Chem.*, 2013, **15**, 1173–1182.
- 97 A. J. Kamphuis, F. Picchioni and P. P. Pescarmona, *Green Chem.*, 2019, **21**, 406–448.
- 98 K. M. Doll and S. Z. Erhan, *Green Chem.*, 2005, **7**, 849–854.
- 99 B. Schäffner, M. Blug, D. Kruse, M. Polyakov, A. Köckritz, A. Martin, P. Rajagopalan, U. Bentrup, A. Brückner, S. Jung, D. Agar, B. Rüngeler, A. Pfennig, K. Müller, W. Arlt, B. Woldt, M. Graß and S. Buchholz, *ChemSusChem*, 2014, **7**, 1133–1139.

- 100 M. Alves, B. Grignard, S. Gennen, C. Detrembleur, C. Jerome and T. Tassaing, *RSC Adv.*, 2015, **5**, 53629–53636.
- 101 L. Peña Carrodegua, Cristòfol, J. M. Fraile, J. A. Mayoral, V. Dorado, C. I. Herrerías and A. W. Kleij, *Green Chem.*, 2017, **19**, 3535–3541.
- 102 W. Natongchai, S. Pornpraprom and V. D'Elia, *Asian J. Org. Chem.*, 2020, **9**, 801–810.
- 103 J. L. Zheng, P. Tolvanen, B. Taouk, K. Eränen, S. Leveneur and T. Salmi, *Chem. Eng. Res. Des.*, 2018, **132**, 9–18.
- 104 V. H. J. M. dos Santos, D. Pontin, R. S. Rambo and M. Seferin, *J. Am. Oil Chem. Soc.*, 2020, **97**, 817–837.
- 105 N. Tenhumberg, H. Büttner, B. Schäffner, D. Kruse, M. Blumenstein and T. Werner, *Green Chem.*, 2016, **18**, 3775–3788.
- 106 H. Büttner, C. Grimmer, J. Steinbauer and T. Werner, *ACS Sustain. Chem. Eng.*, 2016, **4**, 4805–4814.
- 107 R. Giernoth, *Angew. Chem. Int. Ed.*, 2010, **49**, 2834–2839.
- 108 S. K. Singh and A. W. Savoy, *J. Mol. Liq.*, 2020, **297**, 112038.
- 109 T. Chang, X. Gao, L. Bian, X. Fu, M. Yuan and H. Jing, *Chinese J. Catal.*, 2015, **36**, 408–413.
- 110 J. Peng, S. Wang, H. J. Yang, B. Ban, Z. Wei, L. Wang and B. Lei, *Fuel*, 2018, **224**, 481–488.
- 111 S. Wu, B. Wang, Y. Zhang, E. H. M. Elageed, H. Wu and G. Gao, *J. Mol. Catal. A Chem.*, 2016, **418–419**, 1–8.
- 112 L. F. Xiao, D. W. Lv, D. Su, W. Wu and H. F. Li, *J. Clean. Prod.*, 2014, **67**, 285–290.
- 113 H. Büttner, J. Steinbauer, C. Wulf, M. Dindaroglu, H. G. Schmalz and T. Werner, *ChemSusChem*, 2016, **9**, 1–5.
- 114 J. Martínez, F. De La Cruz-Martínez, M. M. De Sarasa Buchaca, M. P.

- Caballero, R. M. Ojeda-Amador, M. D. Salvador, G. Fregapane, J. Tejada, J. A. Castro-Osma and A. Lara-Sánchez, *J. Environ. Chem. Eng.*, 2021, **9**, 105464.
- 115 M. Taherimehr, S. M. Al-Amsyar, C. J. Whiteoak, A. W. Kleij and P. P. Pescarmona, *Green Chem.*, 2013, **15**, 3083–3090.
- 116 Z. Li, Y. Zhao, S. Yan, X. Wang, M. Kang, J. Wang and H. Xiang, *Catal. Lett.*, 2008, **123**, 246–251.
- 117 A. Farhadian, M. B. Gol Afshani, A. Babaei Miyardan, M. R. Nabid and N. Safari, *ChemistrySelect*, 2017, **2**, 1431–1435.
- 118 T. Cai, J. Liu, H. Cao and C. Cui, *Ind. Crops Prod.*, 2020, **145**, 112155.
- 119 M. Hofmann, H. Hofmann, C. Hagelüken and A. Hool, *Sustain. Mater. Technol.*, 2018, **17**, e00074.
- 120 P. Mazo and L. Rios, *J. Am. Oil Chem. Soc.*, 2013, **90**, 725–730.
- 121 G. Rokicki, W. Kuran and B. Pogorzelska-Marciniak, *Monatshefte für Chem.*, 1984, **115**, 205–214.
- 122 J. Steinbauer, A. Spannenberg and T. Werner, *Green Chem.*, 2017, **19**, 3769–3779.
- 123 P. G. Parzuchowski, M. Jurczyk-Kowalska, J. Ryszkowska and G. Rokicki, *J. Appl. Polym. Sci.*, 2006, **102**, 2904–2914.
- 124 L. Longwitz, J. Steinbauer, A. Spannenberg and T. Werner, *ACS Catal.*, 2018, **8**, 665–672.
- 125 G. Rothenberg, *Catalysis. Concepts and Green Applications*, John Wiley and Sons, 2008.
- 126 M. Bähr and R. Mülhaupt, *Green Chem.*, 2012, **14**, 483–489.
- 127 X. Cai, P. Tolvanen, P. Virtanen, K. Eränen, J. Rahkila, S. Leveneur and T. Salmi, *Int. J. Chem. Kinet.*, 2021, **53**, 1203–1219.
- 128 A. Akhdar, K. Onida, N. D. Vu, K. Grollier, S. Norsic, C. Boisson, F. D’Agosto and N. Duguet, *Adv. Sustain. Syst.*, 2020, **5**, 2000218.
- 129 W. Y. Perez-Sena, K. Eränen, N. Kumar, L. Estel, S. Leveneur and T. Salmi, *J.*

- CO2 Util.*, 2022, **57**, 101879.
- 130 B. Grignard, J. Thomassin, S. Gennen, L. Poussard, L. Bonnaud, J. Raquez, P. Dubois, M. Tran, C. B. Park, C. Jerome and C. Detrembleur, *Green Chem.*, 2016, **18**, 2206–2215.
- 131 T. Dong, E. Dheressa, M. Wiatrowski, A. P. Pereira, A. Zeller, L. M. L. Laurens and P. T. Pienkos, *ACS Sustain. Chem. Eng.*, 2021, **9**, 12858–12869.
- 132 O. Figovsky, L. Shapovalov, O. Birukova and A. Leykin, *Polym. Sci. Ser. D*, 2013, **6**, 271–274.
- 133 S. Doley and S. K. Dolui, *Eur. Polym. J.*, 2018, **102**, 161–168.
- 134 A. Z. Yu, R. A. Setien, J. M. Sahouani, J. Docken and D. C. Webster, *J. Coatings Technol. Res.*, 2019, **16**, 41–57.
- 135 J. Pouladi, S. M. Mirabedini, H. E. Mohammadloo and N. G. Rad, *Eur. Polym. J.*, 2021, **153**, 110502–110514.
- 136 S. Jalilian and H. Yeganeh, *Polym. Bull.*, 2015, **72**, 1379–139



# CHAPTER 02

---

## IONIC LIQUID-BASED CATALYSTS FOR THE CYCLOADDITION OF CO<sub>2</sub> TO EPOXIDIZED SOYBEAN OIL

The results presented in this chapter have been published in *Molecular Catalysis* 515 (2021) 11889.



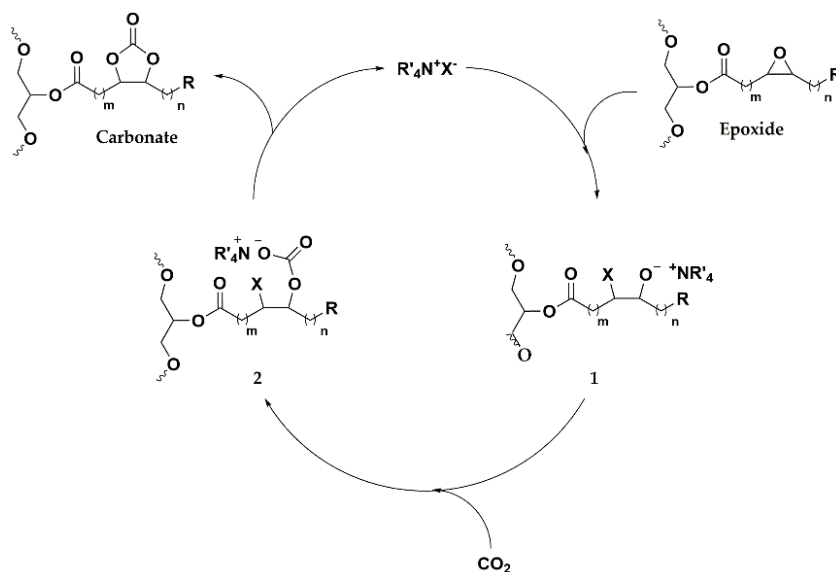
## 2.1 Background

The excessive use of petrochemical resources is considered one of the main concerns of today's society.<sup>1</sup> One of the major causes, among others, is the rise of carbon dioxide (CO<sub>2</sub>) emissions linked mainly to the human consumption of finite petrochemicals to produce energy, commodity and fine chemicals. Hence, scientists are focused on the development of processes in accordance with the Green Chemistry principles.<sup>2</sup> To achieve this ambitious goal, the finding of an abundant, largely available, renewable, low cost and non-toxic feedstock has raised as an important worldwide challenge. In this context, the storage and chemical utilization of CO<sub>2</sub>, a greenhouse gas with low toxicity and anthropogenetic produced in large amounts, has attracted considerable attention as a promising C1 building block source.<sup>3-6</sup> In fact, some value-added products are already produced using CO<sub>2</sub> as feedstock, e.g., methanol,<sup>7,8</sup> urea,<sup>9</sup> salicylic acid<sup>10</sup> among others. Noteworthy, the obtention of cyclic carbonates by atom economic cycloaddition reaction between CO<sub>2</sub> and epoxides is of great interest. As a matter of fact, cyclic carbonates are key compounds in the synthesis of daily use polymers such as non-isocyanate polyurethanes, polycarbonates etc.<sup>11,12</sup> Nevertheless, still most of the epoxides employed in the preparation of cyclic carbonates are obtained from non-renewable fossil sources.<sup>13-17</sup> Therefore, to obtain fully renewable cyclic carbonates from CO<sub>2</sub>, biomass derived epoxides are needed. Among biomass-derived epoxides, those from vegetable oils (VOs) are of special interest due to their availability and easy preparation.<sup>18</sup> In addition, the carbonated vegetable oils produced by cycloaddition of CO<sub>2</sub> to epoxidized vegetable oils offer a range of properties that makes them potentially applicable in several industries focused in the generation of bio-based products.<sup>19</sup> Among the possible applications of carbonated vegetable oils several could be highlighted: monomers for polyesters, polycarbonates and polyurethanes synthesis, industrial lubricants, fuel additives and plasticizers.<sup>17,20,21</sup> One of the plausible applications of carbonated vegetable oils with a major growth potential is their use as monomers in the synthesis of non-isocyanate polyurethanes (NIPUs) by polyaddition or polycondensation reaction with diamines.<sup>22-24</sup> Indeed, the preparation of NIPUs using cyclic and/or linear carbonates and diamines will avoid the use of the highly toxic isocyanate monomers which

handling and use is becoming more restrictive through European regulation.<sup>25</sup> Unfortunately, there are some drawbacks hampering the use of epoxidized vegetable oils and CO<sub>2</sub> as feedstocks to produce carbonated vegetable oils able to be employed as monomers in the synthesis of NIPUs. These drawbacks are the low reactivity of both the oxirane groups of the vegetable oil, mainly due to steric impediments, and the CO<sub>2</sub> molecule that due to its high stability is considered almost an inert molecule. Therefore, the production of carbonated oils by cycloaddition reaction of CO<sub>2</sub> with epoxidized vegetable oils remains a challenge.<sup>26,27</sup> These inherent problems associated to the low reactivity of the feedstocks could potentially be overcome by designing the appropriate catalytic systems or catalyst. In fact, several reports on the cycloaddition reaction of CO<sub>2</sub> to sterically hindered oleochemical internal epoxides have been reported employing different catalytic systems under moderate reaction conditions, such as combination of quaternary ammonium and phosphonium salts with metal complexes<sup>28-34</sup> or hydrogen bond donors,<sup>35,36</sup> crown ether complexes,<sup>21,37,38</sup> ionic liquids,<sup>21,39,40</sup> deep eutectic solvents<sup>41</sup> and organocatalysts.<sup>42</sup> Among the catalysts employed, probably the tetra-*n*-butylammonium bromide [TBA][Br] ionic liquid is the most widely investigated and studied one.<sup>19</sup> However, with this catalyst high temperatures (>100 °C), high CO<sub>2</sub> pressures (>25 bar), high amounts of catalyst (2-7 mol%) and long reaction times (typically >24h) are required in order to obtain good conversion and selectivity towards the desired carbonated product. Consequently, the research on new more effective, efficient, cheaper and more thermally robust catalysts is highly demanded.

Ionic liquids (ILs) are a class of compounds formed exclusively by ions with multiple applications, among them in catalysis, e.g. homogeneous, heterogenized homogeneous catalysis, biphasic systems etc.<sup>43,44</sup> ILs possess several inherent properties that make them special, among other are noteworthy good thermal and chemical stability, low toxicity, negligible vapor pressure, good solubility and easily functionalization for a chosen application.<sup>45,46</sup> Nevertheless, their use as catalysts in the cycloaddition reaction of CO<sub>2</sub> with epoxidized vegetable oils is limited and has not been widely reported with the exception of the above-mentioned IL ([TBA][Br]).<sup>21,39</sup>

The carbonation reaction mechanism proposed elsewhere in the scientific literature is shown in **Scheme 2.1**, in the first step the formation of an alkoxide intermediate takes place by the epoxide opening by a nucleophile species. This is followed by the attack of the alkoxide intermediate to the  $\text{CO}_2$  molecule forming an alkyl carbonate compound. Finally, the cyclic carbonate is obtained after an intramolecular ring-closure.<sup>29</sup> Considering the reaction mechanism, it is clear that the opening of the epoxide is a key step in the cycloaddition reaction otherwise the reaction does not take place. The opening of the epoxide can be achieved 1) by using a good nucleophile species which could be also a good leaving group to allow the formation of the carbonated product, 2) by using a hydrogen bond donor compound to increase the electrophilicity of the carbons in the epoxide ring or 3) by the combination of 1 and 2. In this regard, the bromide anion fulfills both conditions a good nucleophile and good-moderate leaving group.<sup>47</sup> In addition,  $\text{Br}^-$  nucleophilicity could be modified depending on the steric hindrance and rigidity of the selected cation which allows or not the  $\text{Br}^-$  to be close to the electron deficient carbon modifying the electrostatic interaction between them.

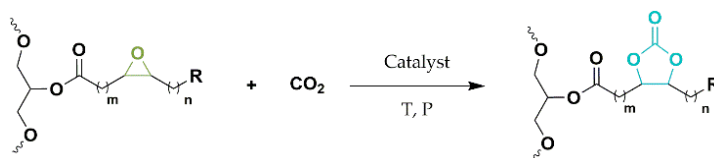


**Scheme 2.1.** General mechanism of  $\text{CO}_2$  cycloaddition to an epoxidized oil, catalysed by a tetralkylammonium halide salt.

## 2.2 Objectives

The main objective of this chapter was to find a catalytic system that improves the reaction conditions of cycloaddition reaction of CO<sub>2</sub> to epoxidized soybean oil (ESBO) to obtain the corresponding carbonated soybean oil (CSBO) under conditions that facilitate the industrial implementation of this reaction.

Due to previously described reasons and taking into account the reaction mechanism, in this work a series of economic and easy to prepare and to isolate ionic liquids based in phosphonium cation (triphenylphosphonium and tricyclohexylphosphonium) and a halogen anion (bromide or iodide) were designed, prepared, fully characterized and tested in the cycloaddition reaction of CO<sub>2</sub> to a reference ESBO to obtain CSBO (**Scheme 2.2**). The influence of the cation and the anion on the performance of the ionic liquid and several reaction parameters such as reaction temperature, catalyst concentration, total pressure and reaction time were studied and are deeply discussed. The results in terms of conversion and selectivity to the carbonated desired product are compared with the most used and reference catalyst [TBA][Br] for the studied reaction.



**Scheme 2.2.** General cycloaddition reaction of CO<sub>2</sub> to an epoxidized vegetable oil.

## 2.3 Experimental

### 2.3.1 Materials

All compounds were used as received unless otherwise stated. 1-bromobutane (99%), 1-bromooctane (99%), 1-iodooctane (98%), 1-bromododecane (97%), 1-bromohexadecane (97%) 1-bromoeicosane ( $\geq 97\%$ ) tetraphenylphosphonium bromide (97%) and tricyclohexylphosphine ( $\geq 98\%$ ) were purchased from Sigma-Aldrich. 4-

bromobutyric acid (98%) and 3-bromopropanol were purchased from Fluorochem. 8-bromooctanoic acid (>97%) was purchased from TCI. Triphenylphosphine (99%) and 1-methylimidazole (99%) were purchased from Across Organics. Tetra-n-butylammonium bromide (98 %) was purchased from Fluka. Toluene (EssentQ), n-pentane (99%), diethyl ether (EssentQ, stabilized by BHT), hexane (EssentQ, fraction from petroleum) and ethyl acetate (EssentQ) were purchased from Scharlau. Epoxidized soybean oil (ESBO) containing 4.19 mmol/g of oxirane was kindly supplied by Hebron (Spain) and the CO<sub>2</sub> (Industrial grade, 99.8%) was purchased from Nippon gases.

### 2.3.2 Synthesis and characterization of the prepared ionic liquids

Ionic liquids were synthesized following similar procedures to those already reported in the scientific literature.<sup>48,49</sup> In a typical synthesis phosphonium based ionic liquids were prepared as follows, in a 100 mL Fischer-Porter reactor under a positive nitrogen pressure, triphenylphosphine (TPP) or tricyclohexylphosphine (TCP) (19 mmol; 1.1 equiv.) was dissolved in toluene (25 mL). Then, 1 equivalent of the selected haloalkane (C < C8) compound was added dropwise and the mixture was heated at reflux temperature for 24h. After, the excess of toluene was removed by decantation and the crude product was washed with toluene (3 x 40 mL) to remove non-ionic residues, and after was washed with n-pentane (2 x 40 mL). Finally, the solid residue was dried overnight under reduced pressure. Ionic liquids based on long alkyl chains (C ≥ C8) were prepared likewise but reaction products were isolated by washing them with diethyl ether (3 x 40 mL) instead of toluene and/or pentane (see **Appendix A1**).

All prepared ionic liquids were characterized by complementary techniques described in **Methods**. The structural characterization of the ILs was determined by means of <sup>1</sup>H and <sup>31</sup>P{<sup>1</sup>H} nuclear magnetic resonance (NMR). Thermal stability was evaluated by thermal gravimetric analysis (TGA). Melting points were measured using capillary melting point technique or by differential scanning calorimetry (DSC) analysis.

### 2.3.3 Catalytic study

Catalytic experiments were carried out in a 100 mL stain-steel Autoclave. In a typical experiment the reactor was loaded with epoxidized soybean oil (ESBO, 25 g containing 104.7 mmol of oxirane) and the desired amount of the previously prepared ionic liquids as catalyst (mol% referred to the oxirane mol). Afterwards, reaction system was heated to the selected reaction temperature and subsequently purged with CO<sub>2</sub>. Then, the reactor was loaded with CO<sub>2</sub> to the desired pressure which was considered as initial reaction time. After the selected reaction time, the reactor was cooled down to room temperature and then the pressure was slowly released.

ESBO conversion into the carbonated soybean oil (CSBO) was determined by <sup>1</sup>H NMR spectroscopy. The conversion and selectivity values were calculated integrating the peaks corresponding to the cyclic carbonates (5.1-4.4 ppm); epoxides (3.25-2.8 ppm) and the unknown peak (2.4-2.3 ppm) and giving a total value to the area of 100% (see **Appendix A5**). All the experiments were performed at least twice in order to check their repeatability. The products (unreacted ESBO, carbonated oil CSBO and unknown product) were isolated by flash chromatography on silica gel (SiO<sub>2</sub>) employing hexane/ethyl acetate as eluent mixture. The epoxide number of ESBO, was determined by a potentiometric determination according to ASTM D 1652-04.

### 2.3.4 Solubility test of the employed catalysts

A solubility test of the employed catalysts was performed in the ESBO used as reaction media. In a typical test, 5 mol % of the corresponding catalyst referred to the oxirane mol was added to 25 g of ESBO containing 0.105 mol of oxirane in a round bottom flask. The mixture was heated at 120 °C for 2h. Catalyst's solubility in the ESBO reaction media was visually inspected.



## 2.4 Results and discussion

### 2.4.1 Synthesis and characterization of ionic liquids

Eleven phosphonium-based ionic liquids (**Figure 2.1 (1-11)**) were synthesized. The prepared ILs were rationally designed and selected on the bases of the cycloaddition mechanism described for [TBA][Br] ionic liquid (**Scheme 2.1**).<sup>29</sup> Consequently, bulky rigid aromatic cations such as triphenylphosphine (TPP) or bulky flexible aliphatic cations such as tricyclohexylphosphine (TCP) and Br<sup>-</sup> and I<sup>-</sup> as anions were selected. The catalytic performance of the presence of functional groups such as hydroxyl (-OH) and carboxyl (-COOH) and the length of the alkyl chain attached to the phosphorus atoms was also evaluated in the studied reaction.

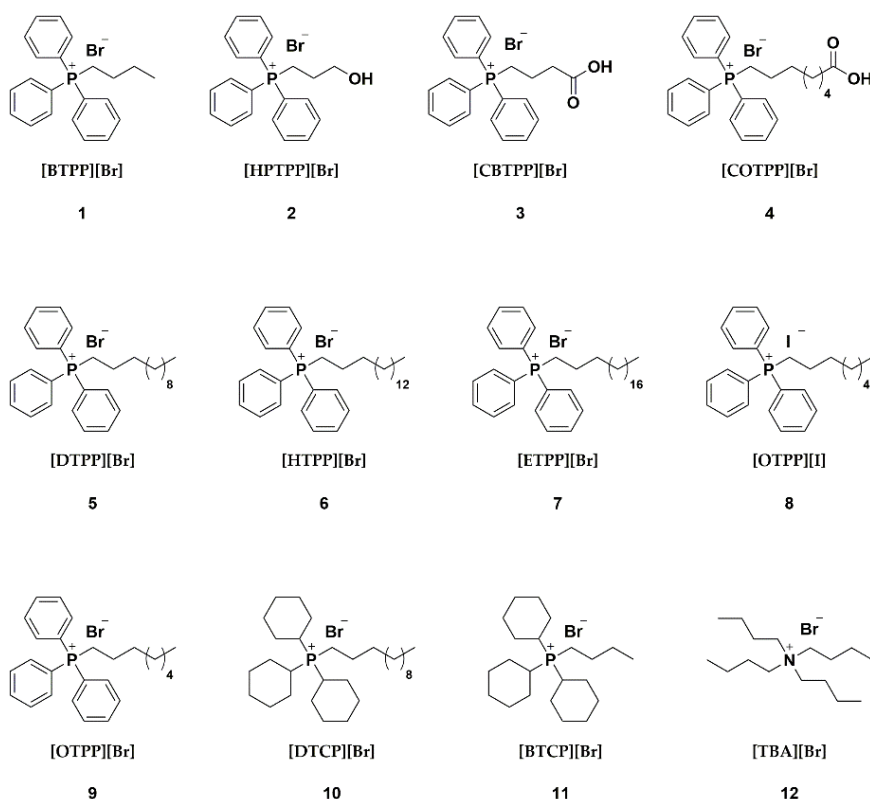


**Figure 2.1.** Prepared phosphonium-based ionic liquids (1-11) and the benchmark ionic liquid (12) employed in this work as catalysts in the cycloaddition reaction of CO<sub>2</sub> to epoxidized soybean oil.

All of the ILs were prepared from inexpensive starting materials in one step and isolated and purified in a very simple way following slightly modified procedures from those found in the scientific literature.<sup>50</sup> The purity of the prepared ILs was confirmed by <sup>1</sup>H and <sup>31</sup>P{<sup>1</sup>H} NMR spectroscopy (see **Appendix A2**) and the thermal properties (melting and stability) were measured by TGA, DSC and/or capillary technique. Within the catalytic study the synthesized ILs were compared with a commercially available IL (**Figure 2.1 (12)**) used as benchmark in the CO<sub>2</sub> cycloaddition reaction with epoxidized vegetable oils to yield carbonated vegetable oils.

The thermal stability of the prepared ionic liquids was determined by TGA. Decomposition onset temperature as well as melting points are showed in **Table 2.1**.

**Table 2.1.** Decomposition temperature ( $T_{\text{onset}}$ ) and melting temperature ( $T_{\text{m}}$ ) of the ionic liquids employed in this work.

Entry	ionic liquid	$T_{\text{onset}}$ (°C)	$T_{\text{m}}$ (°C)
1	[BTPP][Br]	304	245-247
2	[HPTPP][Br]	329	237-239
3	[CBTPP][Br]	326	251-254
4	[COTPP][Br]	318	125-128
5	[DTPP][Br]	293	101-104
6	[HTPP][Br]	291	103-105
7	[ETPP][Br]	289	108-110
8	[OTPP][I]	304	73-76
9	[OTPP][Br]	294	32-34
10	[DTCP][Br]	337	4-6
11	[BTCP][Br]	341	150-153
12	[TBA][Br]	200	102-103

All prepared ILs possess high thermal stability within the range from 287 °C to 341 °C (see **Appendix A3**). Among them, the ILs bearing the tricyclohexylphosphine moiety were found slightly more thermally stable than the ones bearing the

triphenylphosphine moiety (entry 1 *vs.* entry 11 and entry 5 *vs.* entry 10, **Table 2.1**). It is worth noticing that the benchmark IL (12) (entry 12, **Table 2.1**) shows lower thermal stability ca. 200 °C compared to all prepared ILs (1-12). This is in line with what is reported in the literature where phosphonium-based ILs are, in general, thermally more stable than ammonium-based counterparts.<sup>51</sup>

### 2.4.2 Catalytic study

ILs **1** to **11** were tested in the solvent-free synthesis of carbonated soybean oil by cycloaddition of CO<sub>2</sub> to the corresponding epoxidized soybean oil at different reaction conditions. Their performance in the investigated reaction was compared as well with the widely employed in the cited reaction and commercially available ionic liquid (**12**).

Influence of the employed ionic liquid in the studied reaction

Initially, a screening to the different “ad hoc” designed ILs was done in selected standard conditions found elsewhere in the literature for the studied reaction, 20 bar CO<sub>2</sub> pressure, 120 °C, 5 mol% catalyst referred to oxirane mol and 2h reaction. The obtained results are shown in **Figure 2.2**. As can be observed, 3 of the prepared ILs (**1**, **2** and **4**) showed negligible or very low conversion (<2 %) at the studied reaction conditions. On the other hand, 3 out of the 11 prepared ILs (**5**, **6** and **7**) achieved higher conversions than the reference catalyst (**12**). The highest conversion among the tested ILs (45.6%) was obtained with the triphenyl phosphonium-based IL (**5**) bearing a 12-carbon length alkyl chain and a Br<sup>-</sup> as anion. Slightly lower conversions 45.3% and 42.3% were also achieved with the ILs based on triphenyl phosphonium cation bearing an alkyl chain of 16 and 20 carbons length respectively and a Br<sup>-</sup> as anion (**6** and **7**). Conversion closed to the benchmark catalyst (**12**), 37.9 % was achieved with IL (**9**) bearing an alkyl chain of 8 carbons. On the other hand, the other tested IL (**1**) based on the triphenyl phosphonium cation bearing a shorter alkyl chain (C<sub>4</sub>) showed negligible conversion. The presence of a functional group, -OH or -COOH, in the alkyl chain attached to the triphenyl phosphonium cation (**2**, **3** and **4**) in the performance

of the IL in the studied reaction was also investigated. It was expected, on the basis of the reaction mechanism, that the presence of these functional groups could improve the catalytic performance in terms of conversion because these groups could contribute to make more electrophilic the carbon in the epoxide groups due to interaction with the oxygen present in the epoxide ring and consequently facilitated its opening. Nevertheless, unexpected negligible or low conversion, <10 %, was obtained. From the experimental results, it looks that the solubility of the ILs in the reaction media (epoxidized oil) is a key factor that strongly determines the performance of the studied catalyst in the investigated reaction conditions at 2h reaction time. The effect of the solubility was already evidenced in the work of dos Santos et al. by quantitative structure-property relationships modelling and exploratory analysis.<sup>52</sup> It is evident that the reaction rate is strongly dependent on the solubility of the catalyst. Considering previous statement, a study of the solubility of the different tested ILs at 5 mol % in the ESBO, 120 °C and 2h was performed. It was observed that the benchmark catalyst (**12**) was completely soluble in the reaction media at the studied conditions while among the prepared catalysts only **5**, **6**, **7** and **10** were completely soluble under identical conditions. Therefore, only this set of catalysts can be fairly compared to the benchmark catalyst **12**. All the other prepared ILs showed partial (**3**, **4**, **8**, **9** and **11**) or no solubility (**1** and **2**) at all in the studied reaction media and conditions. In fact, we do believe that the lack of solubility masks other effects that were expected to improve the catalytic performance such as alkyl length and/or the presence of -OH, -COOH functional groups in its catalytic performance. In fact, the effect of the catalyst solubility is very well evidenced in the catalytic performance if two similar ILs (**1** and **11**) are compared. The difference between them is the nature of the substituents on the phosphonium cation (aromatic *vs.* aliphatic). As shown in **Figure 2.2**, with the first one a negligible conversion is obtained while with the second one the conversion increased up to 39.5 %. This different behaviour is attributed to the by far higher solubility of the IL (**11**) with the whole-aliphatic cation in a reaction media which has more affinity for aliphatic molecules.

As expected, it has been observed that increasing the length of the alkylic chain has a beneficial effect on the solubility of the IL in the substrate. Therefore, the use of IL with longer aliphatic chains (i.e. C12) in which the solubility is not compromised, permitted us to study the effect of the nature of the phosphonium substituents on the reaction rate. A comparison of catalysts **5** and **10** showed that triphenyl-substituted salt outperformed the analogue tricyclohexyl phosphonium (45.6 % *vs.* 38.5 %). The different reactivity can be attributed to the increased rigidity of the triphenyl phosphonium fragment compared to the more flexible tricyclohexyl counterpart. The more rigid cation keeps the anion (bromide and/or the alkoxide formed during the catalytic reaction) far from the phosphorus atom weakening the electrostatic interaction between anions and the cationic centre, increasing the nucleophilic character of the anion and contributing to an easier and faster epoxide ring opening in the case of the bromide anion or facilitating the attack of the formed alkoxide to the CO<sub>2</sub> molecule to form the final cyclic carbonate.<sup>53</sup>

Concerning the selectivity to the carbonated product, with most of the ILs studied a selectivity above 96 % was achieved. Only in the case of **4** and **8** the selectivity was compromised, 64.8 % and 86.0 % respectively. If fact, <sup>1</sup>H NMR analysis of the reaction mixtures at the end of the reactions showed the formation of an “unidentified” compound (see **Appendix A5**). Intrigued to identified this “unknown” product, a flash-chromatography column was performed to isolated and characterized it. <sup>1</sup>H NMR signals between 2.3 and 2.4 ppm were ambiguously assigned to this new “unidentified” product. Unfortunately, full characterization and the final identification of the “unknown” product was not successful. Nevertheless, considering the <sup>1</sup>H NMR spectra of the isolated “unknown” product (see **Appendix A5**) and the group of signals between 4.0-4.6 ppm and between 5.2-5.4 ppm that are common in ESBO, CSBO and the “unknown” product, we do believe that the “unknown” product is not a decomposition one but most probably derives from CSBO by reaction of the later with the alkoxide resulting from the epoxide ring opening. In summary and taking into account all factors that contribute to the activity and selectivity of the prepared ILs, the catalysts **5**, **6** and **7** yielded the best results in terms of conversion and selectivity outperforming the benchmark catalyst **12** at the

same reaction conditions. Due to the slightly higher conversion achieved with catalyst 5, this IL was selected to further study of other reaction parameters such as temperature, catalysts amount, pressure and time. The benchmark catalyst 12 was also investigated at the same conditions for comparative purposes.

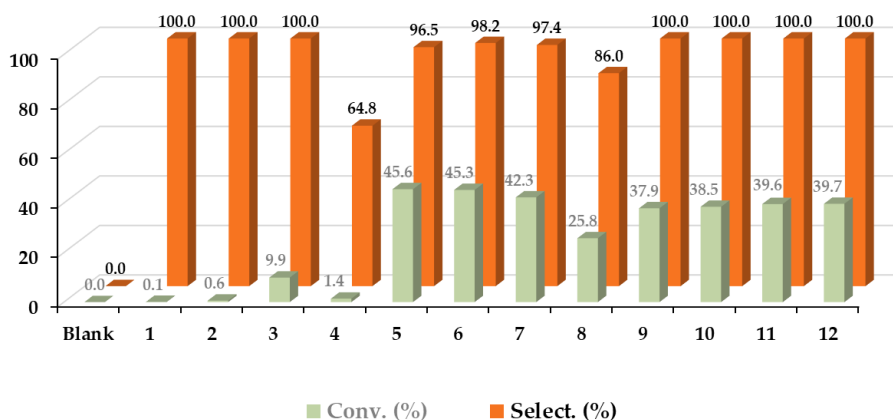


**Figure 2.2.** Conversion and selectivity of ESBO to CSBO after cycloaddition with CO<sub>2</sub> with the different ionic liquid tested as catalysts (1 to 12). Reaction conditions: temperature: 120 °C, CO<sub>2</sub> pressure: 20 bar, reaction time: 2h, 5 mol% of catalyst referred to mol of oxirane.

#### Influence of the catalyst loading

The effect of the catalyst loading (in mol% related to oxirane groups) on the solvent-free cycloaddition reaction of CO<sub>2</sub> to the ESBO was investigated with the selected catalyst 5 and compared to the benchmark catalyst 12. The explored catalyst loadings were 1, 2 and 5 mol%, respectively. The obtained results are depicted in **Figure 2.3**.

As can be seen, with both tested catalysts the conversion increases almost linearly with the catalysts amount in the studied range of concentrations. On the other hand, the selectivity towards the carbonated product was superior at 2 mol % (>99 %) with IL 5. The prepared catalyst 5 showed in all cases better performance in terms of

conversion than the benchmark catalyst **12**. In fact, catalyst **5** increases the conversion achieved by **12** in ca. 43.9%, 0.3% and 14% at 1 mol%, 2 mol% and 5 mol% of catalyst respectively. The highest increment in conversion was obtained at 1 mol % (more than 43 % increment). The better performance of catalysts **5** could be attributed to an increase of the nucleophilic character of the bromide anion due to the presence of the more sterically hindered phosphonium cation and the weaker interaction between the cation and the anion.<sup>53-57</sup>

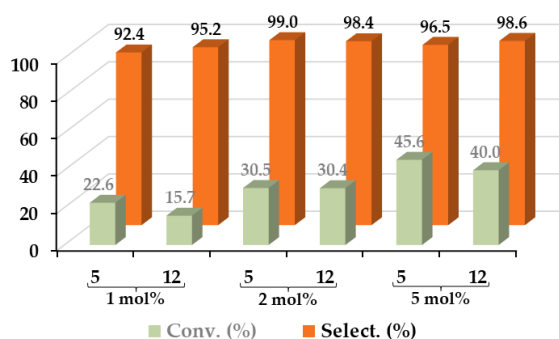


**Figure 2.3.** Conversion and selectivity of ESBO to CSBO after solvent-free cycloaddition with CO<sub>2</sub> at different mol % with catalysts **5** and the reference catalyst **12**. Reaction conditions: temperature: 120 °C; CO<sub>2</sub> pressure: 20 bar; reaction time: 2h; mol % is referred to oxirane mol.

#### Influence of the temperature

Temperature is a key parameter in many catalytic reactions influencing both conversion and selectivity to desired product. The influence of the temperature was studied in the range 60-160 °C with 2 mol% of catalyst and at 2h reaction time.

As can be observed in **Figure 2.4**, the catalytic activity of **5** surpasses that of the benchmark IL (**12**) at all the studied temperatures. In the case of catalyst **5** a continuous increase on the activity with the raise of temperature was observed. On the other hand, with the benchmark catalyst (**12**) the highest conversion was obtained at 140 °C (38.8 %) while it decreased to 26.8 % at 160 °C.

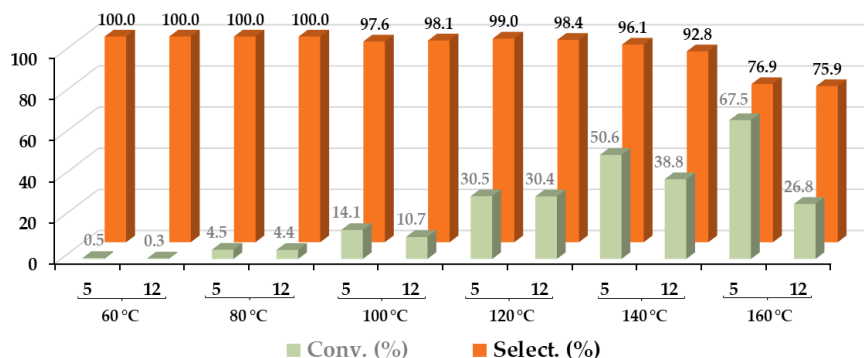


**Figure 2.4.** Conversion and selectivity of ESBO to CSBO after solvent-free cycloaddition with CO<sub>2</sub> at different temperatures with catalyst 5 and the reference catalyst 12. Reaction conditions: catalyst amount: 2 mol % referred to oxirane mol; CO<sub>2</sub> pressure: 20 bar; reaction time: 2h.

This result was somehow unexpected since the decomposition temperature of the benchmark catalyst (12) is reported to be 190 °C.<sup>59</sup> Therefore, it was decided to check the thermal stability of the two tested catalysts at the highest temperature studied by performing an isotherm thermogravimetric analysis at 160 °C for 12h. As suspected, the benchmark catalyst (12) starts degrading after less than 1h at 160 °C while the prepared catalyst 5 shows negligible or no degradation after 12h at 160 °C (Figure 2.5). This finding ambiguously explains why the conversion with 12 decreases when the temperature increases from 140 °C to 160 °C and constituted a clear advantage of IL 5 compared to the benchmark catalyst (12) for scale-up processes at high temperatures.

It is important to highlight that with both catalytic systems the selectivity towards CSBO decreases significantly at temperatures  $\geq 140$  °C, which indicates that the further decomposition of CSBO towards an unidentified product is favoured.



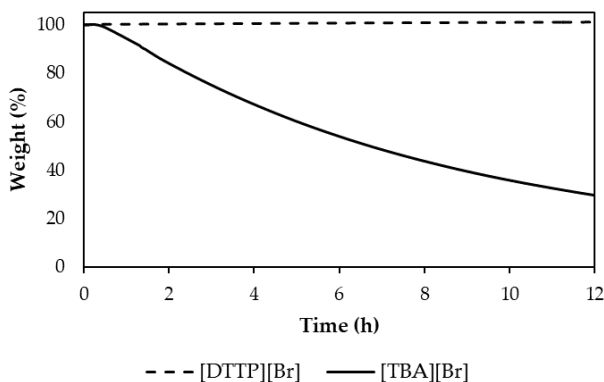


**Figure 2.5.** Catalysts 5 ([DTTP][Br]) and 12 ([TBA][Br]) isothermal thermogravimetric analysis at 160 °C.

Influence of the pressure

The effect of CO<sub>2</sub> pressure was investigated between atmospheric pressure and 40 bar at 120 °C and 2h reaction time (**Figure 2.6**).

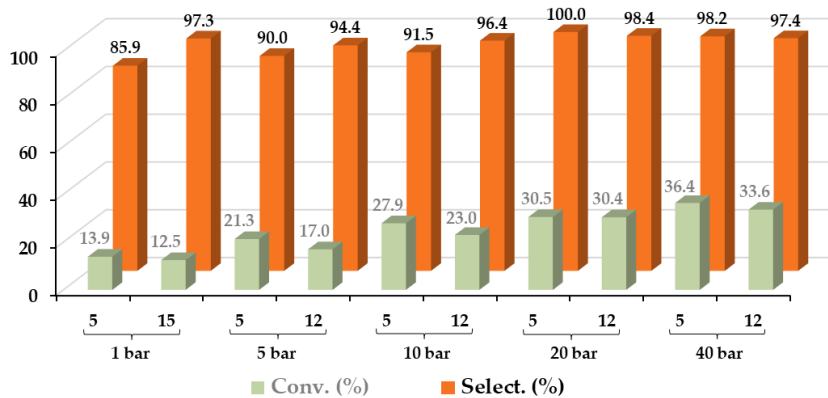


**Figure 2.6.** Conversion and selectivity of ESBO to CSBO after solvent-free cycloaddition with CO<sub>2</sub> at different pressure of CO<sub>2</sub> with catalyst 5 and the reference catalyst 12. Reaction conditions: catalyst amount: 2 mol % referred to oxirane mol; temperature: 120 °C; reaction time: 2h.

The results obtained showed that with both catalytic systems the activity increases when rising the CO<sub>2</sub> pressure. This indicates a positive contribution of the CO<sub>2</sub> partial pressure on the rate-equation law. This result is in agreement with the proposed reaction mechanism and may indicate that attack of the alkoxide intermediate to CO<sub>2</sub> could be involved in the rate-determining step of the process. Nevertheless, a change in the rate determining step depending upon the total CO<sub>2</sub> pressure cannot be discarded. Unexpectedly, an increase of the selectivity towards CSBO was also observed at higher CO<sub>2</sub> pressures with both catalytic systems. This effect could be due to a stabilizing effect of CO<sub>2</sub> avoiding further transformation of the carbonated compounds. In general, catalyst **5** and the benchmark catalyst **12** showed similar behaviour with the pressure achieving slightly higher conversion within the whole range of CO<sub>2</sub> pressures studied when the prepared catalyst **5** was employed.

Influence of the reaction time

A study to follow the conversion of the ESBO and the selectivity towards the CSBO product with time was done with the prepared catalyst **5** at the optimized reaction conditions for this system (160 °C, 40 bar CO<sub>2</sub>, 2 mol% catalyst with respect to oxirane mol). The results obtained are shown in **Figure 2.7**. Under these conditions, full conversion was achieved after 5h reaction although excellent conversions 90.5 % were already obtained after 3h. On the other hand, an excellent selectivity (≥84 %) was observed along the whole process despite the high reaction temperature employed that could contribute to further reaction of the carbonated product. These results show the potential of catalyst **5** that yield among the highest conversion of ESBO to CSBO reported in the literature so far, to the best of our knowledge. In summary, this catalyst that can be readily obtained from commercially available cheap feedstocks shows undoubtedly superior performance and stability in the solvent-free cycloaddition of CO<sub>2</sub> to ESBO reaction compared to the commercially available and widely used in this reaction benchmark catalyst **12**.

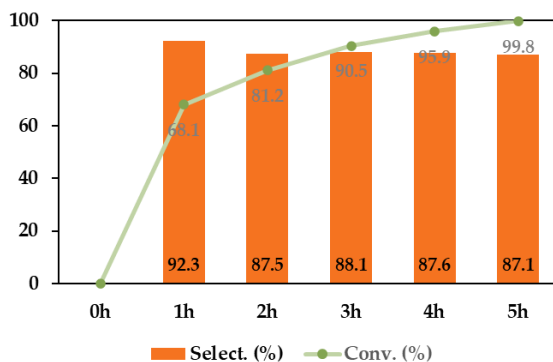


**Figure 2.7.** Conversion and selectivity of ESBO to CSBO after solvent-free cycloaddition with CO<sub>2</sub> at different reaction times with catalyst 5. Reaction conditions: catalyst amount: 2 mol % referred to oxirane mol; temperature: 160 °C; CO<sub>2</sub> pressure: 40 bar.

## 2.5 Conclusions

In the present chapter, a series of eleven ILs were rationally designed and prepared to be employed as catalyst in the obtention of CSBO by solvent-free cycloaddition reaction of CO<sub>2</sub> to ESBO. Most of the ILs were prepared in one step and isolated in a straight-forward manner from economic and widely available feedstock materials, triphenylphosphine and the corresponding haloalkane. Three out of the eleven prepared ionic liquids showed better performance than the benchmark and widely used catalysts (**12**) in this reaction. It was evidenced that the solubility of the employed ionic liquid in the ESBO reaction media is a key factor in the catalyst performance. Additionally, it was shown that the length of the alkylic chain suffices to impart the desired solubility as long as it was of at least 8 carbon atoms-length. The rigidity and the steric hindrance of the substituents on the phosphonium cation was found to affect the nucleophilic character of the Br<sup>-</sup> anion and therefore the catalyst performance that is improved in the case of the triphenylphosphonium (more rigid) compared to tricyclohexylphosphonium (more flexible). Practically full conversion >99 % and excellent selectivity toward the carbonated product 84 % was obtained with 2 mol% of catalyst **5** at 160 °C, 40 bar CO<sub>2</sub> and after 5h reaction while, at the same reaction conditions, the benchmark catalyst **12** showed less than 27% conversion due

to lack of thermal stability. In summary, at least three ionic liquids (**5**, **6** and **7**) with improved catalytic performance in terms of conversion and selectivity compared to the benchmark catalyst **12** in the solvent-free CO<sub>2</sub> cycloaddition to ESBO at moderated reaction conditions, 5h, 40 bar and 160 °C were encountered. Furthermore, these phosphonium-based ionic liquids were synthesized from commercially available and low-cost feedstocks (triphenylphosphine and bromoalkanes) in one step process and were easily isolated. The obtained CSBO can be employed as bio-based compounds with huge application in the field of biopolymers such as polyurethanes and polycarbonates.

## 2.6 References

- 1 R. P. Lee, *J. Clean. Prod.*, 2019, **219**, 786–796.
- 2 P. Anastas and N. Eghbali, *Chem. Soc. Rev.*, 2010, **39**, 301–312.
- 3 T. Sakakura, J. C. Choi and H. Yasuda, *Chem. Rev.*, 2007, **107**, 2365–2387.
- 4 M. Peters, B. Köhler, W. Kuckshinrichs, W. Leitner, P. Markewitz and T. E. Müller, *ChemSusChem*, 2011, **4**, 1216–1240.
- 5 R. Martín and A. W. Kleij, *ChemSusChem*, 2011, **4**, 1259–1263.
- 6 M. Aresta, A. Dibenedetto and A. Angelini, *Chem. Rev.*, 2014, **114**, 1709–1742.
- 7 G. A. Olah, *Angew. Chem. Int. Ed.*, 2005, **44**, 2636–2639.
- 8 S. Wesselbaum, T. Vom Stein, J. Klankermayer and W. Leitner, *Angew. Chem. Int. Ed.*, 2012, **51**, 7499–7502.
- 9 H. Wang, Z. Xin and Y. Li, *Chem. Transform. Carbon Dioxide*, 2017, **375**, 177–202.
- 10 T. Iijima and T. Yamaguchi, *Appl. Catal. A Gen.*, 2008, **345**, 12–17.
- 11 Q. W. Song, Z. H. Zhou and L. N. He, *Green Chem.*, 2017, **19**, 3707–3728.
- 12 A. J. Kamphuis, F. Picchioni and P. P. Pescarmona, *Green Chem.*, 2019, **21**, 406–

- 448.
- 13 T. Chang, X. Gao, L. Bian, X. Fu, M. Yuan and H. Jing, *Chinese J. Catal.*, 2015, **36**, 408–413.
- 14 R. L. Paddock and S. T. Nguyen, *J. Am. Chem. Soc.*, 2001, **123**, 11498–11499.
- 15 J. Meléndez, M. North and R. Pasquale, *Eur. J. Inorg. Chem.*, 2007, 3323–3326.
- 16 J. Q. Wang, D. L. Kong, J. Y. Chen, F. Cai and L. N. He, *J. Mol. Catal. A Chem.*, 2006, **249**, 143–148.
- 17 F. de la Cruz-Martínez, M. Martínez de Sarasa Buchaca, J. Fernández-Baeza, L. F. Sánchez-Barba, A. M. Rodríguez, C. Alonso-Moreno, J. A. Castro-Osma and A. Lara-Sánchez, *Organometallics*, 2021, **40**, 1503–1514.
- 18 V. M. Abbasov, F. A. Nasirov, N. S. Rzayeva, L. I. Nasirova and K. Z. Musayeva, *Ppor*, 2018, **19**, 427–449.
- 19 D. Miloslavskiy, E. Gotlib, O. Figovsky and D. Pashin, *Int. Lett. Chem. Phys. Astron.*, 2014, **8**, 20–29.
- 20 C. Carré, Y. Ecochard, S. Caillol and L. Avérous, *ChemSusChem*, 2019, **12**, 3410–3430.
- 21 B. Schäffner, M. Blug, D. Kruse, M. Polyakov, A. Köckritz, A. Martin, P. Rajagopalan, U. Bentrup, A. Brückner, S. Jung, D. Agar, B. Rüngeler, A. Pfennig, K. Müller, W. Arlt, B. Woldt, M. Graß and S. Buchholz, *ChemSusChem*, 2014, **7**, 1133–1139.
- 22 B. Nohra, L. Candy, J. F. Blanco, C. Guerin, Y. Raoul and Z. Mouloungui, *Macromolecules*, 2013, **46**, 3771–3792.
- 23 L. Maisonneuve, O. Lamarzelle, E. Rix, E. Grau and H. Cramail, *Chem. Rev.*, 2015, **115**, 12407–12439.

- 24 G. Rokicki, P. G. Parzuchowski and M. Mazurek, *Polym. Adv. Technol.*, 2015, **26**, 707–761.
- 25 *Of. J. Eur. Union*, 2009, **552**, 7–31.
- 26 F. Castro-Gómez, G. Salassa, A. W. Kleij and C. Bo, *Chem. A Eur. J.*, 2013, **19**, 6289–6298.
- 27 M. Alves, B. Grignard, R. Mereau, C. Jerome, T. Tassaing and C. Detrembleur, *Catal. Sci. Technol.*, 2017, **7**, 2651–2684.
- 28 Z. Li, Y. Zhao, S. Yan, X. Wang, M. Kang, J. Wang and H. Xiang, *Catal. Lett.*, 2008, **123**, 246–251.
- 29 J. Langanke, L. Greiner and W. Leitner, *Green Chem.*, 2013, **15**, 1173–1182.
- 30 H. Büttner, C. Grimmer, J. Steinbauer and T. Werner, *ACS Sustain. Chem. Eng.*, 2016, **4**, 4805–4814.
- 31 N. Tenhumberg, H. Büttner, B. Schäffner, D. Kruse, M. Blumenstein and T. Werner, *Green Chem.*, 2016, **18**, 3775–3788.
- 32 L. Peña Carrodegua, Cristòfol, J. M. Fraile, J. A. Mayoral, V. Dorado, C. I. Herrerías and A. W. Kleij, *Green Chem.*, 2017, **19**, 3535–3541.
- 33 A. Farhadian, M. B. Gol Afshani, A. Babaei Miyardan, M. R. Nabid and N. Safari, *ChemistrySelect*, 2017, **2**, 1431–1435.
- 34 A. Farhadian, A. Ahmadi, I. Omrani, A. B. Miyardan, M. A. Varfolomeev and M. R. Nabid, *Polym. Degrad. Stab.*, 2018, **155**, 111–121.
- 35 M. Alves, B. Grignard, S. Gennen, C. Detrembleur, C. Jerome and T. Tassaing, *RSC Adv.*, 2015, **5**, 53629–53636.
- 36 W. Natongchai, S. Pornpraprom and V. D’Elia, *Asian J. Org. Chem.*, 2020, **9**, 801–810.

- 37 P. G. Parzuchowski, M. Jurczyk-Kowalska, J. Ryszkowska and G. Rokicki, *J. Appl. Polym. Sci.*, 2006, **102**, 2904–2914.
- 38 L. Longwitz, J. Steinbauer, A. Spannenberg and T. Werner, *ACS Catal.*, 2018, **8**, 665–672.
- 39 M. Bähr and R. Mülhaupt, *Green Chem.*, 2012, **14**, 483–489.
- 40 J. Martínez, F. De La Cruz-Martínez, M. M. De Sarasa Buchaca, M. P. Caballero, R. M. Ojeda-Amador, M. D. Salvador, G. Fregapane, J. Tejada, J. A. Castro-Osma and A. Lara-Sánchez, *J. Environ. Chem. Eng.*, 2021, **9**, 105464.
- 41 W. Liu and G. Lu, *J. Oleo Sci.*, 2018, **67**, 609–616.
- 42 H. Büttner, J. Steinbauer, C. Wulf, M. Dindaroglu, H. G. Schmalz and T. Werner, *ChemSusChem*, 2017, **10**, 1076–1079.
- 43 F. D. Bobbink and P. J. Dyson, *J. Catal.*, 2016, **343**, 52–61.
- 44 A. A. Chaugule, A. H. Tamboli and H. Kim, *Fuel*, 2017, **200**, 316–332.
- 45 O. Soleimani, *J. Chem. Rev.*, 2020, **2**, 169–181.
- 46 N. Nasirpour, M. Mohammadpourfard and S. Zeinali Heris, *Chem. Eng. Res. Des.*, 2020, **160**, 264–300.
- 47 M. North and R. Pasquale, *Angew. Chem. Int. Ed.*, 2009, **48**, 2946–2948.
- 48 S. Livi, J. Duchet-Rumeau, T. N. Pham and J. F. Gérard, *J. Colloid Interface Sci.*, 2010, **349**, 424–433.
- 49 M. Liu, L. Liang, T. Liang, X. Lin, L. Shi, F. Wang and J. Sun, *J. Mol. Catal. A Chem.*, 2015, **408**, 242–249.
- 50 H. Büttner, J. Steinbauer and T. Werner, *ChemSusChem*, 2015, **8**, 2655–2669.
- 51 J. Luo, O. Conrad and I. F. J. Vankelecom, *J. Mater. Chem.*, 2012, **22**, 20574–20579.

- 52 V. H. J. M. dos Santos, D. Pontin, R. S. Rambo and M. Seferin, *J. Am. Oil Chem. Soc.*, 2020, **97**, 817–837.
- 53 J. Sun, L. Wang, S. Zhang, Z. Li, X. Zhang, W. Dai and R. Mori, *J. Mol. Catal. A Chem.*, 2006, **256**, 295–300.
- 54 M. M. Dharman, J. I. Yu, J. Y. Ahn and D. W. Park, *Green Chem.*, 2009, **11**, 1754–1757.
- 55 L. Han, S. J. Choi, M. S. Park, S. M. Lee, Y. J. Kim, M. I. Kim, B. Liu and D. W. Park, *React. Kinet. Mech. Catal.*, 2012, **106**, 25–35.
- 56 S. Narang, D. Berek, S. N. Upadhyay and R. Mehta, *J. Polym. Res.*, 2016, **23**, 1–8.
- 57 L. Wang, T. Huang, C. Chen, J. Zhang, H. He and S. Zhang, *J. CO<sub>2</sub> Util.*, 2016, **14**, 61–66.
- 58 R. J. Wei, X. H. Zhang, B. Y. Du, Z. Q. Fan and G. R. Qi, *J. Mol. Catal. A Chem.*, 2013, **379**, 38–45.
- 59 K. M. Doll and S. Z. Erhan, *J. Agric. Food Chem.*, 2005, **53**, 9608–9614.



# CHAPTER 03

---

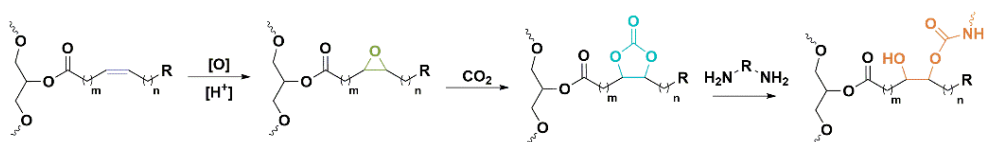
SYNTHESIS AND CHARACTERIZATION  
OF CARBONATED  
SOYBEAN OIL-BASED  
NON-ISOCYANATE POLYURETHANES



### 3.1 Background

The current tendency in both academia and industry is to develop safer and sustainable processes and products. One of the materials that has gained great interest due to its close relationship with Green Chemistry is cyclic carbonates. In fact, the most common and industrially established route for the manufacturing of these products is the cycloaddition of carbon dioxide (CO<sub>2</sub>) to epoxide rings.<sup>1</sup> This route, in addition to showing 100% atomic efficiency, allows the use of a renewable, non-toxic and widely available reagent, CO<sub>2</sub>. Moreover, another feature that brings green character to the process is the possibility of using epoxides from bio-based origin, thus discarding/reducing the use of petrochemical raw materials.<sup>2-5</sup> This has prompted the scientific community to use cyclic carbonates in several fields. Indeed, cyclic carbonates have demonstrated their usefulness in a wide range of applications.<sup>6,7</sup> Especially they have shown potential as starting reagent for the chemical synthesis of "green polyurethanes", allowing to avoid toxic compounds such as phosgene or isocyanates.<sup>8-10</sup> As already mentioned in **Chapter 1**, the reaction of cyclic carbonates with amines generates non-isocyanate polyurethanes (NIPUs), providing a safe and suitable route comparing with conventional synthesis of polyurethanes (PUs), which is based on the reaction of toxic isocyanates and polyols. Hence, due to increasing safety and environmental concerns, researchers have focused their efforts on the development of NIPUs based on renewable sources and CO<sub>2</sub> by polyaddition of cyclic carbonates and amines.

As stated in **Chapter 1**, the several types of vegetable oils (VOs) and their derivatives make them one of the most widely used sources for the synthesis of bio-based polymers, which also includes non-isocyanate polyurethanes. Since Tamami and his co-workers first developed isocyanate-free polyurethanes from oils, the polyaddition reaction between carbonated oils or derivatives and amines has been studied in detail to obtain vegetable oil-based NIPUs (**Scheme 3.1**).<sup>11-28</sup> In many of these works, the influence of several elements, such as the amine structure, carbonate amount, cyclic carbonate amine ratio, and oil type on the final polymer properties has been studied.



**Scheme 3.1.** Route to NIPUs from vegetable oils.

The amine structure has an impact in numerous properties of the final PU. Amines with a rigid structure (aromatic and cycloaliphatic) provide higher Young's modulus, tensile strength and glass transition temperature ( $T_g$ ) than aliphatic amines. In contrast, NIPUs based on carbonated oils and flexible amines show higher elongation at break than their cyclic analogues.<sup>14,15,18</sup> On the other hand, amine functionality is also one of the factors that plays a role in carbonated oil-based NIPUs properties. Increasing the number of functional groups enhances cross-linking density, which results in a higher  $T_g$  and tensile strength comparing with bifunctional analogues.<sup>11</sup>

Another factor that makes possible to obtain polymeric networks with very diverse properties is the percentage of carbonate groups present in the oil. The use of a monomer with a high carbonate content, provides polymeric networks with a higher value of Young's modulus, tensile strength, glass transition temperature, hardness and adhesion in relation to monomers with a lower percentage of carbonates.<sup>13,14,26,29</sup> This results from the fact that these properties are closely related with cross-linking degree and hydroxyl groups concentration. Nevertheless, some properties related to final product applicability, such as anticorrosion properties or capacity to be foamed, are improved by using an oil with lower carbonate content.<sup>17,26</sup>

The amine/cyclic carbonate molar ratio has a significant effect on final product properties. An excess of amine leads to side reaction, harming the crosslinking degree, and therefore decreasing properties such as tensile strength or hardness. Below amine equimolar ratios (excess of cyclic carbonate) amide formation is hardly noticeable. However, not complete cyclic carbonate conversion is obtained, which results in low tensile strength and hardness due to the low cross-linking degree.<sup>11,12,15,18,30</sup>

Another relevant aspect that determines properties of NIPUs is the type of vegetable oil used as precursor. So far, soybean oil has been one of the most used oleochemicals due to its low cost and abundance. However, in recent years other oils such as linseed or algae-derived triglycerides have been used for this goal. Dong et al. evidenced that cyclic carbonate reactivity is one of the factors most influenced by oil type.<sup>28</sup> Indeed, triglycerides with higher carbonate density show greater reactivity associated to the cascading effect of neighbouring groups. Nonetheless, the greater reactivity negatively affects formulation handling, since the gel formation happens before 1 minute, limiting the use of high iodine number oils (algae oil) under standard laboratory conditions. Furthermore, just as high carbonate percentage oils, triglycerides with great carbonate ring density show higher glass-transition temperature and Young's modulus.<sup>14,28</sup>

The influence of carbonate content, amine type or molar ratio in the polymer properties evidence that the variation of these factors could facilitate the development of a new NIPU family with a wide range of properties. This fact indicates that vegetable oil-based NIPUs could be considered a material as versatile as the PUs obtained from the conventional route. This opens the door to the use of vegetable oil-based NIPUs in different fields and applications.

In spite of the potential of vegetable oil-based NIPUs to replace traditional isocyanate-based PU, until now, the research has focused on their synthesis rather than assessing their performance and comparing the NIPUs with vegetable oil-based PU. Not having a direct comparative analysis of the NIPUs with the traditional PU makes difficult to know their potential to substitute them.

## 3.2 Objectives

The main objective of this chapter was to obtain NIPUs with differing features using previously synthesized carbonated soybean oil (CSBO) as a precursor, as well as to determine whether these NIPUs have the potential to replace conventional vegetable oil-based PUs.

To simplify the process and facilitate the industrial implementation, one of the goals of this chapter was to verify that CSBO can be used without purification. For that goal, the influence of the ionic liquid catalyst was studied in a model reaction between monofunctional cyclic carbonate and amine. The main objective of the chapter was to perform a systematic study of the main factors influencing final NIPUs properties, such as molar ratio and amine structure. The synthesis was accompanied by a detailed study of the properties of soybean oil-based NIPUs through a series of characterization techniques to analyse the influence of these parameters in the final properties and determine the versatility of these bio-based NIPUs. A comparison of the properties obtained with those of traditional vegetable oil-based PUs was also carried out.

### 3.3 Experimental

#### 3.3.1 Materials

All the compounds were used as received. 1-bromododecane (97%), 4,4'-methylenebis(cyclohexylamine) (MBCHA, 95%) and cyclohexylamine (CHA, 99%) were purchased from Sigma-Aldrich. 1,8-diaminooctane (DAO, >98%) was purchased from TCI. Propylene carbonate (PPC, 99.5%), n-dodecane (99%) and triphenylphosphine (99%) were purchased from Across Organics. Priamine 1074 was kindly supplied by Covestro. Diethyl ether (EssentQ, stabilized by BHT), dichloromethane (EssentQ, stabilized with approx. 50 ppm of amylene), ethyl acetate (EssentQ) and tetrahydrofuran (THF, 99%) were purchased from Scharlau. Epoxidized soybean oil (ESBO) containing 4.19 mmol/g of oxirane was kindly supplied by Hebron (Spain) and the CO<sub>2</sub> (Industrial grade, 99.8%) was purchased from Nippon gases.

### 3.3.2 Synthesis and characterization of CSBO

Carbonated soybean oil synthesis was performed based on the results obtained in **Chapter 2**. For the preparation of the carbonated oil, a 300 mL stain-steel Parr reactor was loaded with epoxidized soybean oil (ESBO, 150 g containing 628.6 mmol of oxirane) and previously prepared dodecyltriphenylphosphonium bromide ([DTPP][Br]) as catalyst (2 mol% referred to oxirane). Afterward, the reaction system was heated to 160 °C and subsequently purged with CO<sub>2</sub>. Then, the reactor was loaded with 40 bar of CO<sub>2</sub> which was kept constant during the synthesis process. The gas loading time was considered as initial reaction time. After 5h, the reactor was cooled down to room temperature and then the pressure was slowly released. ESBO conversion and selectivity into the CSBO was determined by <sup>1</sup>H NMR spectroscopy. The peak presented in all triglyceride structures at 5.3 ppm (1H) was used as internal standard and the peaks corresponding to the cyclic carbonates (5.1-4.4 ppm), epoxides (3.25-2.8 ppm) and the unknown peak (2.4-2.3 ppm) were integrated and giving a total value to the area of 100%.

Synthesized CSBO was characterized by complementary techniques described in **Methods**. The structural characterization of the prepared CSBO was determined by means of nuclear magnetic resonance (NMR) and Fourier Transform Infrared Spectroscopy (FTIR) equipped with universal Attenuated Total Reflection (ATR) sampling accessory. The epoxide number of ESBO, was determined by a potentiometric determination according to ASTM D 1652-04.

### 3.3.3 Influence of [DTPP][Br] in the reaction between cyclic carbonate and amine

The synthesis of a urethane compound from PPC and CHA was carried out in a 50 mL three neck glass steel reactor equipped with a mechanical stirrer, temperature controller and water condenser. The reactor was loaded with PPC (20.4 g, 200 mmol) and [DTTP][Br] (2 mol% referred to PPC) (in case where catalyst was added). Afterwards the reaction system was heated to 70 °C and subsequently the amine (19.8

g, 200 mmol) was added dropwise, end of addition is considered as initial reaction time. FTIR and GC-MS characterization techniques were used to monitor the reaction described in **Methods**. The changes in the chemical composition of monomers were monitored by Fourier Transform Infrared Spectroscopy (FTIR) equipped with universal Attenuated Total Reflection (ATR) sampling accessory. Gas Chromatography Mass Spectrometry detector (GC-MS) was used for the monitorization of the PPC conversion and unreacted monomer using n-dodecane as an internal standard directly from the crude reaction mixture.

### 3.3.4 Synthesis and characterization of CSBO-based NIPUs

Before preparing CSBO-based NIPUs, in order to eliminate CO<sub>2</sub> bubbles and avoid their formation of it in final film it is necessary to treat the carbonated soybean oil with ultrasound process. The CSBO (150 g) product was dissolved in ethyl acetate (200 mL) until a low viscosity solution was obtained. This was introduced in ultrasound bath under stirring, at 40 °C for 3-4h. Finally, ethyl acetate was eliminated under vacuum.

To obtain NIPU networks, CSBO was mixed with the corresponding amine at different molar ratios without using any solvent and catalyst. In a typical synthesis CSBO-based NIPU networks were prepared as follows: In a 250 mL glass reactor, CSBO (50 g; 171.8 C=O mmol) was mechanically stirred under vacuum at 60 °C until no more bubbles were observed. This process was done to remove and avoid new bubbles formation. Then, vacuum was removed, and amine (137.4-206.1 mmol) was added little by little and mixed by five minutes. Afterwards, the prepared formulations were poured into a Teflon mould (10 cm × 5 cm × 0.5 cm) and cured at 70 °C for 24h, and then for 6h at 100 °C. For coatings, the prepared formulations were applied on degreased aluminium panels using a manual film applicator Model Baker from Neurtek Instruments with a thickness of 100 µm and cured at same conditions. After curing, yellowish coatings and free films were obtained.

Synthesized isocyanate-free polyurethanes were characterized one week after the end of the curing process, to ensure that complete curing. For this purpose, different



complementary techniques described in **Methods** were used. The structural analysis of the prepared CSBO-based NIPUs was performed by Fourier Transform Infrared Spectroscopy (FTIR) equipped with universal Attenuated Total Reflection (ATR) sampling accessory. The thermal analysis of the NIPUs was analysed by thermal gravimetric analysis (TGA) and differential scanning calorimetry (DSC). The cross-linking degree was determined by swelling index (SI) and gel-content (GC) in THF. The pencil hardness and impact resistance of the prepared CSBO-based NIPU coatings were determined according to ASTM D 3363-20 and ISO 6272-1:2012, respectively.

## 3.4 Results and discussion

### 3.4.1 Synthesis and characterization of CSBO

Carbonated soybean oil (CSBO) was prepared by CO<sub>2</sub> cycloaddition to epoxidized soybean oil (ESBO) and according to the conditions previously established in **Chapter 2**.

Successful conversion of epoxide group (ESBO) into cyclic carbonate group (CSBO) was confirmed by ATR-FTIR and <sup>1</sup>H NMR. In **Figure 3.1-a** ATR-FTIR spectra provided the evidence of the CO<sub>2</sub> cycloaddition reaction to epoxide group. The total disappearance of epoxide characteristic bands (840 and 820 cm<sup>-1</sup>) confirmed the complete conversion of ESBO. This is consistent with the formation band associated to cyclic carbonate localized at 1800 cm<sup>-1</sup> and ascribed to C=O group stretching vibration. Conversion of ESBO to CSBO was also confirmed by <sup>1</sup>H NMR analysis (**Figure 3.2-b**). The disappearance of peaks at 3.1-2.7 ppm corresponding to C–H in  $\alpha$ -position of epoxide ring, together with the formation of new peaks at 5.1-4.6 ppm associated to C–H in  $\alpha$ -position of cyclic carbonate corroborate the total conversion of epoxide and the formation of CSBO. The results obtained suggested that highly carbonated soybean oil (yield: 84%) was obtained at 160 °C, 40 bar and 5h, using [DTPP][Br] as catalyst.

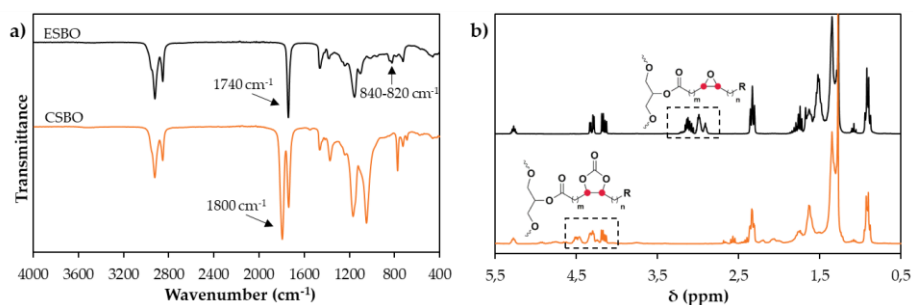


**Figure 3.1.** Comparative ATR-FTIR (a) and  $^1\text{H}$  NMR spectra of the ESBO and CSBO.

### 3.4.2 Influence of [DTTP][Br] in the reaction between cyclic carbonate and amine

After the synthesis of the CSBO and before polymerization, the carbonated oil was not purified to simplify the process and facilitate the industrial implementation. Normally, the separation process of these ionic liquids and carbonated oils is based on a liquid-liquid extraction, which restricts their industrial use. Therefore, to determine the influence of the presence of the catalyst ([DTTP][Br]) on the reaction between cyclic carbonates and amines, propylene carbonate (PPC) and cyclohexylamine (CHA) were chosen as model molecules for CSBO and methylenebis(cyclohexylamine) (MBCHA), respectively. The model reaction between PPC and CHA was carried out at 70 °C for 24h, with and without catalyst, and monitored by FTIR and GC-MS.

**Figure 3.2** shows the reaction monitoring by FTIR. In both cases (with and without catalyst), the disappearance of the C=O stretching vibration band of the cyclic carbonate ( $1800\text{ cm}^{-1}$ ), together with the formation of the O–H and N–H stretching vibration band ( $3400\text{--}3300\text{ cm}^{-1}$ ), urethane C=O stretching vibration band ( $1690\text{ cm}^{-1}$ ) and N–H bending vibration ( $1550\text{ cm}^{-1}$ ) band, associated with hydroxyurethane formation, verified the reaction between PPC and CHA. Moreover, the results showed that at different times the influence of the catalyst was negligible (neither positive nor negative).

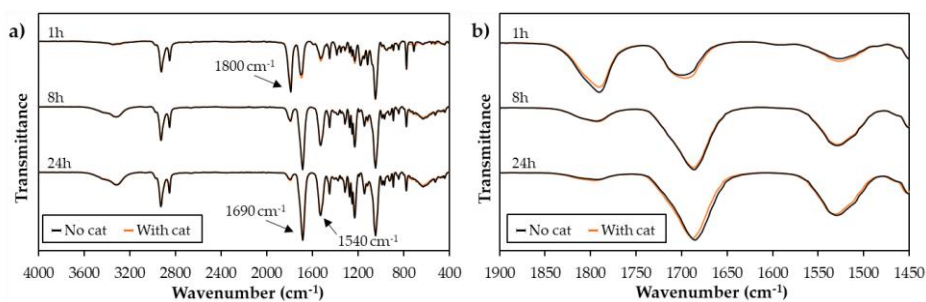


**Figure 3.2.** ATR-FTIR spectra of the reaction between PPC and CHA at different reaction time in a wavelength range of a) 4000-400  $\text{cm}^{-1}$  and b) 1900-1450  $\text{cm}^{-1}$ .

Through GC-MS it was possible to determine the amount/concentration of PPC throughout the reaction. **Figure 3.3** shows the evolution of PPC conversion in the reactions with and without catalyst.

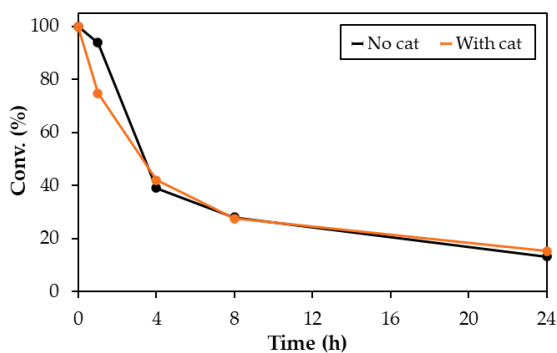


**Figure 3.3.** PPC conversion values at different reaction times, measured by GC-MS.

As can be seen, the conversion of PPC was very similar in the reactions with and without catalyst. The main difference is observed in the first steps of the reaction (1h), where the presence of [DTPP][Br] seems to positively influence the activity compared to the reaction without catalyst (75% *vs.* 94%). However, after 4h of reaction the PPC conversion in both reactions was practically the same until 24h of reaction. Therefore, the FTIR and GC-MS analysis suggest that the presence of [DTPP][Br] does not affect the reactivity between PPC and CHA, allowing to keep the catalyst used in the synthesis of CSBO, in the polyaddition process.

### 3.4.3 Synthesis and characterization of CSBO-based NIPUs

As pointed out above in this chapter, the PUs synthesized via traditional synthesis are limited by process safety and the use of precursors that will not be able to comply with the environmental concern. As previously mentioned in the previous sections, NIPUs from carbonated oils may be a possible solution to develop more sustainable materials. The properties of the prepared CSBO-based NIPUs are detailed in **Table 3.1**.

**Table 3.1.** CSBO-based NIPUs experimental data from DSC, TGA and THF absorption.

Formulations	DSC		TGA			THF absorption		
	$T_g$ (°C)	$T_{5^a}$ (°C)	$T_{50^b}$ (°C)	$T_{Stage\ 1^c}$ (°C)	$T_{Stage\ 2^d}$ (°C)	$T_{Stage\ 3^e}$ (°C)	SI (%)	GC (%)
NIPU MBCHA <sup>g</sup>	21	273	411	335	390	465	897	46
NIPU DAO <sup>h</sup>	1	261	415	324	403	469	282	71
NIPU Priamine 0.8	-25	304	438	321	409	466	555	72
NIPU Priamine 1.0	-18	304	449	321	- <sup>f</sup>	465	503	74
NIPU Priamine 1.2	-29	304	451	320	- <sup>f</sup>	466	604	37

<sup>a</sup>Temperature in which the NIPU loss 5 wt% of its initial mass; <sup>b</sup>Temperature in which the NIPU loss 50 wt% of its initial mass; <sup>c</sup>Temperature for maximum weight loss related with urethane group decomposition; <sup>d</sup>Temperature for maximum weight loss related with ester group decomposition; <sup>e</sup>Temperature for maximum weight loss related with ether bonds and aliphatic hydrocarbon decomposition; <sup>f</sup>The degradation stage maximum is not visible; <sup>g</sup>MBCHA: 4,4'-methylenebis(cyclohexylamine); <sup>h</sup>DAO: 1,8-diaminooctane.

## Influence of molar ratio in CSBO-based NIPUs

In order to investigate the effect of amine/cyclic carbonate ratio on the resulting NIPU performances, different molar ratios (0.8, 1.0 and 1.2) were employed to synthesize CSBO-based NIPUs using bio-based priamine as amine precursor.

The structures of the prepared NIPU were confirmed by ATR-FTIR. **Figure 3.4** shows the ATR-FTIR of the starting CSBO and the prepared CSBO-based NIPUs at different molar ratios.

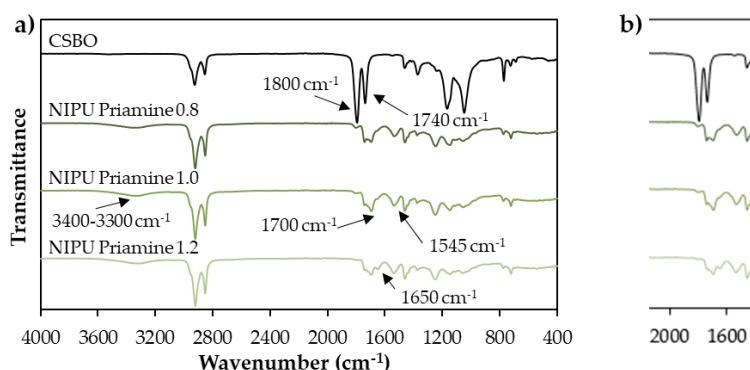
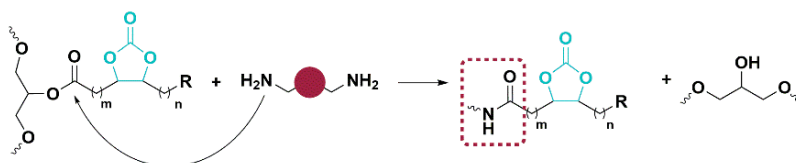


**Figure 3.4.** ATR-FTIR spectra of CSBO and the prepared CSBO-based NIPUs with priamine at different amine/cyclic carbonate molar ratio: a) Wavenumber 400-4000  $\text{cm}^{-1}$  and b) wavenumber 1500-2000  $\text{cm}^{-1}$

In the CSBO FTIR spectra, the C=O stretching vibration band of the cyclic carbonate at 1800  $\text{cm}^{-1}$  and the C=O stretching vibration band of the ester group present in triglyceride structure at 1740  $\text{cm}^{-1}$  are clearly observed. After curing process, the presence of a residual band at 1800  $\text{cm}^{-1}$  (cyclic carbonate C=O stretching vibration), together with the presence of polyhydroxyurethanes (PHUs) characteristic bands at 3400-3300  $\text{cm}^{-1}$  (O-H and N-H stretching vibration), 1700  $\text{cm}^{-1}$  (urethane C=O stretching vibration) and 1545  $\text{cm}^{-1}$  (N-H bending vibration), confirmed carbonate conversion and NIPU formation. The intensity of cyclic carbonate band in the prepared formulation shows that the conversion increased proportionally with the amount of amine used. In fact, at amine/cyclic carbonate molar ratio of 1.2, this band is hardly distinguishable. However, the formation of a new band at 1650  $\text{cm}^{-1}$  assigned

to the amide C=O vibration, suggest the presence of a side reaction. This fact was also observed by other authors in the synthesis of vegetable oil-based NIPUs, which associated the side band to the aminolysis of ester group present in triglyceride structure (**Scheme 3.2**).<sup>12,15,18,28</sup> The NIPUs prepared with an amine/cyclic carbonate molar ratio of 0.8 and 1.0, showed a residual shoulder at this wavelength, suggesting that the transesterification reaction is negligible. Additionally, at a molar ratio lower to equimolar ratios (0.8), the ester band intensity was greater than urethane band. Nevertheless, at an amine/cyclic carbonate ratio of 1.2, the amide absorption band is clearly visible. This evidences that the excess of amine enhances amide formation through transesterification side reaction.



**Scheme 3.2.** Amide formation via triglyceride ester group transesterification.

The influence of the molar ratio on the glass transition temperature ( $T_g$ ) was investigated by comparing the values obtained in NIPUs composed by Priamine at different molar ratios. The  $T_g$  obtained by DSC analysis of the Priamine-containing polymers at different molar ratios are represented in **Figure 3.5** and given in **Table 3.1**. The data showed  $T_g$  between  $-29\text{ }^\circ\text{C}$  and  $-18\text{ }^\circ\text{C}$ , following this order:  $T_{g\text{ NIPU Priamine } 1.0} > T_{g\text{ NIPU Priamine } 0.8} > T_{g\text{ NIPU Priamine } 1.2}$ . At amine/cyclic carbonate molar ratio of 0.8, in which the control of the transesterification reaction was higher, the  $T_g$  increased with the amount of amine. The enhancement of  $T_g$  with increasing stoichiometric ratio may be the result of a lower mobility of the chains as the density of the polymeric network increased. This means that a higher degree of crosslinking was obtained with at high stoichiometric ratio, which is in line with the FTIR results discussed above. However, by increasing amine amount to 1.2 amine/cyclic carbonate molar ratio, the lowest  $T_g$  value was obtained. As mentioned in FTIR results, at amine excess ester group aminolysis occurred to large extend, which led the cleavage of the polymeric network decreasing cross-linking degree (**Figure 3.8**). Therefore, this behaviour may be the

responsible of the lowest  $T_g$  observed using an excess of amine and demonstrated the influence of the molar ratio in NIPUs thermal properties.

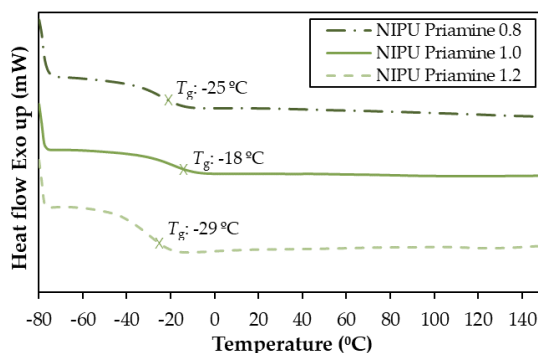


**Figure 3.5.** Comparative DSC curves of the prepared CSBO-based NIPUs with priamine at different amine/cyclic carbonate molar ratio.

As **Table 3.1** shows, the thermal stability in terms of weight loss, was very similar at different molar ratios, exceeding the 300 °C at 5 wt% loss ( $T_5$ ) and 440 °C at 50 wt% loss ( $T_{50}$ ). Nevertheless, as can be seen in **Figure 3.6**, the degradation behaviour was different for NIPUs developed at amine/cyclic carbonate molar ratio of 0.8 and those prepared at a molar ratio equal or greater to equivalent ratios (1.0 and 1.2). It has been reported that the thermal decomposition of NIPUs composed by urethanes and ester groups is based in a triple weight loss trend. The first step is associated to urethane group degradation, the second one with ester group degradation, and the last one, with ether bonds and aliphatic hydrocarbon chains degradation.<sup>31,32</sup> The same behaviour was observed at amine/cyclic carbonate molar ratio of 0.8, where the second degradation step associated with the decomposition of the ester group was well defined in contrast to molar ratio of 1.0 and 1.2. In these cases, the last two degradation stages were merged (**Figure 3.6-b**). The absence of the maximum corresponding to the ester degradation step can be explained by results obtained in FTIR. As it has been mentioned in FTIR results, the excess of amine led to amide formation via transesterification reaction (**Scheme 3.2**). As the concentration of ester group is lower, the intensity of its degradation step is lower too. However, at equivalent molar ratio the formation of amide was hardly noticeable by FTIR.

Therefore, the absence of ester group at this molar ratio may be associated to another factor rather than to the excess of amidation. One of the possible reasons could be that the high molecular weight of the repeating unit leads to a low concentration of the ester group, hindering a well-defined second degradation step.

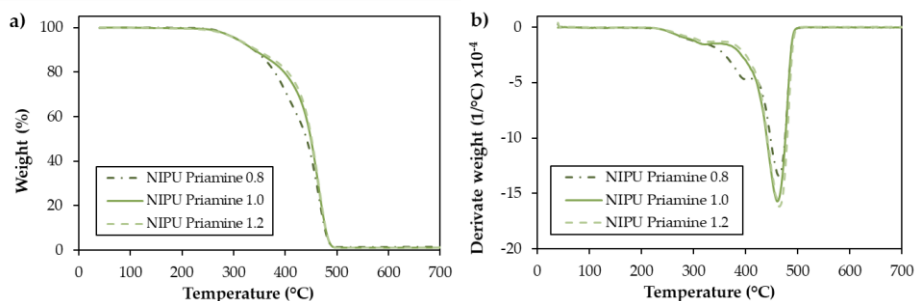


**Figure 3.6.** Comparative thermal profiles of the prepared CSBO-based NIPUs with priamine at different amine/cyclic carbonate molar ratio: a) TG curves and b) dTG curves.

Swelling index (SI) and gel-content (GC) measurements of NIPU materials were performed to study the molar ratio influence in cross-linking degree of CSBO-based NIPUs containing Priamine. Lowest SI and highest GC correspond to the maximum cross-linking of polymer network.<sup>33</sup> Generally, these measurements largely depend on the (1) cross-linking density of the polymers, (2) interaction between polymer and solvent, (3) and the type of amine. As can be observed in **Figure 3.7**, amine/cyclic carbonate molar ratio influenced in SI and GC.

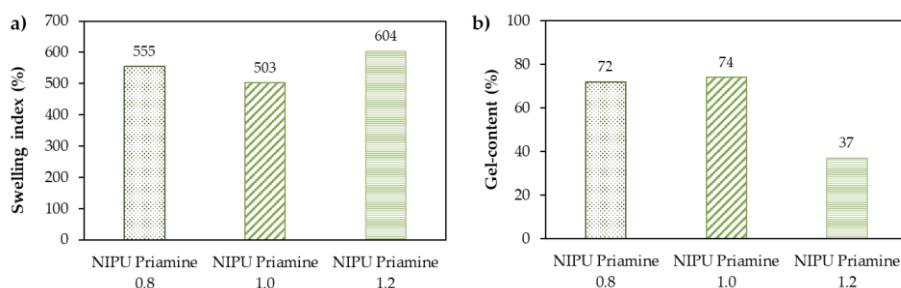


**Figure 3.7.** Comparative SI and GC of the prepared CSBO-based NIPUs with priamine at different amine/cyclic carbonate molar ratio.



The lowest SI and the highest GC was reached at stoichiometry balance. At not stoichiometry amine/cyclic carbonate molar ratios (1.2 and 0.8), the swelling index increased, and gel content decreased. As we concluded from the FTIR results, in the NIPU synthesized with amine/cyclic carbonate molar ratio of 1.2, the amine excess caused chain cleavage (**Figure 3.8**), leading to low crosslink density. Consequently, the NIPU was more susceptible to solvent penetration, which result in the NIPU with highest SI and lowest GC. On the other hand, at amine/cyclic carbonate molar ratio of 0.8 lower cyclic carbonate conversion was obtained, which led to lower cross-linking degree and hence, solvent penetration was facilitated, increasing the SI. Nevertheless, the GC was quite good, achieving a polymeric network with a superior cross-linking of 70%. At amine/cyclic carbonate molar ratio of 1.0, high cyclic carbonate conversion, together with moderate amide formation (polymer network cleavage), caused lower solvent uptake (SI) and weight loss (GC). Hence, these findings revealed that the NIPU synthesized at stoichiometric balance, reached the highest degree of crosslinking due to its lower SI and higher GC. These results are in accordance with the  $T_g$  values obtained for the polymeric network(**Table 3.1**).

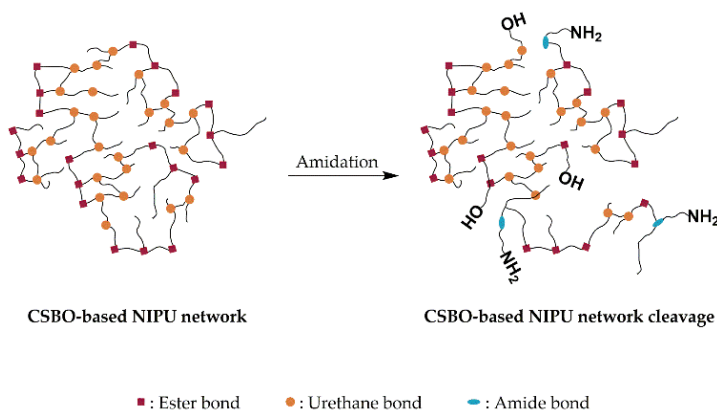


**Figure 3.8.** Thermoset CSBO-based NIPU network cleavage.

#### Influence of amine structure in CSBO-based NIPUs

With the aim of developing materials with different properties and learn about the versatility of CSBO-based NIPUs, three formulations dependent of amine structure

were prepared by step-growth melt polymerization between CSBO and three types of amines: rigid petro-based cycloaliphatic methylenebis(cyclohexylamine) (MBCHA, NIPU MBCHA), petro-based open-chain 1,8-diaminooctane (DAO, NIPU DAO) and bio-based dimeric fatty Priamine 1074 (Priamine, NIPU Priamine). The amine/cyclic carbonate molar ratio was fixed at 1.0 for all the formulations due to the good conversion/cross-linking degree ratio. **Figure 3.9** illustrates the structure of the amine employed for the synthesis of CSBO-based NIPUs.

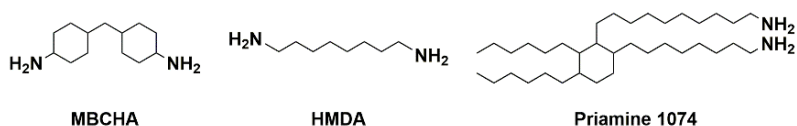


**Figure 3.9.** Amine used for CSBO-based NIPUs synthesis.

ATR-FTIR was used to perform the structural characterization of PHU materials after the curing process. **Figure 3.10** shows the ATR-FTIR spectra of the prepared CSBO-based NIPU materials. In all spectra, NIPU formation is evidenced due to the presence of PHU characteristic bands localized at  $3400\text{--}3300\text{ cm}^{-1}$ ,  $1700\text{ cm}^{-1}$  and  $1545\text{ cm}^{-1}$  and ascribed to O–H and N–H stretching vibration, urethane C=O stretching vibration and N–H bending vibration, respectively. Indeed, the residual band corresponding to cyclic carbonate C=O at  $1800\text{ cm}^{-1}$  in NIPU DAO and NIPU Priamine indicates high conversion. However, in both cases the formation of a new band at  $1650\text{ cm}^{-1}$  in the spectra reveals amide formation via transesterification reaction (**Scheme 3.2**). On the contrary, using a less active amine, such as MBCHA, the intensity of the band corresponding to the C=O stretching vibration of the cyclic carbonate ( $1800\text{ cm}^{-1}$ ) is higher, evidencing a lower conversion. Additionally, the presence of the side band at  $1650\text{ cm}^{-1}$  is barely detectable using the cyclic amine. These findings indicated that open-chain amines exhibited higher activity, which was expressed in higher cyclic carbonate conversion and side reaction formation. It can therefore be said that two of the prepared CSBO-based NIPU are composed by urethane, ester, and amide groups.

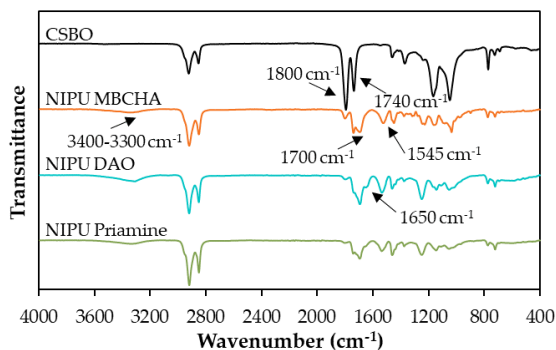


**Figure 3.10.** ATR-FTIR spectra of CSBO and the prepared CSBO-based NIPUs with different amines.

Thermal properties of the synthesized NIPUs were evaluated by DSC and TGA techniques. It is expected that thermal properties of the obtained NIPUs differ from each other due to the differences in molecular structure of the amines employed. In fact, in the thermal analysis by DSC (**Figure 3.11**), the influence of amine nature is obvious in the prepared CSBO-based NIPUs. MBCHA-containing NIPUs present  $T_g$  values 20 °C and 39 °C higher than DAO- and Priamine-containing NIPUs, respectively. The highest  $T_g$  is attributed to the lowest mobility of cyclic structures regarding to linear structure.<sup>15</sup> On the other hand, the long chain carbon linkages present in DAO and Priamine would lead to more flexible components in polymeric network resulting in lower  $T_g$  value, 1 °C and -18 °C respectively. Priamine based NIPU exhibited lowest  $T_g$  owing to structure of the amine precursor, composed of a hydrocarbon cycle with pendant aliphatic chains which generates a free volume and increases the mobility of chains. Moreover, the absence of crystallization and melting processes indicated that the formed NIPU networks do not have crystalline structure.<sup>34,35</sup> These results show how amine structure considerably influenced NIPUs thermal properties, allowing the development of polymer materials with  $T_g$  values in the range superior to 35 °C (from -18 °C to 21 °C).

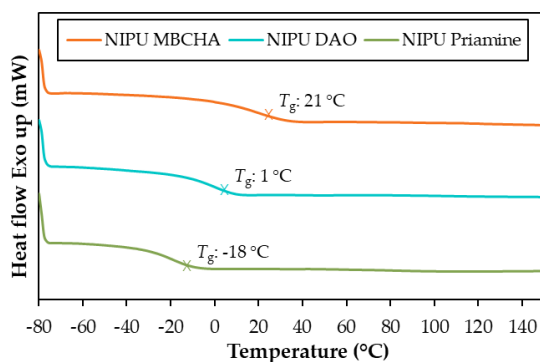


**Figure 3.11.** Comparative DSC curves of the prepared CSBO-based NIPUs with different amines.

The thermal stability of the NIPUs cured with DAO, MBCHA and Priamine was measured with TGA. **Figure 3.12** illustrates the thermal profile of the prepared NIPUs. It is important to underline that TGA results show that in the temperature range explored by DSC, CSBO-based NIPUs were not degraded. As can be seen in **Table 3.1** and **Figure 3.12** the use of different amines has a significant influence on the thermal stability of the final polymer. Indeed, NIPU-Priamine in comparison with NIPU-MBCHA and NIPU-DAO, exhibited a thermal stability up to 43 °C at 5 wt% loss of its initial mass (304 °C *vs.* 273 *vs.* 261 °C). The higher stability obtained by the bio-based (oligo)amine material was also observed by other authors.<sup>29,36</sup> Duval et al. suggested that PU thermal stability is closely related to the molecular weight of the repeating unit. As the molecular weight of the repeating unit increases, the concentration of the urethane group decreases (1<sup>st</sup> degradation stage), resulting in greater thermal stability.<sup>37</sup> This is in line with the results obtained, because NIPU-Priamine is formed by the repeating unit with the highest molecular weight. That may be the reason why the polymer formed by this oligomeric amine reached the highest  $T_5$ . On the other hand, the NIPUs based on lower molecular weight amines exhibited similar thermal degradation behaviour. However, the NIPU composed by cyclic structure (NIPU-MBCHA) achieved slightly higher thermal stability than open aliphatic structure (NIPU-DAO). This was also observed by other authors, that justified the higher thermal stability to the rigid structure of the cyclic amine as compared to long chain carbon linkages present in the open-chain diamines.<sup>18</sup> It is

important to underline that, unlike priamine, the drift of thermogravimetric curves of NIPUs prepared with low molecular weight amines depicts a triple weight loss trend (Figure 3.12-b) as it was reported in literature.<sup>31,32</sup> The obtained results show that prepared CSBO-based NIPUs reached high thermal stability with temperatures up to 304 °C.

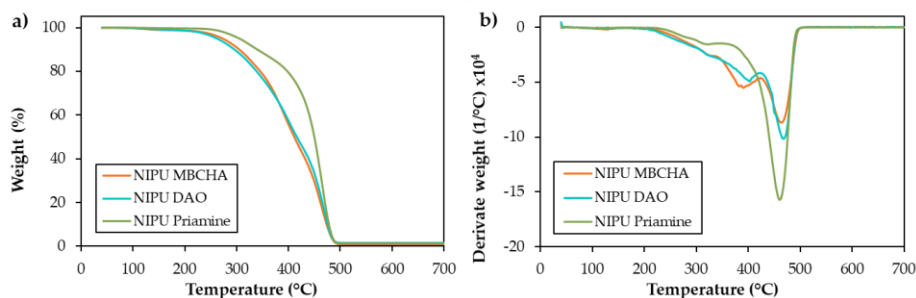


**Figure 3.12.** Comparative thermal profiles of the prepared CSBO-based NIPUs with different amines: a) TG curves and b) dTG curves.

SI and GC measurements of NIPU materials were performed to study amine structure influence in cross-linking degree of CSBO-based NIPUs. As previously mentioned, lowest SI and highest GC correspond to the maximum cross-linking of polymer network.<sup>33</sup> As shown in Figure 3.13, the NIPU MBCHA had the highest SI and lowest GC. This behaviour indicates that the lowest cross-linked material was obtained with less reactive cycloaliphatic amine. These measurements are supported by FTIR results, in which the highest intense cyclic carbonate C=O stretching vibration band was obtained using MBCHA as amine. When comparing open-chain aliphatic amines, the SI was clearly different, but the GC was almost equal. A similar GC value suggested that the cross-linking degree was the same for NIPU-DAO and NIPU-Priamine. Therefore, the remarkable difference in SI must be related to the amine structure and not to the cross-linking degree. The reason was that the number of carbon atoms between amine groups is superior in Priamine (>16C) comparing with DAO (8C). Consequently, the distance between cross-linking nodes increased, allowing the penetration of the solvent through cross-linked network, which led to higher SI. In the case of NIPU MBCHA the GC did not exceed 50%, which confirmed the low reactivity of the cyclic amine in the synthesis of CSBO-based NIPUs.

However, in the most reactive case, the NIPU priamine the GC values did not reach over 74%, which indicated that at least 26% uncross-linked material was left in CSBO-based NIPU network. Therefore, the prepared CSBO-based NIPUs with open-chain diamines exhibited suitable cross-linked networks with a GC superior to 70%, while the CSBO-based NIPUs synthesized with cyclic amine, the GC did not exceed 50%, indicating a low degree of cross-linked network.

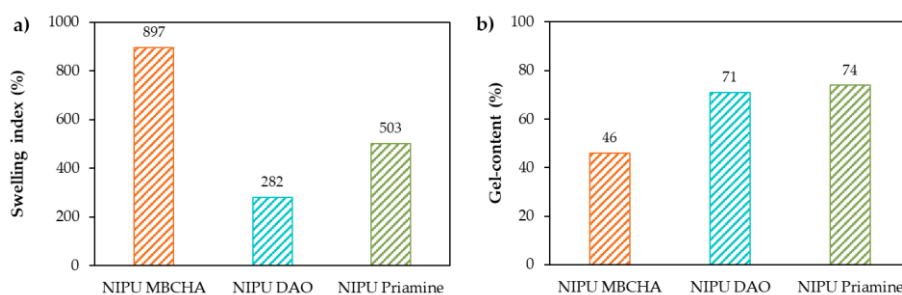


**Figure 3.13.** Comparative SI and GC of the prepared CSBO-based NIPUs with different amines.

The preparation and characterization of CSBO-based NIPU coatings had also been conducted with the aim of determine more specific properties. The coating properties tested for prepared NIPUs included hardness and impact resistance, considered as vital importance in coatings performance. **Table 3.2** details the coating features of NIPUs prepared from CSBO and different amines at same molar ratio.

**Table 3.2.** CSBO-based NIPUs hardness and impact resistance properties

Formulation	DFT <sup>a</sup>	Pencil hardness	Impact d <sup>b</sup> (kg/cm)
NIPU MBCHA	84-97	6B	>100
NIPU DAO	67-101	6B	>100
NIPU Priamine 1.0	58-100	6B	>100

<sup>a</sup>Dry film thickness (DFT); <sup>b</sup>Impact d: Direct impact.

The hardness of the organic coatings was measured by pencil hardness, which ranges from 8B (softest) to 9H (hardest). As shown in **Table 3.2**, soft pencils were able to cut

the coated NIPU, indicating the low hardness of the material. Moreover, it is important to note that the same value of pencil hardness was obtained for all three coatings. This suggests that amine structure had no significant influence on the pencil hardness of the CSBO-based NIPU coatings. On the other hand, MBCHA, DAO and priamine based NIPU coatings had an excellent direct impact resistance. Like in pencil hardness, amine structure has no influence in impact resistance of the CSBO-based NIPU coatings. Therefore, the results obtained revealed that at studied conditions, the triglyceride structure exhibited a greater influence on coating properties than amine structure. This could be attributed to the higher wt% of CSBO present in NIPU network. In fact, among the amines used, priamine is the only one that exceeds 30 wt% of the total mass. Hence, the low hardness and high impact resistance lies in the triglyceride soft structure that increases the softness and flexibility to coatings.<sup>38</sup>

Comparative between CSBO-based NIPUs and traditional PUs from VO<sub>s</sub>

As mentioned previously, most works devoted to carbonated vegetable oil-based NIPUs have concentrated in their synthesis leaving their performance unaddressed. For this reason, a comparative study was carried out between the properties of PUs synthesized via traditional route reported in the literature, and the properties of the CSBO-based NIPUs synthesized in our work. To make the comparison as realistic as possible, only the PU composed by vegetable oil-based polyols through different synthetic routes (without modification, epoxidation/ring-opening, ozonolysis, hydroformylation, thiol-ene coupling, transesterification and transamidation) have been considered. The **Figure 3.14** illustrates the structure of VO-based polyols.

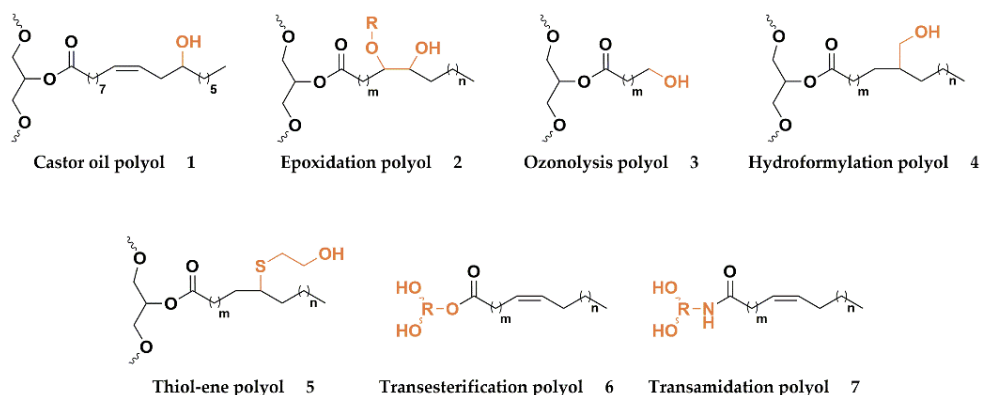


**Figure 3.14.** Vegetable oil-based polyols overall structure.

The comparison of the thermal properties is detailed in **Figure 3.15**. The acronym PU-1 means that the PU is synthesized using polyol 1 (castor oil) as precursor. This description also serves to the other PU acronyms. **Figure 3.15-a** illustrates the range of  $T_g$  value for CSBO-based NIPUs and PUs synthesized from vegetable oil-based polyols. In this comparison the most remarkable point is that NIPU materials exhibited lower  $T_g$  than the isocyanate analogues, with glass transition temperatures around room temperature ( $-18\text{ }^{\circ}\text{C}$  to  $21\text{ }^{\circ}\text{C}$ ). This behaviour must be related to different factors, such as the difference in structure between traditional PUs and PHUs, the lower degree of crosslinking of non-isocyanate materials caused by the lower activity of cyclic carbonates and amines compared to isocyanates and polyols, etc. **Figure 3.15-b** shows the temperature ranges of  $T_5$  for both vegetable oil-based PU and NIPUs. Looking at NIPUs thermal stability, the maximum  $T_5$  value is similar in NIPUs and traditional PUs, with no difference greater than  $50\text{ }^{\circ}\text{C}$ . However, the minimum  $T_5$  value is clearly superior (up to  $160\text{ }^{\circ}\text{C}$ ) to many of the traditional PU. These results reveal a higher thermal stability of NIPUs in relation to vegetable-based PUs. This behaviour is in accordance with the results reported in the literature associated to not-oleochemical PUs and NIPUs. Many authors justify the improvement in thermal stability to the absence of unstable biuret and allophanate units present in traditional PUs, and the extra hydrogen bonds created with O–H groups formed in the polyaddition reaction between cyclic carbonate and amine.<sup>9,39,40</sup>



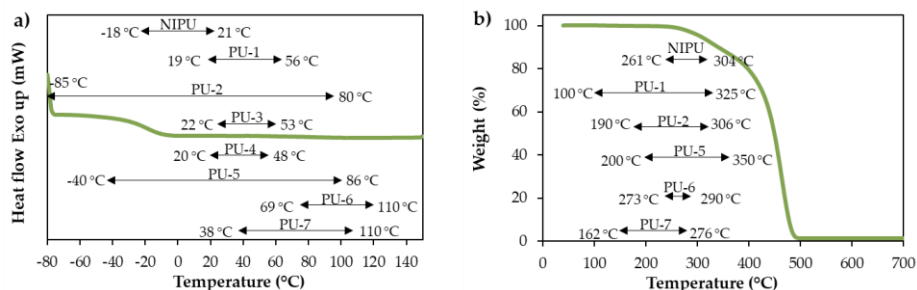


**Figure 3.15.** Comparison of thermal properties between CSBO-based NIPUs and VO-based PUs: (a) DSC curve and b) TG curve.

The comparison of pencil hardness is detailed in **Figure 3.16**. It has been previously mentioned that CSBO-based NIPU coatings exhibited poor pencil hardness. Indeed, the comparison with vegetable oil-based PUs points to the superiority of traditional PU route compared to NIPUs synthesized from cyclic carbonates and amines. The better performance of PUs compared with CSBO-based NIPUs (2H-4H *vs.* 6B) may be associated to the low reactivity of cyclic carbonates comparing with isocyanates.<sup>41–43</sup> This enables for a higher cross-linking degree, which is closely related to the hardness of the coating. Therefore, the results obtained are still far from the values obtained with traditional route.

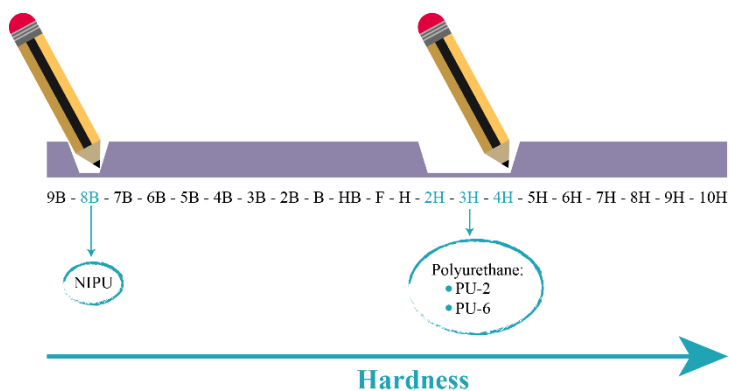


**Figure 3.16.** Comparison of pencil hardness between CSBO-based NIPUs and VO-based PUs.

**Table 3.3** shows the impact resistance of CSBO-based NIPUs and PU synthesized from vegetable oil polyols. It should be noted that very few works have determined this property, only PU synthesized from polyols developed via epoxidation/ring-opening (2) and transesterification (6) have been reported. This comparison reveals the high impact resistance of both vegetable oil-based PUs and NIPUs. Hence, this behaviour clearly reflects the positive influence of the triglyceride structure on impact resistance.

**Table 3.3.** Comparison of direct impact resistance between CSBO-based NIPUs and VO-based PUs.

	NIPU	PU-2	PU-6
Impact d <sup>a</sup> (kg/cm)	>100	>100	90

<sup>b</sup>Impact d: Direct impact.

### 3.5 Conclusions

The use of carbonated soybean oil as precursor for non-isocyanate polyurethanes enabled the synthesis of products with a bio-based content between 73% and 100%. In this chapter, the influence of amine ratio and amine type on the properties of CSBO-based NIPUs has been studied. It was observed that an amine excess had a negative influence due to polymer network cleavage through triglyceride ester group transesterification. At an amine/cyclic carbonate molar ratio below stoichiometric equilibrium, the effect was not negative in terms of NIPU properties, but the conversion of cyclic carbonate was low. The amine/cyclic carbonate molar ratio of 1.0 enables the best cross-linking degree, high cyclic carbonate conversion and amide formation control. The use of different amines had a marked effect on both activity and final product properties. The employment of rigid amines allowed to achieve  $T_g$  near to ambient temperature (21 °C), but due to their low activity, the cross-linking degree obtained was poor. Open-chain amines lead to a  $T_g$  significantly inferior to room temperature ( $\geq 1$  °C), although the higher activity enabled superior cross-linking degree. In addition, it is important to highlight that the use of higher molecular weight

amines, such as triamine, increased the thermal stability of NIPU by more than 40 °C with respect to lower molecular weight amines. Regarding the properties of the coatings, the CSBO-based NIPUs showed poor pencil hardness, while the impact resistance was excellent. Although the thermal stability of NIPUs has been shown to be superior in many cases, the comparison between NIPUs synthesized in this work from CSBO and PUs synthesized from VO polyols suggests that the potential of the isocyanate free pathway is not yet sufficiently competitive in certain properties. In fact, although NIPUs outperform many PUs synthesized from VO in thermal stability, they lag behind in other properties ( $T_g$ , impact toughness).

### 3.6 References

- 1 M. North, R. Pasquale and C. Young, *Green Chem.*, 2010, **12**, 1514–1539.
- 2 E. Darroman, N. Durand, B. Boutevin and S. Caillol, *Prog. Org. Coatings*, 2015, **83**, 47–54.
- 3 Y. H. Kim, E. S. An, S. Y. Park and B. K. Song, *J. Mol. Catal. B Enzym.*, 2007, **45**, 39–44.
- 4 M. Ghasemlou, F. Daver, E. P. Ivanova and B. Adhikari, *Eur. Polym. J.*, 2019, **118**, 668–684.
- 5 C. Carré, Y. Ecochard, S. Caillol and L. Avérous, *ChemSusChem*, 2019, **12**, 3410–3430.
- 6 H. L. Parker, J. Sherwood, A. J. Hunt and J. H. Clark, *ACS Sustain. Chem. Eng.*, 2014, **2**, 1739–1742.
- 7 H. Zhang, C. Li, M. Piszcz, E. Coya, T. Rojo, L. M. Rodriguez-Martinez, M. Armand and Z. Zhou, *Chem. Soc. Rev.*, 2017, **46**, 797–815.
- 8 S. Fukuoka, M. Kawamura, K. Komiyama, M. Tojo, H. Hachiya, K. Hasegawa, M. Aminaka, H. Okamoto, I. Fukawa and S. Konno, *Green Chem.*, 2003, **5**, 497–507.

- 9 L. Maisonneuve, O. Lamarzelle, E. Rix, E. Grau and H. Cramail, *Chem. Rev.*, 2015, **115**, 12407–12439.
- 10 G. Rokicki, P. G. Parzuchowski and M. Mazurek, *Polym. Adv. Technol.*, 2015, **26**, 707–761.
- 11 B. Tamami, S. Sohn and G. L. Wilkes, *J. Appl. Polym. Sci.*, 2004, **92**, 883–891.
- 12 I. Javni, D. P. Hong and Z. S. Petrovic, *J. Appl. Polym. Sci.*, 2008, **108**, 3867–3875.
- 13 Z. Li, Y. Zhao, S. Yan, X. Wang, M. Kang, J. Wang and H. Xiang, *Catal. Lett.*, 2008, **123**, 246–251.
- 14 M. Bähr and R. Mülhaupt, *Green Chem.*, 2012, **14**, 483–489.
- 15 I. Javni, D. P. Hong and Z. S. Petrovic, *J. Appl. Polym. Sci.*, 2013, **128**, 566–571.
- 16 S. Jalilian and H. Yeganeh, *Polym. Bull.*, 2015, **72**, 1379–1392.
- 17 B. Grignard, J. Thomassin, S. Gennen, L. Poussard, L. Bonnaud, J. M. Raquez, P. Dubois, M. P. Tran, C. B. Park, C. Jerome and C. Detrembleur, *Green Chem.*, 2016, **18**, 2206–2215.
- 18 S. Doley and S. K. Dolui, *Eur. Polym. J.*, 2018, **102**, 161–168.
- 19 A. Farhadian, A. Ahmadi, I. Omrani, A. B. Miyardan, M. A. Varfolomeev and M. R. Nabid, *Polym. Degrad. Stab.*, 2018, **155**, 111–121.
- 20 W. Y. Pérez-Sena, X. Cai, N. Kebir, L. Vernières-Hassimi, C. Serra, T. Salmi and S. Leveneur, *Chem. Eng. J.*, 2018, **346**, 271–280.
- 21 S. Hu, X. Chen and J. M. Torkelson, *ACS Sustain. Chem. Eng.*, 2019, **7**, 10025–10034.
- 22 A. Z. Yu, R. A. Setien, J. M. Sahouani, J. Docken and D. C. Webster, *J. Coatings Technol. Res.*, 2019, **16**, 41–57.
- 23 A. F. G. Agudelo, W. Y. Pérez-Sena, N. Kebir, T. Salmi, L. A. Ríos and S. Leveneur, *Chem. Eng. Sci.*, 2020, **228**, 115954.

- 24 J. Dong, B. Liu, H. Ding, J. Shi, N. Liu, B. Dai and I. Kim, *Polym. Chem.*, 2020, **11**, 7524–7532.
- 25 C. Mokhtari and F. Malek, *Mater. Today Proc.*, 2020, **31**, S12–S15.
- 26 J. Pouladi, S. M. Mirabedini, H. E. Mohammadloo and N. G. Rad, *Eur. Polym. J.*, 2021, **153**, 110502–110514.
- 27 S. Doley, A. Bora, P. Saikia, S. Ahmed and S. K. Dolui, *J. Polym. Res.*, 2021, **28**, 1–9.
- 28 T. Dong, E. Dheressa, M. Wiatrowski, A. P. Pereira, A. Zeller, L. M. L. Laurens and P. T. Pienkos, *ACS Sustain. Chem. Eng.*, 2021, **9**, 12858–12869.
- 29 L. Poussard, J. Mariage, B. Grignard, C. Detrembleur, C. Jérôme, C. Calberg, B. Heinrichs, J. De Winter, P. Gerbaux, J. M. Raquez, L. Bonnaud and P. Dubois, *Macromolecules*, 2016, **49**, 2162–2171.
- 30 X. Yang, C. Ren, X. Liu, P. Sun, X. Xu, H. Liu, M. Shen, S. Shang and Z. Song, *Mater. Chem. Front.*, 2021, **5**, 6160–6170.
- 31 C. Carré, L. Bonnet and L. Avérous, *RSC Adv.*, 2014, **4**, 54018–54025.
- 32 K. Błażek, P. Kasprzyk and J. Datta, *Polymer*, 2020, **205**, 122768–122782.
- 33 A. Cornille, G. Michaud, F. Simon, S. Fouquay, R. Auvergne, B. Boutevin and S. Caillol, *Eur. Polym. J.*, 2016, **84**, 404–420.
- 34 M. Kathalewar, A. Sabnis and D. D’Mello, *Eur. Polym. J.*, 2014, **57**, 99–108.
- 35 R. Pathak, M. Kathalewar, K. Wazarkar and A. Sabnis, *Prog. Org. Coatings*, 2015, **89**, 160–169.
- 36 M. Decostanzi, Y. Ecochard and S. Caillol, *Eur. Polym. J.*, 2018, **109**, 1–7.
- 37 C. Duval, N. Kébir, A. Charvet, A. Martin and F. Burel, *J. Polym. Sci. Part A Polym. Chem.*, 2015, **53**, 1351–1359.
- 38 A. Chaudhari, R. Kulkarni, P. Mahulikar, D. Sohn and V. Gite, *J. Am. Oil Chem. Soc.*, 2015, **92**, 733–741.

- 39 O. Figovsky, L. Shapovalov, A. Leykin, O. Birukova and R. Potashnikova, *Chem. Chem. Technol.*, 2013, **7**, 79–87.
- 40 A. Cornille, R. Auvergne, O. Figovsky, B. Boutevin and S. Caillol, *Eur. Polym. J.*, 2017, **87**, 535–552.
- 41 O. Kreye, H. Mutlu and M. A. R. Meier, *Green Chem.*, 2013, **15**, 1431–1455.
- 42 A. Gomez-Lopez, F. Elizalde, I. Calvo and H. Sardon, *Chem. Commun.*, 2021, **57**, 12254–12265.
- 43 Z. Wu, W. Cai, R. Chen and J. Qu, *Prog. Org. Coatings*, 2018, **119**, 116–122.

# CHAPTER 04

---

APPLICATION OF CARBONATED  
SOYBEAN OIL-BASED NON-  
ISOCYANATE POLYURETHANES IN  
THE COATING INDUSTRY





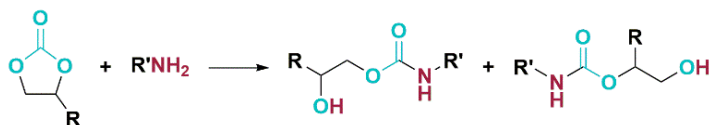
## 4.1 Background

Polyurethanes (PUs) have been used for decades in the coating industry to impart properties such as low temperature flexibility, toughness, resistance to abrasion, corrosion, and chemical resistance. This has enabled the use of PU coatings in many fields, from the automotive industry to those requiring high chemical resistance.<sup>1</sup> In fact, the PU coatings market reached a value of over 18 billion United States Dollar (USD) in 2020 with automotive and transportation being the industries with the largest implementation.<sup>2</sup> Notwithstanding its excellent properties, PU production is affected by the toxicity of the reagents used in their synthesis process. Conventional PUs are synthesized by step-growth copolymerization of polyols and polyisocyanates, The latter are considered as potential dangerous for human's health. In fact, the main effects of hazardous exposures are occupational asthma, irritation of the eyes, nose throat, and skin.<sup>3-5</sup> Additionally, the industrial production of isocyanates is based on the use of phosgene, a highly toxic chemical that causes death upon overcoming the lethal dose.<sup>6,7</sup> In this context, the use of isocyanates has been limited by the REACH regulation.<sup>8</sup>

For this reason and to improve safety in PU production, both academic and industrial research have been focused on "greener" routes to avoid the use of isocyanates.<sup>9-11</sup> The urge for new strategies is one of the biggest challenges for PU industry, since it implies discarding a large-scale optimized synthesis pathway, specific equipment, etc. PUs synthesized via non-isocyanate routes are termed non-isocyanate polyurethanes (NIPUs). Among the developed routes, the 100% atom economy polyaddition reaction between cyclic carbonates and amines has attracted major interest in the scientific community, since the rest of the routes still use highly toxic precursors, such as phosgene, acyl azides, carboxamides, aziridines, etc.<sup>11-13</sup> The growing interest in this route is not only related to the ability to avoid toxic precursors, but to the various benefits compared to other non-isocyanate routes and even traditional PUs.

The NIPUs synthesized through the cyclic carbonate ring opening reaction are called poly(hydroxyurethanes) (PHU) due to the formation hydroxyl dangling groups along

the polymer chain (**Scheme 4.1**). The presence of this functional groups provides different properties compared to conventional PUs. The polyaddition reaction between cyclic carbonates and amines allows the polymerization at moderate temperatures and without catalyst.<sup>13,14</sup> Another relevant benefit is that a wide repertoire of (poly)cyclic carbonates are commercially available or easily synthesizable. Indeed, raw materials from bio-origin (*i. e.* vegetable oils, lignin, etc.) can be used for the synthesis of the starting cyclic carbonates.<sup>12</sup> In addition, the fact that the most used reaction process to produce cyclic carbonates is the cycloaddition of carbon dioxide (CO<sub>2</sub>) to epoxide rings offers a new opportunity to produce highly sustainable and environmentally beneficial PUs.<sup>15</sup> Moreover, in terms of manipulation and long-term storage, the use of cyclic carbonates is beneficial due to the low moisture sensitivity of these products.<sup>16</sup> On the other hand, PU industry is still relying on the use of petroleum-based resources for the synthesis of polyols and polyisocyanates. Hence, this polymer family is transitioning from non-suitable feedstocks to more environmentally-friendly and sustainable ones in order to develop an industry based on renewable resources.<sup>1,17-20</sup>



**Scheme 4.1.** PHU synthesis via the cyclic carbonate ring opening by amine.

In this context, many research groups have synthesized non-isocyanate polyurethanes from vegetable oils due to their availability and low cost.<sup>21-42</sup> Moreover, the use of these bio-based raw materials in NIPU coatings can bring beneficial characteristics. Indeed, vegetable oils can help increasing the bio-based content of coatings, contributing to the environmental sustainability, a big concern in today's society. Besides, the long fatty acid aliphatic chains provide flexibility, while the high functionality helps increasing the cross-linking density, which results in an improvement of coatings properties.<sup>43</sup>

The first carbonated oil-based NIPU coatings were reported by Doley et al.<sup>28</sup> Formulations made of carbonated sunflower oil (CSFO) and 1,2-diaminoethane (EDA), 2,2'-Diaminodiethylamine(DETA) or isophoronediamine (IPDA) were cured for 48h at 90 °C followed by 1h at 140 °C. The presence of cyclic amine in NIPU structure (for the IPDA derivatives) enhanced the hardness, gloss, and resistance against chemicals (acids and water) in comparison with the open-chain analogues. Moreover, potentiodynamic polarization studies and electrochemical impedance spectroscopy revealed that IPDA based coatings exhibited the highest resistance and lowest corrosion rate due to its rigid structure. As a result, the authors suggested the use of these environmentally friendly materials for surface coatings. Yu et al. investigated the influence of cooperative catalysis in thermal curing (120 °C, 3h) of carbonated soybean oil (CSBO) with (tris(2-aminoethyl)amine) (TAEA) for NIPU coatings.<sup>32</sup> The formulation without catalyst provided excellent crosshatch adhesion (5B), a pendulum hardness of 28 s and a methyl ethyl ketone (MEK) resistance to 65 double rubs. The addition of a cooperative catalyst system (DBU 1 mol % and LiOTf 1 mol %) induced the enhancement of coating hardness and MEK resistance to 51 s and 346 double rubs, respectively. Besides, the synergistic effect between the superbase and acid improved the curing process reducing time and temperature to 45 minutes and 80 °C, with minimal influence on coating properties. Recently, Pouladi et al. carried out a systematic study on the curing procedure of carbonated linseed oil (CLSO) and DETA for NIPU coatings.<sup>36</sup> The thermal curing of the CLSO composed by different carbonate contents (45%, 75% and 100%) for 2h at 100 °C and followed by 2h at 180 °C, provided NIPU coatings with an appropriate resistance to impact, cross hatch of 4B to 5B (excellent) and a pendulum hardness of 30 s to 43 s. These authors observed that the improvement of adhesion and hardness properties was directly connected to the increase in carbonate amount. However, the behaviour in anticorrosion properties was different. While coatings cured with CLSO with 75% of carbonate showed the better anticorrosion properties, systems cured with totally carbonated oil were less resistant to corrosion. Actually, the results obtained with partially carbonated samples showed anticorrosion properties comparable to PU-based coated samples.

In these preliminary reports towards the implementation of vegetable oil-based NIPU coatings, many works synthesized NIPUs reacting cyclic carbonates with low molecular weight amines. Nevertheless, the use of the latter restricted the implementation in the industry due to limitations related to low molecular weight. On the one hand, primary short alkyl chain length amines display higher toxicity than long ones.<sup>44,45</sup> On the other hand, the low boiling point associated with low molecular weight brings an increased risk of (toxic) gas formation, even at temperatures close to ambient. Consequently, the handling (and security) of the formulation are compromised. Additionally, in fields that require high temperatures, the implementation is impeded because of the impossibility of performing thermal curing. Thus, despite the use of renewable feedstocks for NIPU coatings synthesis, the use of low molecular weight amines hinders the transition towards Green Chemistry principles. The novelty of this project is the use of industrial amines, which have not been previously reported in vegetable oil-based NIPU coatings.

## **4.2 Objectives**

The main objective of the research explained in this chapter was to obtain CSBO-based NIPU coatings relevant to industry requirements.

In order to achieve the main objective, two strategies were carried out. The first consists in the direct use of CSBO for the synthesis of NIPU coatings through the reaction between CSBO and industrially employed amino hardeners. The second approach was based on the development of hybrid NIPU-epoxy coatings via the synthesis of CSBO-based NIPU amino hardeners (CSBO-AHs).

The obtained NIPU-epoxy hybrid coatings were characterized by means of complementary techniques used by the coating industry and compared to commercial epoxy coating benchmarks. The ultimate goal was to establish the potential of CSBO as a precursor for NIPU coatings for industrial implementation. In fact, with the objective of bringing formulations composed of CSBO closer to industrial formulations, pigmented coatings were also developed.

## 4.3 Experimental

### 4.3.1 Materials

All the compounds were used as received. 1-bromododecane (97%) was purchased from Sigma-Aldrich. Triphenylphosphine (99%) was purchased from Across Organics. Ethyl acetate (EssentQ) was purchased from Scharlau. Epoxidized soybean oil (ESBO) containing 4.19 mmol/g of oxirane was kindly supplied by Hebron (Spain). The CO<sub>2</sub> (Industrial grade, 99.8%) was purchased from Nippon gases. Commercially available amino hardeners (AHs), AH-a (Polyamine adduct hardener), AH-b, AH-c (Mannich base hardener), AH-d (Polyamidoamine hardener), m-xylenediamine (m-XDA), triethylenetetramine (TETA), 1-methoxy-2-propanol, methyl ethyl ketone (MEK) and type 1 epoxy resin (Epo-1) were kindly supplied by Allnex—The coating Resins Company—. Due to intellectual property rights, we are unable to specify the specific names of the resin and amino hardeners used. JEFFAMINE D-400 Polyetheramine (Jeff D400) was purchased Huntsman.

### 4.3.2 Synthesis and characterization of CSBO

The carbonated oil used for this study comes from the same batch used in **Chapter 3**.

### 4.3.3 Synthesis and characterization of NIPU coatings by direct use of CSBO

In order to develop CSBO-based NIPU coatings, the mentioned carbonated oil was reacted (directly) with an amino hardener. Typically, formulations were prepared by mixing carbonated soybean oil (CSBO, 5 g containing 16.8 mmol of C=O), the selected industrial amino hardener (16.8 mmol NH<sub>2</sub>) and 1-methoxy-2-propanol. The latter was added in order to improve reactivity during the reaction and adjust the viscosity to make it suitable for coating application<sup>46</sup>. The solid content of the solvent-based NIPU coatings was kept to around 90 wt%. Afterwards, all formulations were applied on aluminium plates using a manual film applicator Model 360 from Erichsen with a thickness of 200 µm. Finally, the coatings were cured at 100 °C for 4h.

Different and complementary characterization techniques described in **Methods**, were used for CSBO-based coatings characterization. The structural characterization of the prepared NIPU coatings was determined by means of Fourier Transform Infrared Spectroscopy (FTIR) equipped with universal Attenuated Total Reflection (ATR) sampling accessory. The initial viscosity of the prepared formulations was determined by dynamic viscosity measurements. The coating mixture drying was evaluated by dust-free.

#### 4.3.4 Synthesis and characterization of NIPU-epoxy hybrid coatings by modified CSBO

Synthesis and characterization of CSBO-AHs

To develop CSBO-based NIPU amino hardeners (CSBO-AHs), carbonated oil stepwise addition was performed over an excess of amine (**Figure 4.1**). In a typical synthesis, amino hardeners (AHs) were prepared as follows: In a 500 mL three-neck flask glass reactor equipped with a mechanical stirrer, temperature controller and water condenser, amine (40.0 g; 547.14 NH<sub>2</sub> mmol) and a quarter of the total CSBO (16.25 g; 54.8 C=O mmol) amount were dissolved in 1-methoxy-2-propanol (30 wt%). Then, reaction temperature was raised to 80 °C, considered the initial reaction time. The reaction progress was monitored by FTIR. Once the added cyclic carbonate was fully consumed, another batch of CSBO dissolved in 1-methoxy-2-propanol was added (16.25 g; 54.8 C=O mmol; 70 wt%). This process was repeated until an excess equivalent ratio of amine/cyclic carbonate of 2.5–3.3 equiv. was reached (3<sup>rd</sup> or 4<sup>th</sup> step) depending on the amine used. Finally, 1-methoxy-2-propanol was removed and MEK was added dropwise at room temperature to improve the visual aspect and the subsequent drying of the formulation.

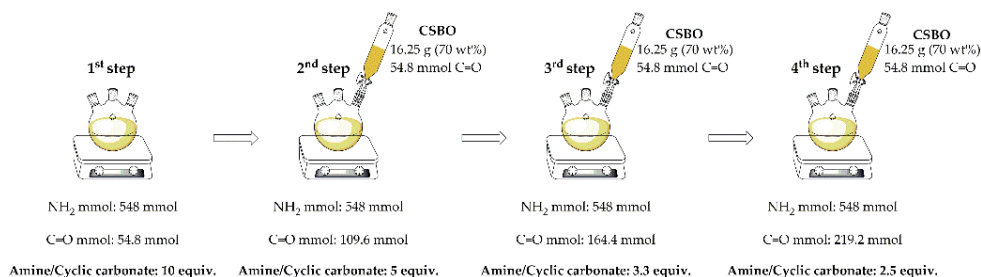


**Figure 4.1.** CSBO-based amino hardeners synthesis via CSBO stepwise addition.

Synthesized CSBO-AHs were characterized by complementary techniques described in **Methods**. Attenuated Total Reflection Fourier Transform Infrared Spectroscopy (ATR-FTIR) was used for the monitorization of the CSBO conversion and the structural analysis the prepared amino hardeners. The structural characterization was complemented by  $^{13}\text{C}$  nuclear magnetic resonance (NMR) in solution. The amine value of prepared CSBO-AHs was determined by a potentiometric determination according to DIN 53176. CSBO-AHs viscosity was determined by means of dynamic viscosity value.

Synthesis and characterization of NIPU-epoxy hybrid coatings by modified CSBO

For clear coatings, amino hardeners were reacted with an epoxy resin. Typically, formulations were prepared by mixing industrially used Epo-1 epoxy resin (75 g; 120 epoxy mmol), the selected amino hardener (90 H active mmol) and MEK (10 wt%). The amine/epoxy molar ratio and solvent addition were selected due to the suitability for anticorrosion properties and to adjust the appropriate viscosity for coating application, respectively. Afterwards, all coatings were applied on glass, OC steel degreased and sand blasted steel panels using a manual film applicator Model 360 from Erichsen with a thickness of 200  $\mu\text{m}$  for glass and OC steel degreased panels and 400  $\mu\text{m}$  for sand blasted steel panels. Finally, coatings were cured at room temperature for at least 7 days.

For pigmented coatings, similar process was carried out. First the addition of pigments and additives to the binder (epoxy resin) of the formulation was done at a binder to pigment ratio of 1 to 2 wt%. Aerosil R 202 and Crayvallac extra were added

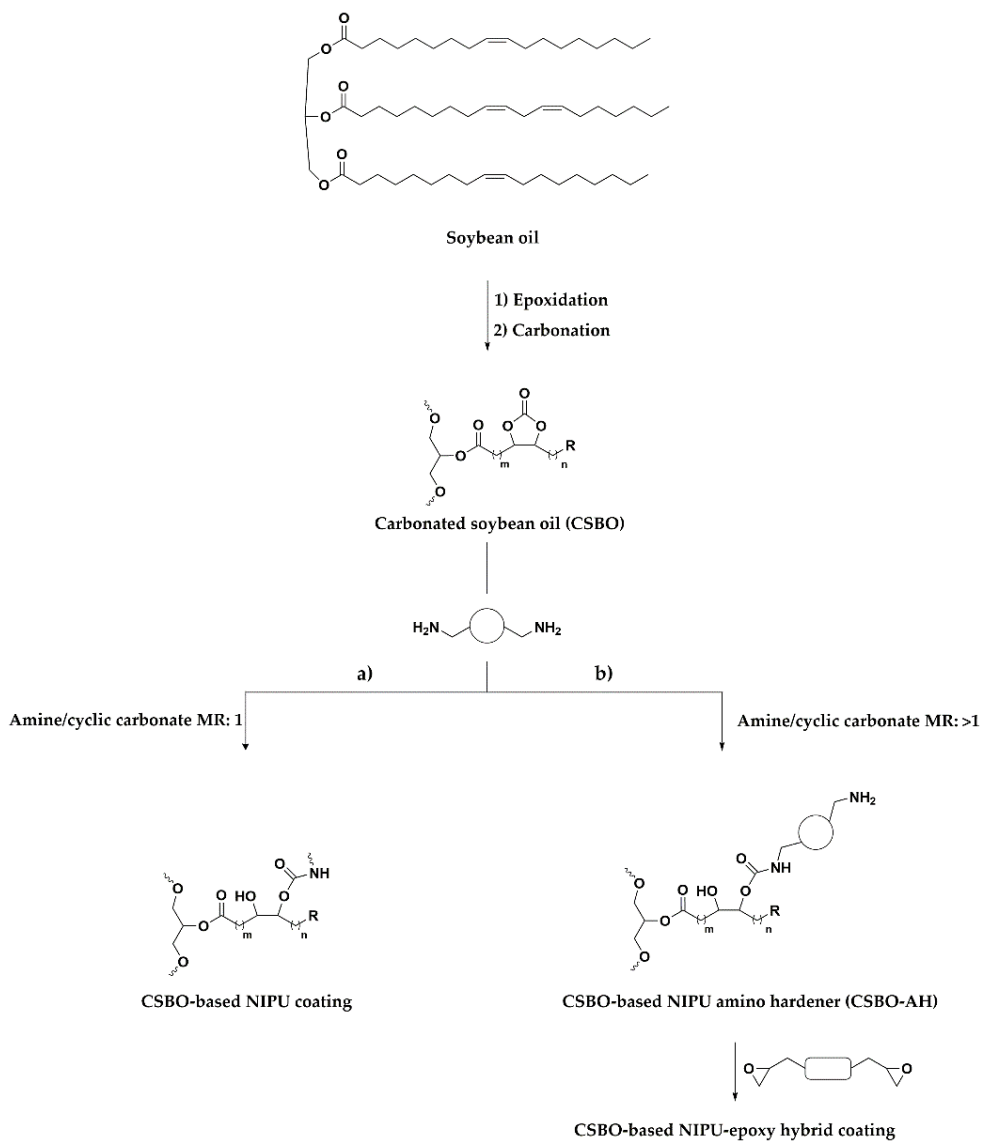
to the composition as rheology modifier. EWO and Winnofil were incorporated as fillers. Tronox CR-828 and Heucophos ZPA were added as pigments. Finally, VXW 6208/60 was added as dispersing and wetting agent, and Plustalc H05 was aggregated as a functional extender. Then, to achieve a homogeneous binder, the mix was dispersed for 30 minutes on pearl mill at 3000 rpm. Once the pigmented binder was prepared, the same process described for clear coatings was followed.

The prepared NIPU-epoxy hybrid coatings from CSBO-AHs were fully characterized by complementary techniques described in **Methods**. Formulation's pot-life was determined by means of dynamic viscosity value. Coating mixture drying was evaluated by dust-free, tack-free, and drying rate according to ISO 9117-5. The thickness of the coatings on the panels was measured with a dualscope MPO from Fischer. General and mechanical coating properties were measured according to standard methods including pendulum hardness (ISO 1522:2006), solvent resistance (EN 13523-11), cross-cut test (ISO 2409:2013), cupping test (ISO 1520:2006) and impact resistance (ASTM D2794). The resistance of pigmented coated samples against corrosion was evaluated by salt spray test according to ISO 9227:2017.

#### 4.4 Results and discussion

The strategies undertaken in order to discover the potential of CSBO as a precursor for NIPU coatings for industrial implementation are summarized in **Scheme 4.2**. The procedure illustrated in this scheme is detailed in the experimental section 4.3.3 and 4.3.4.





**Scheme 4.2.** General scheme of synthesis of NIPU coatings from CSBO: a) Direct use of CSBO and b) via CSBO-based AHs synthesis.

#### 4.4.1 Synthesis and characterization of NIPU coatings by direct use of CSBO

As discussed earlier in this chapter, CSBO-based NIPU coatings are constrained by curing conditions and curing agents. Therefore, in order to be as close as possible to

industrial requirements, we focused on these two parameters. The curing conditions in the coating industry can be divided in two general categories: (1) Long times (1-7 days) at room temperature and (2) short times (minutes or few hours) at high temperatures. Hence, 100 °C and 4h were selected as curing conditions to simulate industrial requirements. Regarding the second factor, the use of industrial curing agents represents a major advantage over low molecular weight amines typically used in academic research. As mentioned before, the low boiling point of these amines limits their use at high temperatures, as they would form toxic fumes and reduce the initial molar ratio. Therefore, the use of oligo-polymeric amines is widespread at the industrial level. The higher thermal stability of the industrial amino hardeners makes them more suitable for their use at high temperatures. Also, in our case, the use of commercial amino hardeners can allow the development of products with structures similar to the ones of current industrial coatings. For this reason, amino hardeners used by Allnex—The coating Resins Company— were tested for CSBO-based NIPU coatings preparation (**Figure 4.2**). The exact structure of amino hardeners AH-a and AH-b is not disclosed for confidentiality.

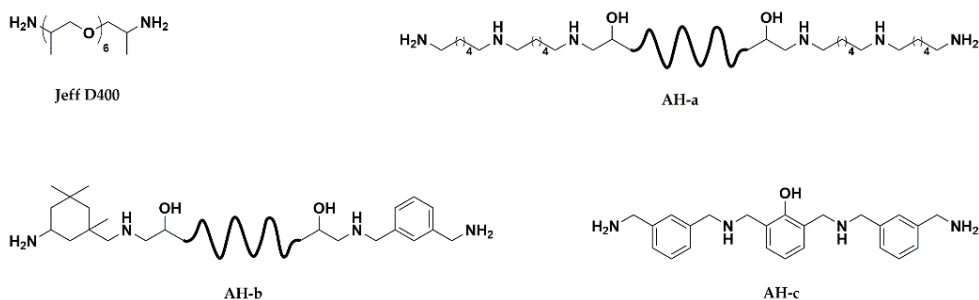


**Figure 4.2.** Industrial amino hardeners used for CSBO-based NIPU coatings synthesis.

The synthesis of CSBO-based NIPU coatings from carbonated soybean oil and four industrially employed amino hardeners and the main data of prepared formulations are represented on **Scheme 4.2-a** and **Table 4.1**.

**Table 4.1.** The main data of the prepared NIPU coatings formulations.

Amino hardener	Carbonated resin	Formulation
Jeff D400		NIPU D400
AH-a	CSBO	NIPU-a
AH-b		NIPU-b
AH-c		NIPU-c

FTIR was used to monitor the changes in the chemical composition after the curing process. **Figure 4.3** shows the ATR-FTIR spectra of the prepared CSBO-based NIPU coatings. The presence of shoulder bands at 3400-3300  $\text{cm}^{-1}$ , 1700  $\text{cm}^{-1}$  and 1545  $\text{cm}^{-1}$  assigned to O–H and N–H stretching vibration, urethane C=O stretching vibration and N–H bending vibration, respectively, to some extent evidence the formation of NIPU. Nevertheless, the intense band corresponding to the C=O stretching vibration band of the cyclic carbonate at 1800  $\text{cm}^{-1}$  observed in all spectra of all the samples points to low conversions. The results obtained indicate a low reactivity between CSBO and industrial amino hardeners at the selected curing conditions.

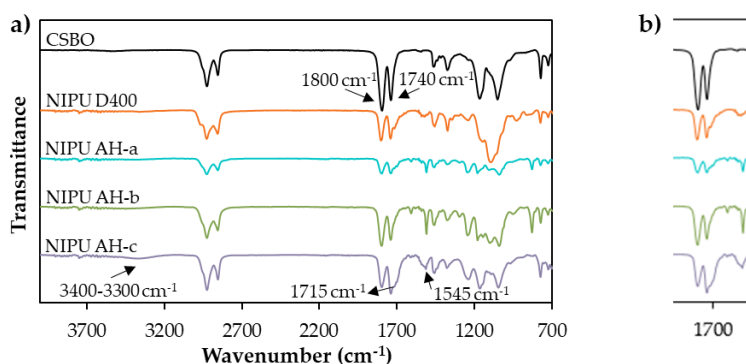


**Figure 4.3.** Comparative ATR-FTIR spectra of CSBO, NIPU D400, NIPU AH-a, NIPU AH-b and NIPU AH-c after curing process: a) Wavenumber 700-4000  $\text{cm}^{-1}$  and b) wavenumber 1500-2000  $\text{cm}^{-1}$ .

Drying is of paramount relevance in the coating industry. The first step of drying is measured via dust-free test, which is related to the physical drying of a coating material. This test determines when dust will no longer stick to the surface. The

drying time should be as short as possible to avoid dirt adhesion on the wet coating, and thereby achieve a satisfactory surface coating. As it can be seen in **Figure 4.4**, the CSBO-based NIPU composed with AH-c did not achieve a dry (dust-free) stage, even after one week. The same behaviour was observed in other NIPU coatings. This means that a significant part of the initial components remained unreacted, which is in line with previously discussed FTIR results. As other research groups have reported before, the low degree of cross-linking exhibited by these formulations could be due to both the low intrinsic reactivity of cyclic carbonates and amines and the high steric impediment of triglyceride structure.<sup>47,48</sup> This suggests that the direct use of CSBO to produce NIPU coatings composed by industrial amino hardeners cured at conditions close to industrial requirements is limited.

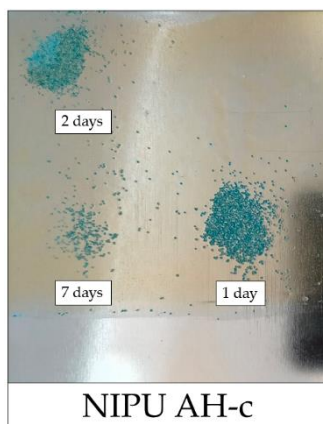


**Figure 4.4.** Dust-free test after 7 days for NIPU AH-c coating.

#### 4.4.2 Synthesis and characterization of NIPU-epoxy hybrid coatings by modified CSBO

The poor performance of NIPU coatings synthesized by direct use of CSBO, impelled us to take another approach for introducing CSBO-based NIPUs in coating industry under requirements in line with this industry. For this reason, it was decided to test a new process through the development of CSBO-based NIPU amino hardeners, with the objective of improving the performance/dryness of the formulation to equal industry requirements.

Recent research has shown that the curing process and the material performance can be synergistically enhanced through the combination of PHU with other chemical components, such as epoxy, acrylic, siloxane, etc.<sup>49,50</sup> This strategy has been applied even in some vegetable oil-based NIPUs.<sup>51-58</sup> Among the hybrid chemistry, PHU-epoxy has gained much attention due to the capacity of epoxy group to react rapidly with amines, and thus accelerate the curing process. Thus, our strategy was the development of CSBO-based NIPU amino hardeners via the reaction between CSBO and amine excess, followed by the reaction between the latter and an industrial epoxy resin, as is depicted in **Scheme 4.2-b**. The real potential of this approach is the opportunity to obtain amino terminal NIPUs that cure at room temperature. Furthermore, it allowed keeping the non-reacted amine with the synthesized amine-terminated hardener, avoiding an extra purifying process, and hence simplifying coating formulations preparative.<sup>49</sup> Moreover, this method avoids the use of low boiling point amines during the curing.

The development process for CSBO-based hybrid NIPU-epoxy coatings is divided into three main stages. First, a preliminary study was carried out to determine the most appropriate conditions to develop CSBO-based NIPU amino hardeners. Second, under optimal reaction conditions and using different amines, CSBO-based NIPUs with amino terminal groups were synthesized. Finally, clear, and pigmented coatings were prepared.

Optimization of the reaction conditions for CSBO-AHs

The high reactivity between amines and epoxy makes it difficult to develop one-component (1K) coatings, which makes this type of formulations into two-component (2K) NIPU coatings. In the latter, to ensure that the properties are not compromised in any way, it is important to avoid the presence of reactive groups that can react intramolecularly within the same component. Therefore, in CSBO-AHs synthesis it is fundamental to achieve a total conversion of the cyclic carbonate. However, the polyfunctionality of the carbonated soybean oil can result in gel formation during the hardener's synthesis by cross-linking, which prevents total conversion and make handling difficult. Consequently, the study of amine/cyclic carbonate ratio, together

with the possibility of a CSBO stepwise addition process was done to know the most suitable amine/cyclic carbonate molar ratio to avoid gel formation and achieve full conversion of cyclic carbonate.

The CSBO-AHs synthesis was done at 80 °C because is considered suitable for the amine addition to cyclic carbonate, and not high enough to facilitate the transesterification of the triglyceride ester group. Additionally, 1-methoxy-2-propanol (50 wt%) was used as reaction solvent, since in previous works it was demonstrated that protic polar solvents can form H bonds with the PHU achieving an adequate viscosity during the reaction.<sup>46</sup> The chemical composition changes during the synthesis process were monitored by FTIR.

The results of the preliminary study for the synthesis of CSBO-based NIPU amino hardener are shown in **Table 4.2**.

**Table 4.2.** Results of the preliminary study for the synthesis of CSBO-based NIPU amino hardeners.

Entry	Amine	MR <sup>a</sup>	T (°C)	Gel formation time (h)	CSBO 1 <sup>st</sup> addition time (h) <sup>b</sup>
1	AH-a	1.1	80	1.5	Batch <sup>e</sup>
2	AH-a	2.5	80	4	Batch <sup>e</sup>
3	AH-a	10–2.5 <sup>c</sup>	80	-	9
4	TETA	10–2.5 <sup>c</sup>	80	-	1.5
5	AH-c	10–2.5 <sup>c</sup>	80	-	1.5
6	AH-c	5–2.5 <sup>d</sup>	80	-	4
7	AH-c	10–2.5 <sup>c</sup>	60	-	3

<sup>a</sup>Amine/cyclic carbonate molar ratio.; <sup>b</sup>The time of addition corresponds to 2<sup>nd</sup> step (amine/cyclic carbonate equiv.: 5); <sup>c</sup>CSBO step by step addition with an initial molar ratio of amine/cyclic carbonate 10 to 2.5; <sup>d</sup>CSBO step by step addition with an initial molar ratio of amine/cyclic carbonate 5 to 2.5; <sup>e</sup>The reaction was done in batch and not by CSBO addition.

As it can be observed, at initial low molar ratios of amine/cyclic carbonate (equal or less to 2.5, **Table 4.2**, entry 1 and 2) gel formation was observed at relatively short

times. As mentioned above, it is desired to avoid gel formation to achieve full conversion of cyclic carbonates present in carbonate oil molecule. At high amine excess (amine/cyclic carbonate ratio 10) and CSBO stepwise addition until a molar ratio amine/cyclic carbonate near to 2.5 (Table 4.2, entry 3–5) gel formation was not observed, and the complete conversion of cyclic carbonate was achieved. Although all tested amines at these conditions did not present gel formation, polymeric amine (AH-a) showed low activity, while lower molecular weight amines (TETA and AH-c) reacted much faster. This evidenced the negative impact of the polymeric structure, and hence the use of AH-a was discarded.

In spite of avoiding gel formation by CSBO stepwise reaction (Table 4.2 entry 3-5), the presence of a side band (1660-1650  $\text{cm}^{-1}$ ) was observed in the ATR-FTIR spectra (Figure 4.5-top).

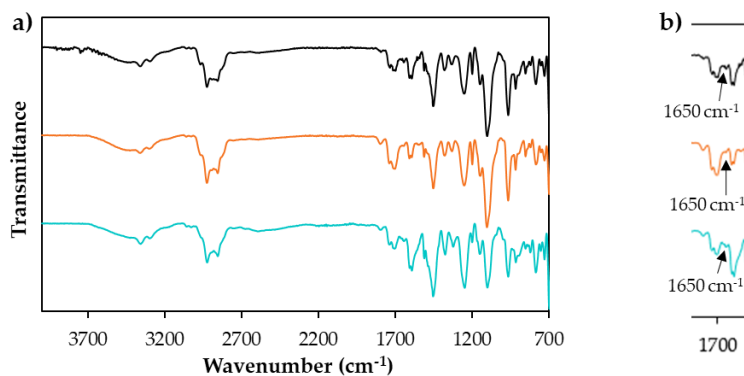
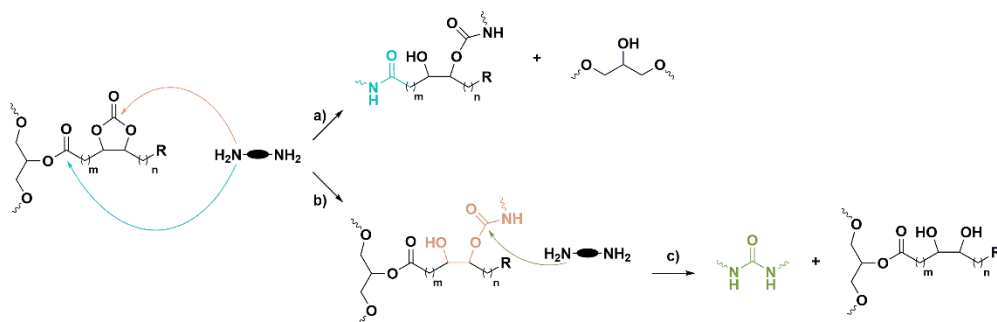


**Figure 4.5.** FTIR-ATR spectra of the CSBO-based NIPU amino hardener's after 1h at MR 10 and 80 °C (top), MR 5 and 80 °C (middle) and MR 10 and 60 °C (bottom): a) Wavenumber 400-4000  $\text{cm}^{-1}$  and b) wavenumber 1500-2000  $\text{cm}^{-1}$ .

In Chapter 3 it has been determined that the side band present in the wavelength 1660-1650  $\text{cm}^{-1}$  corresponds to the amide C=O stretching vibration. However, in the synthesis of CSBO-AHs, the amine excess was so excessively high that in addition to driving the amide formation, it can enhance the formation of urea from transurethanization side reaction. This fact was also observed by other authors.<sup>11,58-61</sup> Scheme 4.3 despite the possible main reaction between CSBO and amines.



**Scheme 4.3.** Main possible reactions between carbonated oil and amine: (a) cyclic carbonate aminolysis, (b) ester group amidation and (c) urea formation by transurethanization.

Therefore, it was decided to reduce initial amine/cyclic carbonate molar ratio and/or temperature in order to prevent side product formation (Table 4.2, entry 6 and 7). However, the Figure 4.5-top and middle and Table 4.2 not only reveals the side group formation at milder conditions, but also more than twofold increase in time for the second addition step in both cases. Therefore, decreasing the initial amine/cyclic carbonate molar ratio and temperature, revealed null impact on selectivity, in addition to the negative effect on the reactivity. Hence, it was established an initial amine excess with an amine/cyclic carbonate molar ratio of 10, and CSBO addition step by step at 80 °C, as suitable reaction conditions to avoid gel-formation, achieve full conversion of cyclic carbonate and form CSBO-based NIPU amino hardener.

It is very common to add a solvent to both the binder and the hardener to achieve a suitable viscosity and facilitate the mixing and application of the coating. Therefore, the solvent used for components storage is another factor to be considered in coatings formulations. Improper selection may negatively affect two fundamental factors related with formulation application: amino hardener's homogeneity and formulation's drying time. Initially, when methoxy propanol was used as both reaction and application solvent resulted in cloudy formulations (Figure 4.6), which can lead the formation of two phases over time.



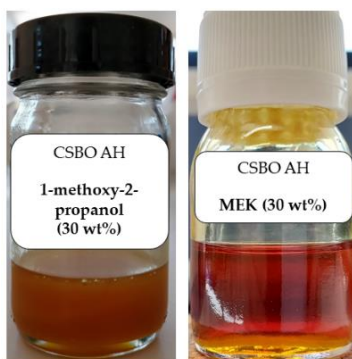
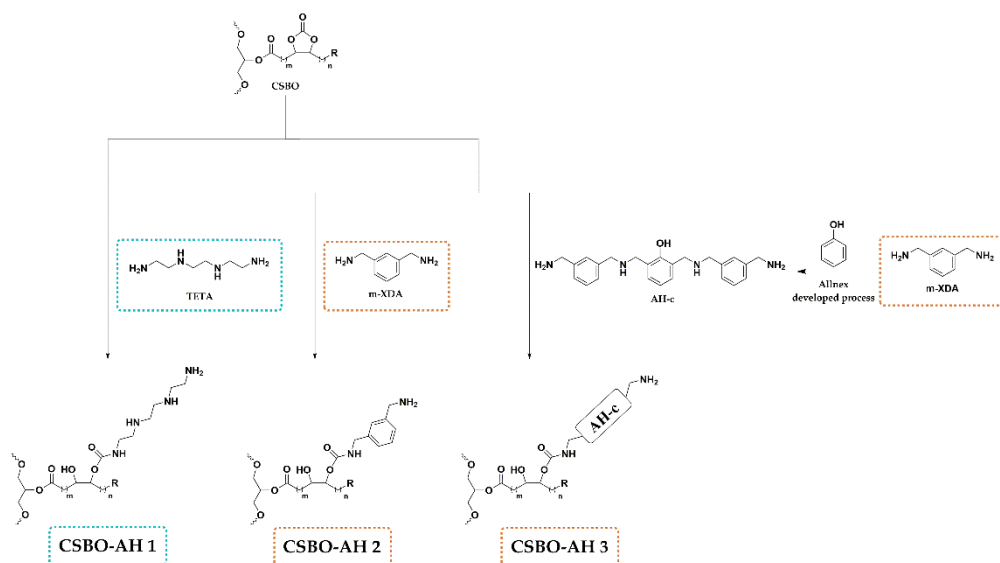


**Figure 4.6.** CSBO-based amino hardener in different solvents.

As for the second factor, high boiling point solvents result in longer formulation drying time. Hence, solvents with lower boiling points are considered a better option. For these reasons, it was concluded that the best option was to keep methoxy propanol as reaction solvent and remove and replace it by the same amount of MEK on a later stage. MEK could not be used also as reaction solvent as the condensation reaction between amine and keto group in MEK would take place.<sup>62</sup> To achieve a suitable viscosity with the selected solvent, a 30 wt% was established as appropriate MEK concentration, for both formulation application and amino hardeners synthesis.

Synthesis and characterization of CSBO-AHs

The CSBO-AHs were prepared according to the previously established procedure. **Scheme 4.4** illustrates the synthesis of three amino hardeners using carbonated soybean oil and TETA, m-XDA or AH-c as starting materials. The diamine selection was due to their use as precursors for commercially available amino hardeners. In fact, the industrially used AH-c is synthesized through the chemical modification of m-XDA. Consequently, the prepared amino hardeners can be divided in two families: TETA-based amino hardeners (CSBO-AH 1) and m-XDA-based amino hardeners (CSBO-AH 2 and CSBO-AH 3).



**Scheme 4.4.** CSBO-based amino hardeners synthesis process.

In **Table 4.3**, are detailed the H equiv. weight and viscosity of the prepared CSBO-AHs using different amine precursors.

**Table 4.3. Properties of synthesized CSBO-based amino hardeners.**

Name	Amine precursor	Final MR <sup>a</sup>	H equiv. weight (g/mol)	Viscosity (mPa.s)
CSBO-AH 1	TETA	2.5	92.0	16689
CSBO-AH 2	m-XDA	3.3	149.2	3345
CSBO-AH 3	AH-c	3.3	205.5	9549

<sup>a</sup>Amine/cyclic carbonate molar ratio.

The influence of amine reactivity on the final amine/cyclic carbonate molar ratio is evident. As mentioned above, achieving a complete conversion of the cyclic carbonate is required to ensure that the properties of the amino hardener components are not compromised. In the m-XDA-based amines, the reaction had to be stopped at amine/cyclic carbonate molar ratio 3.3 (3<sup>rd</sup> step), since at lower molar ratios the conversion of cyclic carbonate is limited. In TETA-based amino hardener the final

amine/cyclic carbonate molar ratio was close to 2.5 (4<sup>th</sup> step). The results obtained indicated that the reactivity of aromatic hardeners is lower for the preparation of CSBO-based amino hardeners, which limited the CSBO addition to the 3<sup>rd</sup> step (amine/cyclic carbonate molar ratio close to 3.3).

ATR-FTIR was used to follow the reaction progress. In **Figure 4.7** the ATR-FTIR spectra of the CSBO-AH 2 is illustrated as an example of the reaction monitoring. The ATR-FTIR spectra provided evidence of the reaction between cyclic carbonate and amine. The progressive disappearance of the cyclic carbonate carbonyl characteristic band ( $1800\text{ cm}^{-1}$ ) confirmed the complete conversion of CSBO and determined the end of the step or reaction. This is consistent with the simultaneous formation of bands associated to PHU formation localized at  $3400\text{--}3300\text{ cm}^{-1}$ ,  $1700\text{ cm}^{-1}$  and  $1545\text{ cm}^{-1}$  and ascribed to O–H and N–H stretching vibration, urethane C=O stretching vibration and N–H bending vibration, respectively. Nevertheless, the formation of a new band at  $1660\text{--}1645\text{ cm}^{-1}$  was also observed. As mentioned in previous section, it is suspected that the amine reacted with the triglyceride ester group for amide formation (**Scheme 4.3-a**) and/or with the formed urethane for urea formation (**Scheme 4.3-c**). As mentioned before, these facts were also observed by other authors, which associated the presence of these side reactions to the excess of amine used.<sup>11,22,25,28,59,61</sup>

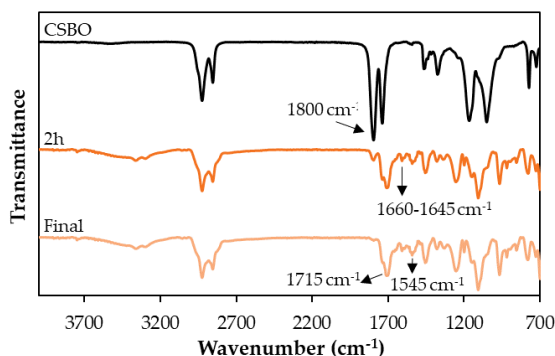


**Figure 4.7.** ATR-FTIR spectra of the reaction between CSBO and m-XDA at different reaction times.

In order to identify the side functional group, and because  $^1\text{H}$  NMR spectra were not conclusive, each of CSBO-AHs was analysed by  $^{13}\text{C}$  NMR. In **Figure 4.8** the  $^{13}\text{C}$  NMR spectra of soybean oil, CSBO and CSBO-AH 2 are illustrated as a representative example. The soybean oil spectrum showed the characteristic peaks of ester group presented in vegetable oil structure at 172 ppm and 69-62 ppm assigned to the ester carbonyl carbon and to the glycerol carbon atoms, respectively.<sup>63</sup> The  $^{13}\text{C}$  NMR spectra of CSBO, in addition to the related peaks characteristic of the ester and glycerol group, confirms the formation of cyclic carbonate through the existence of peaks at 154-153 ppm (cyclic carbonate C=O) and 82 and 79.5 ppm (cyclic carbonate carbon atoms).<sup>28,29</sup> The CSBO-AH 2 spectrum, verified vegetable-oil NIPU formation by the emergence of peaks at 157 ppm (urethane C=O) and 66-63 ppm (OH adjacent carbon).<sup>46,64</sup> In fact, the absence of the peaks at 82 ppm and 79.5 ppm and the existence of low intensity peaks at 154-153 ppm confirmed the high cyclic carbonate conversion. The analysis of these results, together with FTIR spectra, suggested that the presence of cyclic carbonate group was residual. Regarding the side reaction, the presence of peaks at 172 ppm and 69-62 ppm (ester group) and the formation of a new one at 168 ppm (amide C=O), points to partial amidation of ester group.<sup>63</sup> Moreover, the absence of a peak at 160 ppm (urea C=O) discards the hypothesis of urea formation during CSBO-AHs synthesis.<sup>46</sup> Therefore, these results verified that the final CSBO-AHs were mainly composed by urethane, amide, and amino terminal groups, and are consistent with those obtained by FTIR. This means that, in addition to the cyclic carbonate ring-opening reaction (**Scheme 4.3-b**), the transesterification reaction also occurs (**Scheme 4.3-a**). It is important to point out that the use of CSBO as a precursor allowed the development of amino-hardeners with a bio-based content between 46% and 62%.

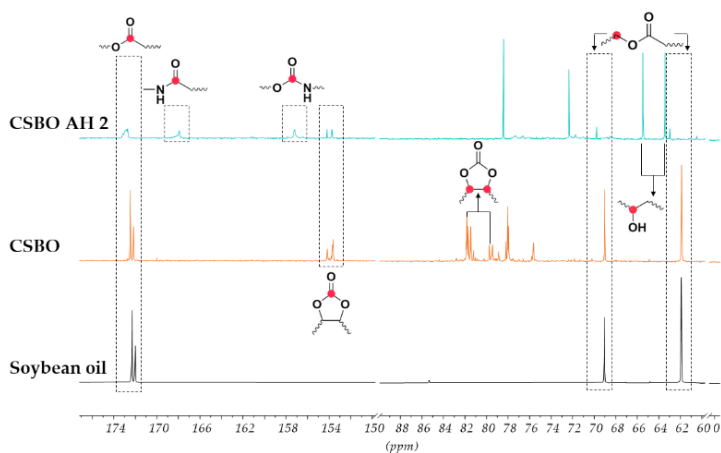


**Figure 4.8.** Comparative  $^{13}\text{C}$ -NMR spectra of soybean oil, CSBO and CSBO-AH 2.

#### Characterization of NIPU-epoxy hybrid clear coatings by modified CSBO

The real potential of coatings must be evaluated through the main formulation, composed only by a component A (epoxy resin) and component B (amino hardener), and named as clear formulation. The NIPU-epoxy hybrid coatings were prepared using CSBO-AHs and industrial epoxy resins as components. Two commercial epoxy coatings were also formulated from commercial amine hardeners synthesized from TETA (AH-d) and m-XDA (AH-c) and used as benchmark. It is important to underline that for a more appropriate comparison, coatings developed from the same amino precursor were compared. In **Figure 4.9** the prepared NIPU-epoxy hybrid formulations nomenclature and components are depicted.

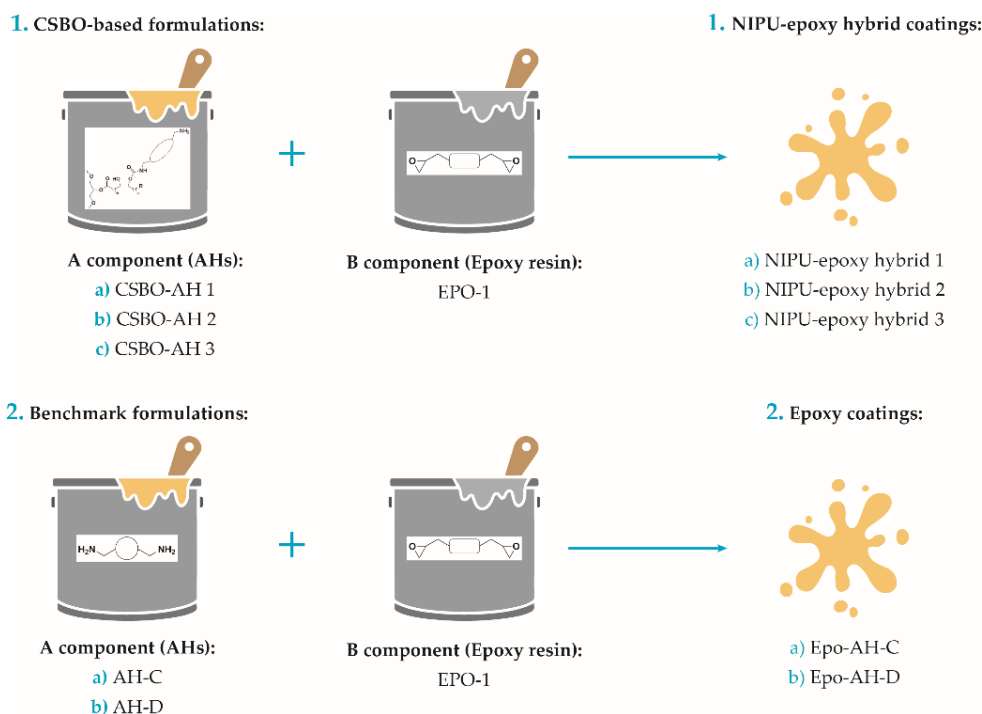


**Figure 4.9.** Preparative of CSBO-based hybrid NIPU-epoxy coatings.

*a) Curing monitoring*

In ambient curing coatings, it is important to know the development of hardness over time after the application on the surface and before properties characterization and thus, determine the end of the curing. This property was monitored in clear coatings over a 28 days period, and the results are summarized in **Figure 4.10**. Monitoring the pendulum hardness value provides relevant data related to the curing behaviour. As can be seen in **Figure 4.10-a**, the TETA-based benchmark (Epo-AH-d) and the Hy-NIPU-Epo 1 formulations showed totally different behaviour. The reference reached a plateau much faster than the formulation composed of CSBO (Hy-NIPU-Epo 1), which did not reach a clear plateau within the monitoring time. These results suggests that the triglyceride structure has a negative effect on amine group reactivity, delaying the complete curing time considerably. On the other hand, all m-XDA-based formulations showed a similar trend in hardness development (**Figure 4.10-b**), where for all prepared coatings a plateau was not reached within the 28 days. These results

suggest that, in this case, the curing time is strongly determined by the aromatic nature of the amino hardener. Nevertheless, it is to be stressed that even if a constant value was not obtained, the slope of the curve decreased considerably after 7 days. It is important to emphasize that a coating reaches its maximum potential when the hardness value reaches a plateau (constant value). In CSBO-based formulations not reaching a constant pendulum hardness value within the monitoring time suggests that perhaps the real potential of the prepared amino hardeners (CSBO-AH 1-3) could be obtained only at even longer curing times (>28 days).

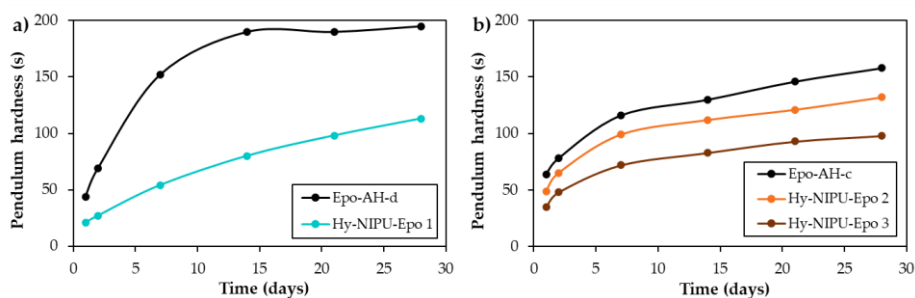


**Figure 4.10.** Pendulum hardness monitoring of prepared coatings (a) TETA-based and (b) m-XDA based.

#### b) Clear coatings properties

Coatings key properties, such as pot-life, drying, hardness and solvent resistance were studied to determine the performance of CSBO-based NIPU-epoxy hybrid clear formulations. After having monitored the curing process, 28 days was selected as coating characterization time. As described before, the hardness value plateau or nearly constant hardness was reached after 28 days of its application in panels. Therefore, it was considered that that curing was complete after this period **Figure 4.11** depicts the coating properties of each formulation.

Formulation's pot-life was defined as the time it takes for the viscosity of the coating mixture to increase by twice its value from the time all the reagents are mixed. In practical terms, it is important to know the pot-life value, as it determines the time

limit of application on a surface due to viscosity increase. The pot-life value of the prepared formulations was similar in both families. However, the benchmark derivatives achieved slightly shorter pot-life than hybrid formulations. This behaviour could be associated to the high steric hindrance of the triglyceride structure, which leads to a decrease in amino groups reactivity. The fact that the pot-life time are relatively long, allows the application of coating mixtures for a broader period of time.

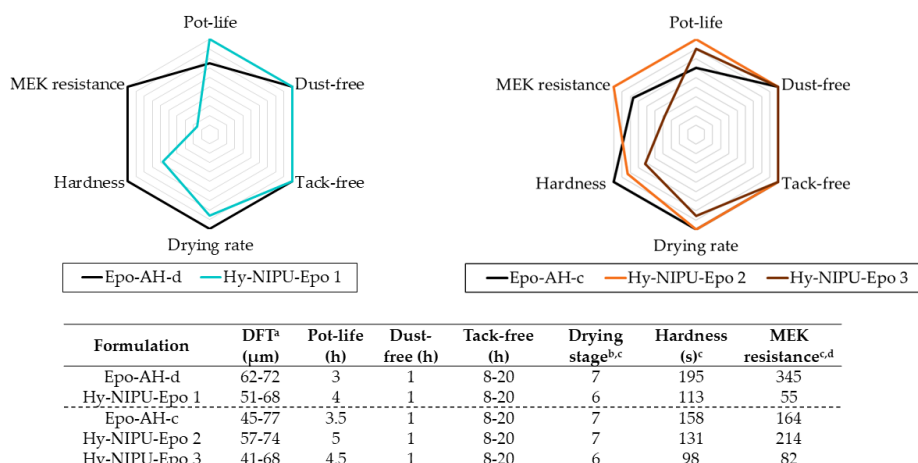
Drying is a property of great relevance in the coating industry. It is fundamental to be as fast as possible to avoid the adhesion of polluting particles, to apply another layer, etc. Coating mixture drying was evaluated by dust-free, tack-free, and drying test according to ISO 9117-5:2012. The nature of the amino hardener used has no influence in dust-free and tack-free times for both TETA-based and m-XDA-based formulations. The physical drying (dust-free) was less than 1h, and the chemical drying (tack-free) did not exceed 24h after application to the surface. The drying test (ISO 9117-5:2012) specifies a method for the determining the drying stage of coatings, in stages ranging from 1 (lowest drying stage) to 7 (maximum drying stage). In this case, two of the three CSBO-based formulations failed to reach the stage of maximum drying (7: maximum drying stage). Considering that the standard specifies that elasto-plastic coatings hardly ever reach a maximum drying value, the lower value obtained by CSBO-based formulations may be due to the softness of the triglyceride structure. However, although, some of the CSBO-based formulations did not achieve the highest drying stage, the potential of hybrid formulations is clear since the value obtained was only 1 point lower than the maximum. Even, Hy-NIPU-Epo 2 achieved the maximum drying stage after the selected characterization period.

The hardness of the prepared coatings was measured by Konig pendulum. In TETA-based formulations, the hardness of the prepared coatings decreased significantly when CSBO-AH was used. This behaviour can be explained by the possible greater cross-linking degree that it is obtained using more active amino hardeners. In contrast, m-XDA based formulations showed slightly lower differences. On the contrary to TETA-based formulations, the lower hardness of formulations composed by CSBO and mXDA could be caused by triglyceride structure. Indeed, the presence



of long fatty acid chains provides a higher softness to the material, decreasing the hardness value.<sup>65</sup> On the other hand, the greater hardness of Hy-NIPU-Epo 2 (CSBO-AH 2, H equiv.: 149.2 g/mol) in relation to Hy-NIPU-Epo 3 (CSBO-AH 3, H equiv.: 205.5 g/mol) may be due to the cross-linking density (See H equiv. values in **Table 4.3**). At low H equiv. value of the hardener, the distance between cross-linking nodes is lower and therefore greater the cross-linking density and coating hardness. Moreover, these results confirmed that hybrid chemistry enhanced coating properties, increasing considerably the hardness compared to carbonated oil-based NIPU coatings, where values did not exceed 51 s.<sup>32,36</sup> This behaviour is in accordance with those reported in the literature where the addition of epoxy resins improved coatings properties.<sup>52,55,66,66</sup>

The solvent resistance was examined by performing MEK rubbing test. TETA-based formulations showed the same trend as previously explained properties, achieving the benchmark formulation the greater solvent resistance. For coatings composed by m-XDA, the highest value was obtained with Hy-NIPU-Epo 2, a CSBO-based formulation. Due to the close relationship between the solvent resistance and cross-linking degree, the results obtained suggested that Epo-AH-d and Hy-NIPU-Epo 2 got the highest cross-linking in their respective families.



<sup>a</sup>Dry film thickness (DFT); <sup>b</sup>The drying rate unit is determined by ISO 9117-5:2012. 1 is the lowest value and 7 the maximum; <sup>c</sup>These properties were measured after 28 days; <sup>d</sup>The unit of MEK resistance is the number of MEK double rubs.

**Figure 4.11.** Properties of the prepared clear coating formulations after 28 days.

### Characterization of NIPU-epoxy hybrid pigmented coatings by modified CSBO

In order to take a step forward on the application of the CSBO-based formulations, pigmented coatings based on a commercial formulation (Allnex – The coating Resins Company –) were prepared (**Figure 4.12**). The principal difference between pigmented and clear coatings is the addition of pigments, additives, etc. to the main formulation composed by the binder (component A–Epoxy resin) and the AH (component B–Amino hardener), also named as clear formulation.



**Figure 4.12.** Prepared pigmented coatings composed by CSBO-AH 2 and applied in glass (left), OC (middle) and sand blasted steel panels (right).

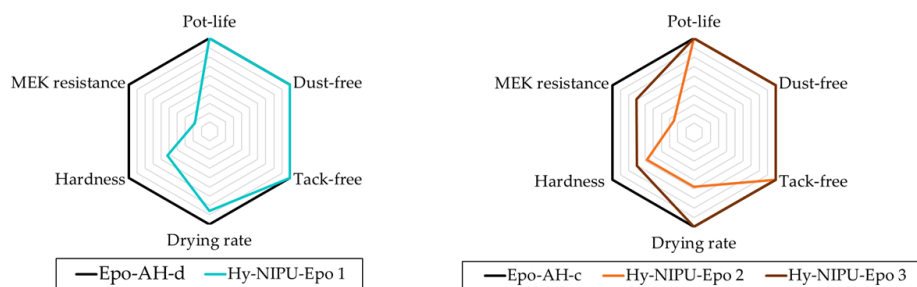
Unlike clear coatings, characterization was done after 7 days, as this is the norm for industrial epoxy resin formulations. In **Figure 4.13** general pigmented coating properties are depicted. A strong influence of additives and pigments was observed compared to clear coatings, particularly in pot-life and MEK resistance. In all the formulations prepared, the pot-life increased significantly to times higher than 20h. This must be attributed to the presence of additives. Furthermore, the MEK resistance decreased considerably, fivefold in most cases, compared with the clear coatings at the same period of time (**Table 4.4**). The increase in pot-life time and reduction of MEK resistance could be because the additives/pigments present in the formulation can act as diluents within the polymeric network. Actually, the presence of these additives in the formulation reduces the concentration of component A (binder) and component B (AH) in the main formulation, which leads to a lower interaction between both components.

**Table 4.4.** MEK resistance of the prepared clear and pigmented coatings after 7 days.

Formulation	Clear coating <sup>a</sup>	Pigmented coating <sup>a</sup>
Epo-AH-d	109	39
HyNIPU-Epo 1	57	7
Epo-AH-c	73	24
HyNIPU-Epo 2	42	6
HyNIPU-Epo 3	51	17

<sup>a</sup>The unit of MEK resistance is the number of MEK double rubs.

Another negative aspect of the presence of additives and pigments was observed in HyNIPU-Epo 2 formulation. The best coatings properties were achieved with this clear formulation. However, the addition of additives and pigments, considerably affected final features, becoming the worst coating in hardness, drying rate and MEK resistance. This indicates that the interaction between the hardener and additives/pigments had a negative influence, suggesting that the additives or pigments employed were not the most suitable ones for the CSBO-AH 2.



Formulation	DFT <sup>a</sup> ( $\mu\text{m}$ )	Pot-life (h)	Dust-free (h)	Tack-free (h)	Drying stage <sup>b,c</sup>	Hardness (s) <sup>c</sup>	MEK resistance <sup>c,d</sup>
Epo-AH-d	33-51	22	1	8-20	7	109	39
Hy-NIPU-Epo 1	43-65	22	1	8-20	6	57	7
Epo-AH-c	49-76	>24	1	8-20	7	73	24
Hy-NIPU-Epo 2	35-62	>24	1	8-20	4	42	6
Hy-NIPU-Epo 3	55-73	>24	1	8-20	7	51	17

<sup>a</sup>Dry film thickness (DFT); <sup>b</sup>The drying rate unit is determined by ISO 9117-5:2012. 1 is the lowest value and 7 the maximum; <sup>c</sup>These properties were measured after 7 days; <sup>d</sup>The unit of MEK resistance is the number of MEK double rubs.

**Figure 4.13.** Properties of the prepared pigmented coating formulations.

The mechanical properties of the pigmented coatings were measured to obtain a broader view of the features of the formulations, including crosshatch adhesion,

cupping, and impact resistance. The mechanical properties obtained are summarized in **Table 4.5**.

**Table 4.5.** Pigmented coating mechanical properties of NIPU-epoxy hybrid formulations after 7 days.

Formulation	Cross-cut <sup>a</sup>	Cupping test (mm)	Impact d <sup>b</sup> (kg/cm)	Impact id <sup>c</sup> (kg/cm)
Epo-AH-d	1	2.7	20	Null
HyNIPU-Epo 1	1	7.5	10	Null
Epo-AH-c	0-1	6.3	40	5
HyNIPU-Epo 2	0-1	5.3	10	10
HyNIPU-Epo 3	0	7.8	40	10

<sup>a</sup>The cross-cut unit is determined by ISO 2409:2013; <sup>b</sup>Impact d: Direct impact; <sup>c</sup>Impact id: Indirect impact.

In TETA-based formulations, the difference in properties such as adhesion or impact resistance was minimal. HyNIPU-Epo 1 achieved the same adhesion strength as that of the commercial epoxy coating. Regarding impact resistance, both direct and indirect impact resistances of the prepared coatings were low or null. In the case of cupping test, which is a slow deformation measurement, better results were obtained with CSBO-based formulation compared to the one based on the commercial epoxy coating. In m-XDA-based formulations all CSBO-based showed excellent adhesion properties, like the benchmark. In addition, the coating composed by HyNIPU-Epo 3 exhibited the highest slow deformation. The impact resistance results revealed a similar value for HyNIPU-Epo 3 and Epo-AH-c, while the formulation composed by HyNIPU-Epo 2 exhibited poorer properties. These results support the negative effect of additives/pigments in HyNIPU-Epo 2 formulation since it became the coating with inferior mechanical properties. Before the measurement of these properties, it was expected an improvement of some of them compared to epoxy benchmarks, since it was reported that the addition of PU/NIPU to an epoxy resin enhances the mechanical properties.<sup>50</sup> Hence, the similarity in many of the mechanical properties may be due to the fact that a significant part of the formulation is composed by pigments/additives (pigment/binder ratio: 2/1 wt%). This suggests that the influence

of pigments/additives in prepared coatings is greater than the nature of the hardener and binder.

The corrosion resistance was investigated by DIN EN ISO 9227 for coatings applied in sand blasted steel panels that were exposed to 5% NaCl-solution for 6 weeks. **Table 4.6** and **Figure 4.14** show the mark length and the photographs from scratch reference of selected samples after different time intervals of exposure to the salt spray test. As can be seen for TETA-based formulations (Epo-AH-d and HyNIPU-Epo 1) the corrosion monitoring was very similar until 28 days. Nevertheless, at the end, better anticorrosion performance was obtained by the benchmark. On the other hand, the samples based on m-XDA (Epo-AH-c, HyNIPU-Epo 2 and HyNIPU-Epo 3) exhibited different behaviour. The HyNIPU-Epo 3 formulation showed the same anticorrosion resistance as the commercial benchmark after 42 days. However, as in previously studied properties, poor results were obtained with HyNIPU-Epo 2 due presumably to the negative interaction between pigments/additives and the amino hardener. It should be emphasized that two of the three prepared CSBO-based formulations exhibited suitable anticorrosion properties since coatings remained stable after 42 days exposed to 5% NaCl-solution. Despite the high anticorrosion performance of CSBO-based pigmented coatings, it is difficult to determine whether this is due to the base formulation (binder + hardener) or the high concentration of additives/pigments.

**Table 4.6.** Salt spray results for prepared NIPU-Epoxy hybrid formulations applied in sand blasted steel panels.

Time (days)	Epo-AH-d (mm) <sup>a</sup>	HyNIPU-Epo 1 (mm) <sup>a</sup>	Epo-AH-c (mm) <sup>a</sup>	HyNIPU-Epo 2 (mm) <sup>a</sup>	HyNIPU-Epo 3 (mm) <sup>a</sup>
0	0	0	0	0	0
14	12	9	6	10	11
28	15	19	8	Null	9
42	15	24	10	Null	10

<sup>a</sup>Mark length from scratch reference.

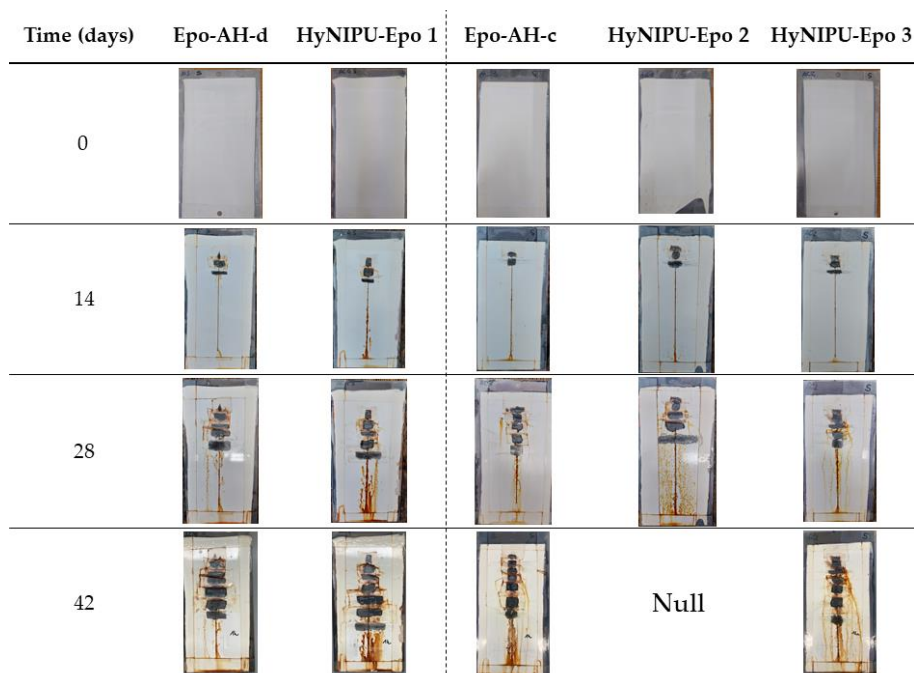


**Figure 4.14.** Photographs of the prepared NIPU-epoxy hybrid formulations applied in sand blasted steel panels after different exposure times to the salt spray test.

The salt spray test was also studied for coatings applied in OC plates (**Table 4.7**). In this instance, similar behaviour as in sand blasted steel plate was observed. However, the lower roughness of OC plates reduced the penetration of the formulation into the plate, exhibiting poorer results for all formulations.

**Table 4.7.** Salt spray results for prepared NIPU-Epoxy hybrid formulations applied in OC panels.

Time (days)	Epo-AH-d (mm) <sup>a</sup>	HyNIPU-Epo 1 (mm) <sup>a</sup>	Epo-AH-c (mm) <sup>a</sup>	HyNIPU-Epo 2 (mm) <sup>a</sup>	HyNIPU-Epo 3 (mm) <sup>a</sup>
0	0	0	0	0	0
14	22	21	6	Null	Null
28	Null	Null	9	Null	Null
42	Null	Null	Null	Null	Null

<sup>a</sup>Mark length from scratch reference.

## 4.5 Conclusions

In this chapter, carbonated soybean oil-based non-isocyanate polyurethane coatings have been explored under conditions required for industrial application, in terms of temperature and time. It was observed that the NIPUs synthesized by the direct use of CSBO hardly met the requirements for industrial implementation. However, the synthesis of NIPU-Epoxy hybrid coatings from CSBO-based amino hardeners allowed a curing process at room temperature and in a relatively short time.

The potential of the development of NIPU-epoxy hybrid formulations is derived from two main factors 1) The possibility of developing CSBO-based amino hardeners at high cyclic carbonate conversion, 2) The possibility of performing the curing of a NIPU formulation under conditions required by the industry.

The reaction conditions for suitable synthesis of CSBO-based NIPU amino hardeners were studied. It was noted that the initial amine/cyclic carbonate molar ratio influenced considerably the gel-formation, and hence the cyclic carbonate conversion. The best conditions to avoid gel formation and achieve complete conversion of cyclic carbonate, were an amine/cyclic carbonate molar ratio of 10 and stepwise addition of CSBO. Reducing the molar ratio of amine/cyclic carbonate and temperature did not prevent amide formation, while diminishing reactivity.

Based in CSBO stepwise process, two family of CSBO-AHs were synthesized using TETA and m-XDA as precursor. It is worth mentioning that in both families complete cyclic carbonate conversion was confirmed by FTIR and  $^{13}\text{C}$ -NMR, which provide a clear opportunity for the development of bio-based NIPU amino hardeners from vegetable oils.

The CSBO amino hardeners were studied in coating application as component of clear and pigmented formulations. The curing time of the prepared formulations was significantly dependent on the presence of triglyceride and aromatic structures, reaching complete curing after 28 days. The drying performance was found to be negligibly dependent to CSBO presence and diamine precursor. However, the final

hardness of the coatings was markedly influenced by the triglyceride structure, with the softest coatings being achieved in the CSBO-based formulations. Moreover, a comparison between commercially available epoxy coatings and hybrid NIPU-epoxy synthesized by the present route suggests, that the potential of bio-based formulations is not so far away from commercial ones. In the case of pigmented formulations, it was observed that additives/pigments addition influenced considerably the final properties. Indeed, in many of the mechanical properties and anticorrosion performance, similar values were obtained for benchmarks and NIPU coatings, probably due to the fact that a significant part of the formulation is composed of pigments/additives (pigment/binder ratio: 2/1 wt%).

To the best of our knowledge, this work addresses for the first time the uses of CSBO-based amino hardeners as a component of NIPU coating formulations. It should be noted that the process carried out for the development of NIPU-epoxy hybrid coatings can bring oil-based formulations closer to a real application since the conditions are similar to those required by the coating industry. On the one hand, the obtention of soybean oil-based NIPU amino hardeners via the stepwise addition of CSBO, represents an alternative for the obtention of high CSBO conversion at relatively short reaction times and mild conditions. In addition, it allows obtaining hardeners with a bio-based content of more than 45%. On the other hand, the synthesis of CSBO-based NIPU amino hardener and the subsequent addition of an epoxy resin, allows room temperature curing carbonated oil-based NIPU coatings due to the capacity of epoxy group to react rapidly with amines. In addition, it was possible to develop pigmented CSBO formulations, which brought these bio-based formulations closer to those used industrially, especially in terms of their visual characteristics. However, the addition of the pigments and/or additives has not improved the properties of the coatings, therefore in the future it would be necessary to focus on the optimization of a pigmented formulations. Additionally, due to the use of petrochemical-based epoxy resin, the final bio-based content in clear coatings was inferior to 10%, which suggest that in order to enhance this percentage, the employment of bio-based epoxy resins must be consider.



## 4.6 References

- 1 A. Noreen, K. M. Zia, M. Zuber, S. Tabasum and A. M. Zahoor, *Prog. Org. Coatings*, 2016, **91**, 25–32.
- 2 Polyurethane (PU) Coatings Market–Growth, Trends, COVID-19 Impact, and Forecasts (2021–2026). <https://www.mordorintelligence.com/industry-reports/polyurethane-market>. (accessed February 5, 2022).
- 3 M. H. Karol and J. A. Kramarik, *Toxicol. Lett.*, 1996, **89**, 139–146.
- 4 C. Bolognesi, X. Baur, B. Marczynski, H. Norppa, O. Sepai and G. Sabbioni, *Crit. Rev. Toxicol.*, 2001, **31**, 737–772.
- 5 L. Pollaris, F. Devos, V. De Vooght, S. Seys, B. Nemery, P. H. M. Hoet and J. A. J. Vanoirbeek, *Arch. Toxicol.*, 2016, **90**, 1709–1717.
- 6 H. W. Engels, H. G. Pirkel, R. Albers, R. W. Albach, J. Krause, A. Hoffmann, H. Casselmann and J. Dormish, *Angew. Chem. Int. Ed.*, 2013, **52**, 9422–9441.
- 7 Y. Suryawanshi, P. Sanap and V. Wani, *Polym. Bull.*, 2019, **76**, 3233–3246.
- 8 *Of. J. Eur. Union*, 2009, **552**, 7–31.
- 9 B. Nohra, L. Candy, J. F. Blanco, C. Guerin, Y. Raoul and Z. Mouloungui, *Macromolecules*, 2013, **46**, 3771–3792.
- 10 L. Maisonneuve, O. Lamarzelle, E. Rix, E. Grau and H. Cramail, *Chem. Rev.*, 2015, **115**, 12407–12439.
- 11 A. Cornille, R. Auvergne, O. Figovsky, B. Boutevin and S. Caillol, *Eur. Polym. J.*, 2017, **87**, 535–552.
- 12 C. Carré, Y. Ecochard, S. Caillol and L. Avérous, *ChemSusChem*, 2019, **12**, 3410–3430.
- 13 M. Ghasemlou, F. Daver, E. P. Ivanova and B. Adhikari, *Eur. Polym. J.*, 2019, **118**, 668–684.
- 14 J. Datta and M. Włoch, *Polym. Bull.*, 2016, **73**, 1459–1496.
- 15 M. North, R. Pasquale and C. Young, *Green Chem.*, 2010, **12**, 1514–1539.

- 16 M. S. Kathalewar, P. B. Joshi, A. J. Sabnis and V. C. Malshe, *Rsc Adv.*, 2013, **3**, 4110–4129.
- 17 T. An Phung Hai, M. Tessman, N. Neelakantan, A. A. Samoylov, Y. Ito, B. S. Rajput, N. Pourahmady and M. D. Burkart, *Biomacromolecules*, 2021, **22**, 1770–1794.
- 18 Z. S. Petrović, *Contemp. Mater.*, 2010, **I-1**, 39–50.
- 19 A. Tenorio-Alfonso, M. C. Sánchez and J. M. Franco, *J. Polym. Environ.*, 2020, **28**, 749–774.
- 20 H. Khatoon, S. Iqbal, M. Irfan, A. Darda and N. K. Rawat, *Prog. Org. Coatings*, 2021, **154**, 106124.
- 21 B. Tamami, S. Sohn and G. L. Wilkes, *J. Appl. Polym. Sci.*, 2004, **92**, 883–891.
- 22 I. Javni, D. P. Hong and Z. S. Petrovic, *J. Appl. Polym. Sci.*, 2008, **108**, 3867–3875.
- 23 Z. Li, Y. Zhao, S. Yan, X. Wang, M. Kang, J. Wang and H. Xiang, *Catal. Lett.*, 2008, **123**, 246–251.
- 24 M. Bähr and R. Mühlhaupt, *Green Chem.*, 2012, **14**, 483–489.
- 25 I. Javni, D. P. Hong and Z. S. Petrovic, *J. Appl. Polym. Sci.*, 2013, **128**, 566–571.
- 26 S. Jalilian and H. Yeganeh, *Polym. Bull.*, 2015, **72**, 1379–1392.
- 27 B. Grignard, J. Thomassin, S. Gennen, L. Poussard, L. Bonnaud, J. M. Raquez, P. Dubois, M. P. Tran, C. B. Park, C. Jerome and C. Detrembleur, *Green Chem.*, 2016, **18**, 2206–2215.
- 28 S. Doley and S. K. Dolui, *Eur. Polym. J.*, 2018, **102**, 161–168.
- 29 A. Farhadian, A. Ahmadi, I. Omrani, A. B. Miyardan, M. A. Varfolomeev and M. R. Nabid, *Polym. Degrad. Stab.*, 2018, **155**, 111–121.
- 30 W. Y. Pérez-Sena, X. Cai, N. Kebir, L. Vernières-Hassimi, C. Serra, T. Salmi and S. Leveneur, *Chem. Eng. J.*, 2018, **346**, 271–280.

- 31 S. Hu, X. Chen and J. M. Torkelson, *ACS Sustain. Chem. Eng.*, 2019, **7**, 10025–10034.
- 32 A. Z. Yu, R. A. Setien, J. M. Sahouani, J. Docken and D. C. Webster, *J. Coatings Technol. Res.*, 2019, **16**, 41–57.
- 33 A. F. G. Agudelo, W. Y. Pérez-Sena, N. Kebir, T. Salmi, L. A. Ríos and S. Leveneur, *Chem. Eng. Sci.*, 2020, **228**, 115954.
- 34 J. Dong, B. Liu, H. Ding, J. Shi, N. Liu, B. Dai and I. Kim, *Polym. Chem.*, 2020, **11**, 7524–7532.
- 35 C. Mokhtari and F. Malek, *Mater. Today Proc.*, 2020, **31**, S12–S15.
- 36 J. Pouladi, S. M. Mirabedini, H. E. Mohammadloo and N. G. Rad, *Eur. Polym. J.*, 2021, **153**, 110502–110514.
- 37 S. Doley, A. Bora, P. Saikia, S. Ahmed and S. K. Dolui, *J. Polym. Res.*, 2021, **28**, 1–9.
- 38 T. Dong, E. Dheressa, M. Wiatrowski, A. P. Pereira, A. Zeller, L. M. L. Laurens and P. T. Pienkos, *ACS Sustain. Chem. Eng.*, 2021, **9**, 12858–12869.
- 39 J. D. O. Rodrigues, C. K. Z. Andrade, R. L. Quirino and M. J. A. Sales, *Prog. Org. Coatings*, 2022, **162**, 106557–106567.
- 40 X. Yang, C. Ren, X. Liu, P. Sun, X. Xu, H. Liu, M. Shen, S. Shang and Z. Song, *Mater. Chem. Front.*, 2021, **5**, 6160–6170.
- 41 X. Yang, S. Wang, X. Liu, Z. Huang, X. Huang, X. Xu, H. Liu, D. Wang and S. Shang, *Green Chem.*, 2021, **23**, 6349–6355.
- 42 H. Gholami and H. Yeganeh, *Eur. Polym. J.*, 2021, **142**, 110142–110152.
- 43 R. Pathak, M. Kathalewar, K. Wazarkar and A. Sabnis, *Prog. Org. Coatings*, 2015, **89**, 160–169.
- 44 H. Greim, D. Bury, H. J. Klimisch, M. Oeben-Negele and K. Ziegler-Skylakakis, *Chemosphere*, 1998, **36**, 271–295.

- 45 M. N. Kim, J. C. Jang, I. M. Lee, H. S. Lee and J. S. Yoon, *J. Environ. Sci. Heal. Part B Pestic. Food Contam. Agric. Wastes*, 2002, **37**, 53–64.
- 46 A. Cornille, M. Blain, R. Auvergne, B. Andrioletti, B. Boutevin and S. Caillol, *Polym. Chem.*, 2017, **8**, 592–604.
- 47 R. P. Tiger, M. V. Zabalov and M. A. Levina, *Polym. Sci. Ser. C*, 2021, **63**, 113–125.
- 48 A. Gomez-Lopez, F. Elizalde, I. Calvo and H. Sardon, *Chem. Commun.*, 2021, **57**, 12254–12265.
- 49 Y. Ecochard and S. Caillol, *Eur. Polym. J.*, 2020, **137**, 109915–109936.
- 50 R. H. Lambeth, *Polym. Int.*, 2020, **70**, 696–700.
- 51 O. Türünç, N. Kayaman-Apohan, M. V. Kahraman, Y. Menceloğlu and A. Güngör, *J. Sol-Gel Sci. Technol.*, 2008, **47**, 290–299.
- 52 O. Figovsky, L. Shapovalov, O. Birukova and A. Leykin, *Polym. Sci. Ser. D*, 2013, **6**, 271–274.
- 53 S. Samanta, S. Selvakumar, J. Bahr, D. S. Wickramaratne, M. Sibi and B. J. Chisholm, *ACS Sustain. Chem. Eng.*, 2016, **4**, 6551–6561.
- 54 S. Panchireddy, B. Grignard, J. M. Thomassin, C. Jerome and C. Detrembleur, *Polym. Chem.*, 2018, **9**, 2650–2659.
- 55 S. Doley, A. Sarmah, C. Sarkar and S. K. Dolui, *Polym. Int.*, 2018, **67**, 1062–1069.
- 56 R. Gharibi, H. Yeganeh and S. Kazemi, *Mater. Sci. Eng. C*, 2019, **99**, 887–899.
- 57 M. A. C. M. Haniffa, H. A. Illias, C. Y. Chee, S. Ibrahim, V. Sandu and C. H. Chuah, *ACS Omega*, 2020, **5**, 10315–10326.
- 58 M. Blain, L. Jean-Gérard, R. Auvergne, D. Benazet, S. Caillol and B. Andrioletti, *Green Chem.*, 2014, **16**, 4286–4291.
- 59 V. Besse, F. Camara, F. Méchin, E. Fleury, S. Caillol, J. P. Pascault and B. Boutevin, *Eur. Polym. J.*, 2015, **71**, 1–11.

- 
- 60 O. Lamarzelle, P. L. Durand, A. L. Wirotius, G. Chollet, E. Grau and H. Cramail, *Polym. Chem.*, 2016, **7**, 1439–1451.
- 61 A. Bossion, R. H. Aguirresarobe, L. Irusta, D. Taton, H. Cramail, E. Grau, D. Mecerreyes, C. Su, G. Liu, A. J. Müller and H. Sardon, *Macromolecules*, 2018, **51**, 5556–5566.
- 62 R. D. Patil and S. Adimurthy, *Asian J. Org. Chem.*, 2013, **2**, 726–744.
- 63 D. Betancourt-Jimenez, J. P. Youngblood and C. J. Martinez, *ACS Sustain. Chem. Eng.*, 2020, **8**, 13683–13691.
- 64 A. Cornille, J. Serres, G. Michaud, F. Simon, S. Fouquay, B. Boutevin and S. Caillol, *Eur. Polym. J.*, 2016, **75**, 175–189.
- 65 A. Chaudhari, R. Kulkarni, P. Mahulikar, D. Sohn and V. Gite, *J. Am. Oil Chem. Soc.*, 2015, **92**, 733–741.
- 66 J. Ke, X. Li, F. Wang, M. Kang, Y. Feng, Y. Zhao and J. Wang, *J. CO2 Util.*, 2016, **16**, 474–485.
- 67 J. Ke, X. Li, F. Wang, S. Jiang, M. Kang, J. Wang, Q. Li and Z. Wang, *RSC Adv.*, 2017, **7**, 28841–28852.



# CHAPTER 05

---

CONCLUSIONS, FUTURE WORK AND  
PUBLISHED RESEARCH





## 5.1 Conclusions

This thesis has been devoted to bringing carbonated soybean oil-based non-isocyanate polyurethanes (CSBO-based NIPUs) closer to the industrial application with the aim to lead to a more sustainable industry. On the one hand, new economical catalysts have been developed to obtain cyclic carbonate precursors under mild reaction conditions. On the other hand, CSBO-based NIPUs have been developed with industrial application in mind, more specifically for the coating industry.

First, related to the synthesis of carbonated soybean oil, it has been possible to reduce the reaction time, from more than 24h with [TBA][Br] (the most used catalyst for carbonated vegetable oils synthesis) to only 5h of reaction with the self-developed catalyst, [DTPP][Br]. These results bring the synthesis of CSBO closer to a possible industrial implementation. Moreover, during this research, several factors with a significant influence on the reaction performance have been identified. (1) The chain length of the substituent attached to the triphenylphosphonium cation: The increase of the number of C atoms allows to enhance the nucleophilicity of the anion and solubility of the catalyst in the reaction medium. (2) The rigidity of the cation: A rigid structure keeps the anion far from the phosphorus atom weakening the electrostatic interaction between anion and the cationic centre, increasing the nucleophilic character of the anion and contributing to an easier and faster epoxide ring opening (considered the rate-determining step). (3) The higher thermal stability of [DTPP][Br] compared with [TBA][Br], allows increasing temperature in the CSBO synthesis, thus reducing the reaction time at least fivefold. Nevertheless, despite these promising results, the still elevated temperature and pressure employed limit the economic viability of the process. In my view, now that we know several factors that considerably influence/improve the catalytic activity, reaction conditions should be improved by reducing or eliminating the required pressure. Ideally, reactions would run at atmospheric pressure. Furthermore, recovering and reusing the catalyst could also mean a great advance in the sustainability of the process, since it would allow using the same catalyst to produce a certain number of batches of CSBO.

Secondly, related with the synthesis of CSBO-based NIPUs, polymers networks with different characteristics were developed from previously synthesized CSBO using different amines and molar ratios. The results obtained suggest that the versatility of the NIPUs was quite similar to that of the isocyanate analogues, achieving very different properties only by varying the amine structure and the molar ratio of the reagents. However, the reaction conditions and the poor performance in relation to traditional polyurethanes clearly shows that CSBO-based NIPUs industrial implementation is still far. In fact, although NIPUs outperform many PUs synthesized from VO in thermal stability, they lag behind in other properties ( $T_g$ , hardness, etc). This means that the potential of the isocyanate free pathway is not yet sufficiently competitive in certain properties, which limits the industrial use and commercialization of these materials.

Finally, among the two strategies studied for applying CSBO-based NIPUs in the coatings industry, unequal results have been achieved. On the one hand, the coatings synthesized through the direct use of CSBO and industrial amino hardeners showed insufficient performance. On the other hand, the development of hybrid NIPU-epoxy coatings via the synthesis of CSBO-based NIPU amino hardeners (CSBO-AHs) shows that this could be one of the solutions with greatest potential for implementing CSBO-based NIPUs in coating industry. Indeed, this process allows a complete conversion of CSBO at a moderate temperature and a short reaction time, in addition to a room temperature curing of carbonated soybean oil-based NIPU formulations. Furthermore, it was possible to develop pigmented CSBO formulations, which brought these biomass-based formulations closer to those used industrially, especially in terms of their visual characteristics. Although the addition of the pigments did not perform as desired, it identifies the optimization of pigmented formulations as future research.

## 5.2 Future work

This thesis has delivered promising results and represents a step forward in the applicability of NIPUs from carbonated soybean oil (CSBO). However, it is still necessary to continue the research to obtain the final goal of reaching their industrial application.

Regarding the synthesis of vegetable carbonated oils, most of the research is focused on the obtention of bio-based cyclic carbonates from commercially available vegetable oils. However, the majority of the available vegetable oils are edible and compete with the food chain. Therefore, the employment of non-edible (e.g., used cooking vegetable oil) should be investigated. To the best of our knowledge, there are no examples in the scientific literature dealing with the carbonatation of epoxidized, used cooking vegetable oil by CO<sub>2</sub> chemical fixation. This remains a huge and exciting challenge. On the other hand, in order to continue bringing this process closer to the industry and develop more sustainable and economical process, it is necessary to research on the recovery and reuse of the catalytic system. This recovery could be done by developing biphasic or heterogenization methods.

In relation to the applicability of CSBO-based NIPUs in the coatings industry, their performance can be extended/improved by two different strategies. On the one hand, expanding the family of CSBO-based NIPU amino-hardeners (CSBO-AHs) by using industrial-grade amines containing different structures to obtain CSBO-AHs with different compositions and properties. On the other hand, by developing new NIPU-epoxy hybrid formulations, using different industrially available epoxy resins. Additionally, the final pigmented formulations need to be optimized to enhance the properties and find the real potential of formulations composed by carbonated vegetable oils. Another point to increase workplace safety and consumer health is to avoid the use of organic solvents. This trend has not gone unnoticed by the coating industry, which in the last decades has focused its efforts on the development of waterborne formulations. Therefore, despite the hydrophobicity of the triglyceride structure, the future research should study the development of waterborne CSBO-based NIPU coatings to meet the environmental and health requirements that

industry is asking for. Finally, once the optimization of one of the formulations has been achieved, the evaluation of the possible fields in which CSBO-based NIPU coatings can be introduced as an alternative to another petrochemical-based formulation may be the first step towards the commercialization of the product.

### 5.3 Published research

#### PAPERS IN SCIENTIFIC JOURNALS

---

**Centeno-Pedraza, A.,** Perez-Arce, J., Prieto-Fernandez, S., Freixa, Z., Garcia-Suarez, E. J. **2021.**

**Phosphonium-based ionic liquids: economic and efficient catalysts for the solvent-free cycloaddition of CO<sub>2</sub> to epoxidized soybean oil to obtain potential bio-based polymers precursors**

Molecular Catalysis. DOI: 10.1016/j.mcat.2021.11889

Impact factor: 5.089 (2021)

Journal Category: Chemistry, Physical

Gómez-de-Miranda-Jiménez-de-Aberasturi, O., **Centeno-Pedraza, A.,** Prieto-Fernández, S., Rodriguez Alonso, R., Medel, S., Cuevas, J. M., Monsegue, L. G., De Wildeman, S., Benedetti, E., Klein, D., Henneken, H., Ochoa-Gómez, J. R. **2021.**

**The future of isosorbide as a fundamental constituent for polycarbonates and polyurethanes.**

Green Chemistry Letters and Reviews. DOI: 10.1080/17518253.2021.1965223

Impact factor: 6.016 (2021)

Journal Category: Green & Sustainable Science & Technology

**Centeno-Pedraza, A.,** Perez-Arce, J., Freixa, Z., Ortiz, P., Garcia-Suarez, E. J. **2022.**

**Catalytic systems for the effective fixation of CO<sub>2</sub> into epoxidized vegetable oils and derivates to obtain bio-based cyclic carbonates as precursors for greener polymers.**

(SUBMITTED)

CONTRIBUTIONS AT INTERNATIONAL SCIENTIFIC  
CONFERENCES

---

---

**Centeno-Pedraza, A.,** Freixa, Z., Garcia-Suarez, E. J.

**Carbonation of epoxidized soybean oil employing deep eutectic solvents as catalysts.**

Workshop- New Materials for a Better Life: Advanced devices and Materials as Key Enabling Technologies for Sustainable Environment (NM4BL), **2019**, Leioa (Spain)

Poster contribution

**Centeno-Pedraza, A.,** Prieto-Fernandez, S., Freixa, Z., Ortiz, P., Garcia-Suarez, E. J.

**Transformation of soybean oil and CO<sub>2</sub> for non-isocyanate polyurethanes (NIPUs) synthesis.**

Brightlands Polymers Days, **2021**, Eindhoven (Netherlands)

Oral contribution

**Centeno-Pedraza, A.,** Feola, R., Freixa, Z., Garcia-Suarez, E. J., Ortiz, P.

**Hybrid non-isocyanate polyurethane coatings from carbonated soybean oil.**

Bordeaux Polymers Conference (BPC), **2022**, Bordeaux (France)

Poster contribution

# LIST OF FIGURES

<i>Chapter 1</i>	<i>Page</i>
<b>Figure 1.1.</b> Main applications of traditional polyurethanes. ....	5
<b>Figure 1.2.</b> Soybean oil chemical composition.....	8
<b>Figure 1.3.</b> Triglyceride structure composed by oleic (top), linoleic (middle) and linolenic (bottom) acid methyl esters and reactive sites highlighted in orange.....	8
<b>Figure 1.4.</b> Ricinoleic and lesquerolic acid chemical structure.....	9
<b>Figure 1.5.</b> Main synthetic routes to form polyols from vegetable-oils. ....	10
<b>Figure 1.6.</b> Main routes known for the synthesis of non-isocyanate polyurethanes..	14
<b>Figure 1.7.</b> Non-functionalized ionic liquid catalyst used in CO <sub>2</sub> cycloaddition to epoxidized oleochemicals.....	22
<b>Figure 1.8.</b> Task-specific ionic liquid catalyst used in CO <sub>2</sub> cycloaddition to epoxidized oleochemicals. ....	28
<b>Figure 1.9.</b> Additives employed as co-catalyst to improve the catalytic performance of alkali metal salts. ....	38
<i>Chapter 2</i>	<i>Page</i>
<b>Figure 2.1.</b> Prepared phosphonium-based ionic liquids ( <b>1-11</b> ) and the benchmark ionic liquid ( <b>12</b> ) employed in this work as catalysts in the cycloaddition reaction of CO <sub>2</sub> to epoxidized soybean oil.....	63
<b>Figure 2.2.</b> Conversion and selectivity of ESBO to CSBO after cycloaddition with CO <sub>2</sub> with the different ionic liquid tested as catalysts ( <b>1</b> to <b>12</b> ). Reaction conditions:	

temperature: 120 °C, CO<sub>2</sub> pressure: 20 bar, reaction time: 2h, 5 mol% of catalyst referred to mol of oxirane. .... 68

**Figure 2.3.** Conversion and selectivity of ESBO to CSBO after solvent-free cycloaddition with CO<sub>2</sub> at different mol % with catalysts **5** and the reference catalyst **12**. Reaction conditions: temperature: 120 °C; CO<sub>2</sub> pressure: 20 bar; reaction time: 2h; mol % is referred to oxirane mol. .... 69

**Figure 2.4.** Conversion and selectivity of ESBO to CSBO after solvent-free cycloaddition with CO<sub>2</sub> at different temperatures with catalyst **5** and the reference catalyst **12**. Reaction conditions: catalyst amount: 2 mol % referred to oxirane mol; CO<sub>2</sub> pressure: 20 bar; reaction time: 2h. .... 70

**Figure 2.5.** Catalysts **5** ([DTTP][Br]) and **12** ([TBA][Br]) isothermal thermogravimetric analysis at 160 °C. .... 71

**Figure 2.6.** Conversion and selectivity of ESBO to CSBO after solvent-free cycloaddition with CO<sub>2</sub> at different pressure of CO<sub>2</sub> with catalyst **5** and the reference catalyst **12**. Reaction conditions: catalyst amount: 2 mol % referred to oxirane mol; temperature: 120 °C; reaction time: 2h. .... 71

**Figure 2.7.** Conversion and selectivity of ESBO to CSBO after solvent-free cycloaddition with CO<sub>2</sub> at different reaction times with catalyst **5**. Reaction conditions: catalyst amount: 2 mol % referred to oxirane mol; temperature: 160 °C; CO<sub>2</sub> pressure: 40 bar. .... 73

### *Chapter 3*

### *Page*

**Figure 3.1.** Comparative ATR-FTIR (a) and <sup>1</sup>H NMR spectra of the ESBO and CSBO. .... 88

**Figure 3.2.** ATR-FTIR spectra of the reaction between PPC and CHA at different reaction time in a wavelength range of a) 4000-400 cm<sup>-1</sup> and b) 1900-1450 cm<sup>-1</sup>. .... 89



---

<b>Figure 3.3.</b> PPC conversion values at different reaction times, measured by GC-MS. .....	89
<b>Figure 3.4.</b> ATR-FTIR spectra of CSBO and the prepared CSBO-based NIPUs with priamine at different amine/cyclic carbonate molar ratio: a) Wavenumber 400-4000 cm <sup>-1</sup> and b) wavenumber 1500-2000 cm <sup>-1</sup> .....	91
<b>Figure 3.5.</b> Comparative DSC curves of the prepared CSBO-based NIPUs with priamine at different amine/cyclic carbonate molar ratio.....	93
<b>Figure 3.6.</b> Comparative thermal profiles of the prepared CSBO-based NIPUs with priamine at different amine/cyclic carbonate molar ratio: a) TG curves and b) dTG curves. ....	94
<b>Figure 3.7.</b> Comparative SI and GC of the prepared CSBO-based NIPUs with priamine at different amine/cyclic carbonate molar ratio.....	94
<b>Figure 3.8.</b> Thermoset CSBO-based NIPU network cleavage. ....	95
<b>Figure 3.9.</b> Amine used for CSBO-based NIPUs synthesis.....	96
<b>Figure 3.10.</b> ATR-FTIR spectra of CSBO and the prepared CSBO-based NIPUs with different amines. ....	97
<b>Figure 3.11.</b> Comparative DSC curves of the prepared CSBO-based NIPUs with different amines. ....	98
<b>Figure 3.12.</b> Comparative thermal profiles of the prepared CSBO-based NIPUs with different amines: a) TG curves and b) dTG curves. ....	99
<b>Figure 3.13.</b> Comparative SI and GC of the prepared CSBO-based NIPUs with different amines. ....	100
<b>Figure 3.14.</b> Vegetable oil-based polyols overall structure.....	102

**Figure 3.15.** Comparison of thermal properties between CSBO-based NIPUs and VO-based PUs: (a) DSC curve and b) TG curve..... 103

**Figure 3.16.** Comparison of pencil hardness between CSBO-based NIPUs and VO-based PUs..... 103

---

## *Chapter 4*

*Page*

---

**Figure 4.1.** CSBO-based amino hardeners synthesis via CSBO stepwise addition.. 117

**Figure 4.2.** Industrial amino hardeners used for CSBO-based NIPU coatings synthesis.  
..... 120

**Figure 4.3.** Comparative ATR-FTIR spectra of CSBO, NIPU D400, NIPU AH-a, NIPU AH-b and NIPU AH-c after curing process: a) Wavenumber 700-4000  $\text{cm}^{-1}$  and b) wavenumber 1500-2000  $\text{cm}^{-1}$ . ..... 121

**Figure 4.4.** Dust-free test after 7 days for NIPU AH-c coating..... 122

**Figure 4.5.** FTIR-ATR spectra of the CSBO-based NIPU amino hardener's after 1h at MR 10 and 80 °C (top), MR 5 and 80 °C (middle) and MR 10 and 60 °C (bottom): a) Wavenumber 400-4000  $\text{cm}^{-1}$  and b) wavenumber 1500-2000  $\text{cm}^{-1}$ ..... 125

**Figure 4.6.** CSBO-based amino hardener in different solvents. .... 127

**Figure 4.7.** ATR-FTIR spectra of the reaction between CSBO and m-XDA at different reaction times. .... 129

**Figure 4.8.** Comparative  $^{13}\text{C}$ -NMR spectra of soybean oil, CSBO and CSBO-AH 2.  
..... 131

**Figure 4.9.** Preparative of CSBO-based hybrid NIPU-epoxy coatings. .... 132

**Figure 4.10.** Pendulum hardness monitoring of prepared coatings (a) TETA-based and (b) m-XDA based..... 133

**Figure 4.11.** Properties of the prepared clear coating formulations after 28 days ....135

**Figure 4.12.** Prepared pigmented coatings composed by CSBO-AH 2 and applied in glass (left), OC (middle) and sand blasted steel panels (right). .....136

**Figure 4.13.** Properties of the prepared pigmented coating formulations. ....137

**Figure 4.14.** Photographs of the prepared NIPU-epoxy hybrid formulations applied in sand blasted steel panels after different exposure times to the salt spray test. ....140

# LIST OF TABLES

<i>Chapter 1</i>	<i>Page</i>
<b>Table 1.1.</b> Non-functionalized ionic liquid catalysts used in carbonated oleochemicals synthesis.....	23
<b>Table 1.2.</b> Task-specific (functionalized) ionic liquid catalysts used in carbonated oleochemicals synthesis. ....	26
<b>Table 1.3.</b> Ionic liquid/Lewis acidic co-catalyst binary catalytic systems used in carbonated oleochemicals synthesis.....	32
<b>Table 1.4.</b> Ionic liquid/HBD co-catalyst binary catalytic systems used in carbonated oleochemicals synthesis. ....	34
<b>Table 1.5.</b> Alkali metal salts/co-catalyst binary catalytic systems used in carbonated oleochemicals synthesis. ....	39
<b>Table 1.6.</b> Heterogeneous catalytic systems used in carbonated oleochemicals synthesis.....	42
 <i>Chapter 2</i>	 <i>Page</i>
<b>Table 2.1.</b> Decomposition temperature ( $T_{\text{onset}}$ ) and melting temperature ( $T_{\text{m}}$ ) of the ionic liquids employed in this work.....	64
 <i>Chapter 3</i>	 <i>Page</i>
<b>Table 3.1.</b> CSBO-based NIPUs experimental data from DSC, TGA and THF absorption.....	90
<b>Table 3.2.</b> CSBO-based NIPUs hardness and impact resistance properties .....	100

---

<b>Table 3.3.</b> Comparison of direct impact resistance between CSBO-based NIPUs and VO-based PUs. ....	104
--	-----

---

**Chapter 4**
**Page**


---

<b>Table 4.1.</b> The main data of the prepared NIPU coatings formulations. ....	121
<b>Table 4.2.</b> Results of the preliminary study for the synthesis of CSBO-based NIPU amino hardeners. ....	124
<b>Table 4.3. Properties of synthesized CSBO-based amino hardeners.</b> ....	128
<b>Table 4.4.</b> MEK resistance of the prepared clear and pigmented coatings after 7 days. ....	137
<b>Table 4.5.</b> Pigmented coating mechanical properties of NIPU-epoxy hybrid formulations after 7 days. ....	138
<b>Table 4.6.</b> Salt spray results for prepared NIPU-Epoxy hybrid formulations applied in sand blasted steel panels. ....	139
<b>Table 4.7.</b> Salt spray results for prepared NIPU-Epoxy hybrid formulations applied in OC panels. ....	140

# LIST OF SCHEMES

<i>Chapter 1</i>	<i>Page</i>
<b>Scheme 1.1.</b> Synthesis of an urethane compound. ....	3
<b>Scheme 1.2.</b> PU from diisocyanate and diol. ....	4
<b>Scheme 1.3.</b> Synthesis of non-isocyanate polyurethanes via polyaddition of bis(cyclic carbonate) to diamine. ....	15
<b>Scheme 1.4.</b> General cycloaddition reaction of CO <sub>2</sub> to an epoxide. ....	16
<b>Scheme 1.5.</b> General three-step mechanism for the cycloaddition to an epoxide catalyzed by a tetraalkylammonium ionic liquid. ....	18
<b>Scheme 1.6.</b> General mechanism of CO <sub>2</sub> cycloaddition to an epoxide catalyzed by a tetraalkylammonium halide salt with hydroxyl terminal group. ....	25
<b>Scheme 1.7.</b> Mechanism proposed by Longwitz et al. for the CO <sub>2</sub> cycloaddition to an epoxide catalyzed by CaI <sub>2</sub> , 18-crown-6-ether and TPP catalytic system (Credit: Longwitz et al.). <sup>124</sup> ....	37
<b>Scheme 1.8.</b> CSBO-based non-isocyanate polyurethanes synthesis process. ....	44
<i>Chapter 2</i>	<i>Page</i>
<b>Scheme 2.1.</b> General mechanism of CO <sub>2</sub> cycloaddition to an epoxidized oil, catalysed by a tetraalkylammonium halide salt. ....	59
<b>Scheme 2.2.</b> General cycloaddition reaction of CO <sub>2</sub> to an epoxidized vegetable oil. ....	60
<i>Chapter 3</i>	<i>Page</i>

---

**Scheme 3.1.** Route to NIPUs from vegetable oils.....82

**Scheme 3.2.** Amide formation via triglyceride ester group transesterification. ....92

---

*Chapter 4*

*Page*

---

**Scheme 4.1.** PHU synthesis via the cyclic carbonate ring opening by amine. ....112

**Scheme 4.2.** General scheme of synthesis of NIPU coatings from CSBO: a) Direct use of CSBO and b) via CSBO-based AHs synthesis. ....119

**Scheme 4.3.** Main possible reactions between carbonated oil and amine: (a) cyclic carbonate aminolysis, (b) ester group amidation and (c) urea formation by transurethanization. ....126

**Scheme 4.4.** CSBO-based amino hardeners synthesis process.....128





# METHODS

---



This section details the experimental procedure for the chemical and structural characterization of synthesized ionic liquids catalyst, carbonated soybean oil (CSBO) and CSBO-based non-isocyanate polyurethanes (CSBO-based NIPUs). In addition to, the specific characterization of the developed NIPUs coatings.

## Epoxide content determination

The epoxide content (O), defined as the weight percent of oxirane oxygen is a suitable determination method to determine the epoxide content in epoxidized soybean oil (ESBO). This was determined according to the ASTM D 1652-04 standard using 702 SM Titrino equipment from Metrohm. The experimental process was performed according to the following procedure:

- i. Dissolve the sample (0.4 g) in  $\text{CH}_2\text{Cl}_2$  (40 mL) under stirring.
- ii. When the ESBO is dissolved, add 10 mL of tetraethylammonium bromide ([TEA][Br]) keeping the stirring.
- iii. Place the beaker in the automatic titrator. Immerse the electrode and shake it with a stir speed that is not too fast. Perform the titration with a standardized perchloric acid ( $\text{HClO}_4$ ) solution (1N solution in acetic acid).

The epoxide content (O) was calculated according to the following equation:

$$\text{Weight percent epoxide (E)} = 4.3 \times V_{\text{HClO}_4} + \frac{N_{\text{HClO}_4}}{\text{sample weight (g)}}$$

$$\text{Weight percent of oxirane (O)} = \frac{16}{43} \times E$$

## Gas Chromatography Mass Spectrometry (GC-MS)

Gas Chromatograph with Mass Spectrometry (GC-MS) measurements were carried out using a Gas Chromatograph Agilent GC 7890B, a MS detector 5977A and a HP5-

ms column of 30 m, 0.25 mm and 0.25 mm. Analytical conditions: samples dissolved in  $\text{CH}_2\text{Cl}_2$ ; injector temperature, 250 °C; detector temperature, 150 °C; split, 25:1; injection volume, 1  $\mu\text{L}$ ; oven temperature was started at 40 °C (3 min), afterwards it was increased at 12 °C  $\text{min}^{-1}$  up to 85 °C and then, it was increased at 30 °C  $\text{min}^{-1}$  up to 250 °C and kept at this temperature for 4 min; injection mode: split; carrier gas: helium at 1.2  $\text{mL min}^{-1}$ ; mass range: 33.0–550.0; running time, 16.25 min.

The determination of propylene carbonate (PPC) content in the samples was determined by means of a calibration curve using PPC as the standard and n-dodecane as the internal standard. The calibration curve was performed with 5 points, in a range of concentrations between 400 and 4000mg /l of PPC in  $\text{CH}_2\text{Cl}_2$ .

### **Nuclear Magnetic Resonance spectroscopy (NMR)**

$^1\text{H}$ ,  $^{13}\text{C}$  and  $^{31}\text{P}\{^1\text{H}\}$  Nuclear Magnetic Resonance (NMR) in solution were recorded on a Bruker 300 MHz spectrometer, using deuterated chloroform ( $\text{CDCl}_3$ ), deuterated dimethyl sulfoxide (DMSO) and deuterated acetone ( $(\text{CD}_3)_2\text{CO}$ ). The experimental conditions were as follows: a) For  $^1\text{H}$  NMR spectroscopy: 10 mg of sample; 0.5 mL of solvent; 5.45 s acquisition time; 1 s delay time, 14  $\mu\text{s}$  pulse, spectral width 60009.61 Hz and 16 scans; b) for  $^{31}\text{P}\{^1\text{H}\}$  NMR spectroscopy: 10 mg of sample, 0.5 mL of solvent, 0.67 s acquisition time, 2 s delay time, 12  $\mu\text{s}$  pulse, spectral width 4919.61 Hz and 512 scans; and for  $^{13}\text{C}$  NMR spectroscopy: 100 mg of sample; 0.75 mL of solvent; 1.81 s acquisition time; 2 s delay time, 10  $\mu\text{s}$  pulse, spectral width 18115.94 Hz and 4096-16384 scans.

### **Thermogravimetric Analysis (TGA)**

Thermal stability was evaluated by thermal gravimetric analysis (TGA) using either Mettler Toledo TGA/DSC 1 STARe System calibrated with indium, aluminium, gold and palladium standards. The experimental conditions were as follows: a) For ionic liquids characterization, the sample (15-20 mg) was heated from room temperature to

100 °C with a heating rate of 10 °C min<sup>-1</sup>, and keep in isothermal conditions (100 °C, 1 h) to eliminate moisture and/or residual solvent, if any. Then, the sample was heated from 100 °C to 700 °C with at a rate of 10 °C min<sup>-1</sup>. Isothermal measurements were performed at 160 °C, 180 °C and 200 °C by heating the sample (15-20 mg) from room temperature to desired temperature at 10 °C min<sup>-1</sup>. Once the desired temperature was reached it was kept for 12h. In all cases, the measurements were done under nitrogen flow (50 mL min<sup>-1</sup>). b) For CSBO-based NIPUs in a typical experiment the sample (15-20 mg) was heated from room temperature to 700 °C with a heating rate of 10 °C min<sup>-1</sup> under nitrogen flow (50 mL min<sup>-1</sup>). All the measurements were performed at least twice in order to check their repeatability.

### **Differential Scanning Calorimetry Analysis (DSC)**

Differential scanning calorimetry (DSC) analysis were carried out using Mettler Toledo DSC 2 STARe System calibrated with indium and zinc standards. The experimental conditions were as follows: a) For ionic liquids melting points characterization, DSC Scans cycles consisted of heating the sample (7-10 mg) up to 200 °C followed by a cooling ramp from 200 °C and -80 °C and a subsequent heating ramp between -80 °C and 200 °C, both at 10 °C/min and under nitrogen atmosphere. b) For CSBO-based NIPUs, DSC scans cycles consisted of heating the sample up to 150 °C followed by a cooling ramp from 150 °C and -80 °C and a subsequent heating ramp between -80 °C and 150 °C, both at 10 °C/min and under nitrogen atmosphere. This cycle was repeated by four times. To analyse the glass transition temperature ( $T_g$ ) the data obtained in second heating ramp were used. All the measurements were performed at least twice in order to check their repeatability.

### **Melting point determination**

Melting points were measured using STUART SMP30 capillary melting point apparatus. Samples were heated from room temperature until the solid phase

changes to the liquid phase. All the measurements were performed at least twice in order to check their repeatability.

## Fourier Transform Infrared Spectroscopy (FTIR)

FTIR spectra were collected using an infrared spectrophotometer ALPHA-P from Bruker Instrument or Spectrum 3 from PerkinElmer, both equipped with attenuated total reflectance (ATR). The spectra were recorded in the range of 4000 to 400  $\text{cm}^{-1}$  at a resolution of 4 $\text{cm}^{-1}$  with 24 registered scans.

## Determination of the degree of cross-linking of the polymeric network

Cross-linking of the final NIPUs was analysed by swelling index (SI) and gel-content (GC). The process has been based on previously reported work<sup>1,2</sup>. These tests were carried out in THF as an appropriate solvent, since it could dissolve the monomers and oligomers, but not the cross-linked NIPU. The cured samples ( $\approx 0.5$  g) were separately put into THF (50:1) for 72h at room temperature. Before weighing, the sample was dried with filter paper to absorb superficial solvent. The swelling index is given by Eq (1), where  $m_0$  and  $m_1$  are the weight of samples before and after swelling, respectively. After swelling index measurement, the samples were dried in vacuum oven at RT during 24h. The gel content is given by following equation (2), where  $m_0$  is initial mass of the sample, and  $m_2$  is mass of the sample after drying. For each sample, the SI and GC measurements were performed in quadruplicate.

$$(1) \text{ Swelling index (\%)} = \frac{m_1 - m_0}{m_0} \times 100$$

$$(2) \text{ Gel - content (\%)} = \frac{m_2}{m_0} \times 100$$

## Amine number determination

The amine number, defined as the number of milligrams of potassium hydroxide (KOH) equivalent to one gram of epoxy hardener resin, is a suitable determination method to determine the amine content in amine functional compounds. This was determined according to the DIN 53176 standard using 799 GPT Titrino equipment from Metrohm. The experimental process was performed according to an Allnex -The coating Resin Company- internal procedure, following this procedure:

- i. Dissolve the reaction sample ( $\approx 0.6$  g) in a propylene carbonate (4): acetic acid (1) solution (28 mL) under stirring.
- ii. Once the amine functional compound is dissolved, place the beaker in the automatic titrator. Immerse the electrode and shake it with a stir speed that is not too fast. Perform the titration with a standardized perchloric acid ( $\text{HClO}_4$ ) solution (0.1 M solution in acetic acid).

The amine number was calculated according to the following equation:

$$\text{Amine number} \left( \frac{\text{KOH mg}}{\text{g}} \right) = 56.1 \times V_{\text{HClO}_4} + \frac{N_{\text{HClO}_4}}{\text{sample weight (g)}}$$

## Viscosity and formulations pot-life determination

Formulation's pot life was determined by means of dynamic viscosity value. Viscosity measurements were done at 23 °C, over a shear rate range of 25 s<sup>-1</sup> using an 7Physica MCR 101 from Anton Parr. In practice, the pot life of the formulation was defined as the time it takes for the viscosity of the coating mixture to increase to twice its value since all the reagents are mixed. In order to know the exact pot-life of each of the formulations, the viscosity was measured every 30 minutes until it doubled its initial value ( $t_0$ ).

## Coating drying determination

Coating mixture drying was evaluated by dust-free, tack-free, and drying test according to ISO 9117-5.

Dust-free time is considered when particles, dust, etc. do not remain adhered to the coating. The experimental process to determine de dust-free time was performed according to the following procedure: Glass particles were added to the coating at 30-minute intervals. Once the particles were no longer adhered, this was defined as the dust-free time of the formulation.

The tack-free time is the time at which the coating is properly adhered and capable of providing maximum protection to a surface without being disrupted or damaged. In test environments, tack-free time can simply be stated as the point at which a film applied to a surface simply ceases to be tacky to the touch. The experimental process to determine de tack-free time was performed according to the following procedure: On a coating that had already reached the dust-free time, the surface was pressed manually with a finger covered with cellulose paper every 30 minutes.

Once no paper remained adhered and no marks were observed on the coating, the coating was considered to have reached the tack-free time.

The drying stage for each coating was determined according to ISO 9117-5 standard and in triplicate. The experimental process was performed according to the following procedure:

- i. Place a paper disc and top of that, a rubber disc on the test panel.
- ii. Place a weight (200 g, 2 kg and/or 20 kg) centrally on the rubber disc and keep it for 60 seconds.
- iii. After that remove the weight and rubber disc and drop the test panel vertically from a height. The adhesion or non-adhesion of the paper disk and the weight used, determine the specific drying stage (**Table M.1**).

The following table indicates the coating requirements for each of the drying stages:



**Table M.1.** Drying stages characteristics.

Drying stage	Type of test	Test result
1	Pouring ballotini on to surface of coating	The ballotini can be brushed away easily and completely with a soft brush.
2	Load with 20 g	The paper does not stick to the coating.
3	Load with 200 g	The paper does not stick to the coating.
4	Load with 2 kg	The paper does not stick to the coating. In the area acted on by the load, the coating surface shows visible changes.
5	Load with 2 kg	The paper does not stick to the coating. In the area acted on by the load, the coating surface shows no visible changes.
6	Load with 20 kg	The paper does not stick to the coating. In the area acted on by the load, the coating surface shows visible changes.
7	Load with 20 kg	The paper does not stick to the coating. In the area acted on by the load, the coating surface shows no visible changes.

## Coating hardness determination

The hardness of the coatings was evaluated by pendulum dumping test via the König pendulum and according to ISO 1522:2006 standard. The tests were performed at  $(23 \pm 2)$  °C and relative humidity of  $(50 \pm 5)$  %. The pendulum damping time was determine on three different parts of the same test panel.

The hardness of the coatings was also evaluated by pencil hardness test according to ASTM D 3363-20 and in duplicate. The tests were performed at  $(23 \pm 2)$  °C and relative humidity of  $(50 \pm 5)$  %. The experimental process was performed according to the following procedure:

- i. The coating thickness is measured.
- ii. Preparation of the grating pencil, removing 5 to 6 mm of wood without damaging the lead, leaving a perfect cylinder. The pencil is then placed vertically on the 400 grit or finer sandpaper and rubbed over it until a perfectly circular and flat point is obtained.
- iii. Making the scratch. Starting with the hardest pencil, it is placed firmly on the coating at approximately a 45° angle to the specimen. The pencil is moved approximately 6.5 mm forward, exerting enough force on the specimen to scratch or cut the coating or break the pencil tip.
- iv. The operation is repeated with successively softer pencils until the one that does not cut the coating by at least 3 mm is reached.

### **Determination of the resistance of coatings to separation from substrate**

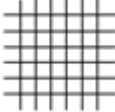
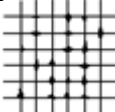
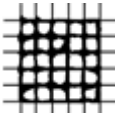
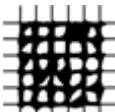
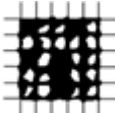
The resistance of coatings to separation from substrate was determined by cross-cut test according to ISO 2409:2013. This specifies a test method for evaluating the resistance of paint coatings to separation from substrates when a right-angle grid pattern is cut into the coating, penetrating the substrate. The experimental process was performed according to the following procedure:

- i. Manually cut the coating using the multi-blade cutting tool and trying to maintain a uniform pressure and speed.
- ii. Remove any loose paint from the area of cutting.
- iii. Place a piece of adhesive tape over the marked area, press and finally pull it off.

- iv. Carefully examine visually the area and determine the separation resistance of the coating to the substrate (**Table M.2**).

The following table indicates the possible coating classification after cross-cut test:

**Table M.2.** Cross-cut test classification.

Classification	Description	Appearance of surface of cross-cut area
0	The edges of the cuts are completely smooth; none of the squares of the lattice is detached.	
1	Detachment of small flakes of the coating at the intersections of the cuts. A cross-cut area not greater than 5 % is affected.	
2	The coating has flaked along the edges and/or at the intersections of the cuts. A cross-cut area greater than 5 %, but not greater than 15 %, is affected.	
3	The coating has flaked along the edges of the cuts partly or wholly in large ribbons, and/or it has flaked partly or wholly on different parts of the squares. A cross-cut area greater than 15 %, but not greater than 35 %, is affected.	
4	The coating has flaked along the edges of the cuts in large ribbons and/or some squares have detached partly or wholly. A cross-cut area greater than 35 %, but not greater than 65 %, is affected.	
5	Any degree of flaking that cannot even be classified by classification 4.	-

## Coating solvent resistance determination

The solvent resistance of the coatings was determined by performing methyl ethyl ketone (MEK) rubbing test using a Werkstoff-prüfgeräte from Hess according to EN 13523-11. The speed of the double rubs was defined as 1s. The test was finished once the material underneath (glass plate) was observed, indicating the removal of the coating.

## Coating gradual deformation resistance determination

The resistance of coatings to gradual deformation was determined by cupping test according to ISO 1520:2006. This Standard specifies an empirical method for assessing the resistance of a coating to cracking and/or detachment from a metal substrate when subjected to gradual deformation by indentation under standard conditions. The experimental process was performed according to the following procedure and in duplicate:

- i. Hold the test panel (with right dimensions) firmly without excessive pressure between the retaining ring and the drawing die with the coating towards the die and with the hemispherical end of the indenter just in contact with the uncoated side of the test panel (zero position of the indenter). Adjust the panel until the central axis of the indenter intersects the panel at least from the edge.
- ii. The hemispherical end of the indenter is advanced into the test piece at a constant speed.
- iii. Once a crack is first observed on the surface of the coating and/or the coating begins to become detached from the substrate, the indenter is stopped, and the depth of indentation is measured.

## Coating rapidly deformation resistance determination

The resistance of coatings to rapidly deformation was according to ASTM D2794 and ISO 6272-1:2012. These equivalent standards specify an empirical method which has been found to be useful in predicting the performance of organic coatings for their ability to resist cracking caused by impacts. The experimental process was performed according to the following procedure:

- i. Place the test panel in the apparatus with the coated side either up (direct impact) or down (indirect impact)
- ii. Lightly place the weight on the indenter and adjust the guide tube so that the lifting pin is at the zero mark and raise the weight (1 kg) up the tube to a height where it is expected that no failure will occur.
- iii. Release the weight so that it drops on the indenter.
- iv. Remove the test panel from the apparatus and observe the impact area for cracks in the coating. If no cracks are evident, repeat the procedure at a greater height.
- v. Once visible cracks are observed, repeat the test five times at each of three heights; slightly above, slightly below, and at that determined in the first trial.
- vi. Examine the impacted areas for cracking by magnifier.

## Coating corrosion resistance determination

The resistance of coated samples against corrosion was evaluated by salt spray test introducing them in a Typ SC 1000 cabin from Weiss Technik GmbH at 35 °C and 47% relative humidity, 5% NaCl-solution. Formulations applied in metal plates were analysed for the corrosion resistance at different time intervals according to ISO 9227:2017.

## References

- 1 I. Javni, D. P. Hong and Z. S. Petrovic, *J. Appl. Polym. Sci.*, 2013, **128**, 566–571.
- 2 X. He, X. Xu, Q. Wan, G. Bo and Y. Yan, *Polymers*, 2017, **9**, 649-661.

# APPENDIX

---





## CHAPTER 2

### A1. Synthesis of ionic liquids

*Butyltriphenylphosphonium bromide ([BTTP][Br])(1)*: In a 100 mL Fischer Porter reactor, under a positive nitrogen pressure, triphenylphosphine (1.1 equiv) was dissolved in toluene (25 mL). Then, 1-bromobutane (1.0 equiv) was added dropwise and the mixture was heated to reflux for 24h. The crude product first was washed with toluene to remove non-ionic residues, and then with pentane. Finally, the white solid was dried under reduced pressure at 55 °C overnight (Yield 56%). Melting point: 245-247 °C. Onset temperature: 304 °C.

$^1\text{H}$  NMR (DMSO- $d_6$ , TMS, 300MHz)  $\delta$ /ppm: 0.90 ( $^3\text{J}$  (HH) = 7.0 Hz, t, 3H), 1.51 (m, 4H), 3.60 (m, 2H), 7.97-7.7 (m, 15H);  $^{31}\text{P}\{^1\text{H}\}$  NMR (DMSO- $d_6$ , TMS, 121 MHz)  $\delta$ /ppm: 24.09.

*(3-hydroxypropyl)triphenylphosphonium bromide ([HPTTP][Br])(2)*: In a 100 mL Fischer Porter reactor, under a positive nitrogen pressure, triphenylphosphine (1.1 equiv) was dissolved in toluene (25 mL). Then, 3-bromopropanol (1.0 equiv) was added dropwise and the mixture was heated to reflux for 24h. The crude product first was washed with toluene to remove non-ionic residues, and then with pentane. Finally, the white solid was dried under reduced pressure at 55 °C overnight (Yield: 87%). Melting point: 237-239 °C. Onset temperature: 329 °C.

$^1\text{H}$  NMR (DMSO- $d_6$ , TMS, 300MHz)  $\delta$ /ppm: 1.68 (m, 2H), 1.22 (m, 16H), 3.67-3.47 (m, 4H), 4.86 ( $^3\text{J}$  (HH) = 5.1 Hz, t, 1H), 7.96-7.71 (m, 15H);  $^{31}\text{P}\{^1\text{H}\}$  NMR (DMSO- $d_6$ , TMS, 121 MHz)  $\delta$ /ppm: 24.54.

*(3-carboxypropyl)triphenylphosphonium bromide ([CBTTP][Br])(3)*: In a 100 mL Fischer Porter reactor, under a positive nitrogen pressure, triphenylphosphine (1.1 equiv) was dissolved in toluene (25 mL). Then, 4-bromobutyric acid (1.0 equiv) was added dropwise and the mixture was heated to reflux for 24h. The crude product first was washed with toluene to remove non-ionic residues, and then with pentane. Finally,

the white solid was dried under reduced pressure at 55 °C overnight (Yield: 63%). Melting point: 251-254 °C. Onset temperature: 326 °C.

$^1\text{H}$  NMR (DMSO- $d_6$ , TMS, 300MHz)  $\delta$ /ppm: 1.74 (m, 2H), 2.51 (m, 2H), 3.60 (m, 2H), 7.97-7.71 (m, 15H), 12.34 (s, 1H);  $^{31}\text{P}\{^1\text{H}\}$  NMR (DMSO- $d_6$ , TMS, 121 MHz)  $\delta$ /ppm: 23.77.

*(7-carboxyheptyl)triphenylphosphonium bromide ([COTPP][Br])(4)*: In a 100 mL Fischer Porter reactor, under a positive nitrogen pressure, triphenylphosphine (1.1 equiv) was dissolved in toluene (25 mL). Then, 8-bromooctanoic acid (1.0 equiv) was added and the mixture was heated to reflux for 24h. The crude product first was washed with toluene to remove non-ionic residues, and then with pentane. Finally, the white solid was dried under reduced pressure at 55 °C overnight (Yield: 78%). Melting point: 125-128 °C. Onset temperature: 318 °C.

$^1\text{H}$  NMR (DMSO- $d_6$ , TMS, 300MHz)  $\delta$ /ppm: 1.24 (m, 4H), 1.45 (m, 6H), 2.17 ( $^3\text{J}$  (HH) = 7.3 Hz, t, 2H), 3.59 (m, 2H), 7.95-7.71 (m, 15H), 11.95 (s, 1H);  $^{31}\text{P}\{^1\text{H}\}$  NMR (DMSO- $d_6$ , TMS, 121 MHz)  $\delta$ /ppm: 24.07.

*Dodecyltriphenylphosphonium bromide ([DTPP][Br])(5)*: In a 100 mL Fischer Porter reactor, under a positive nitrogen pressure, triphenylphosphine (1.1 equiv) was dissolved in toluene (25 mL). Then, 1-bromododecane (1.0 equiv) was added dropwise and the mixture was heated to reflux for 24h. Toluene was eliminated under vacuum and the crude product was washed with ethyl ether under stirring three times. Finally, the white solid was dried under reduced pressure at 55 °C overnight (Yield: 65.3 %). Melting point: 101-104 °C). Onset temperature: 293 °C

$^1\text{H}$  NMR (DMSO- $d_6$ , TMS, 300MHz)  $\delta$ /ppm: 0.87 ( $^3\text{J}$  (HH) = 6.9 Hz, t, 3H), 1.24 (m, 16H), 1.48 (m, 4H), 3.57 (m, 2H), 7.96-7.73 (m, 15H);  $^{31}\text{P}\{^1\text{H}\}$  NMR (DMSO- $d_6$ , TMS, 121 MHz)  $\delta$ /ppm: 24.08.

*Hexadecyltriphenylphosphonium bromide ([HTPP][Br])(6)*: In a 100 mL Fischer Porter reactor, under a positive nitrogen pressure, triphenylphosphine (1.1 equiv) was dissolved in toluene (25 mL). Then, 1-bromohexadecane (1.0 equiv) was added dropwise and the mixture was heated to reflux for 48h. Toluene was eliminated under vacuum and the crude product was washed with ethyl ether under stirring three

times. Finally, the white solid was dried under reduced pressure at 55 °C overnight (Yield: 40%). Melting point: 104 °C. Onset temperature: 291 °C.

$^1\text{H}$  NMR (DMSO- $d_6$ , TMS, 300MHz)  $\delta$ /ppm: 0.87 ( $^3\text{J}$  (HH) = 6.9 Hz, t, 3H), 1.25 (m, 24H), 1.48 (m, 4H), 3.57 (m, 2H), 7.97-7.74 (m, 15H);  $^{31}\text{P}\{^1\text{H}\}$  NMR (DMSO- $d_6$ , TMS, 121 MHz)  $\delta$ /ppm: 24.06.

*Eicosiltriphenylphosphonium bromide ([ETPP][Br])(7)*: In a 100 mL Fischer Porter reactor, under a positive nitrogen pressure, triphenylphosphine (1.1 equiv) was dissolved in toluene (25 mL). Then, 1-bromoeicosane (1.0 equiv) was added little by little and the mixture was heated to reflux for 48h. Toluene was eliminated under vacuum and the crude product was washed with ethyl ether under stirring three times. Finally, the white solid was dried under reduced pressure at 55 °C overnight (Yield: 55%). Melting point: 109 °C. Onset temperature: 289 °C.

$^1\text{H}$  NMR (DMSO- $d_6$ , TMS, 300MHz)  $\delta$ /ppm: 0.87 ( $^3\text{J}$  (HH) = 7.0 Hz, t, 3H), 1.25 (m, 32H), 1.49 (m, 4H), 3.57 (m, 2H), 7.96-7.73 (m, 15H);  $^{31}\text{P}\{^1\text{H}\}$  NMR (DMSO- $d_6$ , TMS, 121 MHz)  $\delta$ /ppm: 24.07.

*Octyltriphenylphosphonium iodine ([OTPP][I])(8)*: In a 100 mL Fischer Porter reactor, under a positive nitrogen pressure, triphenylphosphine (1.1 equiv) was dissolved in toluene (25 mL). Then, 1-iodooctane (1.0 equiv) was added dropwise and the mixture was heated to reflux for 24h. Toluene was eliminated under vacuum and the crude product was washed with ethyl ether under stirring three times. Finally, the yellowish solid was dried under reduced pressure at 55 °C overnight (Yield: 37%). Melting point: 73-77 °C. Onset temperature: 304 °C.

$^1\text{H}$  NMR (DMSO- $d_6$ , TMS, 300MHz)  $\delta$ /ppm: 0.85 ( $^3\text{J}$  (HH) = 6.9 Hz, t, 3H), 1.21 (m, 8H), 1.46 (m, 4H), 3.57 (m, 2H), 7.96-7.73 (m, 15H);  $^{31}\text{P}\{^1\text{H}\}$  NMR (DMSO- $d_6$ , TMS, 121 MHz)  $\delta$ /ppm: 24.07.

*Octyltriphenylphosphonium bromide ([OTPP][Br])(9)*: In a 100 mL Fischer Porter reactor, under a positive nitrogen pressure, triphenylphosphine (1.1 equiv) was dissolved in toluene (25 mL). Then, 1-bromooctane (1.0 equiv) was added dropwise and the mixture was heated to reflux for 24h. Toluene was eliminated under vacuum and the crude product was washed with ethyl ether under stirring three times. Finally, the

colourless viscous liquid was dried under reduced pressure at 55 °C overnight (Yield: 16.4%). Melting point: 33 °C. Onset temperature: 294 °C.

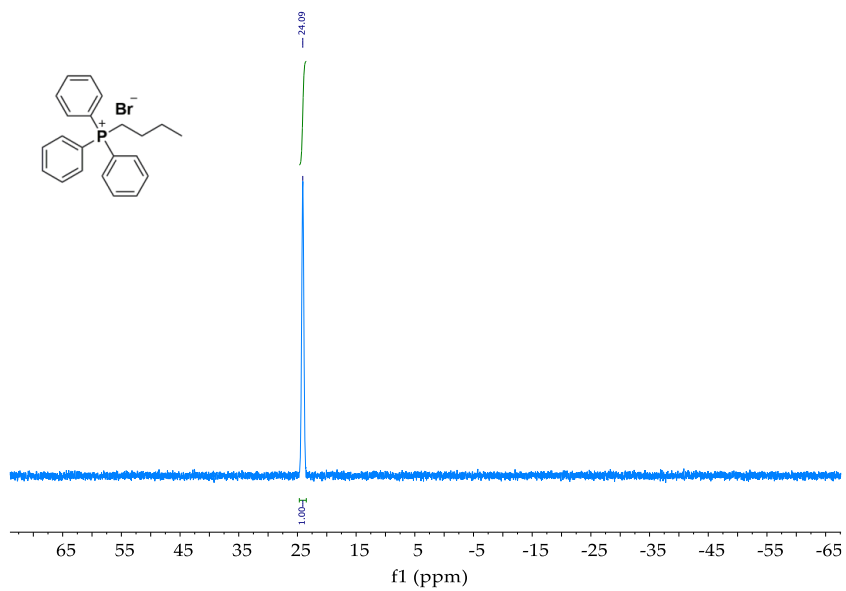
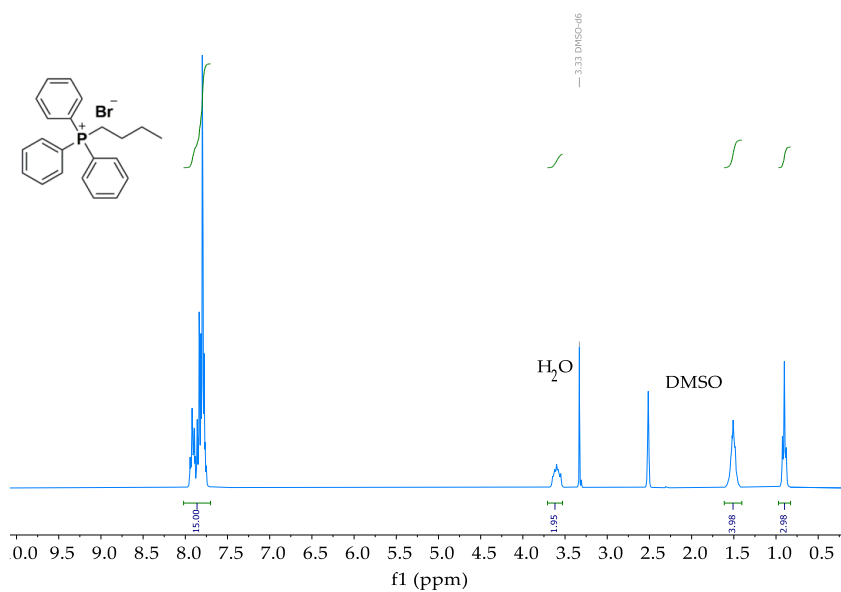
$^1\text{H}$  NMR (DMSO- $d_6$ , TMS, 300MHz)  $\delta$ /ppm: 0.80 ( $^3\text{J}$  (HH) = 6.9 Hz, t, 3H), 1.17 (m, 8H), 1.44 (m, 4H), 3.56 (m, 2H), 7.93-7.68 (m, 15H);  $^{31}\text{P}\{^1\text{H}\}$  NMR (DMSO- $d_6$ , TMS, 121 MHz)  $\delta$ /ppm: 24.10.

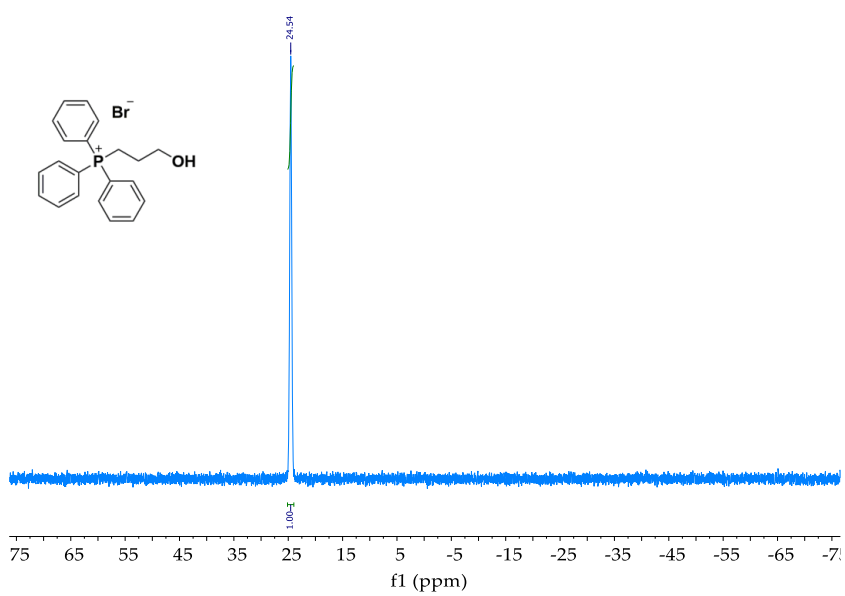
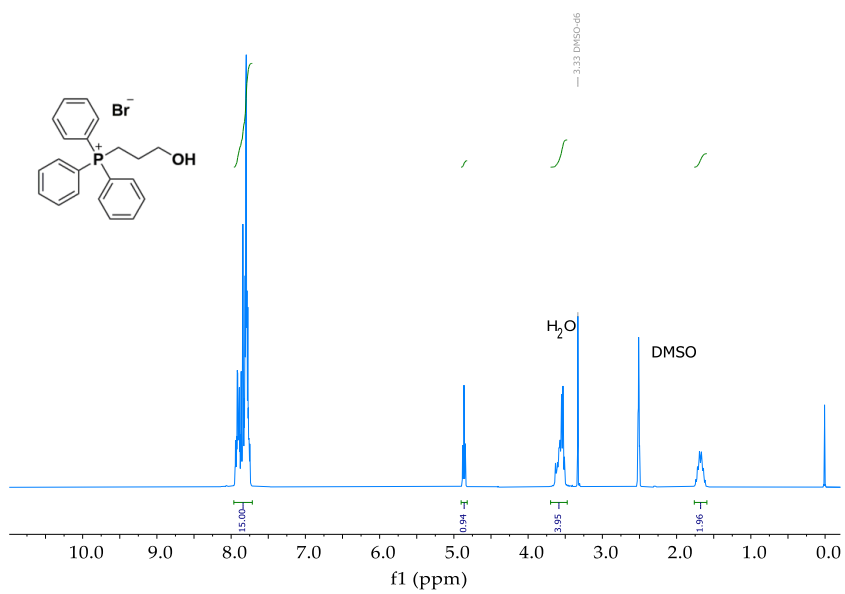
*Dodecyltripcyclohexylphosphonium bromide* ([DTCP][Br])(**10**): In a 100 mL Fischer Porter reactor, under a positive nitrogen pressure, tricyclohexylphosphine (1.1 equiv) was dissolved in toluene (25 mL). Then, 1-bromododecane (1.0 equiv) was added dropwise and the mixture was heated to reflux for 24h. Toluene was eliminated under vacuum and the crude product was washed with ethyl ether under stirring three times. Finally, the colourless viscous liquid was dried under reduced pressure at 55 °C overnight (Yield: 72%). Melting point: 5 °C. Onset temperature: 337 °C.

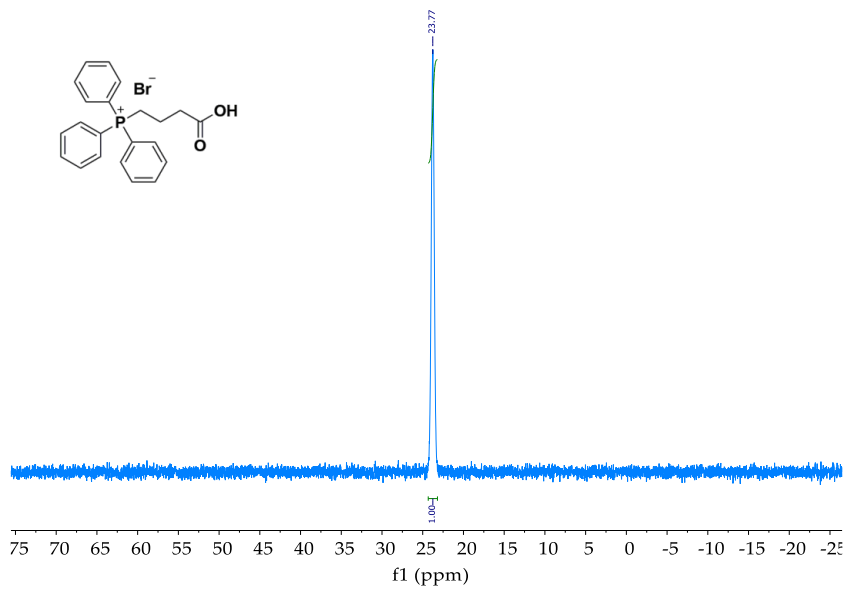
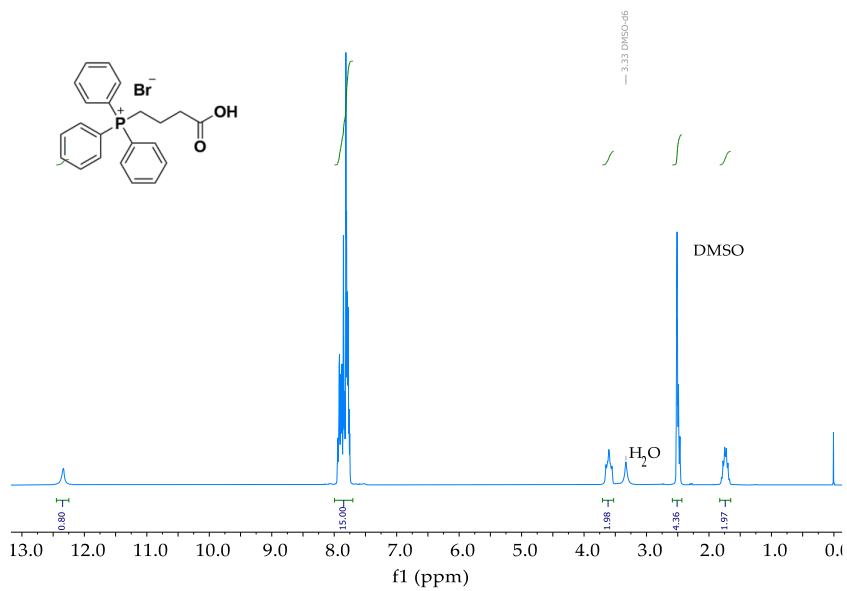
$^1\text{H}$  NMR (CDCl<sub>3</sub>, TMS, 300MHz)  $\delta$ /ppm: 0.84 ( $^3\text{J}$  (HH) = 6.2 Hz, t, 3H), 1.36-1.14 (m, 18H), 1.62-1.39 (m, 16H), 2.08-1.72 (m, 16H), 2.40 (m, 2H), 2.65 (m, 3H);  $^{31}\text{P}\{^1\text{H}\}$  NMR (CDCl<sub>3</sub>, TMS, 121 MHz)  $\delta$ /ppm: 31.67.

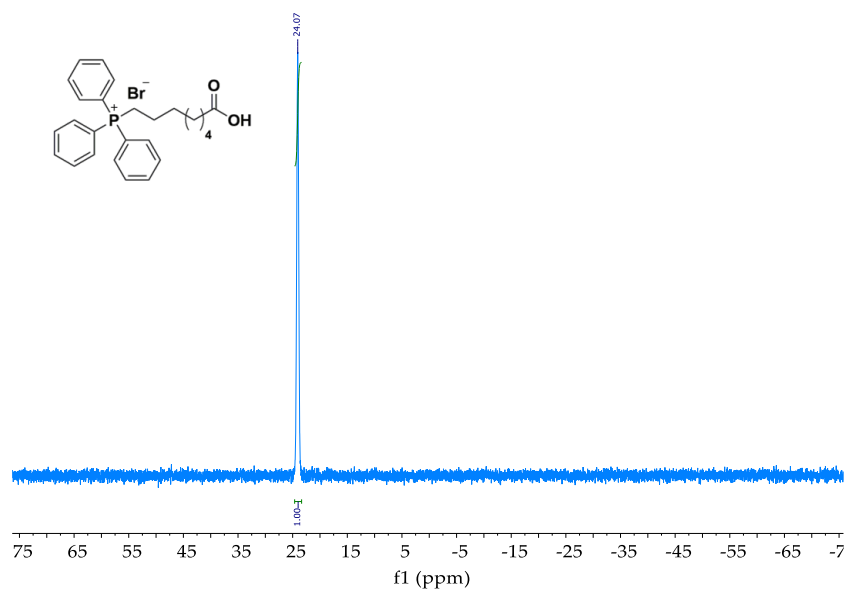
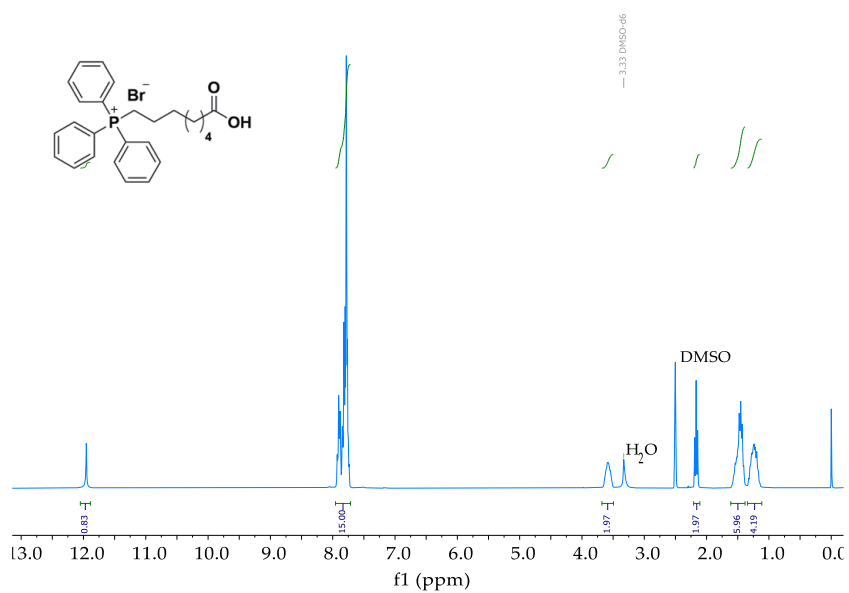
*Butyltripcyclohexylphosphonium bromide* ([BTCP][Br])(**11**): In a 100 mL Fischer Porter reactor, under a positive nitrogen pressure, tricyclohexylphosphine (1.1 equiv) was dissolved in toluene (25 mL). Then, 1-bromobutane (1.0 equiv) was added dropwise and the mixture was heated to reflux for 24h. Toluene was eliminated under vacuum and the crude product was washed with ethyl ether under stirring three times. Finally, the white solid was dried under reduced pressure at 55 °C overnight (Yield: 88%). Melting point: 150-153 °C. Onset temperature: 341 °C.

$^1\text{H}$  NMR (CDCl<sub>3</sub>, TMS, 300MHz)  $\delta$ /ppm: 0.97 ( $^3\text{J}$  (HH) = 7.5 Hz, t, 3H), 1.31 (m, 4H), 1.64-1.39 (m, 16H), 2.17-1.82 (m, 14H), 2.49 (m, 2H), 2.67 (m, 3H);  $^{31}\text{P}\{^1\text{H}\}$  NMR (CDCl<sub>3</sub>, TMS, 121 MHz)  $\delta$ /ppm: 31.68.

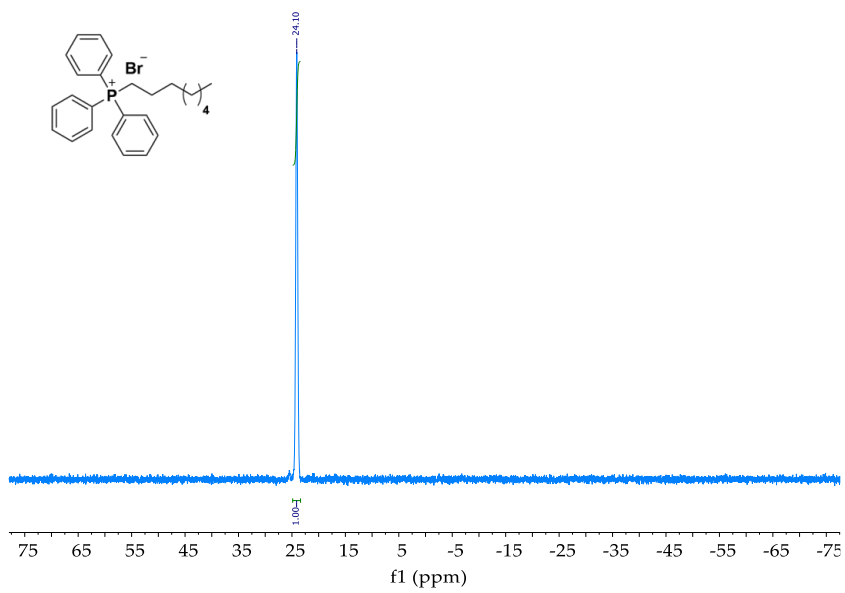
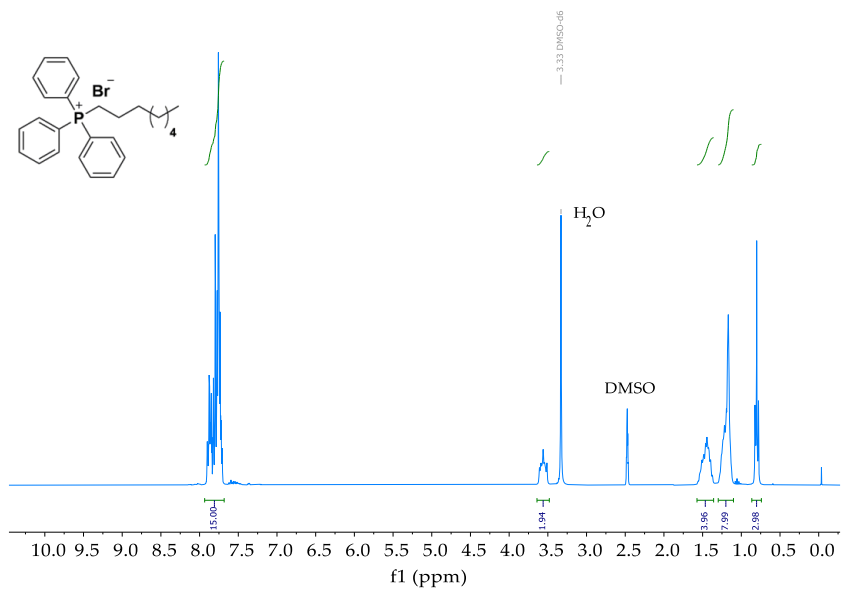
A2.  $^1\text{H}$  and  $^{31}\text{P}\{^1\text{H}\}$  NMR spectra of the prepared ionic liquids



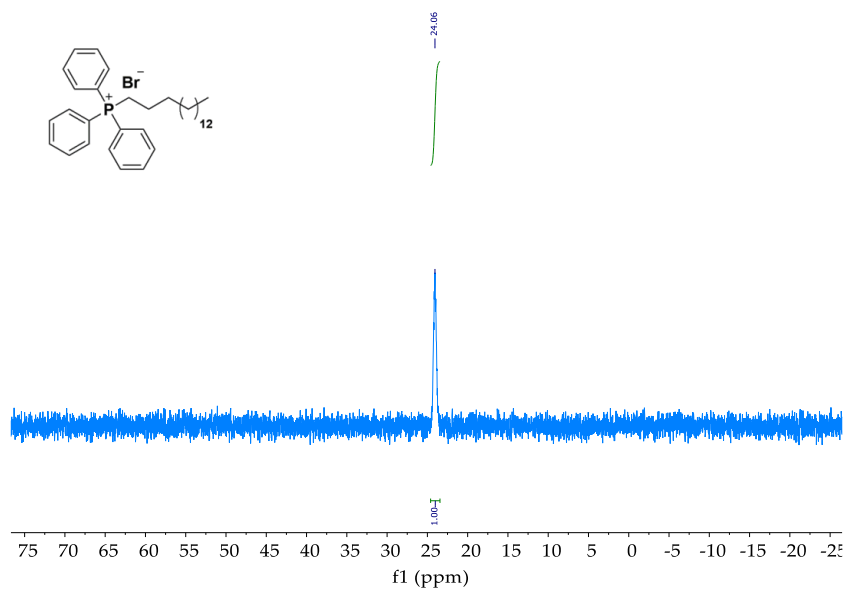
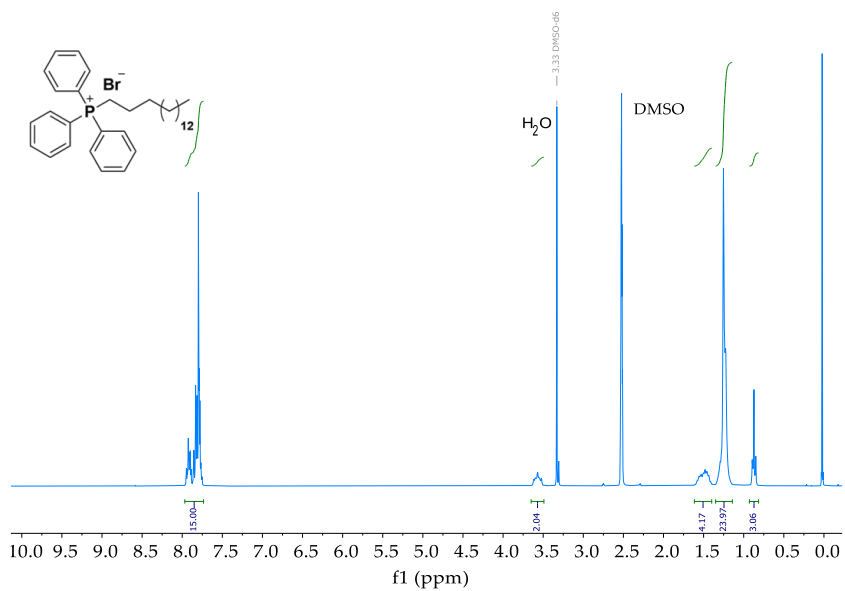






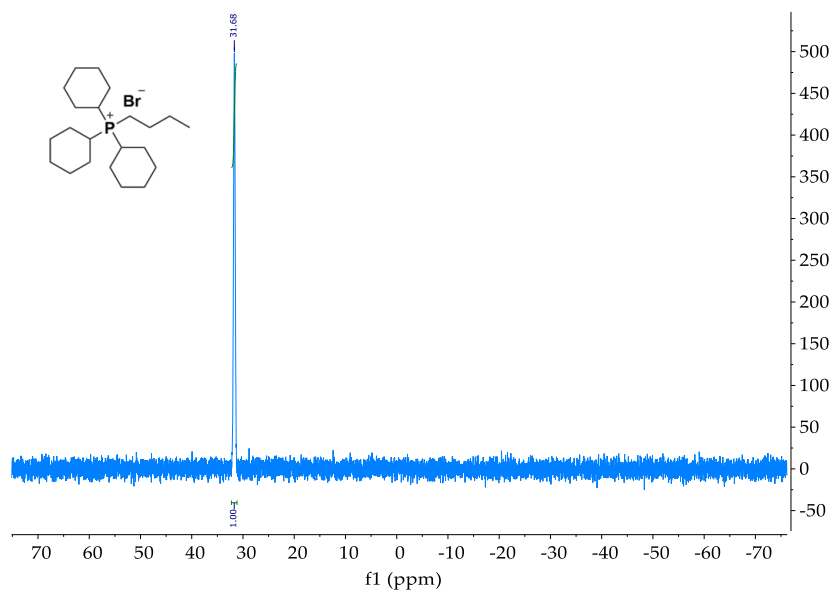
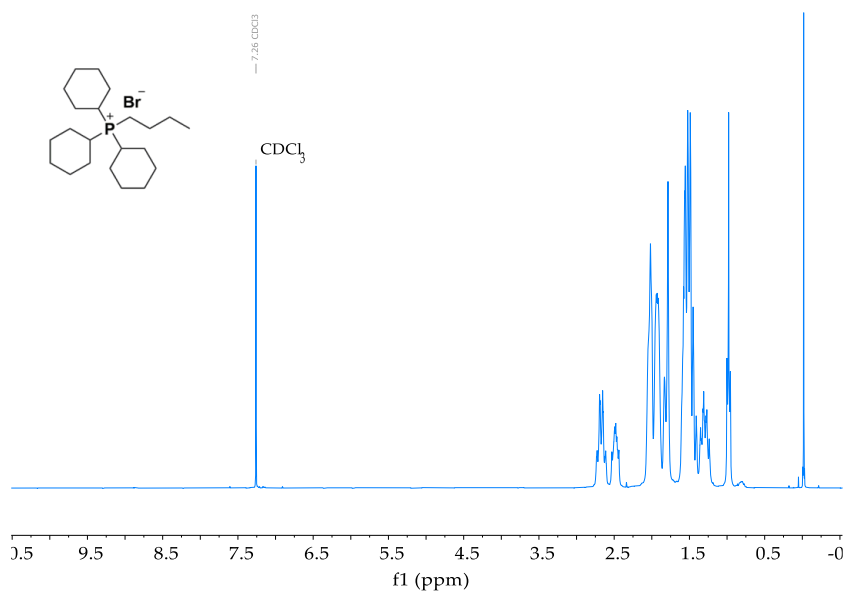


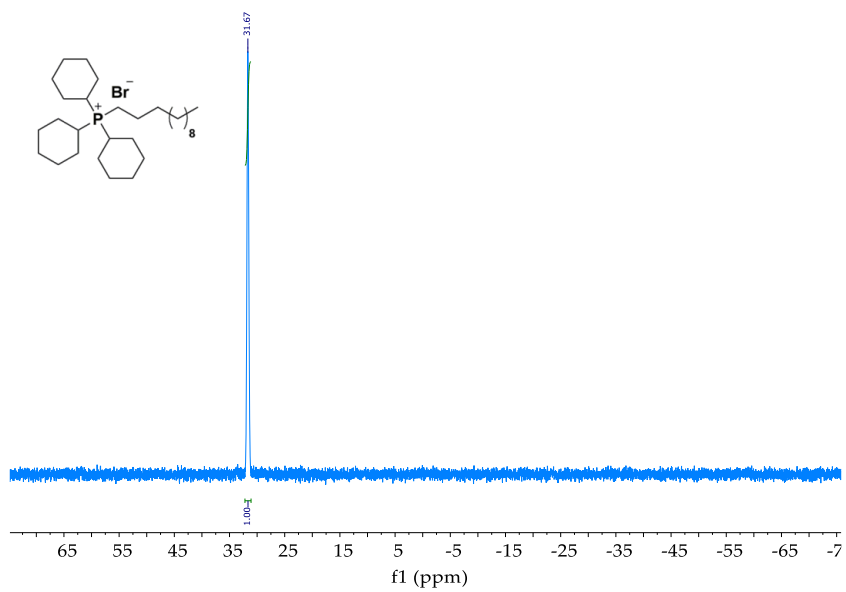
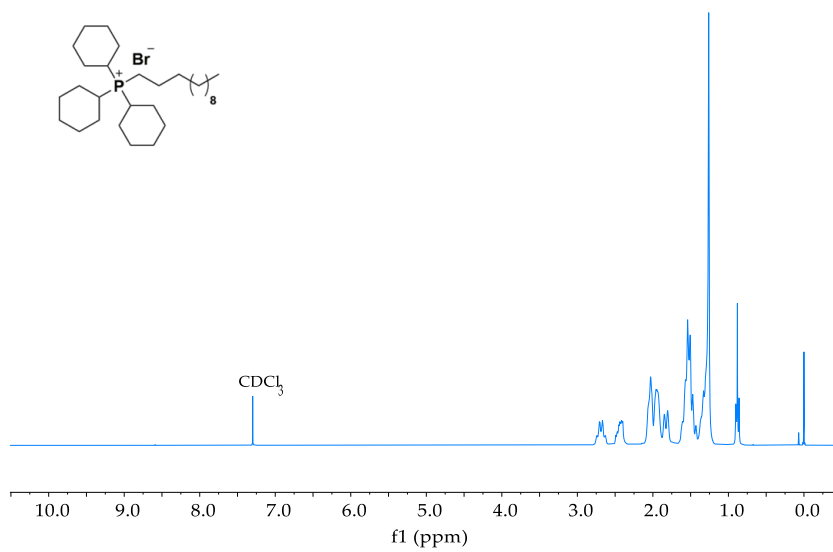




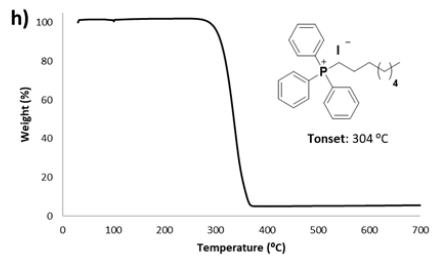
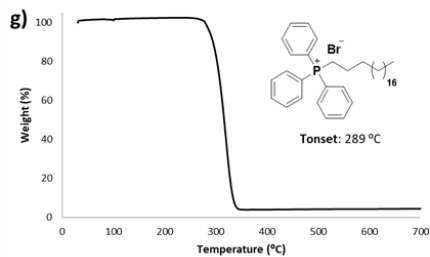
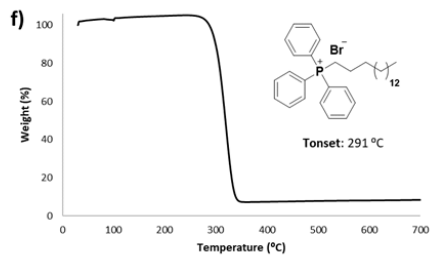
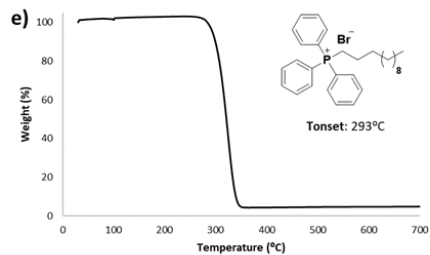
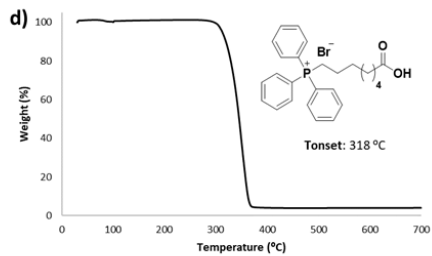
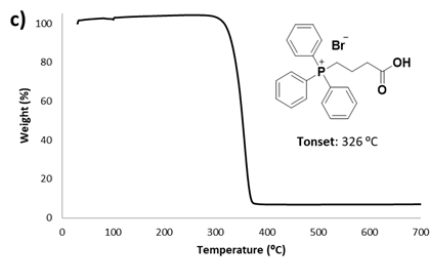
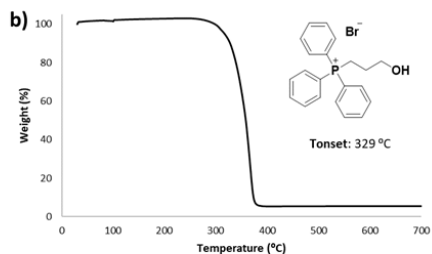
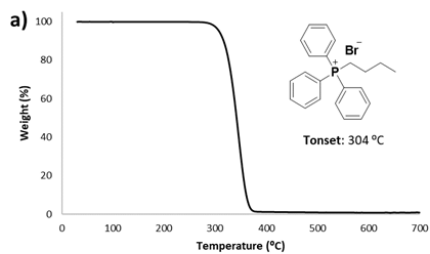






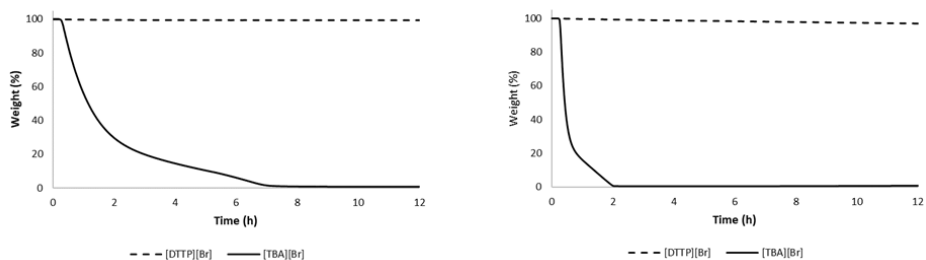


## A3. TG profiles of the prepared and benchmark ionic liquids





A4.TG isothermal profiles of the [TBA][Br] (12) and the prepared [DTPP][Br] (5) ionic liquids: 180 °C (left) and 200 °C (right).



A5. Products isolated by flash chromatography column purification

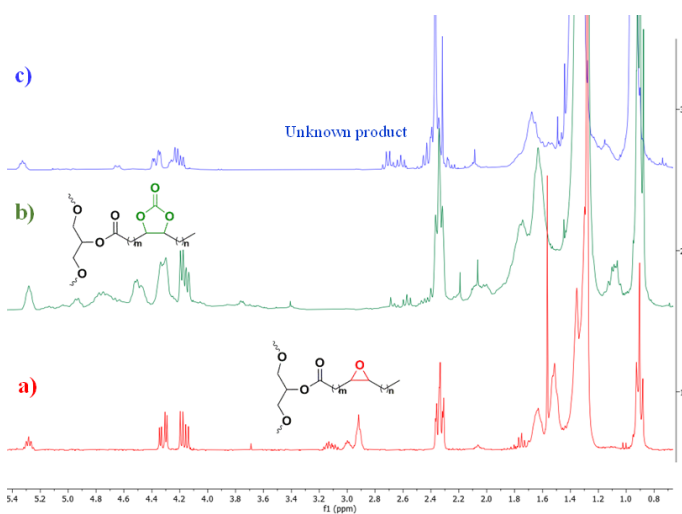


**Figure A.1.** <sup>1</sup>H NMR (CDCl<sub>3</sub>, TMS, 300MHz) of products isolated by flash chromatography purification: **a)** epoxidized soybean oil (ESBO), **b)** carbonated soybean oil (CSBO) and **c)** unknown product.







eman ta zabal zazu  
Universidad del País Vasco Euskal Herriko Unibertsitatea

